Electronic Thesis and Dissertation Repository

2-16-2024 10:15 AM

Frontoparietal Circuitry Underlying Saccade Control in the Common Marmoset

Janahan Selvanayagam, *Western University*

Supervisor: Everling, Stefan, *The University of Western Ontario*
A thesis submitted in partial fulfillment of the requirements for the Doctor of Philosophy degree in Neuroscience
© Janahan Selvanayagam 2024

Recommended Citation

Abstract

Our visual world is full of far more stimuli than can be processed simultaneously. Yet we are able to efficiently extract behaviourally relevant information from a scene, primarily by performing rapid saccadic eye movements. These processes are under the control the frontoparietal network, two critical nodes of which are: the lateral intraparietal area (LIP) and the frontal eye fields (FEF). Extensive research in the macaque has causally implicated these areas in visual attention and oculomotor control. However, the organization of the activity of single neurons in these areas across cortical layers remains poorly understood as these regions are deep within sulci in the macaque. The marmoset, with a lissencephalic cortex, largely homologous frontoparietal network, and comparable oculomotor repertoire, presents a unique opportunity to address these questions.

First, the homology of these cortical areas must be established. Recent work from our group supports marmoset LIP homology, however, FEF remains to be explored. The first aim of this dissertation was identify and characterize marmoset FEF. Using intracortical microstimulation (ICMS), we restricted marmoset FEF to areas 8a, 45, 6D and 8C, and demonstrated frontal cortical organization consistent with other primates, supporting the use of marmosets for neurophysiological investigations of oculomotor control and attention.

The subsequent aims of this work were to examine the laminar dynamics of LIP and FEF in marmosets completing a target selection task. We observed neurons in both LIP and FEF involved in target selection, with FEF showing a stronger link to motor control. Interestingly, organization in LIP followed the canonical circuit model (CCM), with input in the granular, target selection in supragranular, and output in infragranular layers. In contrast, FEF displayed a unique bilaminar visual input in superficial layers and target selection in deeper layers, resembling recent observations in other frontal areas more than the traditional CCM.

These findings suggest that while models developed in primary sensory areas might apply to some regions of association cortex, their generalizability to frontal areas is limited. This work underscores the marmoset's value as a model for studying attention and cognition, and broadens our knowledge of cortical organization underlying these phenomena.

Keywords: Common Marmoset; Visual Attention; Target Selection; Laminar Electrophysiology; Lateral Intraparietal Area; Frontal Eye Fields; Saccadic Eye Movements

Lay Summary

In our busy visual world, we rapidly scan scenes to focus on important details. This process, attention, is largely governed by two brain areas: the lateral intraparietal area (LIP) and the frontal eye fields (FEF). Our understanding of how neurons in these areas function comes primarily from macaque studies. We know that these regions can be separated into distinct layers, but we know little about how neurons in different layers differ functionally. Uncovering this organization would provide a greater understanding of how the brain directs attention, and generally deepen our understanding of brain organization.

However, due to the many folds in the macaque brain, as in the human brain, it is challenging to study neurons from these different layers simultaneously. Here, the more distantly related, common marmoset monkey, with its smooth brain, presents an opportunity to answer this very question. Now we are able to use long, high-density electrodes to record activity from multiple layers and reconstruct this organization.

However, we first have to determine if marmoset LIP and FEF resemble what we see in other primates. We have previously shown that this is the case for LIP, and in the first project of this thesis, using intracortical microstimulation (ICMS), we show this for FEF.

Having established this similarity, we studied regions as marmosets completed a task where they must quickly look towards a target item presented on a screen while ignoring any distractors. First, we replicated patterns of neural activity observed in macaques for such a target selection task. Interestingly, we found that in LIP, activity is consistent with existing models which suggest there are distinct input, processing, and output layers. However, while FEF showed some similarities, we observed two input layers here and a different layer was responsible for processing than expected.

These findings show that while our current models apply to some brain areas and functions, they may not be entirely generalizable. Our findings show the value of the marmoset for studying the neuroscience of attention, and provides a deeper understanding of how the brain is organized.

Co-Authorship Statement

For all chapters, Janahan Selvanayagam is the primary author. Kevin D Johnston and Stefan Everling are co-authors for **Chapter 2**, **Chapter 3**, and **Chapter 4**. David J Schaeffer and Lauren K Schaeffer are co-authors for **Chapter 2**.

Acknowledgements

Contents

List of Figures

List of Tables

Acronyms

A1 primary auditory cortex

ACC anterior cingulate cortex

ANOVA analysis of variance

auROC area under the receiver operating characteristics curve

BSG brainstem saccade generator

CCM canonical circuit model

CI confidence interval

dFEF dorsomedial frontal eye fields

dlPFC dorsolateral prefrontal cortex

EBN excitatory burst neuron

FEF frontal eye fields

FIT feature integration theory

fMRI functional magnetic resonance imaging

FV frontal ventral visual area

GAM generalized additive model

IBN inhibitory burst neuron

ICMS intracortical microstimulation

IPS intraparietal sulcus

IT inferotemporal cortex

LGN lateral geniculate nucleus

LIP lateral intraparietal area

LLBN long-lead burst neuron

M1 primary motor cortex

MD medial dorsal nucleus of the thalamus

MF movement field

MRI magnetic resonance imaging

MST medial superior temporal area

MT middle temporal visual area

OPN omnipause neuron

PFC prefrontal cortex

PPC posterior parietal cortex

PPRF paramedian pontine reticular formation

PV parvalbumin

RF receptive field

riMLF rostral interstitial nucleus of the medial longitudinal fasciculus

ROC receiver operating characteristics

RT reaction time

SC superior colliculus

SCi intermediate layers of the superior colliculus

SCs superficial layers of the superior colliculus

SEF supplementary eye fields

SNpr substantia nigra *pars reticulata*

SOM somatostatin

SRT saccade reaction time

V1 primary visual area

V4 visual area V4

vFEF ventrolateral frontal eye fields

List of Appendices

Chapter 1

Introduction

We are continuously inundated with far more information than can be processed simultaneously (James, 1890). It is the role of the nervous system to prioritize certain bits of information over others, taking into account external stimulus properties and the internal state of the subject. Within the visual domain, selective visual attention permits preferential processing of behaviourally relevant stimuli, a key component of visually guided behaviour (Moore & Zirnsak, 2017). Shifting the current locus of attention can be achieved both by moving the eyes to look at a particular location and by covertly shifting attention to the periphery without eye movements (Findlay & Gilchrist, 2003). Primates in particular possess foveate retinas permitting high acuity vision at the point of fixation and especially require frequent eye movements to bring features of interest onto the fovea (Bringmann et al., 2018). These eye movements may include reflexive movements such as the vestibulo-ocular reflex and the optokinetic response or voluntary movements such as ocular pursuit movements and perhaps most commonly, saccadic eye movements. Saccades are generally rapid, ballistic movements, which abruptly shift the point of fixation to a new target location (Dodge & Cline, 1901). Humans on average perform 3-4 saccades a second, fixating on points of interest while simultaneously covertly selecting the target of and preparing the motor plan for the upcoming saccade (Fischer & Boch, 1983). This complex operation requires the coordination of several cortical and subcortical brain regions which in part comprise the frontoparietal network (Corbetta, 1998). The lateral intraparietal area (LIP) and the frontal eye fields (FEF) are two critical cortical nodes in the control of saccadic eye movements and visual attention, and have been the focus of extensive investigation in primates. Decades of neurophysiological investigations in the prevailing non-human primate model, the rhesus macaque (*Macaca mulatta*), have provided valuable insight into the the properties of single neurons in these regions as they relate to the control of visual attention and saccadic eye movements (Johnston & Everling, 2011; Paré & Dorris, 2011; Schall & Thompson, 1999). Determining the correspondence between the attention related activity observed here and anatomical properties, such as cortical layer or morphological cell types, would deepen our understanding of the underlying circuits, and how they instantiate such complex functions. However, due to the challenges of conducting laminar investigations in these regions of the macaque cortex, the unique contributions of the distinct cortical laminae of these regions remains unknown, presenting a major obstacle in understanding the underlying local circuits.

In this introductory chapter, I will (1) review the study of saccades and visual attention,

(2) and how the frontoparietal network supports their function with a particular focus on LIP and FEF. (3) I will then review our current understanding of the cortical microcircuit as well as theoretical models for how it may extend to LIP and FEF, and (4) present the common marmoset as a valuable model for empirical investigations of these concepts.

1.1   Saccadic eye movements and visual attention

1.1.1   A brief history of eye movements

The integral nature that saccadic eye movements play in forming a visual percept in our daily lives is well demonstrated in the case of patient A.I (Gilchrist et al., 1998; Gilchrist et al., 1997). A.I., due to extraocular muscle fibrosis, was unable to move their eyes and as such developed a system of performing small head movements resembling those of saccades in amplitude and frequency despite the strain of such frequent movements of the head. Accordingly, there is a long history of interest in the eye, eye movements and vision. Sushruta, in the *Suśrutasaṃhitā*, "Sushruta's Compendium", circa 600 BCE, described detailed opthalmological records and provided accounts of the eye comprised of the five basic elements: earth, fire, air, fluid and void (Loukas et al., 2010; see for translation Sushruta, 1907). Similarly, Empedocles, circa 500 BCE, proposed the eye was crafted of the four elements, and the fire within shone light from the eye permitting vision; this extramission theory of sight was popularized by Plato and Euclid, persisting for centuries (Finger, 2001; Wade, 2010). In the 2nd century CE, moving away from more mystical and metaphysical explanations, Galen provided detailed descriptions of the six extraocular muscles responsible for eye movements and how they operate to move the eyes in two dimensions (Magnus, 1901; Wade, 2010). These works were preserved by the efforts of Islamic scholars such as ibn Is-hâq, who translated them into Arabic books. Subsequently, ibn al-Haytham, referred to as "the father of modern optics", first described an account of vision where light is reflected from objects and passes into one's eyes permitting vision to occur in the brain (Wade, 2010). He also provided detailed accounts of binocular vision and coordinated eye movements (Wade, 2010).

However, it was not until the late 19th century that saccadic eye movements were first described. In *Über Muskelgeräusche des Auges*, "on the muscle noises of the eye", Hering leveraged a technique of applying a rubber tube to the eyelid and "heard a surprisingly strong and whirring roar", which he confirmed corresponded to muscle contractions of the eyes (Hering, 1879). Indeed, when applied to subjects reading text, he noted (Hering, 1879, p137) that this corresponded to a rapid jerking motion of the eye as opposed to a smooth scanning motion as expected by his contemporaries (Cattell, 1900). Javal (1879) made similar observations and termed these quick movements "saccades", derived from the French word *saccader*, meaning "to jerk".

Thirty years later, Edmund Huey (1908) developed the first known eye tracker, using a custom lens attached to a pointer. Following the development of less intrusive eye tracking methods (Dodge & Cline, 1901; Judd et al., 1905), Buswell (1935) examined how individuals viewed a variety of image stimuli. Buswell famously employed art in these experiments, including "The Great Wave off Kanagawa" by Katsushika Hokusai, and reported the locations and durations of fixations and contrasted early vs late fixations. He noted that not all objects in

a scene are fixated and that certain features such as the large wave and the small white mountain were points of interest across subjects. Further, he observed great individual differences in these gaze patterns, or "scan paths", which he indicated for an artist (red trace in Figure 1.1) corresponds to the subject guiding perception based on artistic elements in the image. Buswell also demonstrated that gaze patterns are radically different when subjects are given a task, such as identifying a person looking out of a window in a photo of a tower.

Yarbus (1967) extended these observations by showing scan paths for images of faces and scenes with and without explicit instructions. When presented with a face, such as in the photograph by Semyon Fridlyand, "Girl from the Volga region", a striking triangular pattern of fixations between the eyes and the mouth could be observed, highlighting the unique importance of face stimuli. Yarbus also presented subjects with "They Did Not Expect Him" by Ilya Repin, and assigned a variety of tasks. When tasked with estimating physical characteristics such as age or infer information such as the length of absence of the visitor, subjects directed gaze towards faces to extract information; in contrast, when tasked with estimating the material wealth of the family, gaze was directed to features of the home such as the art and furniture. These observations highlight how bottom-up features such as salient components of scenes or face stimuli as well as top-down features such as task demands can guide perception and attention. This work sets the stage for examining eye movements in the context of visual attention and cognition in general.

1.1.2 Investigating the spatiotemporal components of gaze

With the incorporation of computers in eye tracking, the ease of acquiring precise measurements of saccadic eye movements permitted the computation of saccade metrics such as direction, amplitude, duration, peak velocity and latency. A notable early observation by Bahill (1975) described a tight linear relationship between saccade amplitude and peak velocity (as well as duration), and borrowing from astrophysics, named this the *main sequence relationship* (see also Carpenter, 1988). That this relationship is observed across nearly all contexts demonstrates that while saccade control is complex and may index many cognitive phenomena, the specifics of saccade production itself is under the tight control of oculomotor circuitry (see Chapter 1.2.1) which produces highly stereotyped motor output. This provides an exemplary effector system for the study of cognition.

Of these saccade metrics, saccade direction and amplitude are of interest in examining the "where" and saccade latency for the "when" of the gaze control system (see for review Findlay & Gilchrist, 2003, p75-78). The spatial and temporal components of saccade control are in fact under the control of distinct albeit parallel networks (e.g., see EBNs vs OPNs in Chapter 1.2.2). The pioneering work of Buswell and Yarbus (Buswell, 1935; Yarbus, 1967) for example leverage the study of the spatial components of gaze to gain insight into the functions of the gaze control system. Similarly, examining the temporal components and how they are affected by subtle experimental manipulations, provide valuable insight in to the organization, capacities and limitations of this system. When examining gaze patterns, saccade latency can be measured as the time between saccades (i.e. the intersaccadic interval), though more commonly in an experimental setting, saccade latency is measured as the time between the onset of some event (such as the onset of a visual stimulus) and saccade onset (i.e. the saccade reaction time (SRT), see Figure 1.2). Saccade latency distributions are often broad and positively skewed
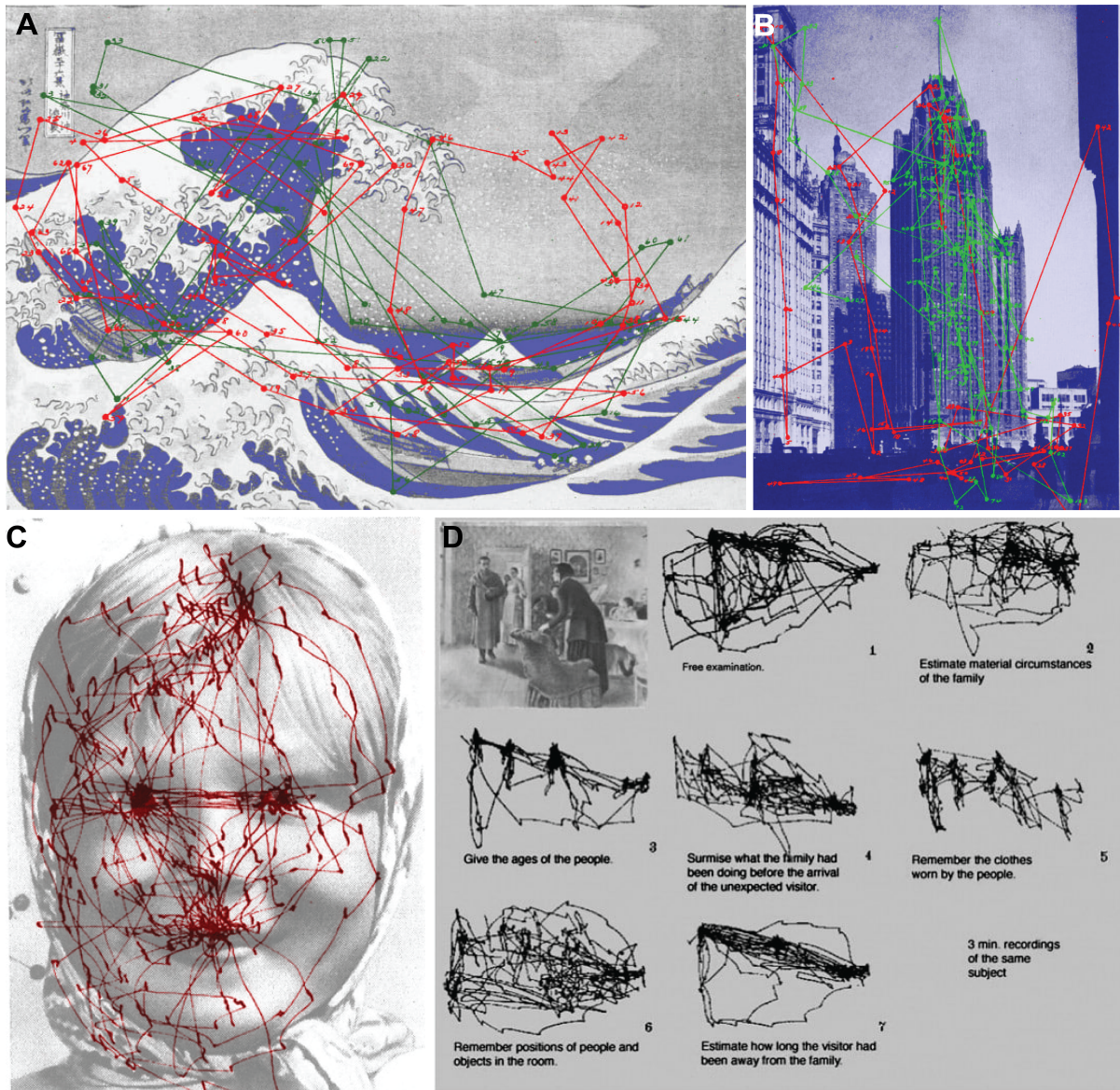
Figure 1.1: Example scan paths. Example scan paths from early recordings by Buswell (1935) (A, B) and Yarbus (1967) (C, D) showing examples of bottom-up (A, C) and top-down (B, D) influences on gaze.
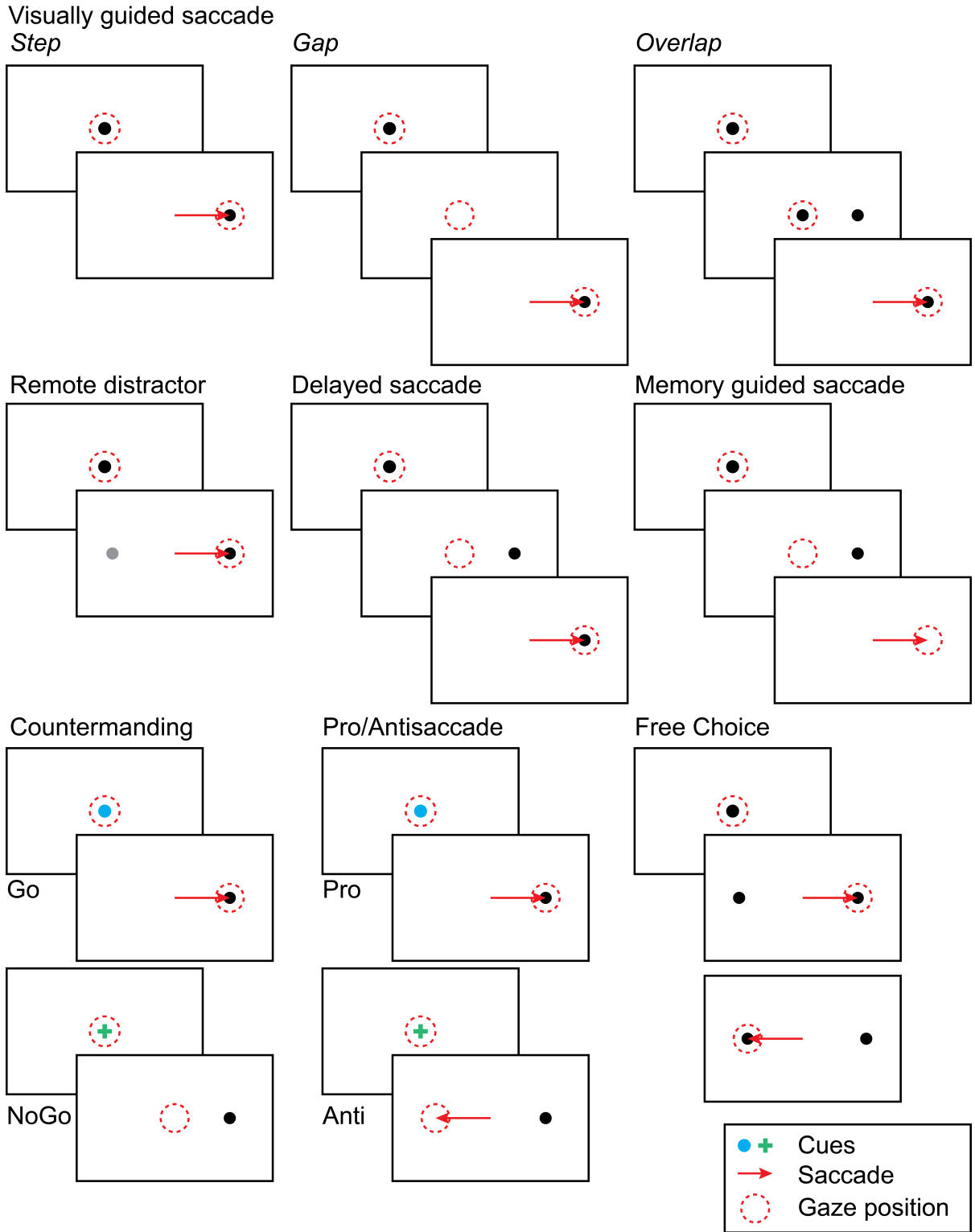
Figure 1.2: Visually guided saccade task schematics.

(Carpenter & Williams, 1995). Some of the variability here can be explained by basic stimulus properties such as luminance, motion, flicker, spatial frequency, etc (e.g., Kalesnykas & Hallett, 1994).

Beyond basic stimulus properties, one experimental manipulation known to affect saccade latency is the "remote distractor effect" (Findlay & Walker, 1999; Walker et al., 1997). Here, the presentation of a distractor stimulus in a distant location from the target stimulus delays the production of saccades to the target (see Figure 1.2). This is thought to reflect competing saccade generation processes for the corresponding vectors resulting from a failure to filter out the irrelevant stimulus when preparing the saccade. Critically, this is not simply a delay resulting from visual processing of a new stimulus as observed from the impact of the spatial and temporal characteristics on remote distractor effect. Namely, the presentation of the distractor must be close in time with the saccade generation to interfere. Additionally, the distractor must be distant from the target or a faciliative effect can be observed. This facilitation can be accounted for by vector averaging for nearby items, highlighting an interesting non-linear spatial interaction underlying saccade generation.

Another manipulation that affects saccade latency is found in the "gap task" (Saslow, 1967). Here subjects are required to fixate on some central stimulus and perform a saccade to a target stimulus flashed in the periphery, but the offset time of the fixation stimulus relative to target onset is manipulated (see Figure 1.2). The fixation stimulus can be removed prior to target onset, producing a "gap" between fixation offset and target onset; fixation offset can be coincident with target onset in a "step"-like manner; or, fixation offset can follow target onset resulting in a temporal "overlap". It is commonly observed that saccade latency is shortened on "gap" trials, termed the "gap effect", and lengthened on "overlap" trials as compared to "step" trials (Saslow, 1967). This faciliative gap effect is thought to result from two factors: the offset of the fixation cue alerts the animal in advance allowing preparation of a saccade and the offset of the fixation disengages the fixation system and disinhibits saccade preparation (Forbes & Klein, 1996). In contrast, "overlap" trials are thought to engage this latter system, delaying saccade production. Gap trials in particular often show a bimodal SRT distribution (Fischer & Boch, 1983), with a shorter latency distribution, known as "express saccades", which are thought to correspond to the most rapid response to a visual stimulus that is physiologically possible, i.e., the sum of minimum afferent and efferent latencies.

Additionally, even when holding the stimuli and task constant, a broad distribution of saccade latencies can be observed across trials. Together, this work suggests that these durations can be considered the sum time of the processes underlying saccade generation (e.g., the LATER model, Carpenter & Williams, 1995): the processing of the visual stimulus, accumulation of evidence for a decision process to select a target, and the preparation and execution of a motor plan for the upcoming saccade. Isolating these selection processes using experimental manipulations provides a way to examine visual attention in saccade paradigms.

1.1.3   The interdependence of saccades and visual attention

Saccadic eye movements and visual attention are tightly linked. During the process of saccade preparation, visual spatial attention benefits can be observed for the future saccade landing position, and these benefits are aligned to the time of saccade execution. Identification and discrimination of stimuli presented at this location are greatly facilitated as compared to those

presented elsewhere (T. Collins & Doré-Mazars, 2006; Peterson et al., 2004). Attention in turn influences the execution of saccades. For example, presenting stimuli or otherwise instructing subjects to attend to a location during saccade execution or late in saccade planning can result in curvature towards or away from the intervening stimulus/location (Doyle & Walker, 2001; Kustov & Robinson, 1996; McPeek & Keller, 2001; Sheliga et al., 1995; van Leeuwen & Belopolsky, 2018).

These observations may potentially be explained by the *premotor theory of attention*, which suggests that although attention shifts can be conducted in the absence of eye movements, they are an obligatory stage in the process of saccade generation and as such rely on the same neural circuits (Rizzolatti et al., 1987). Such a model implies that shifting visual attention across space effectively requires a motor plan analagous to an actual eye movement. Evidence in support of this can be seen in the "meridian crossing effect", wherein an additional cost is incurred for shifting attention across the vertical or horizontal medians (Hughes & Zimba, 1987).

These effects are typically observed when a peripheral cue is presented which redirects attention to the location of that stimulus (see above for a discussion of the remote distractor effect). This abrupt onset acts as a bottom-up or exogenous cue, namely, flicker, which drives attention. In contrast, presenting a central cue which corresponds to a peripheral location may act as a top-down or endogenous cue for directing attention. For example, when presenting an arrow in the center, the direction of which indicates an upcoming peripheral stimulus location, congruent trials where the upcoming stimulus location coincides with the cued location incur a behavioural benefit (e.g., shorter SRTs) whereas incongruent trials results in impaired performance (see Figure 1.3). These findings formalize the early observations by Buswell and Yarbus, as discussed above, regarding the role of bottom-up, exogenous and top-down, endogenous factors in directing gaze and attention.

1.1.4 Visual search

Perhaps the most common paradigm used to investigate visual attention is visual search (see for review, Treisman & Gelade, 1980; Wolfe & Horowitz, 2004). In the visual search paradigm, one or more target stimuli are presented in a multistimulus array and the subject is tasked with identifying the location of a target with an eye movement (see Figure 1.3). Alternatively, the subject may be tasked with identifying the presence of a target that is omitted from the array on a subset of trials. Stimuli may be presented in a concentric ring as subjects fixate some central stimulus and are required to respond with a manual response upon target detection while maintaining fixation or generating a saccade directly to the target. In contrast, in so called "free search" or "foraging" paradigms, stimuli may be presented in a grid and subjects are permitted unrestricted gaze until the target is identified. Many other variations of this task, including delayed saccades, memory guided saccades, antisaccades, etc., have been utilised in the dissection of visual attention and search behaviour (see for examples, Juan et al., 2004; Wen et al., 2023).

An early observation in such visual search paradigms is that search in some stimulus configurations is easy and efficient whereas in others it is not (Wolfe & Horowitz, 2004). It has been observed that when target and distractor stimuli differ on some features such as colour or size, search was extremely efficient. In contrast, if they differed on the basis of certain features such as alphanumeric characters (T's vs L's) or the combination of multiple features such as
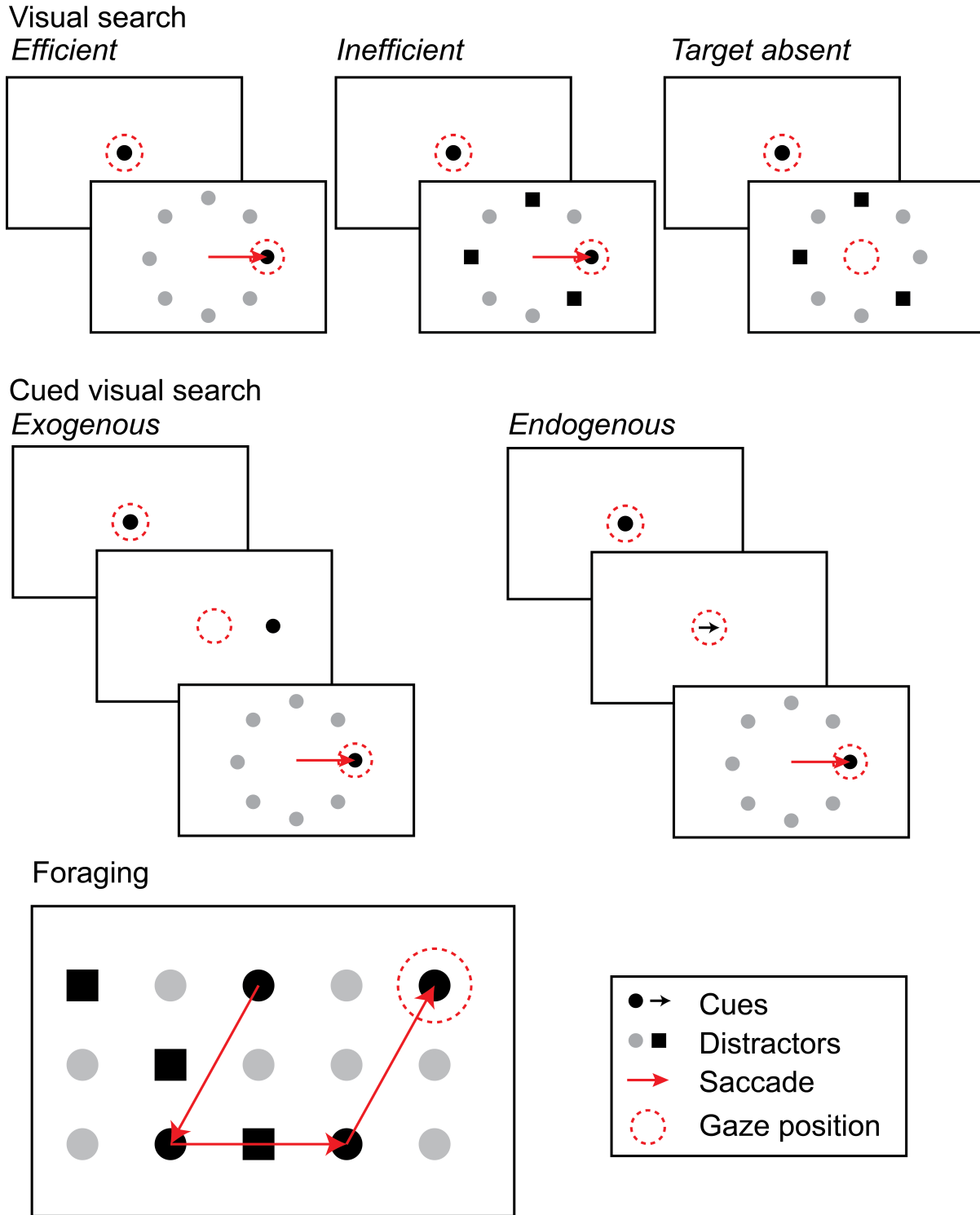
Figure 1.3: Visual search task schematics.

colour and shape (i.e. identifying a red square amidst green squares and red triangles), search is inefficient (see Figure 1.3). The highly influential feature integration theory (FIT) (Treisman & Gelade, 1980) frames these findings under a two-stage architecture wherein some basic features are first extracted in parallel and subsequently these features are "bound" together. Thus efficient search, on the basis of these feature, is parallel; inefficient search, requiring complex features or conjunctions are serial. This can be indexed by the relationship between set-size and reaction times (RTs) on target absent trials (Wolfe & Horowitz, 2004). In parallel search, RTs should be largely invariant to the number of stimuli, whereas in serial search, the subject will need to scan each item individually to correctly reject the presence of a target, meaning RTs scale linearly with the number of distractors.

However, this early model of visual attention has some shortcomings. Critically, it suggests attention results from sequences of filters within the visual hierarchy between early, so-called "pre-attentive" vision and the attentional bottleneck. However, more recent models suggest a separate attention module interacts with the visual system at multiple stages while using similar, often non-overlapping representations to guide attention (Wolfe & Horowitz, 2004; see also, Wolfe, 2021). In this "guided search model", some attributes, termed "guiding features", can be processed efficiently in parallel, to guide attention, and are not always the same as features used in visual processing. Indeed, when examing target-distractor and distractor-distractor dissimilarity, it is clear that the differences required for guidance are much greater in magnitude and sometimes qualitatively different from those required for object classification (Duncan & Humphreys, 1989). Thus, under this framework, it is proposed that there exists in the brain a priority map, which accumulates evidence from a variety of bottom-up, guiding features in parallel, and represents the priority of stimuli across the visual field. Stimuli with the greatest activations are then attended to serially. However, in contrast with FIT, this model suggests guidance is simultaneously parallel and serial, evolves dynamically over time, and interacts with many systems. On the basis of these interactions, this framework can then be extended to incorporate top-down features, such as comparing incoming visual activity with stimulus representations in working memory. Thus, this activation map represents salience, the behavioural relevance or priority of stimuli, in each location in the visual field. Altogether, visual search paradigms offer a powerful way to examine how stimuli are selected from complex visual environments as the target of overt eye movements or covert shifts of attention. The guided search model, built on findings from this paradigm, provides a framework for understanding the interactions between vision, eye movements and attention.

In sum, the long history of studying eye movements and attention using behavioural and psychophysical approaches have provided strong theoretical frameworks for these phenomena. Critically, they suggest these processes are tightly linked; an extreme view of this framework is that covert attentional shifts are in fact oculomotor in nature, whereas a more temperate view suggests these processes are interdependent but distinct (see for review, Corbetta, 1998). The challenges in disentangling these processes highlights the necessity of neurophysiological investigations with high temporal and spatial resolution to uncover the underlying neural circuitry. To this end, in the next section, I will provide an overview of our current understanding of the neural basis of eye movements and attention starting from the muscles and motor neurons controlling the eye to the higher level structures that represent salience and direct visual attention.

1.2   Neural basis of eye movements and visual attention

1.2.1   The oculomotor plant

Eye movements are under the control of three pairs of antagonistic extraocular muscles which allow the rotation of the eye in 3D (see for review, Angelaki, 2011, see Figure 1.4). These muscles are innervated by three cranial nerves: the oculomotor (III), trochlear (IV) and abducens (VI) nerves. The oculomotor nerve innervates the superior rectus, inferior rectus, medial rectus, and inferior oblique muscles, responsible for elevation, depression, adduction and extorsion respectively. The trochlear and abducens nerve innervate the superior oblique and lateral rectus muscles respectively which are responsible for intorsion and abduction respectively. This "oculomotor plant", is well characterized, and in contrast to the skeletomotor system, is highly constrained and stereotyped in its movements. In fact, while the oculomotor plant is capable of free rotation in three dimensions, as outlined by Listing's Law, in the case of voluntary eye movements, the rotation of the eye is restricted to two dimensions (Hepp, 1994). As such, the control of saccadic eye movements relies on premotor neurons responsible for the horizontal and vertical components of the movement found in the paramedian pontine reticular formation (PPRF) and the rostral interstitial nucleus of the medial longitudinal fasciculus (riMLF) respectively (see for review, Cullen and Horn, 2011, see Figure 1.4).

1.2.2   Brainstem saccade generators

In the rostral PPRF, EBNs drive the ipsilateral abducens motor neurons to contract the corresponding lateral rectus muscle and via the inhibitory burst neurons (IBNs) in the caudal PPRF silence the antagonist muscle (i.e. contralateral lateral rectus via the contralateral abducens) (Hikosaka et al., 1978; Hikosaka & Kawakami, 1977; Moschovakis, Scudder, & Highstein, 1991; Moschovakis, Scudder, Highstein, & Warren, 1991; Sasaki & Shimazu, 1981). These neurons are selectively active for horizontal saccades directed to the ipsilateral hemisphere, are tightly coupled in time with saccade onset, and the burst duration, spike count and peak rate encode the saccade duration, amplitude and peak velocity respectively. Another class of neurons, the long-lead burst neurons (LLBNs), resemble EBN in their discharge properties but their saccade-related activity emerges much earlier and have fewer direct projections to cranial nerve motoneurons. Their role in saccade generation may be less direct but rather have a role in saccade initiation and act as a relay between other regions such as the superior colliculus (SC) and EBNs. The final class of brain stem neurons responsible for the control of saccades are OPNs which act as an inhibitory gate to saccades. OPNs tonically inhibit the saccadic burst neurons in PPRF and riMLF, tonically discharging at a constant rate while gaze is fixed and pausing for saccades in all directions (Everling et al., 1998; Horn et al., 1994; Keller, 1974). Indeed the pause is well correlated with saccade duration and stimulation of OPNs results in complete cessation of eye movements (Keller, 1974). Altogether, the oculomotor plant, and the premotor neurons that comprise the brainstem saccade generators (BSGs), form a well characterized and highly constrained effector system for the investigation of higher order cognitive phenomena. Taken together with the obvious role of eye movements in constructing a visual percept and the tight coupling between eye movements and visual attention, this presents an excellent system for the study of attention.

Frontal Eye Fields

Dorsolateral prefrontal cortex

Lateral Intraparietal Area

Primary Visual Cortex

Thalamus

Superior colliculus

rostral interstitial nucleus
of the medial longitudinal
fasciculus

Inferior colliclus

Oculmotor Nerve (CN III)

Trochlear Nerve (CN IV)

Medial longitudinal
fasciculus

Cerebellum

Paramedian pontine
reticular formation

Abducens Nerve (CN VI)

Spinal Cord

superior oblique

superior rectus

lens

retina

iris

macula

pupil

foveal pit

cornea

lateral
rectus

medial
rectus

inferior rectus

inferior oblique

Nasal

Optic Nerve
(CN II)

Figure 1.4: The neural basis of eye movements.

Figure 1.4: *The neural basis of eye movements (continued).* Cortical areas subserving the control of visually guided saccadic eye movements (top) and the brainstem saccade generator (middle). Schematic diagrams of muscles controlling eye movement, with axes of rotation for each muscle (bottom left) and medial saggital view of the eye (bottom right).
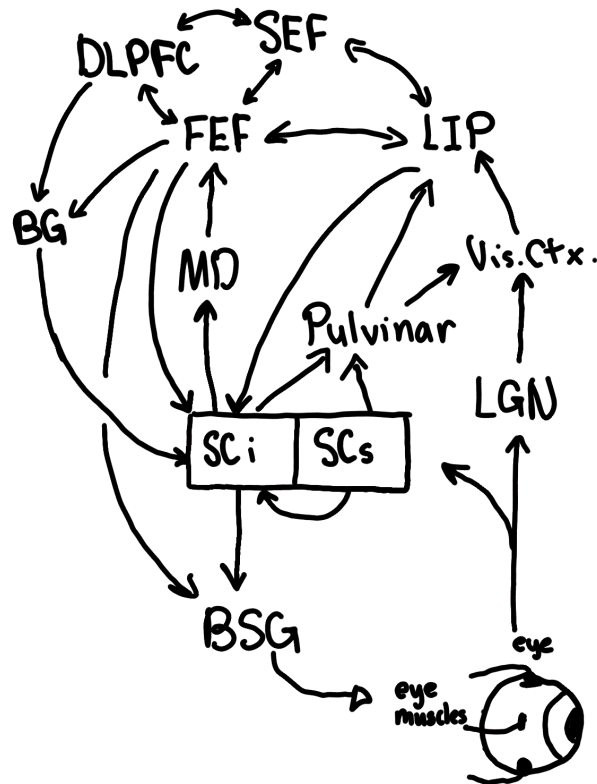
Figure 1.5: Schematic diagram of the frontoparietal network.

While saccades can be generated in complete darkness, generally they are elicited in response to a stimulus that attracts attention. The incoming visual information has to be integrated with the expectations and goals of the observer to generate an appropriate saccade vector. This is largely under the control of the SC and, in particular for voluntary eye movements, FEF; these regions are also tightly interconnected with LIP, which modulates their activity and plays a role in the control of eye movements and attention (see for review Johnston & Everling, 2008; McDowell et al., 2008). In this section, I will outline the contributions of these three regions to the control of eye movements and attention, focusing on neurophysiological evidence from single neuron investigations in the macaque, and discuss their interactions.

1.2.3   Superior colliculus

The SC is ideally situated for its role in guiding eye movements and attention as it receives direct retinotectal afferents and can directly drive the BSGs (Harting, 1977; Moschovakis et al., 1988; Rodgers et al., 2006). In fact, the primate SC receives a broad range of sensory

inputs and can evoke an orienting response recruiting not only the eyes but also the neck and shoulder muscles and even arm movements (Corneil et al., 2008; Pruszynski et al., 2010). The mammalian SC can be subdivided into seven anatomically distinct layers. Of these, the *stratum griseum superficiale* and *stratum opticum* form the superficial layers, SCs, which are primarily concerned with vision and the *stratum griseum intermediale* and the *stratum album intermediale* form the intermediate layers, SCi, which are concerned with multisensory and motor representations (Drager & Hubel, 1975a; Drager & Hubel, 1975b; Meredith & Stein, 1983; Mohler & Wurtz, 1976; Robinson, 1972; Wurtz & Mohler, 1976; Wurtz & Goldberg, 1971). These layers of the SC have a well understood organization representing the visual world continuously across its surface in retinocentric coordinates, i.e., a retinotopic representation. Each SC represents the contralateral hemifield of visual space with the foveal to eccentric visual field being represented along the rostro-caudal axis and the upper to lower visual field being represented along the medial-lateral axis (Savjani et al., 2018). As such, many SCs and SCi neurons respond to visual stimuli presented in a location in space relative to the retina corresponding to the neurons location in this retinotopic map and many SCi neurons increase their discharge activity preceding saccades with an amplitude and direction corresponding to the same retinocentric coordinates.

Decades of anatomical and neurophysiological investigations support the organization of the SC and the separation of function across depth. SCs receives visual inputs from the retina and V1 as mentioned above. Although in primates the geniculostriatal system (i.e. retina to the lateral geniculate nucleus (LGN) to the primary visual area (V1)) supersedes the retinotectal system in terms of volume of projections (8:1 in primates as compared to 1:3 in rodents, Schiller and Malpeli, 1977), the SC still plays a major role in visual processing and its visual activity persists even following lesions of visual cortex (but not in the event of transient LGN inactivation, see Katz et al., 2023). SCs neurons have a rapid, transient response to visual stimulus onset, though deeper layer SCs neurons may also have a more sustained visual response (Goldberg & Wurtz, 1972a, 1972b; Li & Basso, 2008; Mays & Sparks, 1980; McPeek & Keller, 2002; Sparks & Mays, 1980). The activity of these neurons are largely feature agnostic, but rather signify stimulus intensity, i.e., the sensory qualities of a stimulus that make it distinct from the background (Li & Basso, 2008). As such, SCs neurons form a representation aggregating across visual feature maps to indicate the location of the highest intensity stimuli in retinocentric space, reflecting the bottom-up processes of visual attention. SCs neurons in turn modulate cortical visual activity via substantial projections back to striate and extrastriate visual cortex as well as posterior parietal cortex (PPC) through LGN and the pulvinar nucleus (Berman & Wurtz, 2008). SCs also has intrinsic connections to SCi premotor neurons which permits rapid control for visually guided behaviour even in the absence of cortical involvement (Fecteau & Munoz, 2006; Isa, 2002; Isa et al., 1998). Via these projections, the SC can bias visual processing and ultimately direct gaze to the pertinent stimulus in a scene.

In contrast, SCi primarily receives corticotectal input from FEF, LIP, the supplementary eye fields (SEF), the dorsolateral prefrontal cortex (dlPFC), and the anterior cingulate cortex (ACC) (Fries, 1984; Lock et al., 2003). Indeed when visual cortex is inactivated, visual activity in SCi is completely abolished (Schiller et al., 1974). This region also receives blanket tonic inhibitory nigrotectal input; this is under the indirect control of FEF and SEF which project to the caudate nucleus which in turn inhibits the the substantia nigra *pars reticulata* (SNpr), the source of this inhibitory input (see for review, Hikosaka et al., 2000). This pathway provides

another system, alongside OPNs, which permits gating of saccade initiation. As with deeper SCs neurons, SCi neurons have sustained visual responses and critically many increase their discharge activity prior to a saccade (Mohler & Wurtz, 1976; Sparks & Mays, 1980; Wurtz & Goldberg, 1972) and via projections to LLBNs in PPRF and riMLF, these neurons can program saccades directly (Moschovakis et al., 1988; Rodgers et al., 2006; Sparks, 2002; as well as head movements, Corneil et al., 2008; Corneil et al., 2004). As mentioned above, neurons with saccade-related activity are generally tuned to the amplitude and direction of the saccade corresponding to a specific location in retinocentric space known as a movement field (MF), though some neurons have open-ended MFs, i.e., the neuron responds to all saccades in a particular direction of atleast a certain minimum amplitude, but lack a distal border. Accordingly, intracortical microstimulation (ICMS) applied to SC elicits saccadic eye movements of a consistent amplitude and direction, and prolonged stimulation results in "staircases" of saccades each with the same vector (Donders, 1872; Robinson, 1972). These observations are consistent with SCi possessing a retinocentric saccade motor map. Interestingly, temporary inactivation of a portion of this map does not abolish saccades with the corresponding vector, as the average activity of the neighbouring ring of neurons function together to produce a vector average to guide saccades to this location (Lee et al., 1988). Indeed simultaneous stimulation of multiple sites in SC results in an intensity weighted, average vector for the elicited saccade (Robinson, 1972). In particular, neurons in the rostral SC have foveal representations and in SCi, these neurons are related to very small saccadic eye movements (i.e., microsaccades) and fixations. In fact, stimulation of the rostral pole delays saccade initiation and pharmacological inactivation of the area impairs saccade suppression (Munoz et al., 1996; Munoz & Wurtz, 1993). As mentioned above, SCi premotor neurons receive input from SCs and allow for rapid orienting responses. Indeed neural correlates of express saccades (see Chapter 1.1), the fastest possible saccadic eye movements for a visual stimulus, best observed in the "gap task", can be seen in SCi neurons. These neurons are disinhibited by the release of fixation neurons following the offset of the fixation stimulus and the onset of the target stimulus drives neurons representing the appropriate saccade vector (Dorris & Munoz, 1995; Dorris et al., 1997).

In addition to projections to the BSGs, SCi also relays back to FEF and LIP via the medial dorsal nucleus of the thalamus (MD) and pulvinar respectively (Sommer & Wurtz, 2004). These projections feed back to these regions and can convey an efference copy of the saccade motor command, i.e., corollary discharge (Sommer & Wurtz, 2008). This process is thought to assist in updating the visual field after the saccade to maintain stability following a rapid shift in gaze. Finally, evidence suggests SCi has a lateral inhibitory network wherein neurons with distinct spatial tuning inhibit each other to enforce a winner-takes-all mechanism, ensuring the activity of this structure represents a singular locus of gaze/visual attention. Such a framework is necessary for SCi to act as a saliency map, integrating the bottom-up information of a saliency map and the top-down signals relating to the behavioural goals of the animal. Indeed, in a visual search task, discharge activity of SCi neurons evolve to discriminate between target and distractor stimuli prior to the saccade signalling a target selection process (McPeek & Keller, 2002; Shen et al., 2011). Further, SCi inactivation impairs target selection and stimulation biases selection to stimuli in the contralateral hemifield (McPeek & Keller, 2004).

In sum, the anatomical positioning of the SC between early visual processing and direct access to the saccade control machinery as well as its extensive feedback to many stages of

the cortical visual processing hierarchy makes it an ideal structure for the control of saccadic eye movements and visual attention. The functional organization of the SC is relatively well understood: superficial layers represent the bottom up processes of saliency, whereas the intermediate layers are responsible for visuomotor integration and the top-down control of visual attention. While much remains to be uncovered about the organization of the SC, our extensive knowledge of this region provides a framework for investigating other nodes of this network with which the SC shares many properties.

1.2.4   Lateral intraparietal area

The lateral intraparietal area, found in the lateral bank of the intraparietal sulcus (IPS) in the macaque, is an evolutionarily more recent addition to the oculomotor network as it has no clear homologue in non-primate mammals, and appears to be less extensively developed in primates phylogenetically more distant from humans; that is LIP in platyrrhine primates, i.e. "New world" monkeys (e.g., owl monkeys, squirrel monkeys, marmoset monkeys) and pro-simians (e.g., galagos), appear to have less dense projections to the SC and FEF, whereas catarrhine primates, (i.e. "Old world" monkeys and hominoids), demonstrate strong innervation of these regions (Andersen et al., 1985; C. E. Collins et al., 2005; Krubitzer & Kaas, 1990; see also Stepniewska et al., 2007; but see Baldwin & Kaas, 2012; Stepniewska et al., 2016).

As a node of the oculomotor and visual attention network that is largely exclusive to primates, LIP has garnered much interest from neurophysiologists. Mountcastle and colleagues (Lynch et al., 1977; Yin & Mountcastle, 1977) first described pre-saccadic activity in area 7 neurons, which in part included LIP neurons. Subsequently, Andersen and colleagues (1987) narrowed the source of this activity to the area that later became known as LIP (see also Barash et al., 1991a, 1991b); these neurons demonstrated significant visual and saccade-related activity. Additionally, early ICMS experiments have shown that stimulation in the PPC can evoke skeletomotor movements, eye blinks and eye movements (Shibutani et al., 1984). Thier and Andersen (1996; 1998) showed that the region where saccades could be elicited is restricted to LIP; saccades elicited here are either fixed-vector (i.e. consistent direction and amplitude regarless of the initial eye position) or convergent (i.e. saccades converged to one location in space). As such, in primates, and particularly catarrhine primates, LIP can be defined on the basis of its cytoarchitectural properties, its anatomical connections, the properties of ICMS evoked eye movements, and the characteristic visual and saccade-related responses of single neurons in this region.

Many LIP neurons exhibit visual responses with similar properties to SC and FEF neurons, representing salience in a retinocentric manner. Unlike SC, LIP does not possess a smooth retinotopy: adjacent neurons represent overlapping RF and saccade vectors and nearby neurons tend to represent nearby locations in retinocentric space but frequent interruptions can be observed (Blatt et al., 1990; Thier & Andersen, 1996). Also, although the majority of RFs for visual LIP neurons are in the contralateral hemifield, they can be bilateral or entirely in the ipsilateral hemifield. LIP RFs also increase in radius with eccentricity, and can often times be open-ended. Generally, visual activity of LIP neurons can be modulated by colour, contrast and movement particularly when these features produce high contrast with background, suggesting that LIP neurons encode stimulus intensity (Shadlen & Newsome, 1996). However, LIP neurons do not possess feature selectivity, but rather reflect behavioural relevance and any apparent

feature selectivity is better explained by exogenous or endogenous salience or overtraining.

Consistent with behaviour discussed above, in response to the flickering on of an intense "popout" stimulus, LIP neurons transiently increase their activity for the rapid onset of this distracting stimulus; this effect is attenuated in the case of behaviourally irrelevant stimuli (Gottlieb et al., 1998; Ipata et al., 2006; Powell & Goldberg, 2000). LIP neurons do not modulate their activity when a behaviourally irrelevant stimulus that is already present is brought into its RF by an eye movement, but they do so when the stimulus is made relevant (Gottlieb et al., 1998). These observations demonstrate the role of LIP in representing behavioural relevance; it has been shown that LIP neurons, in addition to representing stimulus dimensions such as motion coherence, also represent associated reward value and decision processes (Rorie et al., 2010).

Although the visual response properties of LIP neurons resemble FEF and SC, and as in these areas, neurons significantly increase their discharge activity prior to saccades (Barash et al., 1991a, 1991b), the pre-saccadic activity of this region has since been shown to be more closely correlated with the presence of visual stimuli. Accordingly, this activity is greatly reduced for saccades made in the absence of visual stimuli (Ferraina et al., 2002; Gottlieb & Goldberg, 1999; Paré & Wurtz, 1997, 2001) or in the presence of multiple visual stimuli (Balan et al., 2008; Thomas & Paré, 2007). In contrast, this activity is not well correlated with SRTs (Bisley & Goldberg, 2003; Bisley et al., 2011; Goldberg et al., 2002; Kusunoki et al., 2000). Additionally, relatively larger current intensities are required for saccades to be elicited here via ICMS (Shibutani et al., 1984; Thier & Andersen, 1998), and lesion to this area does not impair saccade production, but rather biases saccades to the ipsilateral field in the presence of competing stimuli (Wardak et al., 2002, 2004). Indeed, although corticopontine projections are observed from LIP, these neurons target more dorsal aspects of the brainstem; LIP does not project directly to the BSGs (May & Andersen, 1986). This is in contrast with FEF and SC, wherein direct projections to the BSGs are observed, low current stimulation reliably elicits saccades, lesions significantly impair saccade production, and the discharge activity of saccade-related neurons correlates well with saccade occurence (see Chapters 1.2.3 and 1.2.5).

A classic task for examining the necessity of a region for saccade production is the countermanding task (see Figure 1.2, Hanes et al., 1995), in which subjects are tasked with performing visually guided saccades but on a subset of trials, when presented with a stop cue, must suppress the saccade and maintain central fixation. In FEF or SC, saccade-related neurons reliably signal that a saccade must be cancelled instead of executed well prior to the saccade (Hanes et al., 1998; Paré & Hanes, 2003), whereas LIP neurons generally showed changes in activity after the saccade was cancelled or not at all (Brunamonti & Pare, 2023). Similar observations can be made for the antisaccade task, for which LIP neurons better represent the visual cue than the saccade target on antisaccade trials (Gottlieb & Goldberg, 1999). However, in a delayed antisaccade task, LIP neurons evolve to signal the saccade direction, suggesting this information is fed back to LIP from other areas (Zhang & Barash, 2000, 2004).

Bisley and Goldberg (2003) examined this discrepancy further by investigating the activity of LIP neurons corresponding to the spatiotemporal dynamics of covert attentional shifts in a contrast sensitivity task. Here the animal is presented with a peripheral cue that is the target of a saccade, the location of which must be maintained in working memory during a delay epoch. During this delay, a probe is presented at the target location or elsewhere, the identity of which indicates whether the saccade must be performed or cancelled. On a subset of trials, a

distractor is flashed at the target location or elsewhere. Consistent with reports cited above, the presence of a distractor transiently draws the focus of attention, and accordingly the activity of LIP neurons, to its location, before it returns to the location of the previously planned saccade. Interestingly, both the distractor and planned saccade show a similar facilitation in the processing of the probe: the perceptual advantage is the same regardless of the reason for the attentional shift. This is true even though the absolute value of LIP activity was different for these different stimulus conditions. Indeed while the absolute activity of LIP neurons does not predict the locus of attention, the activity of LIP neurons together represents a saliency map, where the highest activity reflects the locus of attention. This relative encoding allows more flexible representations of attention across task contexts. Additionally, these results show that during the delay period, the activity of LIP neurons reflects the locus of attention and not the motor plan for the upcoming saccade, when there is conflict between the two. Thus, as there is generally a strong correlation between attended objects and saccade targets, the activity of LIP neurons can reflect the motor plan for saccades in most contexts. However, when these are dissociated, LIP flexibly integrates additional information and no longer faithfully represents oculomotor plans; it must then be ignored by the oculomotor system. It is worth noting however that recent evidence shows that LIP inactivation has a greater impact on biasing free choice tasks employing saccades as compared to those using reach, suggesting there is still some effector specificity to this region (Christopoulos et al., 2018). Altogether, this evidence suggests LIP is neither necessary nor sufficient for the generation of saccades but does represent the locus of attention as the highest activity point in a saliency map, albeit more weakly in non-oculomotor contexts.

As discussed above (see Chapter 1.1), overt shifting of perceptual resources in the visual system is generally accomplished by saccades, however this process is paired with covert shifts of attention responsible for saccade target selection. As with the psychophysical visual attention research, how the activity of LIP neurons relates to these covert processes has been most extensively investigated using the visual search paradigm. Indeed pharmacological inactivation of LIP impairs visual search performance (i.e. an increase in RTs for contralateral targets, Wardak et al., 2002) and these impairments are greater for difficult search than for efficient search (Wardak et al., 2004). LIP neurons discriminate reliably between target and distractor stimuli presented in their receptive fields (Ipata et al., 2006; Mirpour et al., 2009; Schwemmer et al., 2015; Thomas & Paré, 2007) and this activity scales with the number of stimuli (i.e. set-size, Balan et al., 2008; Thomas & Paré, 2007). This discrimination is mediated by both facilitation for target and suppression for distractor stimuli, consistent with a lateral inhibitory network as suggested above for SC (see Chapter 1.2.3). Consistent with this, examining the activity of LIP neurons for target-present and target-absent search arrays reveals separable target-facilitation and distractor-suppression effects in neurons (Nishida et al., 2013). LIP neurons primarily exhibit target-facilitation exclusively or both target-facilitation and distractor-suppression whereas they rarely exhibit distractor-suppression alone. Additionally, distractor-suppression components tended to follow target-facilitation. These observations are consistent with a lateral inhibitory network and by extension a winner-takes-all mechanism for selecting the locus of attention from a saliency map (Zénon et al., 2009).

Altogether, we see that LIP, similar to SC and FEF, has visual responses, and these responses tend to represent salience. However, unlike these regions with which it is tightly interconnected, LIP neurons are not strictly involved in saccade generation despite their activ-

ity reflecting motor plans in some contexts, and the observation of some oculomotor effector specificity. The representation of salience across the visual field however permits LIP to represent the most important stimuli in a scene, and dynamically update this representation with incoming top-down and bottom-up information, from which the focus of attention can be selected. Such a representation is entirely consistent with models, such as the guided search model, described above.

1.2.5   Frontal eye fields

Described originally by Ferrier (1875) as a cortical area in macaque monkeys where electrical stimulation elicited contralateral eye and head movements, FEF in macaques and humans are now increasingly regarded as not only a motor area for saccades and head movements but also as a critical region for visual processing and the deployment of overt and covert spatial attention (Bruce et al., 1985; Mohler et al., 1973; Schall, 1991).

Over the past 40 years, most of our knowledge regarding the neural processes in the FEF has come from experiments in awake behaving macaque monkeys. In these Old-World primates, FEF is defined as an area within the rostral bank and fundus of the arcuate sulcus from which ICMS evokes saccades at low current intensities ($< 50\mu A$). Such experiments have also revealed a topography of saccade amplitudes in macaque FEF. Small saccades are evoked by stimulation of ventrolateral frontal eye fields (vFEF), spanning areas 45b and 8Av, and larger saccades from dorsomedial frontal eye fields (dFEF), spanning area 8Ad (Bruce et al., 1985; Robinson & Fuchs, 1969). As with SC, FEF ICMS also elicits fixed vector saccadic eye movements, with prolonged stimulation resulting in staircases of saccades and simultaneous stimulation resulting in vector averaging (Bruce et al., 1985; Robinson & Fuchs, 1969). ICMS applied to dFEF often additionally elicits neck and shoulder responses and combined contralateral eye and head movements in unrestrained animals (Elsley et al., 2007; Knight & Fuchs, 2007), corresponding to a larger orienting response, resembling observations in the SC. In humans, Foerster (1926) observed a similar organization when examining eye and head movements evoked by epileptic seizures; he referred to these regions as the frontal eye fields (*frontales Augenfelds*) and the frontal adversive field (*frontales Adversivsfeld*) respectively. Interestingly, ICMS of FEF below saccade thresholds in a change detection task can facilitate performance in spatially specific manner (Moore & Armstrong, 2003; Moore & Fallah, 2004). Further experiments revealed these attentional affects may be mediated by feedback projections to earlier visual areas such as visual area V4 (V4), in the ventral visual stream, known to be modulated strongly by attention (Moran & Desimone, 1985); ICMS of FEF resulted in modulation of spatially overlapping V4 neurons (Armstrong et al., 2006; Armstrong & Moore, 2007; Moore & Armstrong, 2003). ICMS at these levels are also able to evoke head movements without a saccade (Corneil et al., 2010). Such observations lend support to a premotor theory of attention.

However, the lesion of FEF alone does not remove the ability of a monkey to perform saccades permanently; transient deficits are observed which are rapidly recovered (Schiller et al., 1980). Yet deficits can still be observed in more cognitively difficult saccade paradigms such as memory guided saccades or antisaccades following lesion (Deng et al., 1986; Keller et al., 2008; Munoz & Everling, 2004) and cryogenic inactivation (Peel et al., 2021). In contrast, joint lesion of SC and FEF permanently abolishes saccade generation (Schiller et al., 1980).

This is because FEF possesses parallel channels to saccade generation: a direct pathway to the BSGs and an indirect pathway via SC (Segraves, 1992).

FEF neurons exhibit more diverse response patterns than merely pre-saccadic activity. In general, FEF neurons may respond following the onset of a visual stimulus (visual), preceding the onset of a saccade (motor[1]) or both (visuomotor) (Bruce & Goldberg, 1985) and are directly interconnected with other visual and oculomotor regions (Barone et al., 2000; Huerta et al., 1986, 1987; Stanton et al., 1988). Visual activity in FEF also follows the gross retinotopic organization observed following ICMS, with peripheral and foveal visual field representations being observed in dFEF and vFEF respectively (Bruce & Goldberg, 1985). These observations are similar to what can be observed in the SC, though the topography of FEF is much coarser. Nevertheless, the patterns of projections to and from FEF with other retinotopic visual areas reflect this organization. In the macaque, Schall and colleagues (1995) showed that retinotopically organized areas such as LIP, the middle temporal visual area (MT) and V4 project topographically on to FEF with dFEF receiving afferents from regions of these areas corresponding to peripheral visual field representations and vFEF corresponding to foveal visual field afferents. Further, the vFEF is the primary target of temporal cortical regions involved in foveal vision and form recognition such as inferotemporal cortex (IT) (Bullier et al., 1996). Thus, FEF's engagement in visual processing and oculomotor production make it an ideal structure for the investigation of visual attention.

As with LIP, the role of FEF in visual attention has been extensively investigated using the visual search paradigm. In this task, single neurons in FEF have been shown to have an initially indiscriminate visual response which evolves to discriminate between targets and distractors; this results in an increased response to targets in their receptive fields and a supressed response for distractors before the saccade is made (Schall & Hanes, 1993; Schall, Hanes, et al., 1995; Thompson et al., 1996). Lesions to FEF result in impairments in visual search paradigms (Schiller & Chou, 2000; van der Steen et al., 1986; Wardak et al., 2006) and, as mentioned above, ICMS in FEF facilitates covert attention. This process of target selection is dissociable from saccade generation as this activity has been demonstrated to be modulated by visual similarity to target and target history (Bichot & Schall, 1999) and can still be observed in the absence of a saccade or when the response is made manually (Monosov & Thompson, 2009; Schall, 2004; Thompson et al., 2005; Thompson et al., 1997). Additionally, increases in discharge activity can be observed for when a cue indicates a target may appear within that neuron's receptive field (Monosov & Thompson, 2009) even in the absence of any stimuli within the receptive field (Zhou & Thompson, 2009), highlighting the role of FEF as a source of a top-down spatial attention signal.

Thus, FEF is causally implicated in but not necessary for saccade generation. FEF additionally represents salient locations in retinocentric coordinates allowing it to select the target of upcoming covert and overt shifts of attention. It does so even in the absence of visual stimuli or oculomotor responses. It would seem then that there is a high degree of overlap in the visual, motor and attention related functions of SC, LIP and FEF neurons. In the following section, I describe the differences and interactions between these structures and the insights

---

[1]Note that 'motor' here does not refer to motor neurons in the conventional sense, which for eye movements are the oculomotor neurons in the cranial nerves. Rather, this is a convention referring to neurons with premotor activity that can drive eye movements.

these provide for current theories of attenton.

1.2.6   The frontoparietal network and theories of attention

Altogether, the muscular and neural circuitry underlying saccade production is well characterized, and the structure and function of the SC, a major controller of covert and overt orienting responses, has been extensively investigated. The SC synthesizes both bottom-up information from the retina and early visual cortex, as well as top-down signals from a variety of cortical regions to direct eye movements and visual attention to behaviourally relevent stimuli in a scene. Two major co-conspirators of this function are LIP and FEF, which both play overlapping but distinct roles in the flexible control of saccadic eye movements and visual attention. LIP neurons more closely represent saliency and decision making processes whereas FEF neurons are involved in covert and overt attentional shifts.

Indeed this delineation of function is supported by investigations contrasting the differential effects of LIP and FEF inactivation. LIP inactivation prolongs SRTs for contralateral targets in the presence of distractors, which scales with task difficulty, but does not affect saccade metrics otherwise (Wardak et al., 2002, 2004). In contrast, FEF inactivation induced massive saccade deficits which also did not scale with task difficulty in visual search paradigms (Wardak et al., 2012; Wardak et al., 2006; c.f. Peel et al., 2021). These findings demonstrate a role for LIP in salience representation and attentional selection whereas FEF represents the locus of attention and controls attentional shifts. While the properties of single neurons in these regions underlying these processes have been well investigated in visual search paradigms, much remains to be known about how these discharge properties map on to anatomical neuronal features such as cell types and cortical layers. Insights into this organization would prove valuable for evaluating current models of attention.

One approach for examining these anatomical features has been leveraging the known laminar distribution of different populations of projecting neurons. While reciprocal connections with LIP are found predominantly in supragranular layers, FEF neurons projecting to the SC are found almost exclusively in layer 5 (Fries, 1984; Pouget et al., 2009; Sommer & Wurtz, 2001). One approach for disentangling these features leverages antidromic identification. In these experiments, extracellularly recorded neurons from one region are classified as having projections to some target area via ICMS in the target area and antidromically stimulating (i.e. "back-firing") the collaterals of these neurons (Humphrey & Schmidt, 1990; Lemon, 1984). These neurons can be confirmed as being antidromically stimulated (as opposed to by orthodromic or polysynaptic means) on the basis of the latency of the elicited spike, the variability in this latency, and a collision test. A collision test is where ICMS is triggered by the recorded neuron's spiking activity: for an antidromically identified neuron, the resulting orthodromic and antidromic spikes should "collide" and cancel out, preventing the stimulation from eliciting a spike. This technique simultaneously identifies the cell type (cortical projection neurons are obligatorily pyramidal neurons) and a target region of its collaterals. This indirectly provides some insight into the laminar organization as well due to the known biases of certain projection patterns as mentioned above i.e., the superficial vs deep bias for corticocortical vs corticotectal projecting neurons. Using this technique a series of experiments by Pare, Wurtz and colleagues (Everling & Munoz, 2000; Ferraina et al., 2002; Paré & Wurtz, 1997, 2001; Sommer & Wurtz, 2001) have identified the response properties of neurons projecting between

FEF, LIP and the SC. They observed that while visual and motor neurons can be identified in all populations, corticocortical neurons were more likely to have stimulus-related responses whereas corticotectal neurons were more likely to have motor-related responses.

In sum, a major theory of visual attention suggests that the overt control of eye movements and the covert deployement of visual attention are inextricably linked. However, contrasting the response properties of LIP and FEF neurons, and the outputs of these regions to each other and the SC, suggests they may be distinct but interdependent processes. This latter view might be supported by interlaminar differences consistent with frameworks such as the canonical circuit model (CCM). Next, I will summarize the CCM as it was first described and discuss how it may extend to LIP and FEF.

1.3   The canonical circuit: Primary visual cortex and beyond

The six-layered mammalian neocortex provides a widely accepted framework with which to describe anatomical and physiological cortical features (Douglas & Martin, 2004). Since its earliest description, the lamination of cortex has prompted questions regarding its function. Application of Golgi staining, detailed histological analysis and electrophysiological mapping allowed pioneering neurophysiologists and anatomists to describe many laminar specific projection patterns of cortical neurons. A general organizing principle of cortex was proposed: superficial cortical layers received and processed input whereas deeper layers had corticofugal outputs. The sophistication of laminar organization could truly be appreciated with the advent of retrograde tracers, which were rapidly employed in the study of many cortical areas across a number of species. These observations outlined that all aspects of cortical organization: inputs, intrinsic connections, and outputs, were structured with respect to lamination.

An early functional model of these anatomical patterns was proposed by Gilbert and Wiesel (C. D. Gilbert, 1983; C. D. Gilbert & Wiesel, 1983) on the basis of intracellular recordings and retrograde tracers employed in cat area 17 (i.e. V1). In this model, granular layer IV receives visual afferents from the thalamus, which then feeds forward to supragranular layers II/III. These layers project to infragranular layers V then VI and feeds back to layer IV. It is worth noting that such a model only accounts for interlaminar excitatory projections, which are mediated exclusively by spiny, pyramidal neurons, and discounts the contributions of intralaminar projections and of other cell types. Indeed many inter- and intralaminar projections are mediated by a diverse population of spiny and aspiny interneurons (Binzegger et al., 2004; Douglas & Martin, 1991).

Incorporating these observations, the CCM is built on the idea that there exists a fundamental computational unit, characterized by strong intralaminar connections and weak interlaminar ones, that is iterated across and subserves functions in all areas of cerebral cortex. This model was devised by Douglas and Martin following their observations in cat visual cortex (areas 17 and 18) in 1991. They observed that supragranular excitation was driven polysynaptically from the thalamus and not directly, and that this excitation was maintained by strong intralaminar connections. This excitation is regulated by intra- and interlaminar inhibitory influences, which are also driven by thalamocortical afferents. Also, they observed a fast and slow phase of inhibition mediated by $GABA_A$ and $GABA_B$ receptors respectively, with the former being more present in deeper layers. Taking together these observations as well as anatomical and

physiological observations made above, the CCM was born. This has since been extended to multiple cortical regions and species, rodent barrel cortex, including tree shrew striate cortex, monkey areas V1, primary auditory cortex (A1) and primary motor cortex (M1) (e.g., Anderson et al., 1993; Ghosh & Porter, 1988; Ojima et al., 1992; Usrey & Fitzpatrick, 1996; see for review, Douglas & Martin, 2004; Swadlow, 2002).

A quantitative analysis of synapses from a 3d reconstruction of neurons from cat area 17 recapitulates the feed-forward cortical loop orginating in layer IV described above (Binzegger et al., 2004). However, this only accounted for a fifth of the asymmetric synapses between excitatory neurons. A large portion of these synapses are in fact involved in recurrent, self-innervation of layers. A high degree of intralaminar connectivity is also observed in synapses between inhibitory neurons as well as between inhibitory and excitatory neurons. Surprisingly, thalamic afferents only accounted for a small proportion of synapses in layer IV, despite being a major driver of the activity in this region. This highlights the heterogeneity of synaptic weights and the sometimes counterintuitive importance of anatomical connection density; understanding the importance of these connections necessitates neurophysiological investigations *in vivo*. Additionally, these observations highlight the importance of feedforward inhibitory circuits. Such circuits are described in rodent barrel cortex (Swadlow, 2002), a region of primary somatosensory cortex representing deflections of individual whiskers on the snout. Here, inhibitory interneurons such as parvalbumin (PV) and somatostatin (SOM) expressing interneurons, receive largely indiscriminate thalamic input either directly or indirectly via local excitatory neurons. This then serves to inhibit subsequent thalamocortical input and regulate the excitation of excitatory neurons enhancing the contrast and precision of their activity.

Altogether these findings in primary cortical areas provide a framework for investigating the laminar contributions of higher order areas such as LIP and FEF, though little is known about how these models could extend to association cortices. This has been examined in one cortical area, SEF, by Schall and colleagues (Godlove et al., 2014; Ninomiya et al., 2015; Sajad et al., 2022; Sajad et al., 2019) using light flashes and a countermanding paradigm. Notably however, SEF is agranular, i.e. it does not possess a granular layer IV. In response to light flashes, SEF exhibits two current sinks: in layer III and layer V (Godlove et al., 2014). This is consistent with corticocortical (from LIP, FEF, the medial superior temporal area (MST), 7a, etc.) and thalamocortical (MD) visual afferents in SEF terminating in layers III and V as compared to the layer IV inputs observed in granular cortical areas. However, this is in conflict with the CCM which relies on a singular input layer. Despite this, they observed a similar spread from middle, to superficial and finally deep layers. Also, excitatory-inhibitory balances in single neuron activity following light flashes were consistent with Douglas and Martin's (1991) observations of local recurrent excitation regulated by inhibition and laminar differences in $GABA_A$ and $GABA_B$ receptor expression in pyramidal neurons (Godlove et al., 2014). Examining the activity of SEF in the countermanding task revealed a bias for superficial neurons in goal maintenance and error monitoring and a bias for reward processing in deeper layers, though this activity can be observed everywhere (Sajad et al., 2022; Sajad et al., 2019). Contrasting these observations with those in V1 reveals patterns consistent with bilaminar input, little to no interlaminar inhibition and weaker interlaminar coupling suggesting the CCM requires significant modification to be extended to some cortical areas such as agranular cortex (Beul & Hilgetag, 2015).

Although FEF and LIP do possess a granular layer IV, some modification is still required

to adapt the CCM to their function. Heinzle and colleagues (2007) used the known activity of FEF neurons to extend the CCM to this region with small modifications of proposed excitatory-inhibitory balance and projection weights. This model recapitulates the classic feedforward loop and ascribes distinct functions to cortical layers consistent with previous observations: layer IV is the visual input layer, layers II/III are responsible for attentional selection and layer V serves the motor output. As mentioned above, target selection related activity can be observed in both FEF (Schall & Hanes, 1993; Schall, Hanes, et al., 1995; Schiller & Chou, 2000; Thompson et al., 1996; Wardak et al., 2006) and LIP (Ipata et al., 2006; Thomas & Paré, 2007; Wardak et al., 2002). Examining the activity of neurons projecting within these regions and to the SC, which should correspond to supragranular and infragranular neurons respectively, exhibit a visual and motor bias respectively (Ferraina et al., 2002; Paré & Wurtz, 1997, 2001; Segraves & Goldberg, 1987; Sommer & Wurtz, 2001). These observations appear to be consistent with the CCM adapted for cortical areas higher in the visual processing hierarchy but relies on assumptions based on weights of anatomical projections, which do not necessarily correspond to physiological importance (Binzegger et al., 2004). Yet, due to the challenge of conducting laminar recordings in regions like LIP and FEF, which are located deep within sulci in the macaque, this remains to be investigated directly with *in vivo* electrophysiology. To this end, we turn to a relatively lissencephalic New world monkey, the common marmoset, *Callithrix jacchus*. In the next section, I examine the merits of the marmoset model as a companion to the macaque for investigations of oculomotor control and visual attention.

1.4 Saccades, visual attention, and the frontoparietal network in the common marmoset

A promising alternative nonhuman primate model for studying LIP and FEF cortical microcircuits may be the New World common marmoset (*Callithrix jacchus*). These small, New-world primates have a largely lissencephalic cortex well suited to modern neurophysiological techniques including high density electrophysiological recordings and optical imaging (Mitchell & Leopold, 2015). In addition to this, a host of practical and scientific advantages, discussed below, have accelerated the use of the marmoset as a neuroscientific model (see for review Johnston et al., 2018; Miller et al., 2016; Mitchell & Leopold, 2015; Mitchell et al., 2014; Preuss, 2019). The marmoset is small (300-600g) which confers advantages in housing and presents fewer risks when handling as compared to larger primates such as macaques. Their smaller sizes, faster developmental trajectory (5-6 month gestation, 12-18 months to adulthood) and propensity to give birth to fraternal twins (if not triplets and quadruplets) facilitates breeding colonies in house for easier access to subjects. This permits experiments requiring larger sample sizes and faster growth such as transgenic manipulations, developmental studies and disease modelling. Marmosets are also very social animals: they live in large family units, partake in cooperative care of young, and exhibit a rich communicative repertoire with diverse vocalizations and body language. These advantages motivate the use of the marmoset as a complementary non-human primate model in neurophysiological investigations of cognition. However, to establish this model for use in oculomotor and visual attention research, we must (1) ascertain that marmosets naturally produce eye movements resembling those of humans

and are capable of being trained on oculomotor tasks. Additionally, we must (2) evaluate the homology of the marmoset frontoparietal network with those of macaques and humans.

1.4.1 Marmoset oculomotor behaviour

Marmosets have been shown to be an excellent model for investigating the oculomotor system as they make saccadic and smooth pursuit eye movements and have natural gaze behaviour resembling other primates (C.-Y. Chen et al., 2021; Johnston et al., 2018; Mitchell & Leopold, 2015; Mitchell et al., 2015; Mitchell et al., 2014). More recent work from our group has shown that when examining the scan-paths of head-restrained marmosets viewing a variety of visual stimuli images and videos of scenes, conspecifics (Zanini et al., 2023) and conspecific faces (Hung et al., 2015; Schaeffer et al., 2020; Selvanayagam et al., 2021), abstract stimuli such as the Frith-Happé theory of mind animations (Dureux et al., 2023), and even live interactions with conspecifics (K. M. Gilbert et al., 2021), many similarities can be observed with those of humans and macaques (Dureux et al., 2023; Hori et al., 2021; Zanini et al., 2023). Additionally, pharmacological manipulations such as administering oxytocin or ketamine alters scanpaths for marmosets and humans in similar ways (Kotani et al., 2017; Selvanayagam et al., 2021). Finally, despite a smaller preferred oculomotor range and greater reliance on head movements, marmosets can be trained to perform saccadic eye movement tasks while being head-restrained (Johnston et al., 2018; Johnston et al., 2019; Ma et al., 2020).

1.4.2 Marmoset frontoparietal network

Regarding the homology of the networks underlying this behaviour, it is known that the sub-cortical and early visual cortical pathways are highly conserved across primates and indeed most mammals. However, the development of the PPC and granular prefrontal cortex (PFC) are unique to primates. In particular, the strength of connections LIP shares with the rest of the network such as the SC differs across primate taxa (see Chapter 1.2.4). This suggests the homology of marmoset LIP and FEF with other primates warrants closer inspection. As discussed above (see Chapter 1.2), LIP and FEF can be defined on the basis of cytoarchitectural properties, anatomical and functional connectivity with other oculomotor and visual regions, ICMS evoked behaviours and response properties of single neurons. The cytoarchitectural classification of marmoset cortex is well characterized in the atlas of Paxinos and colleagues (2012), and although this is insufficient to provide evidence for homology, it provides a strong starting point for identifying homologous regions, especially in the absence of clear sulcal landmarks. Below I review evidence from anatomical and functional magnetic resonance imaging (fMRI) investigations establishing the homology of these regions with macaques and humans. Additionally, I review recent work from our lab using ICMS and single neuron recordings in LIP and putative FEF providing further evidence for its homology.

Marmoset lateral intraparietal area

Rosa and colleagues (2009) separated marmoset PPC into a dorsal and ventral aspect on the basis of cyto- and myeloarchitecture. The dorsal PPC region contained characteristic large layer 5 pyramidal neurons and a similar pattern of myelination to macaque LIP, suggesting

this region may contain the marmoset LIP. This observation is corroborated by anatomical retrograde tracer investigations triangulating connectivity between FEF (Reser et al., 2013), the SC (C. E. Collins et al., 2005) and LIP, albeit slightly weaker than in the macaque. Additionally, resting-state functional connectivity with SC highlights a region of high functional connectivity coinciding with putative marmoset LIP (Ghahremani et al., 2017). A subsequent task-based fMRI study in awake, free-viewing marmosets revealed a "visuo-saccadic" network with activity in SC as well as putative FEF and LIP (Schaeffer et al., 2019). Thus a region of marmoset PPC presents a likely candidate for LIP, but neurophysiological investigation of this region was required to establish common functional properties.

To this end, our group employed ICMS using 32-channel Utah arrays implanted over the putative LIP of two adult marmosets (Ghahremani et al., 2019). Here, we were able to elicit saccades at most electrode sites with a few sites evoking eye blinks or no oculomotor or skeletomotor responses. Most saccades at these sites were fixed-vector, i.e., saccade amplitude and direction was consistent regardless of initial gaze position. At these sites, increasing current intensity increased the probability of eliciting a saccade and reduced saccade latency, but had minimal effect on saccade amplitude and duration. Additionally, prolonged stimulation at these sites resulted in "staircases" of saccades, i.e., the orbit was continuously driven toward the edge with consistent direction and amplitude, providing further evidence for fixed-vector saccades being elicited at this site. Saccades elicited here were exclusively directed towards the contralateral hemifield and tended towards the upper visual field. Current thresholds ($40 - 240\mu A$) and saccade latencies ($64 - 87ms$) were slightly larger in the marmoset as compared to previous reports in macaques (Shibutani et al., 1984; Thier & Andersen, 1998). This may be due to the use of chronically implanted Utah arrays, where the depth of the 1 mm shanks cannot be adjusted to optimize the depth (i.e. the large layer 5 pyramidal neurons that project to SC) where the thresholds and latencies will be lowest. However, this may point to a true species difference, mediated by relative differences in projection strength or soma size which are smaller in marmosets. In addition to the sites where fixed-vector saccades could be elicited, at a subset of sites, saccades that converged in craniocentric space could be observed. These so-called "convergent" or "goal-directed" saccades, which are directed to one location in space regardless of initial gaze position have been also been elicited in macaque LIP (Thier & Andersen, 1998; see also Constantin et al., 2007). In sum, ICMS in marmoset LIP elicits oculomotor behaviour that is comparable to that of macaque LIP, though some differences in thresholds and latencies can be observed.

Having demonstrated some evidence for the homology of marmoset LIP, our group conducted single neuron recordings targeting this area as marmosets completed the gap task. Here we observed neural correlates of the gap effect in single marmoset LIP neurons consistent with observations in the macaque (M. Chen et al., 2016; M. Chen et al., 2013) and its role in the modulation of saccadic eye movements and visual attention (Ma et al., 2020). Altogether, a convergence of evidence from cytoarchitectonic, anatomical, fMRI, ICMS and extracellular electrophyisological investigations support the homology of marmoset LIP and its use in neurophysiological investigations of oculomotor control and visual attention.

Marmoset frontal eye fields

In contrast with LIP, detailed ICMS experiments in awake behaving marmosets have yet to be conducted for FEF. However, some early investigations with anaesthetized marmosets have provided some insight into the putative location of marmoset FEF. In the early 20th century, Mott and colleagues (1910) reported that eye and combined eye and head movements could be evoked by electrical stimulation at several frontal cortical sites. A subsequent study by Blum and colleagues (1982) confirmed this earlier result: they were able to elicit ipsilateral and contralateral saccades, eye movements in all directions, and slow drifting movements from areas 6DC, 6DR, 8Ad, and 46 with no clear patterns or boundaries. However, the defining characteristic of low current thresholds for fixed vector saccadic eye movements cannot be estimated from the experiments in anaesthetized subjects due to the known influence of anaesthesia on the properties of evoked eye movements (Robinson & Fuchs, 1969). Nevertheless, these early observations provide a starting point for identifying marmoset FEF.

Recent study of cytoarchitectural properties of marmoset frontal cortex reveals that areas 8aV and 45 possess the large layer V pyramidal neurons characteristic of FEF (Burman et al., 2006). Additionally, these regions share anatomical connections with oculomotor areas including SC (C. E. Collins et al., 2005), area MT (Krubitzer & Kaas, 1990), LIP and extrastriate visual cortex (Lyon & Kaas, 2001; Reser et al., 2013). Notably, projections to SC could be separated into two regions, which Collins and colleagues (2005) labeled as FEF and the frontal ventral visual area (FV). These regions project to caudal (peripheral visual field) and rostral (foveal) portions of the SC respectively. A similar distinction between FEF and FV was made when examining connections with MT (Krubitzer & Kaas, 1990). Thus, FEF and FV have been proposed to correspond to macaque and human dFEF and vFEF respectively (Bakola et al., 2015). Consistent with these anatomical observations, areas 8, 45 and 6 have also been implicated in a saccade network on the basis of resting-state functional connectivity with SC (Ghahremani et al., 2017) and task-based fMRI (Schaeffer et al., 2019). Altogether, early ICMS, anatomical, and fMRI studies, suggest the marmoset FEF exists at the confluence of areas 8a, 6D, 45, and 46.

On this basis, our group has conducted single neuron recordings in area 8aD, as marmosets complete a modified antisaccade paradigm (Johnston et al., 2019). This paradigm is comprised of alternating blocks of trials requiring the subject to perform a saccade towards a large, high-luminance stimulus (prosaccade) or suppress this prepotent response and instead perform a saccade towards a smaller, low-luminance stimulus (antisaccade). This paradigm is often used as the final stage of antisaccade training and these saccades generally have the same properties as true antisaccades (Bell et al., 2000). Here, preparatory activity in saccade-related neurons was lower for antisaccade trials than for prosaccade trials, which is consistent with macaque FEF (Everling & Munoz, 2000). Thus early ICMS as well as detailed anatomical, fMRI, and electrophysiological investigations provide evidence for a homologous marmoset FEF, but ICMS in awake behaving marmosets is required to confirm this homology and define the bounds of this region.

In sum, the challenge of investigating laminar microcircuitry of regions underlying the control of saccades and visual attention is complicated by the location of such regions deep within sulci in the macaque. The common marmoset, with a largely lissencephalic brain, and highly homologous oculomotor behavioural repertoire and frontoparietal network, presents an

ideal opportunity to address these questions (D'Souza et al., 2021). Recent work supports the homology of marmoset LIP with that of macaques and humans, though a thorough ICMS experiment in awake behaving marmosets remains to be conducted for FEF. In the following section, I will outline the objectives of this dissertation, in which I establish the homology of marmoset FEF using ICMS, as well as conduct laminar electrophysiological investigations in marmoset LIP and FEF to investigate the circuitry underlying the control of visual attention.

1.5 Objectives

Interacting with our visual world requires covert shifts of visual attention, selection of targets of interests and overt saccadic eye movements to fixate on these targets for detailed visual analysis. These behaviours rely on the coordinated activity of the frontoparietal network, the primary cortical nodes of which are LIP and FEF. Single neurons in these regions have been demonstrated to modulate their discharge activity at all stages of visual processing and oculo-motor production, making them ideal structures for the investigation of visual attention. Subsequent lesion studies and pharmacological investigations have demonstrated a causal role for these regions in the process of visual target selection. Indeed activity in these regions can be separated from the stimulus and motor related activity, highlighting the role of these regions as true sources of a top-down spatial attention signal. Determining how this target selection related activity correlates with anatomical properties such as cortical layer or morphological cell type is of particular interest for disentangling the underlying circuit. While anatomical and physiological investigations provide some insight into this organization on the basis of separable corticocortical and corticotectal projection patterns, due to the challenges of conducting laminar investigations in the macaque, the local laminar circuit of LIP and FEF remains unknown. Here we will address this gap by leveraging the relatively lissencephalic cortex and largely homologous frontoparietal network of the common marmoset. As discussed above (see Chapter 1.4) recent work has demonstrated evidence from anatomical connectivity, resting-state and task-based fMRI, single neuron recordings, and ICMS for the homology of marmoset LIP with that of macaques and humans. The first objective of this work was to extend this work to FEF using ICMS to functionally identify the bounds of and assess the homology of marmoset FEF. The second and third objectives of this work were to investigate the laminar dynamics underlying target selection behaviour in marmoset LIP and FEF respectively.

1.5.1 Localization of the frontal eye fields in the common marmoset using microstimulation

The first objective was to explore marmoset frontal cortex using the classical approach of ICMS in the awake behaving marmoset to physiologically identify the marmoset FEF. We broadly surveyed marmoset frontal cortex by implanting 4 mm x 4 mm microelectrode arrays in the frontal cortex of 3 adult marmosets, targeting regions with high functional and anatomical connectivity with the SC and LIP. We stimulated across these arrays and observed evoked skeletomotor and oculomotor movements. We identified a region of frontal cortex wherein low current ($< 50\mu A$) stimulation elicited fixed vector saccadic eye movements characteristic of FEF. This region was anterior to sites where stimulation elicited skeletomotor movements resembling premotor

or primary motor cortex, and coincided with cytoarchitectural areas suggested to be the site of marmoset FEF on the basis of tracer and fMRI studies. We also observed a gross topograpy of saccade direction and amplitude consistent with findings in macaques and humans: small saccades in ventrolateral FEF and large saccades combined with contralateral neck and shoulder movements encoded in dorsomedial FEF. These data provide compelling evidence supporting the homology of marmoset and macaque FEF and highlight its value as a useful primate model for investigating FEF microcircuitry.

1.5.2 Laminar dynamics underlying target selection in lateral intraparietal area of the common marmoset

The second objective was to examine the activity of LIP neurons using high-density laminar electrophysiology as animals completed a visual search task to investigate the laminar dynamics underlying target selection. In this task, marmosets were required to generate saccades towards a target stimulus presented in either the presence or absence of a distractor in the opposite hemifield. We recorded from 1366 single neurons in 23 recordings sessions across 2 marmoset. Here, we observed for the first time in the marmoset, neural correlates of target selection in single LIP neurons. Although neurons in all cortical layers and cell types had stimulus-related activity and discriminated between target and distractor stimuli ultimately at the same degree, we observed subtle differences in the timing of this activity. Namely, stimulus-related activity emerged first in the putative interneurons of granular layer neurons followed by the earliest target discriminating activity emerging in putative supragranular pyramidal neurons. These observations are consistent with the roles of granular layer as an input neuron and supragranular layers in attention and target selection as suggested by models based on the CCM.

1.5.3 Laminar dynamics underlying target selection in frontal eye fields of the common marmoset

As for the second objective with LIP, the third objective was to examine the activity of FEF neurons to investigate the laminar dynamics underlying target selection in this region. We recorded from 1452 neurons across 24 recordings sessions in 2 marmosets. As in LIP, we observed neurons across all cortical layers with stimulus related and target discriminating activity, and an overwhelming number of neurons (though to a lesser extent than in LIP) which responded post-saccadically. Additionally, we observed a greater proportion of neurons than in LIP with pre-saccadic activity, which often correlated with SRTs. These observations are consistent with the role of FEF in visual attention, with a greater role in saccade control than LIP. As in LIP, the timing and information carried by single neurons did not differ across cortical laminae or putative cell types, though it did at the population level. Indeed consistent with LIP, putative granular and supragranular interneurons had the earliest stimulus response latencies. However, it was the putative infragranular interneurons that had the earliest target discrimination times. Taken together with the observations in LIP, these findings suggest that ultimately neurons in all layers receive similar information required for target selection, though subtle timing differences can be observed that are partially consistent with the CCM. However,

the laminar organization becomes more nuanced as we ascend the visual hierarchy. Altogether these findings provide a framework for extending the CCM beyond primary sensory cortical areas to association cortex, and deepen our understanding of the cortical circuits underlying eye movements and visual attention.

1.6 References

Andersen, R. A., Asanuma, C., & Cowan, W. M. (1985). Callosal and prefrontal associational projecting cell populations in area 7A of the macaque monkey: A study using retrogradely transported fluorescent dyes. *The Journal of Comparative Neurology*, *232*(4), 443–455. https://doi.org/10.1002/cne.902320403

Andersen, R. A., Essick, G. K., & Siegel, R. M. (1987). Neurons of area 7 activated by both visual stimuli and oculomotor behavior. *Experimental Brain Research*, *67*(2), 316–322. https://doi.org/10.1007/BF00248552

Anderson, J. C., Martin, K. A. C., & Whitteridge, D. (1993). Form, Function, and Intracortical Projections of Neurons in the Striate Cortex of the Monkey Macacus nemestrinus. *Cerebral Cortex*, *3*(5), 412–420. https://doi.org/10.1093/cercor/3.5.412

Angelaki, D. E. (2011, August 18). The oculomotor plant and its role in three-dimensional eye orientation. In S. P. Liversedge, I. Gilchrist, & S. Everling (Eds.), *The Oxford Handbook of Eye Movements*. Oxford University Press. https://doi.org/10.1093/oxfordhb/9780199539789.013.0008

Armstrong, K. M., Fitzgerald, J. K., & Moore, T. (2006). Changes in Visual Receptive Fields with Microstimulation of Frontal Cortex. *Neuron*, *50*(5), 791–798. https://doi.org/10.1016/j.neuron.2006.05.010

Armstrong, K. M., & Moore, T. (2007). Rapid enhancement of visual cortical response discriminability by microstimulation of the frontal eye field. *Proceedings of the National Academy of Sciences*, *104*(22), 9499–9504. https://doi.org/10.1073/pnas.0701104104

Bahill, A. T., Clark, M. R., & Stark, L. (1975). The main sequence, a tool for studying human eye movements. *Mathematical Biosciences*, *24*(3), 191–204. https://doi.org/10.1016/0025-5564(75)90075-9

Bakola, S., Burman, K. J., & Rosa, M. G. P. (2015). The cortical motor system of the marmoset monkey (Callithrix jacchus). *Neuroscience Research*, *93*, 72–81. https://doi.org/10.1016/j.neures.2014.11.003

Balan, P. F., Oristaglio, J., Schneider, D. M., & Gottlieb, J. P. (2008). Neuronal Correlates of the Set-Size Effect in Monkey Lateral Intraparietal Area. *PLoS Biology*, *6*(7). https://doi.org/10.1371/journal.pbio.0060158

Baldwin, M. K., & Kaas, J. H. (2012). Cortical Projections to the Superior Colliculus in Prosimian Galagos (Otolemur garnetti). *The Journal of comparative neurology*, *520*(9), 2002–2020. https://doi.org/10.1002/cne.23025

Barash, S., Bracewell, R. M., Fogassi, L., Gnadt, J. W., & Andersen, R. A. (1991a). Saccade-related activity in the lateral intraparietal area. II. Spatial properties. *Journal of Neurophysiology*, *66*(3), 1109–1124. https://doi.org/10.1152/jn.1991.66.3.1109

Barash, S., Bracewell, R. M., Fogassi, L., Gnadt, J. W., & Andersen, R. A. (1991b). Saccade-related activity in the lateral intraparietal area. I. Temporal properties; comparison with

area 7a. *Journal of Neurophysiology*, *66*(3), 1095–1108. https://doi.org/10.1152/jn. 1991.66.3.1095

Barone, P., Batardiere, A., Knoblauch, K., & Kennedy, H. (2000). Laminar Distribution of Neurons in Extrastriate Areas Projecting to Visual Areas V1 and V4 Correlates with the Hierarchical Rank and Indicates the Operation of a Distance Rule. *The Journal of Neuroscience*, *20*(9), 3263–3281. https://doi.org/10.1523/JNEUROSCI.20-09-03263.2000

Bell, A. H., Everling, S., & Munoz, D. P. (2000). Influence of Stimulus Eccentricity and Direction on Characteristics of Pro- and Antisaccades in Non-Human Primates. *Journal of Neurophysiology*, *84*(5), 2595–2604. https://doi.org/10.1152/jn.2000.84.5.2595

Berman, R. A., & Wurtz, R. H. (2008). Exploring the pulvinar path to visual cortex. *Progress in brain research*, *171*, 467–473. https://doi.org/10.1016/S0079-6123(08)00668-7

Beul, S. F., & Hilgetag, C. C. (2015). Towards a "canonical" agranular cortical microcircuit. *Frontiers in Neuroanatomy*, *8*. Retrieved November 18, 2023, from https://www. frontiersin.org/articles/10.3389/fnana.2014.00165

Bichot, N. P., & Schall, J. D. (1999). Saccade target selection in macaque during feature and conjunction visual search. *Visual Neuroscience*, *16*(1), 81–89. https://doi.org/10.1017/S0952523899161042

Binzegger, T., Douglas, R. J., & Martin, K. A. C. (2004). A Quantitative Map of the Circuit of Cat Primary Visual Cortex. *Journal of Neuroscience*, *24*(39), 8441–8453. https://doi.org/10.1523/JNEUROSCI.1400-04.2004

Bisley, J. W., & Goldberg, M. E. (2003). Neuronal Activity in the Lateral Intraparietal Area and Spatial Attention. *Science*, *299*(5603), 81–86. https://doi.org/10.1126/science.1077395

Bisley, J. W., Mirpour, K., Arcizet, F., & Ong, W. S. (2011). The Role of the Lateral Intraparietal Area in Orienting Attention and its Implications for Visual Search. *The European journal of neuroscience*, *33*(11), 1982–1990. https://doi.org/10.1111/j.1460-9568.2011.07700.x

Blatt, G. J., Andersen, R. A., & Stoner, G. R. (1990). Visual receptive field organization and cortico-cortical connections of the lateral intraparietal area (area LIP) in the macaque. *Journal of Comparative Neurology*, *299*(4), 421–445. https://doi.org/10.1002/cne. 902990404

Blum, B., Kulikowski, J., Carden, D., & Harwood, D. (1982). Eye Movements Induced by Electrical Stimulation of the Frontal Eye Fields of Marmosets and Squirrel Monkeys. *Brain, Behavior and Evolution*, *21*(1), 34–41. https://doi.org/10.1159/000121613

Bringmann, A., Syrbe, S., Görner, K., Kacza, J., Francke, M., Wiedemann, P., & Reichenbach, A. (2018). The primate fovea: Structure, function and development. *Progress in Retinal and Eye Research*, *66*, 49–84. https://doi.org/10.1016/j.preteyeres.2018.03.006

Bruce, C. J., & Goldberg, M. E. (1985). Primate frontal eye fields. I. Single neurons discharging before saccades. *Journal of Neurophysiology*, *53*(3), 603–635. https://doi.org/10.1152/jn.1985.53.3.603

Bruce, C. J., Goldberg, M. E., Bushnell, M. C., & Stanton, G. B. (1985). Primate frontal eye fields. II. Physiological and anatomical correlates of electrically evoked eye movements. *Journal of Neurophysiology*, *54*(3), 714–734. https://doi.org/10.1152/jn.1985. 54.3.714

Brunamonti, E., & Pare, M. (2023). Neuronal activity in posterior parietal cortex area LIP is not sufficient for saccadic eye movement production. *Frontiers in Integrative Neuroscience*, *17*. https://doi.org/10.3389/fnint.2023.1251431

Bullier, J., Schall, J. D., & Morel, A. (1996). Functional streams in occipito-frontal connections in the monkey. *Behavioural Brain Research*, *76*(1), 89–97. https://doi.org/10.1016/0166-4328(95)00182-4

Burman, K. J., Palmer, S. M., Gamberini, M., & Rosa, M. G. P. (2006). Cytoarchitectonic subdivisions of the dorsolateral frontal cortex of the marmoset monkey (Callithrix jacchus), and their projections to dorsal visual areas. *Journal of Comparative Neurology*, *495*(2), 149–172. https://doi.org/10.1002/cne.20837

Buswell, G. T. (1935). *How People Look at Pictures: A Study of the Psychology of Perception in Art*. University of Chicago Press.

Carpenter, R. H. S. (1988). *Movements of the eyes, 2nd rev. & enlarged ed*. Pion Limited.

Carpenter, R. H. S., & Williams, M. L. L. (1995). Neural computation of log likelihood in control of saccadic eye movements. *Nature*, *377*(6544), 59–62. https://doi.org/10.1038/377059a0

Cattell, J. M. (1900). On relations of time and space in vision. *Psychological Review*, *7*(4), 325–343. https://doi.org/10.1037/h0065432

Chen, C.-Y., Matrov, D., Veale, R., Onoe, H., Yoshida, M., Miura, K., & Isa, T. (2021). Properties of visually guided saccadic behavior and bottom-up attention in marmoset, macaque, and human. *Journal of Neurophysiology*, *125*(2), 437–457. https://doi.org/10.1152/jn.00312.2020

Chen, M., Li, B., Guang, J., Wei, L., Wu, S., Liu, Y., & Zhang, M. (2016). Two subdivisions of macaque LIP process visual-oculomotor information differently. *Proceedings of the National Academy of Sciences of the United States of America*, *113*(41), E6263–E6270. https://doi.org/10.1073/pnas.1605879113

Chen, M., Lui, Y., Wei, L., & Zhang, M. (2013). Parietal Cortical Neuronal Activity Is Selective for Express Saccades. *The Journal of Neuroscience*, *33*(2), 814–823. https://doi.org/10.1523/JNEUROSCI.2675-12.2013

Christopoulos, V. N., Kagan, I., & Andersen, R. A. (2018). Lateral intraparietal area (LIP) is largely effector-specific in free-choice decisions. *Scientific Reports*, *8*(1), 8611. https://doi.org/10.1038/s41598-018-26366-9

Collins, C. E., Lyon, D. C., & Kaas, J. H. (2005). Distribution across cortical areas of neurons projecting to the superior colliculus in new world monkeys. *The Anatomical Record Part A: Discoveries in Molecular, Cellular, and Evolutionary Biology*, *285A*(1), 619–627. https://doi.org/10.1002/ar.a.20207

Collins, T., & Doré-Mazars, K. (2006). Eye movement signals influence perception: Evidence from the adaptation of reactive and volitional saccades. *Vision Research*, *46*(21), 3659–3673. https://doi.org/10.1016/j.visres.2006.04.004

Constantin, A. G., Wang, H., Martinez-Trujillo, J. C., & Crawford, J. D. (2007). Frames of Reference for Gaze Saccades Evoked During Stimulation of Lateral Intraparietal Cortex. *Journal of Neurophysiology*, *98*(2), 696–709. https://doi.org/10.1152/jn.00206.2007

Corbetta, M. (1998). Frontoparietal cortical networks for directing attention and the eye to visual locations: Identical, independent, or overlapping neural systems? *Proceedings of*

the National Academy of Sciences of the United States of America, *95*(3), 831–838. Retrieved July 3, 2023, from https://www.ncbi.nlm.nih.gov/pmc/articles/PMC33805/

Corneil, B. D., Elsley, J. K., Nagy, B., & Cushing, S. L. (2010). Motor output evoked by sub-saccadic stimulation of primate frontal eye fields. *Proceedings of the National Academy of Sciences of the United States of America*, *107*(13), 6070–6075. https://doi.org/10.1073/pnas.0911902107

Corneil, B. D., Munoz, D. P., Chapman, B. B., Admans, T., & Cushing, S. L. (2008). Neuro-muscular consequences of reflexive covert orienting. *Nature Neuroscience*, *11*(1), 13–15. https://doi.org/10.1038/nn2023

Corneil, B. D., Olivier, E., & Munoz, D. P. (2004). Visual Responses on Neck Muscles Reveal Selective Gating that Prevents Express Saccades. *Neuron*, *42*(5), 831–841. https://doi.org/10.1016/S0896-6273(04)00267-3

Cullen, K. E., & Horn, M. R. V. (2011, August 18). Brainstem pathways and premotor control. In S. P. Liversedge, I. Gilchrist, & S. Everling (Eds.), *The Oxford Handbook of Eye Movements*. Oxford University Press. https://doi.org/10.1093/oxfordhb/9780199539789.013.0009

Deng, S.-Y., Goldberg, M. E., Segraves, M. A., Ungerleider, L. G., & Mishkin, M. (1986). The effect of unilateral ablation of the frontal eye fields on saccadic performance in the monkey. In E. L. Keller & D. S. Zee (Eds.), *Adaptive Processes in the Visual and Oculomotor Systems* (pp. 201–208). Pergamon Press.

Dodge, R., & Cline, T. S. (1901). The angle velocity of eye movements. *Psychological Review*, *8*(2), 145–157. https://doi.org/10.1037/h0076100

Donders, F. C. (1872). Ueber angeborene und erworbene Association. *Albrecht von Graefes Archiv für Ophthalmologie*, *18*(2), 153–164. https://doi.org/10.1007/BF02262657

Dorris, M. C., & Munoz, D. P. (1995). A neural correlate for the gap effect on saccadic reaction times in monkey. *Journal of Neurophysiology*, *73*(6), 2558–2562. https://doi.org/10.1152/jn.1995.73.6.2558

Dorris, M. C., Paré, M., & Munoz, D. P. (1997). Neuronal Activity in Monkey Superior Colliculus Related to the Initiation of Saccadic Eye Movements. *The Journal of Neuroscience*, *17*(21), 8566–8579. https://doi.org/10.1523/JNEUROSCI.17-21-08566.1997

Douglas, R. J., & Martin, K. A. (1991). A functional microcircuit for cat visual cortex. *The Journal of Physiology*, *440*, 735–769. Retrieved July 23, 2021, from https://www.ncbi.nlm.nih.gov/pmc/articles/PMC1180177/

Douglas, R. J., & Martin, K. A. (2004). Neuronal Circuits of the Neocortex. *Annual Review of Neuroscience*, *27*(1), 419–451. https://doi.org/10.1146/annurev.neuro.27.070203.144152

Doyle, M., & Walker, R. (2001). Curved saccade trajectories: Voluntary and reflexive saccades curve away from irrelevant distractors. *Experimental Brain Research*, *139*(3), 333–344. https://doi.org/10.1007/s002210100742

Drager, U. C., & Hubel, D. H. (1975a). Responses to visual stimulation and relationship between visual, auditory, and somatosensory inputs in mouse superior colliculus. *Journal of Neurophysiology*, *38*(3), 690–713. https://doi.org/10.1152/jn.1975.38.3.690

Drager, U. C., & Hubel, D. H. (1975b). Physiology of visual cells in mouse superior colliculus and correlation with somatosensory and auditory input. *Nature*, *253*(5488), 203–204. https://doi.org/10.1038/253203a0

D'Souza, J. F., Price, N. S. C., & Hagan, M. A. (2021). Marmosets: A promising model for probing the neural mechanisms underlying complex visual networks such as the frontal–parietal network. *Brain Structure and Function*. https://doi.org/10.1007/s00429-021-02367-9

Duncan, J., & Humphreys, G. W. (1989). Visual search and stimulus similarity. *Psychological Review*, *96*(3), 433–458. https://doi.org/10.1037/0033-295X.96.3.433

Dureux, A., Zanini, A., Selvanayagam, J., Menon, R. S., & Everling, S. (2023). Gaze patterns and brain activations in humans and marmosets in the Frith-Happé theory-of-mind animation task (M. Irish & T. E. Behrens, Eds.). *eLife*, *12*, e86327. https://doi.org/10.7554/eLife.86327

Elsley, J. K., Nagy, B., Cushing, S. L., & Corneil, B. D. (2007). Widespread Presaccadic Recruitment of Neck Muscles by Stimulation of the Primate Frontal Eye Fields. *Journal of Neurophysiology*, *98*(3), 1333–1354. https://doi.org/10.1152/jn.00386.2007

Everling, S., & Munoz, D. P. (2000). Neuronal Correlates for Preparatory Set Associated with Pro-Saccades and Anti-Saccades in the Primate Frontal Eye Field. *Journal of Neuroscience*, *20*(1), 387–400. https://doi.org/10.1523/JNEUROSCI.20-01-00387.2000

Everling, S., Paré, M., Dorris, M. C., & Munoz, D. P. (1998). Comparison of the Discharge Characteristics of Brain Stem Omnipause Neurons and Superior Colliculus Fixation Neurons in Monkey: Implications for Control of Fixation and Saccade Behavior. *Journal of Neurophysiology*, *79*(2), 511–528. https://doi.org/10.1152/jn.1998.79.2.511

Fecteau, J. H., & Munoz, D. P. (2006). Salience, relevance, and firing: A priority map for target selection. *Trends in Cognitive Sciences*, *10*(8), 382–390. https://doi.org/10.1016/j.tics.2006.06.011

Ferraina, S., Paré, M., & Wurtz, R. H. (2002). Comparison of Cortico-Cortical and Cortico-Collicular Signals for the Generation of Saccadic Eye Movements. *Journal of Neurophysiology*, *87*(2), 845–858. https://doi.org/10.1152/jn.00317.2001

Ferrier, D. (1875). The Croonian Lecture: Experiments on the Brain of Monkeys (second series). *Philosopical Transactions of the Royal Society of London*, *165*, 433–488. https://royalsocietypublishing.org/doi/pdf/10.1098/rstl.1875.0016

Findlay, J. M., & Walker, R. (1999). A model of saccade generation based on parallel processing and competitive inhibition. *The Behavioral and Brain Sciences*, *22*(4), 661–674, discussion 674–721. https://doi.org/10.1017/s0140525x99002150

Findlay, J. M., & Gilchrist, I. D. (2003). *Active vision: The psychology of looking and seeing*. Oxford University Press. https://doi.org/10.1093/acprof:oso/9780198524793.001.0001

Finger, S. (2001). *Origins of Neuroscience: A History of Explorations Into Brain Function*. Oxford University Press.

Fischer, B., & Boch, R. (1983). Saccadic eye movements after extremely short reaction times in the monkey. *Brain Research*, *260*(1), 21–26. https://doi.org/10.1016/0006-8993(83)90760-6

Foerster, O. (1926). Zur operativen Behandlung der Epilepsie. *Deutsche Zeitschrift für Nervenheilkunde*, *89*(1), 137–147. https://doi.org/10.1007/BF01653863

Forbes, K., & Klein, R. M. (1996). The Magnitude of the Fixation Offset Effect with Endogenously and Exogenously Controlled Saccades. *Journal of Cognitive Neuroscience*, *8*(4), 344–352. https://doi.org/10.1162/jocn.1996.8.4.344

Fries, W. (1984). Cortical projections to the superior colliculus in the macaque monkey: A retrograde study using horseradish peroxidase. *Journal of Comparative Neurology*, *230*(1), 55–76. https://doi.org/10.1002/cne.902300106

Ghahremani, M., Hutchison, R. M., Menon, R. S., & Everling, S. (2017). Frontoparietal Functional Connectivity in the Common Marmoset. *Cerebral Cortex*, *27*, 3890–3905. https://doi.org/10.1093/cercor/bhw198

Ghahremani, M., Johnston, K. D., Ma, L., Hayrynen, L. K., & Everling, S. (2019). Electrical microstimulation evokes saccades in posterior parietal cortex of common marmosets. *Journal of Neurophysiology*, *122*(4), 1765–1776. https://doi.org/10.1152/jn.00417.2019

Ghosh, S., & Porter, R. (1988). Morphology of pyramidal neurones in monkey motor cortex and the synaptic actions of their intracortical axon collaterals. *The Journal of Physiology*, *400*(1), 593–615. https://doi.org/10.1113/jphysiol.1988.sp017138

Gilbert, C. D. (1983). Microcircuitry of the Visual Cortex. *Annual Review of Neuroscience*, *6*(1), 217–247. https://doi.org/10.1146/annurev.ne.06.030183.001245

Gilbert, C. D., & Wiesel, T. N. (1983, January 1). Functional Organization of the Visual Cortex. In J. .-. Changeux, J. Glowinski, M. Imbert, & F. E. Bloom (Eds.), *Progress in Brain Research* (pp. 209–218). Elsevier. https://doi.org/10.1016/S0079-6123(08)60022-9

Gilbert, K. M., Cléry, J. C., Gati, J. S., Hori, Y., Johnston, K. D., Mashkovtsev, A., Selvanayagam, J., Zeman, P., Menon, R. S., Schaeffer, D. J., & Everling, S. (2021). Simultaneous functional MRI of two awake marmosets. *Nature Communications*, *12*, 6608. https://doi.org/10.1038/s41467-021-26976-4

Gilchrist, I. D., Brown, V., Findlay, J. M., & Clarke, M. P. (1998). Using the eye-movement system to control the head. *Proceedings of the Royal Society B: Biological Sciences*, *265*(1408), 1831–1836. Retrieved November 20, 2023, from https://www.ncbi.nlm.nih.gov/pmc/articles/PMC1689378/

Gilchrist, I. D., Brown, V., & Findlay, J. M. (1997). Saccades without eye movements. *Nature*, *390*(6656), 130–131. https://doi.org/10.1038/36478

Godlove, D. C., Maier, A., Woodman, G. F., & Schall, J. D. (2014). Microcircuitry of Agranular Frontal Cortex: Testing the Generality of the Canonical Cortical Microcircuit. *The Journal of Neuroscience*, *34*(15), 5355–5369. https://doi.org/10.1523/JNEUROSCI.5127-13.2014

Goldberg, M. E., & Wurtz, R. H. (1972a). Activity of superior colliculus in behaving monkey. I. Visual receptive fields of single neurons. *Journal of Neurophysiology*, *35*(4), 542–559. https://doi.org/10.1152/jn.1972.35.4.542

Goldberg, M. E., & Wurtz, R. H. (1972b). Activity of superior colliculus in behaving monkey. II. Effect of attention on neuronal responses. *Journal of Neurophysiology*, *35*(4), 560–574. https://doi.org/10.1152/jn.1972.35.4.560

Goldberg, M. E., Bisley, J., Powell, K. D., Gottlieb, J. P., & Kusunoki, M. (2002). The Role of the Lateral Intraparietal Area of the Monkey in the Generation of Saccades and Visuospatial Attention. *Annals of the New York Academy of Sciences*, *956*(1), 205–215. https://doi.org/10.1111/j.1749-6632.2002.tb02820.x

Gottlieb, J. P., & Goldberg, M. E. (1999). Activity of neurons in the lateral intraparietal area of the monkey during an antisaccade task. *Nature Neuroscience*, *2*(10), 906–912. https://doi.org/10.1038/13209

Gottlieb, J. P., Kusunoki, M., & Goldberg, M. E. (1998). The representation of visual salience in monkey parietal cortex. *Nature*, *391*(6666), 481–484. https://doi.org/10.1038/35135

Hanes, D. P., Patterson, W. F., & Schall, J. D. (1998). Role of Frontal Eye Fields in Countermanding Saccades: Visual, Movement, and Fixation Activity. *Journal of Neurophysiology*, *79*(2), 817–834. https://doi.org/10.1152/jn.1998.79.2.817

Hanes, D. P., Thompson, K. G., & Schall, J. D. (1995). Relationship of presaccadic activity in frontal eye field and supplementary eye field to saccade initiation in macaque: Poisson spike train analysis. *Experimental Brain Research*, *103*(1), 85–96. https://doi.org/10.1007/BF00241967

Harting, J. K. (1977). Descending pathways from the superior colliculus: An autoradiographic analysis in the rhesus monkey (Macaca mulatta). *Journal of Comparative Neurology*, *173*(3), 583–612. https://doi.org/10.1002/cne.901730311

Heinzle, J., Hepp, K., & Martin, K. A. C. (2007). A Microcircuit Model of the Frontal Eye Fields. *Journal of Neuroscience*, *27*(35), 9341–9353. https://doi.org/10.1523/JNEUROSCI.0974-07.2007

Hepp, K. (1994). Oculomotor control: Listing's law and all that. *Current Opinion in Neurobiology*, *4*(6), 862–868. https://doi.org/10.1016/0959-4388(94)90135-x

Hering, E. (1879). Über Muskelgeräusche des Auges. *Sitzberichte der kaiserlichen Akademie der Wissenschaften in Wien. Mathematisch-naturwissenschaftliche Klasse*, *79*, 137–154. Retrieved November 18, 2023, from https://iiif.wellcomecollection.org/pdf/b21642667

Hikosaka, O., Igusa, Y., Nakao, S., & Shimazu, H. (1978). Direct inhibitory synaptic linkage of pontomedullary reticular burst neurons with abducens motoneurons in the cat. *Experimental Brain Research*, *33*(3-4), 337–352. https://doi.org/10.1007/BF00235558

Hikosaka, O., & Kawakami, T. (1977). Inhibitory reticular neurons related to the quick phase of vestibular nystagmus–their location and projection. *Experimental Brain Research*, *27*(3-4), 377–386. https://doi.org/10.1007/BF00235511

Hikosaka, O., Takikawa, Y., & Kawagoe, R. (2000). Role of the Basal Ganglia in the Control of Purposive Saccadic Eye Movements. *Physiological Reviews*, *80*(3), 953–978. https://doi.org/10.1152/physrev.2000.80.3.953

Hori, Y., Cléry, J. C., Schaeffer, D. J., Menon, R. S., & Everling, S. (2021). Functional Organization of Frontoparietal Cortex in the Marmoset Investigated with Awake Resting-State fMRI. *Cerebral Cortex (New York, NY)*, *32*(9), 1965–1977. https://doi.org/10.1093/cercor/bhab328

Horn, A. K., Buttner-Ennever, J. A., Wahle, P., & Reichenberger, I. (1994). Neurotransmitter profile of saccadic omnipause neurons in nucleus raphe interpositus. *The Journal of Neuroscience*, *14*(4), 2032–2046. https://doi.org/10.1523/JNEUROSCI.14-04-02032.1994

Huerta, M. F., Krubitzer, L. A., & Kaas, J. H. (1986). Frontal eye field as defined by intracortical microstimulation in squirrel monkeys, owl monkeys, and macaque monkeys: I. Subcortical connections. *Journal of Comparative Neurology*, *253*(4), 415–439. https://doi.org/10.1002/cne.902530402

Huerta, M. F., Krubitzer, L. A., & Kaas, J. H. (1987). Frontal eye field as defined by intracortical microstimulation in squirrel monkeys, owl monkeys, and macaque monkeys

II. cortical connections. *Journal of Comparative Neurology*, *265*(3), 332–361. https://doi.org/10.1002/cne.902650304

Huey, E. B. (1908). A Study of Visual Fixation. *Science*, *27*(691), 501–502. https://doi.org/10.1126/science.27.691.501

Hughes, H. C., & Zimba, L. D. (1987). Natural boundaries for the spatial spread of directed visual attention. *Neuropsychologia*, *25*, 5–18. https://doi.org/10.1016/0028-3932(87)90039-X

Humphrey, D. R., & Schmidt, E. M. (1990). Extracellular Single-Unit Recording Methods. In A. A. Boulton, G. B. Baker, & C. H. Vanderwolf (Eds.), *Neurophysiological Techniques: Applications to Neural Systems* (pp. 1–64). Humana Press. https://doi.org/10.1385/0-89603-185-3:1

Hung, C.-C., Yen, C. C.-C., Ciuchta, J. L., Papoti, D., Bock, N. A., Leopold, D. A., & Silva, A. C. (2015). Functional Mapping of Face-Selective Regions in the Extrastriate Visual Cortex of the Marmoset. *The Journal of Neuroscience*, *35*(3), 1160. https://doi.org/10.1523/JNEUROSCI.2659-14.2015

Ipata, A. E., Gee, A. L., Gottlieb, J. P., Bisley, J. W., & Goldberg, M. E. (2006). LIP responses to a popout stimulus are reduced if it is overtly ignored. *Nature neuroscience*, *9*(8), 1071–1076. https://doi.org/10.1038/nn1734

Isa, T. (2002). Intrinsic processing in the mammalian superior colliculus. *Current Opinion in Neurobiology*, *12*(6), 668–677. https://doi.org/10.1016/S0959-4388(02)00387-2

Isa, T., Endo, T., & Saito, Y. (1998). The Visuo-Motor Pathway in the Local Circuit of the Rat Superior Colliculus. *The Journal of Neuroscience*, *18*(20), 8496–8504. https://doi.org/10.1523/JNEUROSCI.18-20-08496.1998

James, W. (1890). *The principles of psychology, Vol I*. Henry Holt and Co. https://doi.org/10.1037/10538-000

Javal, L. E. (1879). Essai sur la physiologie de la lecture [Essay on the physiology of reading]. *Annales d'Oculistique*, *82*, 242–253. Retrieved November 18, 2023, from https://pure.mpg.de/rest/items/item_2350899/component/file_2350898/content

Johnston, K. D., Barker, K., Schaeffer, L., Schaeffer, D. J., & Everling, S. (2018). Methods for chair restraint and training of the common marmoset on oculomotor tasks. *Journal of Neurophysiology*, *119*, 1636–1646.

Johnston, K. D., & Everling, S. (2008). Neurophysiology and neuroanatomy of reflexive and voluntary saccades in non-human primates. *Brain and Cognition*, *68*(3), 271–283. https://doi.org/10.1016/j.bandc.2008.08.017

Johnston, K. D., & Everling, S. (2011, August 18). Frontal cortex and flexible control of saccades. In *The Oxford Handbook of Eye Movements*. Oxford University Press. https://doi.org/10.1093/oxfordhb/9780199539789.013.0015

Johnston, K. D., Ma, L., Schaeffer, L., & Everling, S. (2019). Alpha Oscillations Modulate Preparatory Activity in Marmoset Area 8Ad. *Journal of Neuroscience*, *39*(10), 1855–1866. https://doi.org/10.1523/JNEUROSCI.2703-18.2019

Juan, C.-H., Shorter-Jacobi, S. M., & Schall, J. D. (2004). Dissociation of spatial attention and saccade preparation. *Proceedings of the National Academy of Sciences of the United States of America*, *101*(43), 15541–15544. https://doi.org/10.1073/pnas.0403507101

Judd, C. H., McAllister, C. N., & Steele, W. M. (1905). General introduction to a series of studies of eye movements by means of kinetoscopic photographs. *Psychological Review*

Monographs, *7*(1), 1–16. Retrieved November 18, 2023, from https://hdl.handle.net/11858/00-001M-0000-002C-0464-C

Kalesnykas, R. P., & Hallett, P. E. (1994). Retinal eccentricity and the latency of eye saccades. *Vision Research*, *34*(4), 517–531. https://doi.org/10.1016/0042-6989(94)90165-1

Katz, L. N., Yu, G., & Krauzlis, R. J. (2023). Effects of inactivating primate lateral geniculate nucleus on visual and movement-related activity in the superior colliculus.

Keller, E. L. (1974). Participation of medial pontine reticular formation in eye movement generation in monkey. *Journal of Neurophysiology*, *37*(2), 316–332. https://doi.org/10.1152/jn.1974.37.2.316

Keller, E. L., Lee, K.-M., Park, S.-W., & Hill, J. A. (2008). Effect of Inactivation of the Cortical Frontal Eye Field on Saccades Generated in a Choice Response Paradigm. *Journal of Neurophysiology*, *100*(5), 2726–2737. https://doi.org/10.1152/jn.90673.2008

Knight, T. A., & Fuchs, A. F. (2007). Contribution of the Frontal Eye Field to Gaze Shifts in the Head-Unrestrained Monkey: Effects of Microstimulation. *Journal of Neurophysiology*, *97*(1), 618–634. https://doi.org/10.1152/jn.00256.2006

Kotani, M., Shimono, K., Yoneyama, T., Nakako, T., Matsumoto, K., Ogi, Y., Konoike, N., Nakamura, K., & Ikeda, K. (2017). An eye tracking system for monitoring face scanning patterns reveals the enhancing effect of oxytocin on eye contact in common marmosets. *Psychoneuroendocrinology*, *83*, 42–48. https://doi.org/10.1016/j.psyneuen.2017.05.009

Krubitzer, L. A., & Kaas, J. H. (1990). Cortical connections of MT in four species of primates: Areal, modular, and retinotopic patterns. *Visual Neuroscience*, *5*(2), 165–204. https://doi.org/10.1017/S0952523800000213

Kustov, A. A., & Robinson, D. L. (1996). Shared neural control of attentional shifts and eye movements. *Nature*, *384*(6604), 74–77. https://doi.org/10.1038/384074a0

Kusunoki, M., Gottlieb, J. P., & Goldberg, M. E. (2000). The lateral intraparietal area as a salience map: The representation of abrupt onset, stimulus motion, and task relevance. *Vision Research*, *40*(10), 1459–1468. https://doi.org/10.1016/S0042-6989(99)00212-6

Lee, C., Rohrer, W. H., & Sparks, D. L. (1988). Population coding of saccadic eye movements by neurons in the superior colliculus. *Nature*, *332*(6162), 357–360. https://doi.org/10.1038/332357a0

Lemon, R. (1984, February 15). *Methods for Neuronal Recording in Conscious Animal* (1st edition). Wiley.

Li, X., & Basso, M. A. (2008). Preparing to Move Increases the Sensitivity of Superior Colliculus Neurons. *The Journal of Neuroscience*, *28*(17), 4561–4577. https://doi.org/10.1523/JNEUROSCI.5683-07.2008

Lock, T. M., Baizer, J. S., & Bender, D. B. (2003). Distribution of corticotectal cells in macaque. *Experimental Brain Research*, *151*(4), 455–470. https://doi.org/10.1007/s00221-003-1500-y

Loukas, M., Lanteri, A., Ferrauiola, J., Tubbs, R. S., Maharaja, G., Shoja, M. M., Yadav, A., & Rao, V. C. (2010). Anatomy in ancient India: A focus on the Susruta Samhita. *Journal of Anatomy*, *217*(6), 646–650. https://doi.org/10.1111/j.1469-7580.2010.01294.x

Lynch, J. C., Mountcastle, V. B., Talbot, W. H., & Yin, T. C. (1977). Parietal lobe mechanisms for directed visual attention. *Journal of Neurophysiology*, *40*(2), 362–389. https://doi.org/10.1152/jn.1977.40.2.362

Lyon, D. C., & Kaas, J. H. (2001). Connectional and Architectonic Evidence for Dorsal and Ventral V3, and Dorsomedial Area in Marmoset Monkeys. *Journal of Neuroscience*, *21*(1), 249–261. https://doi.org/10.1523/JNEUROSCI.21-01-00249.2001

Ma, L., Selvanayagam, J., Ghahremani, M., Hayrynen, L. K., Johnston, K. D., & Everling, S. (2020). Single-unit activity in marmoset posterior parietal cortex in a gap saccade task. *Journal of Neurophysiology*, *123*(3), 896–911. https://doi.org/10.1152/jn.00614.2019

Magnus, H. (1901). *Die Augenheilkunde der Alten*. Georg Olms Verlag.

May, J., & Andersen, R. A. (1986). Different patterns of corticopontine projections from separate cortical fields within the inferior parietal lobule and dorsal prelunate gyrus of the macaque. *Experimental Brain Research*, *63*(2). https://doi.org/10.1007/BF00236844

Mays, L. E., & Sparks, D. L. (1980). Dissociation of visual and saccade-related responses in superior colliculus neurons. *Journal of Neurophysiology*, *43*(1), 207–232. https://doi.org/10.1152/jn.1980.43.1.207

McDowell, J. E., Dyckman, K. A., Austin, B., & Clementz, B. A. (2008). Neurophysiology and Neuroanatomy of Reflexive and Volitional Saccades: Evidence from Studies of Humans. *Brain and cognition*, *68*(3), 255–270. https://doi.org/10.1016/j.bandc.2008.08.016

McPeek, R. M., & Keller, E. L. (2001). Short-term priming, concurrent processing, and saccade curvature during a target selection task in the monkey. *Vision Research*, *41*(6), 785–800. https://doi.org/10.1016/S0042-6989(00)00287-X

McPeek, R. M., & Keller, E. L. (2002). Saccade Target Selection in the Superior Colliculus During a Visual Search Task. *Journal of Neurophysiology*, *88*(4), 2019–2034. https://doi.org/10.1152/jn.2002.88.4.2019

McPeek, R. M., & Keller, E. L. (2004). Deficits in saccade target selection after inactivation of superior colliculus. *Nature Neuroscience*, *7*(7), 757–763. https://doi.org/10.1038/nn1269

Meredith, M. A., & Stein, B. E. (1983). Interactions Among Converging Sensory Inputs in the Superior Colliculus. *Science*, *221*(4608), 389–391. https://doi.org/10.1126/science.6867718

Miller, C. T., Freiwald, W. A., Leopold, D. A., Mitchell, J. F., Silva, A. C., & Wang, X. (2016). Marmosets: A Neuroscientific Model of Human Social Behavior. *Neuron*, *90*(2), 219–233. https://doi.org/10.1016/j.neuron.2016.03.018

Mirpour, K., Arcizet, F., Ong, W. S., & Bisley, J. W. (2009). Been There, Seen That: A Neural Mechanism for Performing Efficient Visual Search. *Journal of Neurophysiology*, *102*(6), 3481–3491. https://doi.org/10.1152/jn.00688.2009

Mitchell, J. F., & Leopold, D. A. (2015). The marmoset monkey as a model for visual neuroscience. *Neuroscience Research*, *93*, 20–46. https://doi.org/10.1016/j.neures.2015.01.008

Mitchell, J. F., Priebe, N. J., & Miller, C. T. (2015). Motion dependence of smooth pursuit eye movements in the marmoset. *Journal of Neurophysiology*, *113*(10), 3954–3960. https://doi.org/10.1152/jn.00197.2015

Mitchell, J. F., Reynolds, J. H., & Miller, C. T. (2014). Active Vision in Marmosets: A Model System for Visual Neuroscience. *Journal of Neuroscience*, *34*(4), 1183–1194. https://doi.org/10.1523/JNEUROSCI.3899-13.2014

Mohler, C. W., & Wurtz, R. H. (1976). Organization of monkey superior colliculus: Intermediate layer cells discharging before eye movements. *Journal of Neurophysiology*, *39*(4), 722–744. https://doi.org/10.1152/jn.1976.39.4.722

Mohler, C. W., Goldberg, M. E., & Wurtz, R. H. (1973). Visual receptive fields of frontal eye field neurons. *Brain Research*, *61*, 385–389. https://doi.org/10.1016/0006-8993(73)90543-X

Monosov, I. E., & Thompson, K. G. (2009). Frontal Eye Field Activity Enhances Object Identification During Covert Visual Search. *Journal of Neurophysiology*, *102*(6), 3656–3672. https://doi.org/10.1152/jn.00750.2009

Moore, T., & Armstrong, K. M. (2003). Selective gating of visual signals by microstimulation of frontal cortex. *Nature*, *421*(6921), 370–373. https://doi.org/10.1038/nature01341

Moore, T., & Fallah, M. (2004). Microstimulation of the Frontal Eye Field and Its Effects on Covert Spatial Attention. *Journal of Neurophysiology*, *91*(1), 152–162. https://doi.org/10.1152/jn.00741.2002

Moore, T., & Zirnsak, M. (2017). Neural Mechanisms of Selective Visual Attention. *Annual Review of Psychology*, *68*(1), 47–72. https://doi.org/10.1146/annurev-psych-122414-033400

Moran, J., & Desimone, R. (1985). Selective Attention Gates Visual Processing in the Extrastriate Cortex. *Science*, *229*(4715), 782–784. https://doi.org/10.1126/science.4023713

Moschovakis, A. K., Karabelas, A. B., & Highstein, S. M. (1988). Structure-function relationships in the primate superior colliculus. I. Morphological classification of efferent neurons. *Journal of Neurophysiology*, *60*(1), 232–262. https://doi.org/10.1152/jn.1988.60.1.232

Moschovakis, A. K., Scudder, C. A., & Highstein, S. M. (1991). Structure of the primate oculomotor burst generator. I. Medium-lead burst neurons with upward on-directions. *Journal of Neurophysiology*, *65*(2), 203–217. https://doi.org/10.1152/jn.1991.65.2.203

Moschovakis, A. K., Scudder, C. A., Highstein, S. M., & Warren, J. D. (1991). Structure of the primate oculomotor burst generator. II. Medium-lead burst neurons with downward on-directions. *Journal of Neurophysiology*, *65*(2), 218–229. https://doi.org/10.1152/jn.1991.65.2.218

Mott, F. W., Schuster, E., & Halliburton, W. D. (1910). Cortical Lamination and Localisation in the Brain of the Marmoset. *Proceedings of the Royal Society of London. Series B, Containing Papers of a Biological Character*, *82*(553), 124–134. http://www.jstor.org/stable/80317

Munoz, D. P., Waitzman, D. M., & Wurtz, R. H. (1996). Activity of neurons in monkey superior colliculus during interrupted saccades. *Journal of Neurophysiology*, *75*(6), 2562–2580. https://doi.org/10.1152/jn.1996.75.6.2562

Munoz, D. P., & Wurtz, R. H. (1993). Fixation cells in monkey superior colliculus. II. Reversible activation and deactivation. *Journal of Neurophysiology*, *70*(2), 576–589. https://doi.org/10.1152/jn.1993.70.2.576

Munoz, D. P., & Everling, S. (2004). Look away: The anti-saccade task and the voluntary control of eye movement. *Nature Reviews Neuroscience*, *5*(3), 218–228. https://doi.org/10.1038/nrn1345

Ninomiya, T., Dougherty, K., Godlove, D. C., Schall, J. D., & Maier, A. (2015). Microcircuitry of agranular frontal cortex: Contrasting laminar connectivity between occipital

and frontal areas. *Journal of Neurophysiology*, *113*(9), 3242–3255. https://doi.org/10.
1152/jn.00624.2014

Nishida, S., Tanaka, T., & Ogawa, T. (2013). Separate evaluation of target facilitation and
distractor suppression in the activity of macaque lateral intraparietal neurons during
visual search. *Journal of Neurophysiology*, *110*(12), 2773–2791. https://doi.org/10.
1152/jn.00360.2013

Ojima, H., Honda, C. N., & Jones, E. G. (1992). Characteristics of Intracellularly Injected
Infragranular Pyramidal Neurons in Cat Primary Auditory Cortex. *Cerebral Cortex*,
2(3), 197–216. https://doi.org/10.1093/cercor/2.3.197

Paré, M., & Dorris, M. C. (2011, August 18). *The role of posterior parietal cortex in the
regulation of saccadic eye movements*. Oxford University Press. https://doi.org/10.
1093/oxfordhb/9780199539789.013.0014

Paré, M., & Hanes, D. P. (2003). Controlled Movement Processing: Superior Colliculus Ac-
tivity Associated with Countermanded Saccades. *The Journal of Neuroscience*, *23*(16),
6480–6489. https://doi.org/10.1523/JNEUROSCI.23-16-06480.2003

Paré, M., & Wurtz, R. H. (1997). Monkey Posterior Parietal Cortex Neurons Antidromically
Activated From Superior Colliculus. *Journal of Neurophysiology*, *78*(6), 3493–3497.
https://doi.org/10.1152/jn.1997.78.6.3493

Paré, M., & Wurtz, R. H. (2001). Progression in Neuronal Processing for Saccadic Eye Move-
ments From Parietal Cortex Area LIP to Superior Colliculus. *Journal of Neurophysiol-
ogy*, *85*(6), 2545–2562. https://doi.org/10.1152/jn.2001.85.6.2545

Paxinos, G., Charles, W., Michael, P., Rosa, M. G. P., & Hironobu, T. (2012). *The marmoset
brain in stereotaxic coordinates*. Academic
OCLC: 794295103.

Peel, T. R., Dash, S., Lomber, S. G., & Corneil, B. D. (2021). Frontal eye field inactiva-
tion alters the readout of superior colliculus activity for saccade generation in a task-
dependent manner. *Journal of Computational Neuroscience*, *49*(3), 229–249. https://
doi.org/10.1007/s10827-020-00760-7

Peterson, M. S., Kramer, A. F., & Irwin, D. E. (2004). Covert shifts of attention precede invol-
untary eye movements. *Perception & Psychophysics*, *66*(3), 398–405.

Pouget, P., Stepniewska, I., Crowder, E. A., Leslie, M. W., Emeric, E. E., Nelson, M. J., &
Schall, J. D. (2009). Visual and Motor Connectivity and the Distribution of Calcium-
Binding Proteins in Macaque Frontal Eye Field: Implications for Saccade Target Selec-
tion. *Frontiers in Neuroanatomy*, *3*, 2. https://doi.org/10.3389/neuro.05.002.2009

Powell, K. D., & Goldberg, M. E. (2000). Response of Neurons in the Lateral Intraparietal
Area to a Distractor Flashed During the Delay Period of a Memory-Guided Saccade.
Journal of Neurophysiology, *84*(1), 301–310. https://doi.org/10.1152/jn.2000.84.1.301

Preuss, T. M. (2019). Critique of Pure Marmoset. *Brain, Behavior and Evolution*, *93*(2-3), 92–
107. https://doi.org/10.1159/000500500

Pruszynski, J. A., King, G. L., Boisse, L., Scott, S. H., Flanagan, J. R., & Munoz, D. P. (2010).
Stimulus-locked responses on human arm muscles reveal a rapid neural pathway link-
ing visual input to arm motor output. *European Journal of Neuroscience*, *32*(6), 1049–
1057. https://doi.org/10.1111/j.1460-9568.2010.07380.x

Reser, D. H., Burman, K. J., Yu, H.-H., Chaplin, T. A., Richardson, K. E., Worthy, K. H., &
Rosa, M. G. P. (2013). Contrasting Patterns of Cortical Input to Architectural Subdi-

visions of the Area 8 Complex: A Retrograde Tracing Study in Marmoset Monkeys. *Cerebral Cortex*, *23*(8), 1901–1922. https://doi.org/10.1093/cercor/bhs177

Rizzolatti, G., Riggio, L., Dascola, I., & Umiltá, C. (1987). Reorienting attention across the horizontal and vertical meridians: Evidence in favor of a premotor theory of attention. *Neuropsychologia*, *25*(1), 31–40. https://doi.org/10.1016/0028-3932(87)90041-8

Robinson, D. A. (1972). Eye movements evoked by collicular stimulation in the alert monkey. *Vision Research*, *12*(11), 1795–1808. https://doi.org/10.1016/0042-6989(72)90070-3

Robinson, D. A., & Fuchs, A. F. (1969). Eye movements evoked by stimulation of frontal eye fields. *Journal of Neurophysiology*, *32*(5), 637–648. https://doi.org/10.1152/jn.1969.32.5.637

Rodgers, C. K., Munoz, D. P., Scott, S. H., & Paré, M. (2006). Discharge Properties of Monkey Tectoreticular Neurons. *Journal of Neurophysiology*, *95*(6), 3502–3511. https://doi.org/10.1152/jn.00908.2005

Rorie, A. E., Gao, J., McClelland, J. L., & Newsome, W. T. (2010). Integration of Sensory and Reward Information during Perceptual Decision-Making in Lateral Intraparietal Cortex (LIP) of the Macaque Monkey. *PLOS ONE*, *5*(2), e9308. https://doi.org/10.1371/journal.pone.0009308

Rosa, M. G. P., Palmer, S. M., Gamberini, M., Burman, K. J., Yu, H.-H., Reser, D. H., Bourne, J. A., Tweedale, R., & Galletti, C. (2009). Connections of the Dorsomedial Visual Area: Pathways for Early Integration of Dorsal and Ventral Streams in Extrastriate Cortex. *Journal of Neuroscience*, *29*(14), 4548–4563. https://doi.org/10.1523/JNEUROSCI.0529-09.2009

Sajad, A., Errington, S. P., & Schall, J. D. (2022). Functional architecture of executive control and associated event-related potentials in macaques. *Nature Communications*, *13*(1), 6270. https://doi.org/10.1038/s41467-022-33942-1

Sajad, A., Godlove, D. C., & Schall, J. D. (2019). Cortical microcircuitry of performance monitoring. *Nature Neuroscience*, *22*(2), 265–274. https://doi.org/10.1038/s41593-018-0309-8
Bandiera_abtest: a Cg_type: Nature Research Journals Primary_atype: Research Subject_term: Cognitive control;Cortex;Psychology;Schizophrenia Subject_term_id: cognitive-control;cortex;psychology;schizophrenia

Sasaki, S., & Shimazu, H. (1981). Reticulovestibular Organization Participating in Generation of Horizontal Fast Eye Movement*. *Annals of the New York Academy of Sciences*, *374*(1), 130–143. https://doi.org/10.1111/j.1749-6632.1981.tb30866.x

Saslow, M. G. (1967). Effects of Components of Displacement-Step Stimuli Upon Latency for Saccadic Eye Movement. *JOSA*, *57*(8), 1024–1029. https://doi.org/10.1364/JOSA.57.001024

Savjani, R. R., Katyal, S., Halfen, E., Kim, J. H., & Ress, D. (2018). Polar-angle representation of saccadic eye movements in human superior colliculus. *NeuroImage*, *171*, 199–208. https://doi.org/10.1016/j.neuroimage.2017.12.080

Schaeffer, D. J., Gilbert, K. M., Hori, Y., Hayrynen, L. K., Johnston, K. D., Gati, J. S., Menon, R. S., & Everling, S. (2019). Task-based fMRI of a free-viewing visuo-saccadic network in the marmoset monkey. *NeuroImage*, *202*, 116147. https://doi.org/10.1016/j.neuroimage.2019.116147

Schaeffer, D. J., Selvanayagam, J., Johnston, K. D., Menon, R. S., Freiwald, W. A., & Everling, S. (2020). Face selective patches in marmoset frontal cortex. *Nature Communications*, *11*(1), 4856. https://doi.org/10.1038/s41467-020-18692-2

Schall, J. D. (1991). Neuronal activity related to visually guided saccades in the frontal eye fields of rhesus monkeys: Comparison with supplementary eye fields. *Journal of Neurophysiology*, *66*(2), 559–579. https://doi.org/10.1152/jn.1991.66.2.559

Schall, J. D. (2004). On the role of frontal eye field in guiding attention and saccades. *Vision Research*, *44*(12), 1453–1467. https://doi.org/10.1016/j.visres.2003.10.025

Schall, J. D., & Hanes, D. P. (1993). Neural basis of saccade target selection in frontal eye field during visual search. *Nature*, *366*(6454), 467–469. https://doi.org/10.1038/366467a0

Schall, J. D., Hanes, D. P., Thompson, K. G., & King, D. J. (1995). Saccade target selection in frontal eye field of macaque. I. Visual and premovement activation. *The Journal of Neuroscience*, *15*(10), 6905–6918. https://doi.org/10.1523/JNEUROSCI.15-10-06905.1995

Schall, J. D., Morel, A., King, D. J., & Bullier, J. (1995). Topography of visual cortex connections with frontal eye field in macaque: Convergence and segregation of processing streams. *The Journal of Neuroscience*, *15*(6), 4464–4487. https://doi.org/10.1523/JNEUROSCI.15-06-04464.1995

Schall, J. D., & Thompson, K. G. (1999). Neural Selection and Control of Visually Guided Eye Movements. *Annual Review of Neuroscience*, *22*(1), 241–259. https://doi.org/10.1146/annurev.neuro.22.1.241

Schiller, P. H., & Malpeli, J. G. (1977). Properties and tectal projections of monkey retinal ganglion cells. *Journal of Neurophysiology*, *40*(2), 428–445. https://doi.org/10.1152/jn.1977.40.2.428

Schiller, P. H., Stryker, M., Cynader, M., & Berman, N. (1974). Response characteristics of single cells in the monkey superior colliculus following ablation or cooling of visual cortex. *Journal of Neurophysiology*, *37*(1), 181–194. https://doi.org/10.1152/jn.1974.37.1.181

Schiller, P. H., True, S. D., & Conway, J. L. (1980). Deficits in eye movements following frontal eye-field and superior colliculus ablations. *Journal of Neurophysiology*, *44*(6), 1175–1189. https://doi.org/10.1152/jn.1980.44.6.1175

Schiller, P. H., & Chou, I.-H. (2000). The effects of anterior arcuate and dorsomedial frontal cortex lesions on visually guided eye movements: 2. Paired and multiple targets. *Vision Research*, *40*(10), 1627–1638. https://doi.org/10.1016/S0042-6989(00)00058-4

Schwemmer, M. A., Feng, S. F., Holmes, P. J., Gottlieb, J., & Cohen, J. D. (2015). A Multi-Area Stochastic Model for a Covert Visual Search Task. *PLoS ONE*, *10*(8), e0136097. https://doi.org/10.1371/journal.pone.0136097

Segraves, M. A. (1992). Activity of monkey frontal eye field neurons projecting to oculomotor regions of the pons. *Journal of Neurophysiology*, *68*(6), 1967–1985. https://doi.org/10.1152/jn.1992.68.6.1967

Segraves, M. A., & Goldberg, M. E. (1987). Functional properties of corticotectal neurons in the monkey's frontal eye field. *Journal of Neurophysiology*, *58*(6), 1387–1419. https://doi.org/10.1152/jn.1987.58.6.1387

Selvanayagam, J., Johnston, K. D., Wong, R. K., Schaeffer, D., & Everling, S. (2021). Ketamine disrupts gaze patterns during face viewing in the common marmoset. *Journal of Neurophysiology*, *126*(1), 330–339. https://doi.org/10.1152/jn.00078.2021

Shadlen, M. N., & Newsome, W. T. (1996). Motion perception: Seeing and deciding. *Proceedings of the National Academy of Sciences*, *93*(2), 628–633. https://doi.org/10.1073/pnas.93.2.628

Sheliga, B. M., Riggio, L., Craighero, L., & Rizzolatti, G. (1995). Spatial attention-determined modifications in saccade trajectories. *NeuroReport*, *6*(3), 585. Retrieved November 1, 2023, from https://journals.lww.com/neuroreport/abstract/1995/02000/spatial_attention_determined_modifications_in.44.aspx

Shen, K., Valero, J., Day, G. S., & Paré, M. (2011). Investigating the role of the superior colliculus in active vision with the visual search paradigm. *The European Journal of Neuroscience*, *33*(11), 2003–2016. https://doi.org/10.1111/j.1460-9568.2011.07722.x

Shibutani, H., Sakata, H., & Hyvärinen, J. (1984). Saccade and blinking evoked by microstimulation of the posterior parietal association cortex of the monkey. *Experimental Brain Research*, *55*(1). https://doi.org/10.1007/BF00240493

Sommer, M. A., & Wurtz, R. H. (2001). Frontal Eye Field Sends Delay Activity Related to Movement, Memory, and Vision to the Superior Colliculus. *Journal of Neurophysiology*, *85*(4), 1673–1685. https://doi.org/10.1152/jn.2001.85.4.1673

Sommer, M. A., & Wurtz, R. H. (2004). What the Brain Stem Tells the Frontal Cortex. I. Oculomotor Signals Sent From Superior Colliculus to Frontal Eye Field Via Mediodorsal Thalamus. *Journal of Neurophysiology*, *91*(3), 1381–1402. https://doi.org/10.1152/jn.00738.2003

Sommer, M. A., & Wurtz, R. H. (2008). Visual Perception and Corollary Discharge. *Perception*, *37*(3), 408–418. Retrieved August 3, 2023, from https://www.ncbi.nlm.nih.gov/pmc/articles/PMC2807735/

Sparks, D. L. (2002). The brainstem control of saccadic eye movements. *Nature Reviews Neuroscience*, *3*(12), 952–964. https://doi.org/10.1038/nrn986

Sparks, D. L., & Mays, L. E. (1980). Movement fields of saccade-related burst neurons in the monkey superior colliculus. *Brain Research*, *190*(1), 39–50. https://doi.org/10.1016/0006-8993(80)91158-0

Stanton, G. B., Goldberg, M. E., & Bruce, C. J. (1988). Frontal eye field efferents in the macaque monkey: I. Subcortical pathways and topography of striatal and thalamic terminal fields. *Journal of Comparative Neurology*, *271*(4), 473–492. https://doi.org/10.1002/cne.902710402

Stepniewska, I., Preuss, T. M., & Kaas, J. H. (2007). Thalamic connections of the dorsal and ventral premotor areas in New World owl monkeys. *Neuroscience*, *147*(3), 727–745. https://doi.org/10.1016/j.neuroscience.2007.03.054

Stepniewska, I., Cerkevich, C. M., & Kaas, J. H. (2016). Cortical Connections of the Caudal Portion of Posterior Parietal Cortex in Prosimian Galagos. *Cerebral Cortex (New York, NY)*, *26*(6), 2753–2777. https://doi.org/10.1093/cercor/bhv132

Sushruta. (1907). *An English Translation of The Sushruta Samhita* (K. K. L. Bhishagratna, Trans.).

Swadlow, H. A. (2002). Thalamocortical control of feed-forward inhibition in awake somatosensory 'barrel' cortex. *Philosophical Transactions of the Royal Society B: Biological Sciences*, *357*(1428), 1717–1727. https://doi.org/10.1098/rstb.2002.1156

Thier, P., & Andersen, R. A. (1996). Electrical microstimulation suggests two different forms of representation of head-centered space in the intraparietal sulcus of rhesus monkeys. *Proceedings of the National Academy of Sciences*, *93*(10), 4962–4967. https://doi.org/10.1073/pnas.93.10.4962

Thier, P., & Andersen, R. A. (1998). Electrical Microstimulation Distinguishes Distinct Saccade-Related Areas in the Posterior Parietal Cortex. *Journal of Neurophysiology*, *80*(4), 1713–1735. https://doi.org/10.1152/jn.1998.80.4.1713

Thomas, N. W. D., & Paré, M. (2007). Temporal Processing of Saccade Targets in Parietal Cortex Area LIP During Visual Search. *Journal of Neurophysiology*, *97*(1), 942–947. https://doi.org/10.1152/jn.00413.2006

Thompson, K. G., Bichot, N. P., & Sato, T. R. (2005). Frontal Eye Field Activity Before Visual Search Errors Reveals the Integration of Bottom-Up and Top-Down Salience. *Journal of neurophysiology*, *93*(1), 337–351. https://doi.org/10.1152/jn.00330.2004

Thompson, K. G., Bichot, N. P., & Schall, J. D. (1997). Dissociation of Visual Discrimination From Saccade Programming in Macaque Frontal Eye Field. *Journal of Neurophysiology*, *77*(2), 1046–1050. https://doi.org/10.1152/jn.1997.77.2.1046

Thompson, K. G., Hanes, D. P., Bichot, N. P., & Schall, J. D. (1996). Perceptual and motor processing stages identified in the activity of macaque frontal eye field neurons during visual search. *Journal of Neurophysiology*, *76*(6), 4040–4055. https://doi.org/10.1152/jn.1996.76.6.4040

Treisman, A. M., & Gelade, G. (1980). A feature-integration theory of attention. *Cognitive Psychology*, *12*(1), 97–136. https://doi.org/10.1016/0010-0285(80)90005-5

Usrey, W. M., & Fitzpatrick, D. (1996). Specificity in the axonal connections of layer VI neurons in tree shrew striate cortex: Evidence for distinct granular and supragranular systems. *Journal of Neuroscience*, *16*(3), 1203–1218. https://doi.org/10.1523/JNEUROSCI.16-03-01203.1996

van der Steen, J., Russell, I. S., & James, G. O. (1986). Effects of unilateral frontal eye-field lesions on eye-head coordination in monkey. *Journal of Neurophysiology*, *55*(4), 696–714. https://doi.org/10.1152/jn.1986.55.4.696

van Leeuwen, J., & Belopolsky, A. V. (2018). Distractor displacements during saccades are reflected in the time-course of saccade curvature. *Scientific Reports*, *8*, 2469. https://doi.org/10.1038/s41598-018-20578-9

Wade, N. J. (2010). Pioneers of eye movement research. *i-Perception*, *1*(2), 33–68. https://doi.org/10.1068/i0389

Walker, R., Deubel, H., Schneider, W. X., & Findlay, J. M. (1997). Effect of Remote Distractors on Saccade Programming: Evidence for an Extended Fixation Zone. *Journal of Neurophysiology*, *78*(2), 1108–1119. https://doi.org/10.1152/jn.1997.78.2.1108

Wardak, C., Ben Hamed, S., Olivier, E., & Duhamel, J.-R. (2012). Differential effects of parietal and frontal inactivations on reaction times distributions in a visual search task. *Frontiers in Integrative Neuroscience*, *6*. https://doi.org/10.3389/fnint.2012.00039

Wardak, C., Ibos, G., Duhamel, J.-R., & Olivier, E. (2006). Contribution of the Monkey Frontal Eye Field to Covert Visual Attention. *The Journal of Neuroscience*, *26*(16), 4228–4235. https://doi.org/10.1523/JNEUROSCI.3336-05.2006

Wardak, C., Olivier, E., & Duhamel, J.-R. (2002). Saccadic Target Selection Deficits after Lateral Intraparietal Area Inactivation in Monkeys. *The Journal of Neuroscience*, *22*(22), 9877–9884. https://doi.org/10.1523/JNEUROSCI.22-22-09877.2002

Wardak, C., Olivier, E., & Duhamel, J.-R. (2004). A Deficit in Covert Attention after Parietal Cortex Inactivation in the Monkey. *Neuron*, *42*(3), 501–508. https://doi.org/10.1016/S0896-6273(04)00185-0

Wen, W., Guo, S., Huang, H., & Li, S. (2023). Causal investigation of mid-frontal theta activity in memory guided visual search. *Cognitive Neuroscience*, *14*(3), 115–120. https://doi.org/10.1080/17588928.2023.2227787

Wolfe, J. M. (2021). Guided Search 6.0: An updated model of visual search. *Psychonomic Bulletin & Review*, *28*(4), 1060–1092. https://doi.org/10.3758/s13423-020-01859-9

Wolfe, J. M., & Horowitz, T. S. (2004). What attributes guide the deployment of visual attention and how do they do it? *Nature Reviews Neuroscience*, *5*(6), 495–501. https://doi.org/10.1038/nrn1411

Wurtz, R. H., & Goldberg, M. E. (1972). Activity of superior colliculus in behaving monkey. 3. Cells discharging before eye movements. *Journal of Neurophysiology*, *35*(4), 575–586. https://doi.org/10.1152/jn.1972.35.4.575

Wurtz, R. H., & Mohler, C. W. (1976). Organization of monkey superior colliculus: Enhanced visual response of superficial layer cells. *Journal of Neurophysiology*, *39*(4), 745–765. https://doi.org/10.1152/jn.1976.39.4.745

Wurtz, R. H., & Goldberg, M. E. (1971). Superior Colliculus Cell Responses Related to Eye Movements in Awake Monkeys. *Science*, *171*(3966), 82–84. https://doi.org/10.1126/science.171.3966.82

Yarbus, A. L. (1967). *Eye Movements and Vision* (L. A. Riggs, Ed.; B. Haigh, Trans.). Plenum Press.

Yin, T. C. T., & Mountcastle, V. B. (1977). Visual Input to the Visuomotor Mechanisms of the Monkey's Parietal Lobe. *Science*, *197*(4311), 1381–1383. https://doi.org/10.1126/science.408924

Zanini, A., Dureux, A., Selvanayagam, J., & Everling, S. (2023). Ultra-high field fMRI identifies an action-observation network in the common marmoset. *Communications Biology*, *6*, 553. https://doi.org/10.1038/s42003-023-04942-8

Zénon, A., Hamed, S. B., Duhamel, J.-R., & Olivier, E. (2009). Attentional guidance relies on a winner-take-all mechanism. *Vision Research*, *49*(12), 1522–1531. https://doi.org/10.1016/j.visres.2009.03.010

Zhang, M., & Barash, S. (2000). Neuronal switching of sensorimotor transformations for anti-saccades. *Nature*, *408*(6815), 971–975. https://doi.org/10.1038/35050097

Zhang, M., & Barash, S. (2004). Persistent LIP Activity in Memory Antisaccades: Working Memory For a Sensorimotor Transformation. *Journal of Neurophysiology*, *91*(3), 1424–1441. https://doi.org/10.1152/jn.00504.2003

Zhou, H.-H., & Thompson, K. G. (2009). Cognitively-directed spatial selection in the frontal eye field in anticipation of visual stimuli to be discriminated. *Vision research*, *49*(10), 1205–1215. https://doi.org/10.1016/j.visres.2008.03.024

Chapter 2

Localization of the marmoset frontal eye fields using microstimulation

2.1 Introduction

Described originally by Ferrier (1875) as a cortical area in macaque monkeys where electrical stimulation elicited contralateral eye and head movements, the frontal eye fields (FEF) in macaques and humans are now increasingly regarded as not only a motor area for saccades and head movements, but also as a critical region for the deployment of overt and covert spatial attention (Awh et al., 2006). Over the past 40 years, most of our knowledge regarding the neural processes in the FEF has come from experiments in awake behaving macaque monkeys. In these Old-World primates, FEF is defined as an area within the rostral bank and fundus of the arcuate sulcus from which electrical microstimulation evokes saccades at low currents ($< 50 \, \mu A$) (Bruce et al., 1985). Stimulation, recording, and pharmacological manipulation studies in trained macaque monkeys have and continue to provide critical insights into the neural processes in FEF that underlie saccade control and visual attention. However, the local FEF microcircuitry remains poorly understood as, due to its location within a sulcus, macaque FEF is virtually inaccessible to intralaminar recordings and manipulations.

The New-World common marmoset (*Callithrix jacchus*) is a promising alternative primate model for studying FEF microcircuitry. These small primates have a largely lissencephalic cortex and can be trained to perform saccadic eye movement tasks head-restrained (Johnston et al., 2018; Johnston et al., 2019; Mitchell et al., 2014). A first step towards such experiments is the physiological identification of the FEF in marmosets. Existing evidence for the location of this area in this species, however, remains limited and unclear. An early marmoset study by Mott and colleagues (1910) reported that both eye and combined eye and head movements could be evoked by electrical stimulation at several frontal cortical sites. Subsequently, Blum and colleagues (1982) confirmed and extended these earlier results. They observed movements including ipsilateral and contralateral saccades, eye movements in all directions, and slow drifting movements. It seems that these eye movements were evoked in areas 6DC, 6DR, 8aD, and 46 with no clear topography of direction or amplitude. Interpretation of these earlier studies is difficult, however, as the anaesthetized preparations used most likely influenced the properties of the eye movements evoked (Robinson & Fuchs, 1969).

More recently, anatomical evidence has suggested that marmoset FEF lies within areas 45 and 8aV (Reser et al., 2013). Both areas have widespread connections with extrastriate visual areas, and areas labelled FEF and FV by (Collins et al., 2005), which may correspond to areas 45 and 8aV, contain clusters of neurons projecting to the SC, an area critical for the initiation of saccadic and orienting movements. Area 8aV in marmosets also contains large layer V pyramidal neurons, a cytoarchitectonic characteristic of macaque FEF (Stanton et al., 1989). Consistent with this notion, fMRI studies in marmosets have reported BOLD activation in areas 45 and 8aV in response to visual stimuli and saccades (Hung et al., 2015a; Schaeffer, Gilbert, Hori, Gati, et al., 2019), though a resting-state fMRI functional connectivity study found the strongest SC connectivity in area 8aD, at the border of area 6DR (Ghahremani et al., 2017). The authors proposed that this region either corresponded to the marmoset FEF or that it may encode large amplitude saccades, while area 8aV may encode small amplitude saccades.

Here, we set out to physiologically identify the marmoset FEF using the classical approach of intracortical electrical microstimulation (ICMS). We applied microstimulation trains via chronically implanted 96-channel electrode arrays placed to target a broad range of frontal cortical areas in three awake marmosets. Our findings revealed a topography of contralateral saccade amplitude in marmoset frontal cortex similar to that observed in macaques (Bruce et al., 1985; Schall, 1997) and humans (Foerster, 1926), with small saccades being encoded in area 45 and lateral parts of area 8aV, and larger saccades combined with contralateral neck and shoulder movements encoded in the medial posterior portion of area 8aV, area 8C, and area 6DR.

2.2 Methods

2.2.1 Subjects

We obtained data from 3 adult common marmosets (Callithrix jacchus; M1 male, 17 months; M2 female 20 months; M3 male 23 months). All experimental procedures conducted were in accordance with the Canadian Council of Animal Care policy on the care and use of laboratory animals and a protocol approved by the Animal Care Committee of the University of Western Ontario Council on Animal Care. The animals were under the close supervision of university veterinarians.

Prior to the commencement of microstimulation experiments, each animal was acclimated to restraint in a custom primate chair (Johnston et al., 2018). Animals then underwent an aseptic surgical procedure under general anaesthesia in which 96 channel Utah arrays (4mm x 4mm; 1mm electrode length; 400μm pitch; iridium oxide tips) were implanted in left frontal cortex. During this surgery, a microdrill was used to initially open 4mm burr holes in the skull and were enlarged as necessary using a rongeur. Arrays were manually inserted; wires and connectors were fixed to the skull using dental adhesive (Bisco All-Bond, Bisco Dental Products, Richmond, BC, Canada). Once implanted, the array site was covered with silicone adhesive to seal the burr hole (Kwik Sil, World Precision Instruments, Sarasota, FLA, USA). A screw-hole was drilled into the skull on the opposite side to the location of the implanted array to place the ground screw. The ground wire of the array was then tightly wound around the base of the screw to ensure good electrical connection. A combination recording chamber/head

holder (Johnston et al., 2018) was placed around the array and connectors and fixed in place using further layers of dental adhesive. Finally, a removable protective cap was placed on the chamber.

2.2.2   Localizing the array

To precisely determine array locations, high-resolution T2-weighted structural magnetic resonance images (MRI; obtained pre-surgery) were co-registered with computerized tomography (CT) scans (obtained post-surgery). The MRI images provided each marmoset's brain geometry with reference to the location of the skull, while the CT images allowed for localization of the skull and the array boundaries. By co-registering the skulls across the two modalities, the precise array-to-brain location was determined for each animal.

Pre-surgical MRIs were acquired using an 9.4 T 31 cm horizontal bore magnet (Varian/Agilent, Yarnton, UK) and Bruker BioSpec Avance III console with the software package Paravision-6 (Bruker BioSpin Corp, Billerica, MA) and a custom-built high performance 15 cm diameter gradient coil with 400 mT/m maximum gradient strength (xMR, London, CAN; Peterson et al., 2018). A geometrically optimized 8-channel phased array receive coil was designed in-house, for SNR improvement and to allow for acceleration of the echo planar imaging of marmoset cohorts (Gilbert et al., 2019). Preamplifiers were located behind the animal and the receive coil was placed inside a quadrature birdcage coil (12-cm inner diameter) used for transmission. Prior to each imaging session, anaesthesia was induced with ketamine hydrochloride at 20 mg/kg. During scanning, marmosets were anaesthetized with isoflurane and maintained at a level of 2% throughout the scan by means of inhalation. Oxygen flow rate was kept between 1.75 and 2.25 l/min throughout the scan. Respiration, SpO2, and heart rate were continuously monitored and were observed to be within the normal range throughout the scans. Body temperature was also measured and recorded throughout, maintained using warm water circulating blankets, thermal insulation, and warmed air. All animals were head-fixed in stereotactic position using a custom-built MRI bed with ear bars, eye bars, and a palate bar housed within the anaesthesia mask (Gilbert et al., 2019). All imaging was performed at the Centre for Functional and Metabolic Mapping at the University of Western Ontario. T2-weighted structural scans were acquired for each animal with the following parameters: TR = 5500 ms, TE = 53 ms, field of view = 51.2×51.2 mm, matrix size = 384×384, voxel size = $0.133 \times 0.133 \times 0.5$ mm, slices = 42, bandwidth = 50 kHz, GRAPPA acceleration factor: 2.

CT scans were obtained on a micro-CT scanner (eXplore Locus Ultra, GR Healthcare Biosciences, London, ON) after array implantation. Prior to the scan, marmosets were anaesthetized with 15mg/kg Ketamine mixed with 0.025mg/kg Medetomidine. X-ray tube potential of 120 kV and tube current of 20 mA were used for the scan, with the data acquired at 0.5° angular increment over 360°, resulting in 1000 views. The resulting CT images were then reconstructed into 3D with isotropic voxel size of 0.154 mm. Heart rate and SpO2 were monitored throughout the session. At the end of the scan, the injectable anaesthetic was reversed with an IM injection of 0.025mg/kg Ceptor.

The raw MRI and CT images were converted to NifTI format using dcm2niix (Li et al., 2016) and the MRIs were reoriented from the sphinx position using FSL software (Smith et al., 2004). Then, using FSL (FSLeyes nudge function), each animal's CT image was manually aligned to their MRI image based on the skull location - this allowed for co-localization of

the array and brain surface. The array position from the CT image was determined by a hyper-intensity concomitant with the metallic contacts contained within the array; this hyper-intensity stood out against the lower intensities of the skull and surrounding tissues. A region of interest (ROI) was manually drawn within the array location for each animal to be displayed on the NIH marmoset brain atlas surface (Liu et al., 2018) for ease of viewing. The NIH marmoset brain atlas is an ultra-high resolution ex vivo MRI image dataset that contains the locations of cytoarchitectonic boundaries (Liu et al., 2018). As such, to determine the array location with reference to the cytoarchitectonic boundaries, we non-linearly registered the NIH template brain to each marmoset's T2-weighted image using Advanced Normalization Tools (ANTs Avants et al., 2011) software. The resultant transformation matrices were then applied to the cytoarchitectonic boundary image included with the NIH template brain atlas. The olfactory bulb was manually removed from the marmoset T2-weighted image of each animal prior to registration, as it was not included in the template image. As a result of the transformations, the template brain surface, the cytoarchitectonic boundaries, and the array location (ROI described above) could be rendered on each animals' individual native-space brain surface.

We expect that this alignment procedure will be useful for future studies interested in transforming a relatively large functional patch of interest (e.g., ventrolateral FEF) in template space (i.e., with reference to cytoarchitectonic boundaries) to individual animal's MRI native space to determine array implantation loci. Indeed, some variability in cytoarchitecture (or perhaps more importantly, functional architecture) can be expected to occur across individual animals. As such, highly specific localization, like that of individual electrode implantation may require additional mapping to optimize the localization of the saccade vector and amplitude of interest.

2.2.3 Data collection

Following recovery, we verified that electrode contacts were within the cortex by monitoring extracellular neural activity using the Open Ephys acquisition board (http://www.open-ephys.org) and digital headstages (Intan Technologies, Los Angeles, CA, USA). Upon observing single or multiunit activity at multiple sites in the array, we commenced microstimulation experiments.

Animals were head restrained in a custom primate chair (Johnston et al., 2018) mounted on a table in a sound attenuating chamber (Crist Instruments Co., Hagerstown, MD, USA). A spout was placed at the monkey's mouth to deliver a viscous preferred reward of acacia gum. This was delivered via infusion pump (Model NE-510, New Era Pump Systems, Inc., Farmingdale, New York, USA).

In each session, eye position was calibrated by rewarding 300 to 600ms fixations on a marmoset face presented at one of five locations on the display monitor using the CORTEX real-time operating system (NIMH, Bethesda, MD, USA). Faces were presented at the display centre, at 6 degrees to the right and left of centre, and at 6 degrees directly above and below centre. All stimuli were presented on a CRT monitor (ViewSonic Optiquest Q115, 76 Hz non-interlaced, 1600 x 1280 resolution).

Monkeys freely viewed short repeating video clips to sustain their alertness while we applied manually triggered microstimulation trains. Monkeys were intermittently rewarded at random time intervals to maintain their interest. Microstimulation trains were delivered using the Intan RHS2000 Stimulation/Recording Controller system and digital stimulation/recording

headstages (Intan Technologies, Los Angeles, CA, USA). Stimulation trains consisted of 0.2-0.3ms biphasic current pulses delivered at 300 Hz for a duration of 100-400ms, at current amplitudes varying between 5 and 300 μA. At sites where skeletomotor or saccadic responses were evoked, we carried out a current series to determine thresholds. The threshold was defined as the minimum current at which a given response was evoked on 50% of stimulation trials. Skeletomotor responses were observed and recorded manually by two researchers. Eye position was digitally recorded at 1 kHz via video tracking of the left pupil (EyeLink 1000, SR Research, Ottawa, ON, Canada).

2.2.4   Data analysis

Analysis was performed with custom python code. Eye velocity (visual deg/s) was obtained by smoothing and numerical differentiation. Saccades were defined as horizontal or vertical eye velocity exceeding 30 deg/s. Blinks were defined as the radial eye velocity exceeding 1500 deg/s. Slow eye movements were manually identified by inspection of the eye traces.

As we did not require marmosets to fixate during stimulation, saccades following stimulation could be spontaneous. A bootstrap analysis was used to quantitatively determine if saccades were more probable following stimulation than at any other time during a session. In a single session, 60-80 trains were delivered at a single site holding stimulation parameters constant over a 2-minute period. Stimulation onset times were shuffled (time points were randomly sampled without replacement with millisecond resolution over the duration of the session) and the probability of a saccade occurring in a 200ms window following the selected timepoints was computed. This was repeated 1000 times for each session to obtain a distribution of probabilities of saccade occurrence. The percentile rank of the probability of stimulation evoking a saccade with respect to this distribution was computed; the 95th percentile marked the 5% significance criterion indicating a session where stimulation significantly increased the probability of saccade occurrence.

2.3   Results

2.3.1   Evoked skeletomotor and oculomotor responses

Array locations were confirmed using CT scans obtained after the surgery, which were co-registered with MR scans obtained before the surgery (see Figure 2.1a). Microstimulation was conducted at 288 sites across 3 marmosets. We observed a range of skeletomotor and oculomotor responses across the frontal cortex (Figure 2.1b, c).

At the most posterior sites, we observed primarily single joint movements with a gross medio-lateral topography. We observed hindlimb movements (leg, foot, toes) most medially, followed by forelimb (arm, hand, finger) and facial movements (eyelid, ear, nose, jaw) most laterally - an organization characteristic of primary motor cortex (area 4) (Burish et al., 2008; Wakabayashi et al., 2018). Anterior to this, we observed overlapping representation of forelimb, facial, shoulder, and neck musculature with no obvious organization, similar to that observed in the marmoset premotor cortex (area 6) (Burish et al., 2008, c.f. Wakabayashi et al., 2018).
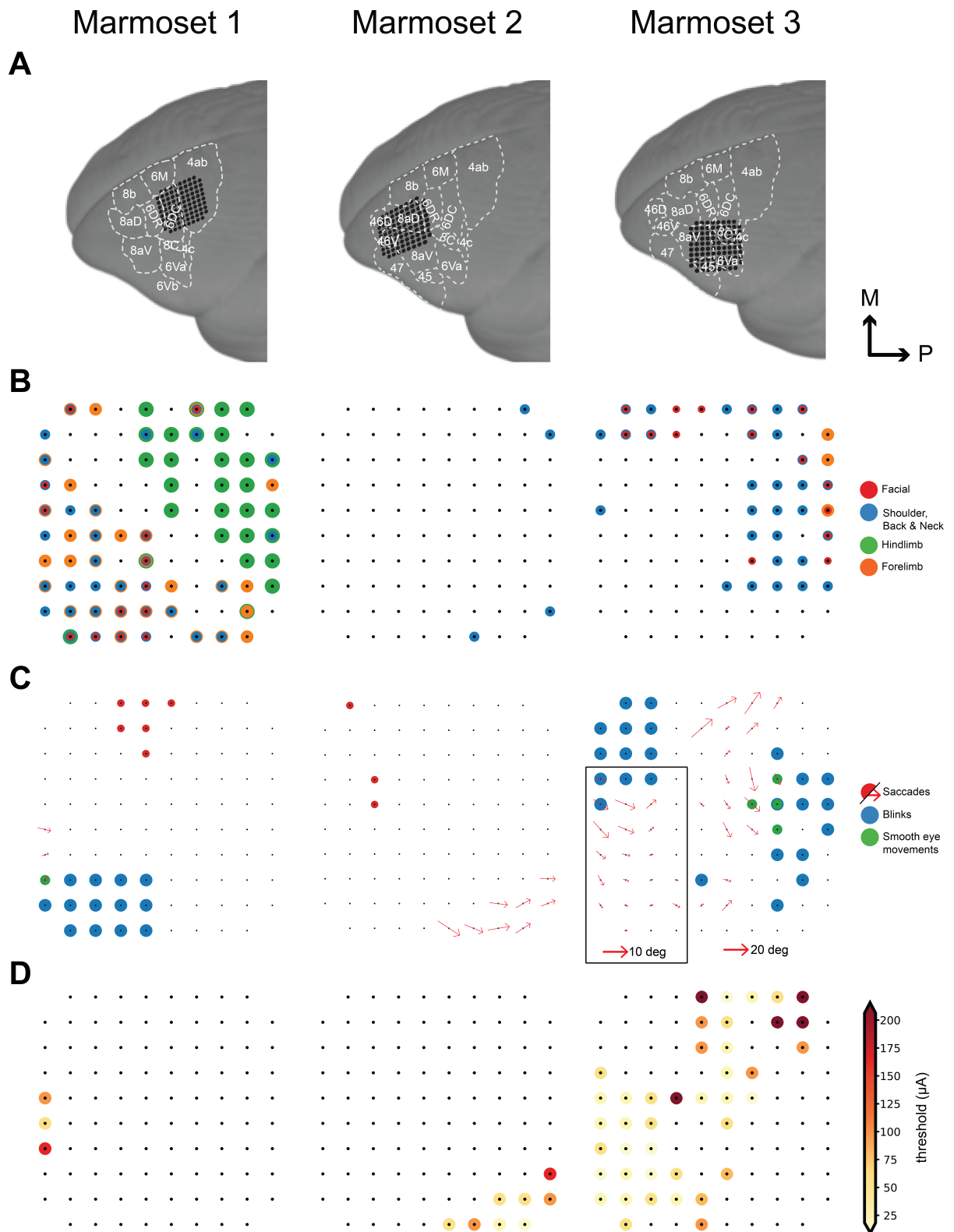
Figure 2.1: Evoked motor responses.

Figure 2.1: *Evoked motor responses (continued).* (A) Array locations in each marmoset reconstructed using MR and CT images (see Localizing the array). (B) Pattern of evoked skeletomotor responses in each marmoset. (C) Pattern of evoked oculomotor responses in each marmoset. At sites where fixed vector saccades were observed, mean saccade vector is plotted. Mean saccade vectors were computed at the minimum current where saccades are evoked at least 75% of the time. Inset shows small saccade vectors at 2x scale for Marmoset 3. (D) Thresholds for saccades at sites where saccades were evoked at currents ≤ $300\mu A$.
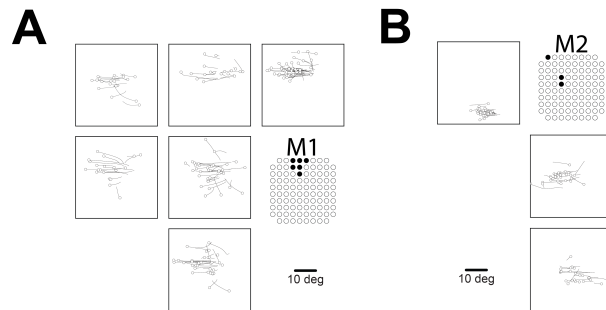
Figure 2.2: Saccades evoked in non-FEF sites. Representative traces for goal-directed saccades from dorsomedial sites in Marmoset 1 (A) and saccades from rostral sites in Marmoset 2 (B). Open circles indicate eye position at saccade onset.

We elicited saccades at 61 sites across 3 marmosets (see Figure 2.1c). At 6 sites on the border of area 6DC and 6M, we observed goal directed saccades characteristic of the supplementary eye fields (SEF), albeit at long latencies (70-110ms) and high currents (200 µA) (see Figure 2.2a). At 3 sites in area 46D and the anterior portion of area 8aD, we elicited saccades with no clear pattern at long latencies (75-90ms) and high currents (300 µA) (see Figure 2.2b). Saccades evoked from these sites were mostly directed to the hemifield contralateral to the stimulated site, though some saccades directed to the ipsilateral hemifield were observed.

We elicited fixed vector saccades at 52 sites across areas 6DR, 8C, 8aV and 45. Mean saccade vectors are plotted in Figure 2.1c. Representative saccade traces are plotted in Figure 2.3. In areas 6DR, 8C and the medial portion of 8aV, we observed larger saccades often coupled with shoulder, neck, and ear movements with the most common response being a shoulder rotation that resembled orienting towards contralateral side. In area 45 and the lateral portion of area 8aV, we observed smaller saccades with no visible skeletomotor responses. Slow eye movements could be elicited at 5 sites in areas 6DR and 8C.

2.3.2   Saccade thresholds and latencies

At sites where we observed fixed vector saccades, we conducted current series to determine thresholds and characterize any current-related changes in saccade metrics. Current series from five representative sites are shown in Figure 2.4a-e. Thresholds were defined as the minimum current at which saccades could be evoked 50% of the time (see Figure 2.4g). Thresholds ranged from 12-300 µA. Saccades were evoked at low thresholds (< 50 µA) at 35 of the 52 sites from which we were able to evoke fixed vector saccades (see Figure 2.1d). Saccade
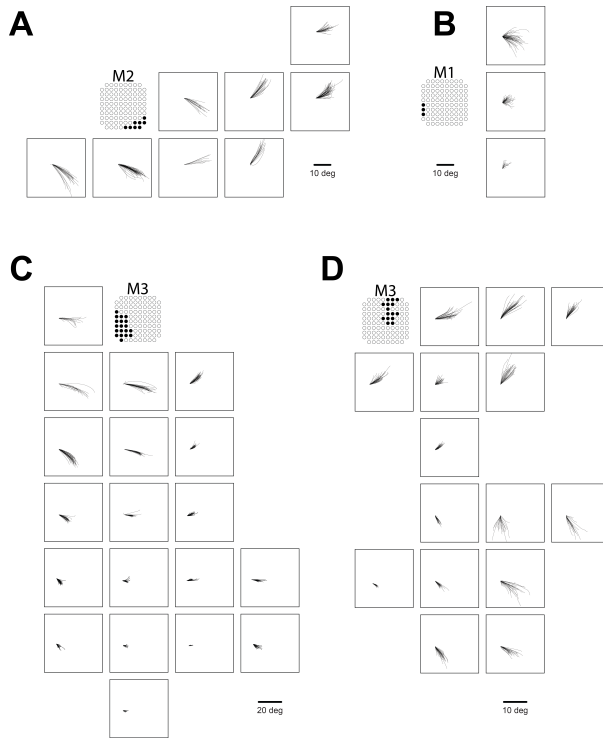
Figure 2.3: Saccades evoked in FEF sites. Representative traces for fixed vector saccades in (A) Marmoset 2 (A), Marmoset 1 (B) and Marmoset 3 (C, D).

metrics were computed at the minimum current at which saccades could be evoked 75% of the time.

Each site had a stereotypical saccade latency, though we found no systematic variation in saccade latency with respect to site coordinates nor any other saccade metrics. Saccade latencies ranged from 25-85ms, with the majority falling in the range between 40-60ms (see Figure 2.4h). Saccade latencies were generally longer and more variable near the current threshold for a given site. When using high currents well above threshold (200-300 µA), uniformly short saccade latencies were observed (15-45ms).

2.3.3 Topography of evoked saccades

Evoked saccades were directed contralateral to the stimulated hemisphere and mostly fixed vector (see Figure 2.1c, Figure 2.3, Figure 2.4a-e), exhibiting relatively consistent directions and amplitudes independent of the initial eye position. Although we did not systematically vary initial eye positions, the fact that marmosets were allowed to freely direct their gaze across video clips on the display monitor during experimental sessions ensured a wide range of initial eye positions at the time of microstimulation onset. Most initial eye positions fell within a 13 degree range similar to observations elsewhere in marmosets (Mitchell et al., 2014) and other New World monkeys (Heiney & Blazquez, 2011). 90% of initial eye positions fell within the following ranges for each marmoset: Marmoset 1: -13.6 to 12.4 abscissa, -10.7 to 11.4 ordinate; Marmoset 2: -12.7 to 15.7 abscissa, -11.7 to 9.6 ordinate; Marmoset 3: -12.9 to 12.7 abscissa, -18.5 to 14.3 ordinate. Amplitude decreased progressively from medial (large
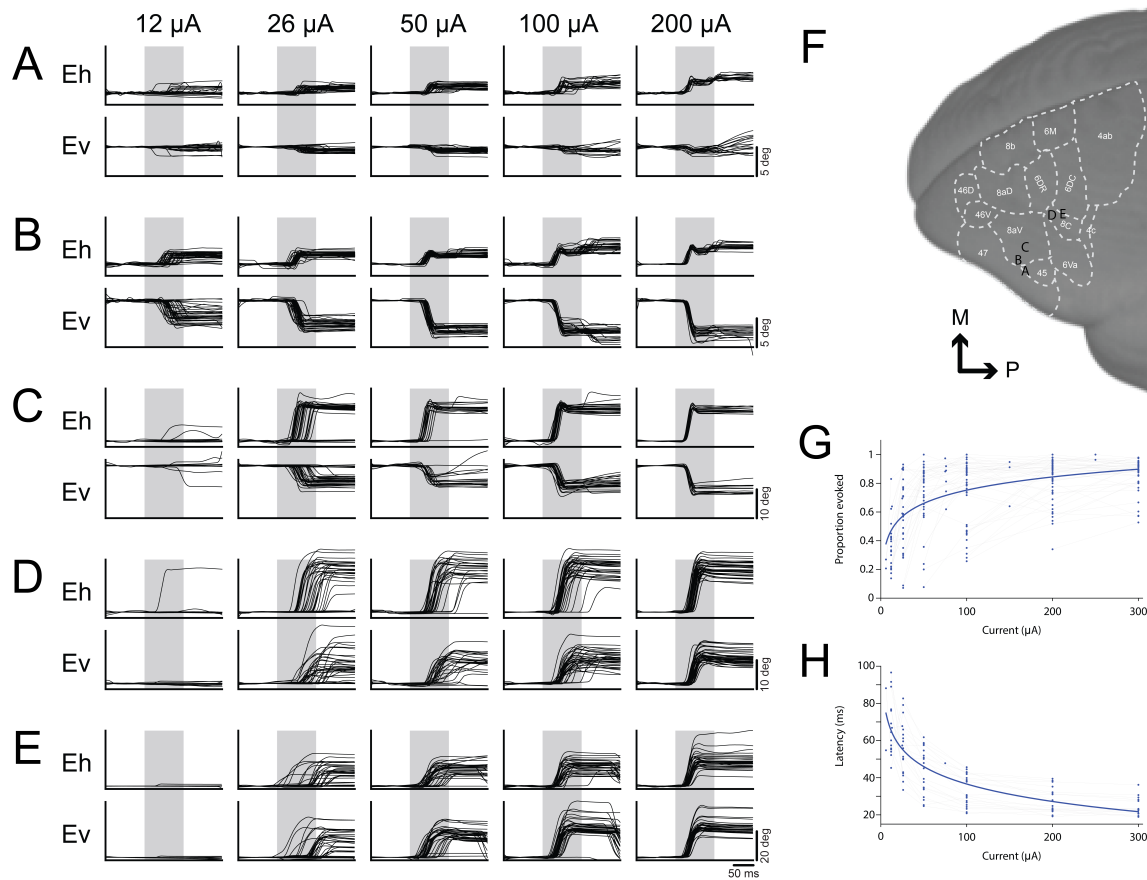
Figure 2.4: Current series at representative saccade sites. Current series at a representative small (A-C) and large (D-E) saccade sites. Baseline correction was applied by subtracting the mean gaze position during a 100ms period preceding stimulation onset in the horizontal and vertical components separately. Grey bars indicate stimulation train duration. Location of array sites for series in (A-E) show in (F). (G) Effect of current on proportion of saccades evoked at all FEF sites in Marmoset 3. (H) Effect of current on saccade latency at low threshold (¡50 µA) sites in Marmoset 3.
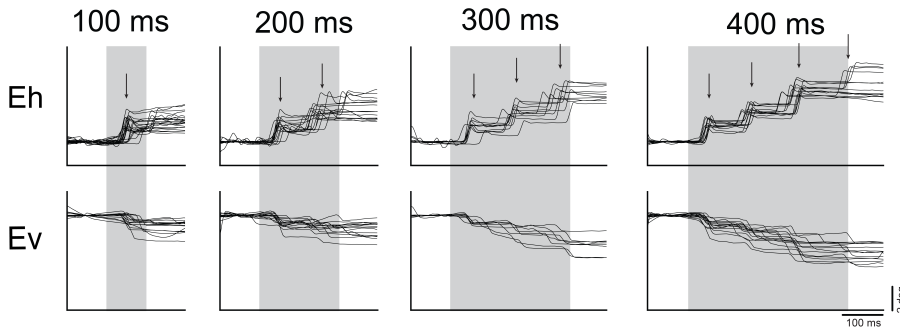
Figure 2.5: Current series at a representative site with staircase saccades. Arrows indicate median saccade onset latency. Baseline correction was applied by subtracting the mean gaze position during a 100ms period preceding stimulation onset in the horizontal and vertical components separately. Grey bars indicate stimulation train duration.

saccades; > 20 visual degrees) to lateral (small saccades; < 2 visual degrees) sites. Direction varied systematically from upper visual field at posterior medial sites to lower visual field at anterior lateral sites.

2.3.4 Staircase saccades

At a subset of sites from which saccades were evoked, we additionally observed staircases of multiple saccades. To investigate this further, we applied stimulation trains of increasing duration at these sites and found that the number of saccades increased as a function of train duration at the majority of these sites (12/15). A representative site is depicted in Figure 2.5. Staircases consisted of 2-5 consecutive saccades with consistent amplitudes and directions, in many cases ultimately driving the eye to the extent of its oculomotor range. At a given site, consecutive saccades occurred at fixed intervals. The intersaccadic interval ranged from 70-120 ms across sites and we observed no systematic variation in intersaccadic interval with respect to site coordinates nor any other saccade metrics.

2.3.5 Slow eye movements

Posterior to where we evoked saccades, in areas 6DR and 8C (see Figure 2.1c), we were able to elicit slow eye movements. These eye movements often followed a saccade and continued until stimulation ended at which point, they stopped abruptly (see Figure 2.6a for a representative site). Slow eye movement duration ranged from 50-75ms varying as a function of stimulation site. While the direction of these movements tended to be consistent at a site, the velocity increased as a function of stimulation current intensity, consistent with what is observed in the smooth pursuit region of the FEF in macaques (see Figure 2.6b for a current series at a representative site) (Gottlieb et al., 1993). Radial eye velocity ranged from 10-200 visual degrees/s, varying as a function of stimulation site and current intensity.
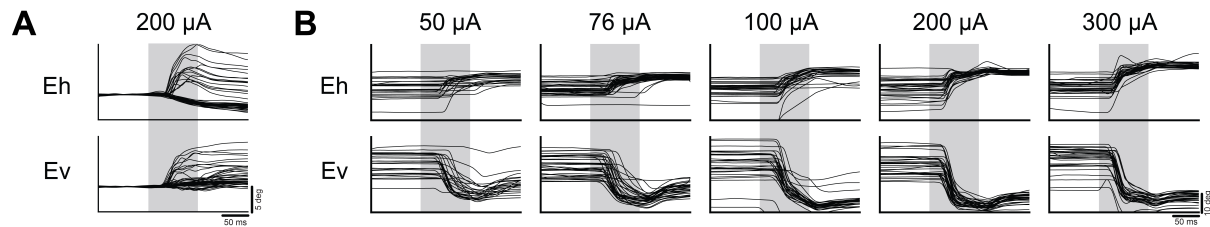
Figure 2.6: Evoked smooth eye movements. (A) Smooth eye movement site at 200 µA from Marmoset 1 Baseline correction was applied by subtracting the mean gaze position during a 100ms period preceding stimulation onset in the horizontal and vertical components separately. (B) Current series from a smooth eye movement site in Marmoset 3. Grey bars indicate stimulation train duration.

2.3.6   Effects of initial gaze position

While evoked saccades were mostly fixed vector, an effect of initial gaze position was observed at some sites. At those sites, saccades tended to be of greater amplitude if the gaze position at the time of stimulus onset was within the hemifield ipsilateral to the stimulated hemisphere. Further, the probability of evoking a saccade was lower if the initial eye position was within the hemifield contralateral to the stimulated hemisphere.

We quantified the magnitude of the effect of initial eye position at each site by computing the linear regression of the difference in final eye position as a function of the initial eye position separately for horizontal (Kh) and vertical (Kv) components of evoked saccades at these sites (Russo & Bruce, 1993). Correlation coefficients of 0 would be expected for sites at which the saccade vector did not change with varying initial eye positions (i.e. strictly fixed-vector saccades), whereas coefficients of -1 would be expected for sites at which evoked saccades terminated at the same eye position irrespective of initial eye position (i.e. goal-directed saccades). An example of this is shown for representative sites from FEF (see Figure 2.7a, b) and SEF (see Figure 2.7c).

Sites in FEF were mostly fixed vector, however, as observed by Russo and Bruce (1993), an effect of initial eye position was observed which increased in magnitude with the mean amplitude of saccades evoked at that site (see Figure 2.7d). This corresponds with the eye position terminating at the edge of the orbit for very large saccades. In contrast, in SEF sites, mostly convergent saccades were observed with correlation coefficients close to -1 and saccades converging on locations well within the oculomotor range of the animal.

2.4   Discussion

The common marmoset is a promising model for investigating the microcircuitry of the FEF (Mitchell & Leopold, 2015). The location of the FEF in marmosets, however, remains controversial. To address this, we systematically applied intracortical microstimulation (ICMS) to marmoset frontal cortex through chronically implanted electrode arrays to investigate the oculomotor and skeletomotor responses evoked in this region (see Figure 2.8 for a schematic summary). We observed patterns of skeletomotor responses consistent with previous ICMS investigations of marmoset motor and premotor cortex (Burish et al., 2008; Wakabayashi et
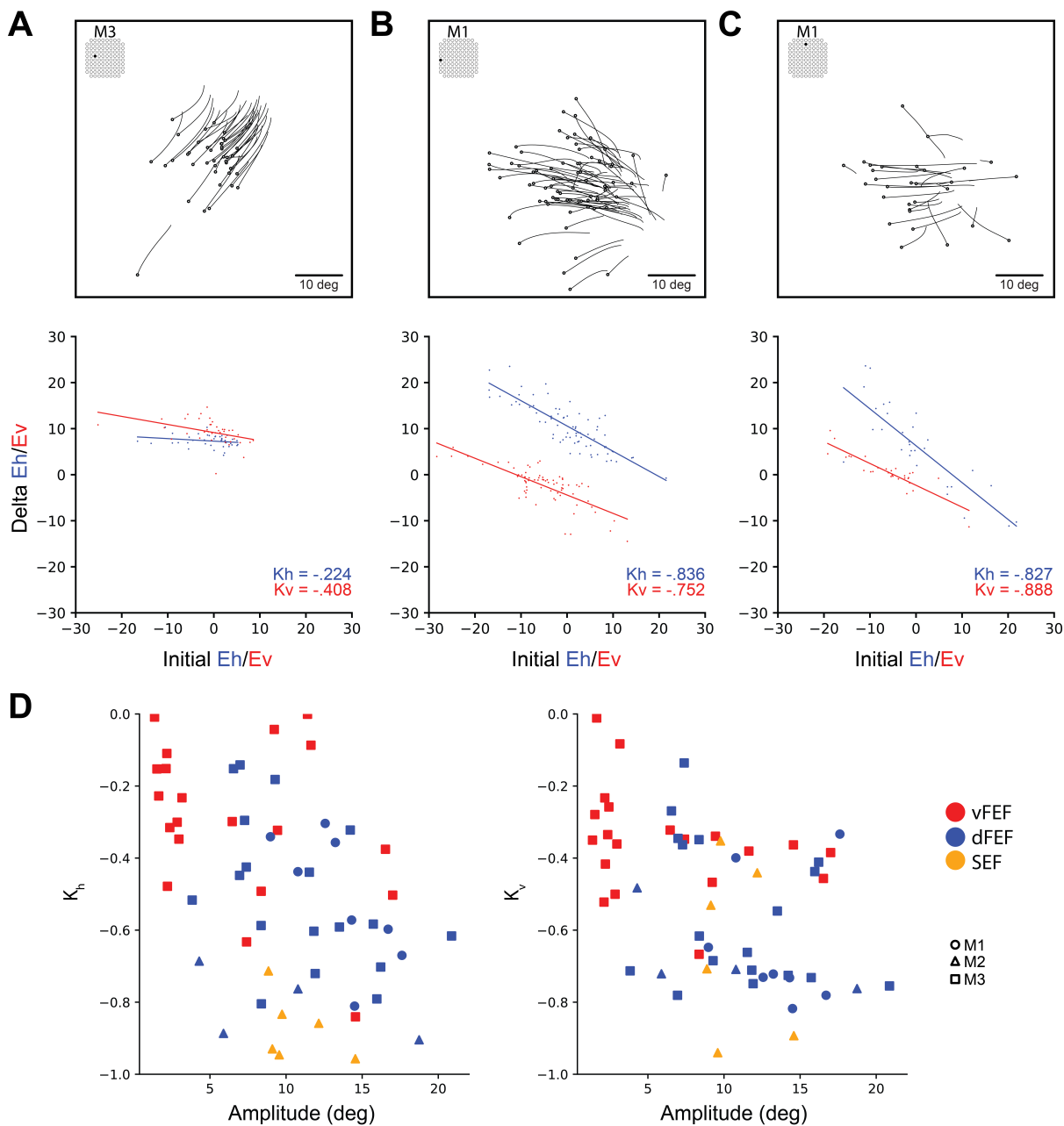
Figure 2.7: Effect of initial eye position. Saccade traces (above) and effect of initial position on delta (below) for representative sites from vFEF (A), dFEF (B) and SEF (C). Open circles indicate eye position at saccade onset. (C) Across all sites, the relationship between Kh and Kv values (correlation coefficients from effect of initial eye position analysis) and amplitude. More negative values indicate a greater effect of initial eye position.
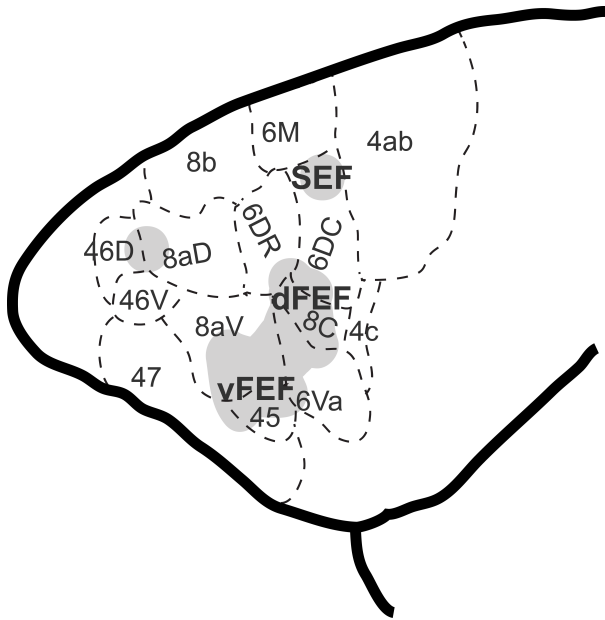
Figure 2.8: Schematic representation of cortical eye fields in marmoset frontal cortex.

al., 2018). Anterior to these motor areas, we observed a suite of oculomotor responses across frontal cortex which we propose correspond to three cortical eye fields. ICMS in area 45 and in the lateral part of area 8aD evoked small contraversive saccades at very low currents, consistent with the properties of the ventrolateral FEF (vFEF) in macaques (Bruce et al., 1985). In areas 6DR, 6DC, 8C, and medial 8aV, ICMS evoked larger saccades that were often associated with shoulder, neck and ear movements. This is consistent with ICMS experiments in dorsomedial macaque FEF (dFEF) (Corneil et al., 2010; Elsley et al., 2007). We also observed goal-oriented saccades characteristic of the supplementary eye field (SEF) at dorsomedial sites. In prefrontal areas 46 and anterior 8aD, ICMS elicited saccades with no consistent organization of direction or amplitude. These findings are consistent with the organization of FEF and SEF in macaques (Bruce et al., 1985; Gottlieb et al., 1993; Knight & Fuchs, 2007; Robinson & Fuchs, 1969; Russo & Bruce, 1993; Schlag-Rey et al., 1997).

A characteristic feature of the FEF observed in macaque ICMS experiments is the ability to evoke short latency fixed vector saccades at low currents. While the threshold to evoke saccades can be as high as 2 mA in frontal cortex (Robinson & Fuchs, 1969), FEF is defined in macaque as the restricted region in which thresholds are below 50 μA (Bruce et al., 1985). Here, we observed a large number of sites with thresholds below 50 μA, with a lower bound of 12 μA, similar to the 10 μA observed in macaque (Bruce et al., 1985). This is despite the limitations of fixed-length chronic electrode arrays which did not allow us optimally target layer V output neurons and in contrast to previous reports of higher thresholds in marmoset motor cortex compared to macaques (Burish et al., 2008). However, saccade latencies were slightly longer than those observed in macaques. We found a range of 25-85ms as compared to 20-60ms observed by Bruce and colleagues (1985) at near threshold currents, and 15-45ms as compared to 15-25ms by Robinson and Fuchs (1969) at higher currents. It has been proposed that longer latency saccades are evoked through an indirect route (e.g., superior colliculus), whereas shorter latency saccades are evoked by recruiting neurons that project directly to the brain stem (Bruce

et al., 1985). Investigations employing single unit recordings in the marmoset FEF and studies investigating the connectivity of marmoset FEF and brain stem oculomotor nuclei should provide insight into these differences.

In macaque FEF, saccades evoked by ICMS are fixed-vector with little variability in amplitude and direction (Bruce et al., 1985; Robinson & Fuchs, 1969). While saccades evoked here were predominantly fixed vector, some effects of initial gaze position were observed in which saccades were larger when the initial gaze position was in the hemifield ipsilateral to the site of stimulation. Similar observations have been made in macaque FEF (Robinson & Fuchs, 1969; Russo & Bruce, 1993) in which the magnitude of this effect is greater for larger saccades. However, this effect is greater here than previously observed with macaques. This may be a result of the eye being driven to the edge of the oculomotor range. In marmosets, this is limited to approximately 12 degrees as compared to 30 degrees in the macaque (Heiney & Blazquez, 2011; Mitchell et al., 2014; Tomlinson & Bahra, 1986). Head-restraint also prevents marmosets from using head movements to shift gaze, which they depend on to a greater extent than larger primates (Mitchell et al., 2014). Investigations in head unrestrained marmosets would clarify these differences.

Previous studies of macaque FEF have revealed a topographic representation of saccade amplitude and direction. Bruce and colleagues (1985) demonstrated a medio-lateral gradient in which large saccades were evoked medially and small saccades laterally. We observed a similar organization of saccade amplitude in marmosets, with small saccades being elicited in areas 45 and lateral area 8aV (vFEF) and larger saccades being evoked in areas 6DR, 6C, 8C, and medial 8aV (dFEF). Bruce and colleagues (1985) observed systematic changes in saccade direction with small advances along the depth of the arcuate sulcus in macaques, though they often encountered disruptions and reversals of direction. We observed a rostro-caudal organization of saccade direction in marmosets in which direction gradually changed from lower to upper visual field, though there were occasional direction reversals. Assuming that frontal cortex in marmoset is roughly a flattened version of that in macaque, the rostro-caudal axis would correspond roughly to traversing the depth of the arcuate sulcus from lip to fundus in macaques. We additionally observed a more continuous medio-lateral organization of saccade direction, such that the upper visual field was represented medially. This organization would be difficult to observe in the macaque FEF due to its more complex morphology.

At more posterior-medial sites where larger saccades are represented (dFEF), we observed skeletomotor responses resembling an orienting response while we only observed oculomotor responses at the more anterior-lateral sites. This is in line with what Knight and Fuchs (2007) found in awake head-unrestrained macaques. Indeed, Foerster (1926) already reported two saccade-related fields in humans: (1) FEF where epileptic seizures evoked contralateral saccades and (2) a more posterior field that he termed frontal adversive field (frontales Adversivsfeld) where seizures were associated with contralateral saccades and head movements.

At posterior medial sites, at the border of area 6D and 6M, we observed goal-directed saccades characteristic of SEF (Schlag & Schlag-Rey, 1987). Contrary to observations at more anterior lateral sites, convergence of saccades could not be explained by physical limitation of the orbit. We observed saccades converging at locations well within the animal's oculomotor range and, albeit infrequently, saccades directed to the hemifield ipsilateral to the stimulated hemisphere. These findings are similar to observations in the macaque by Schlag and Schlag-Rey (1987). However, we observed that saccade latencies were much longer at these sites

(70-110ms) than those observed by Schlag and Schlag-Rey (1987) (40-60ms). Further, they observed low current thresholds, at many sites less than 20 µA, whereas we observed few saccades at currents as high as 200 µA. Taken together, these findings suggest the observed responses may be evoked due to current spread to dorsomedial regions not covered by our arrays. We propose that area 6M may contain the putative marmoset SEF. Further investigation employing ICMS and single unit electrophysiology in marmoset dorsomedial frontal cortex is required to fully investigate this putative homology

We were also able to elicit saccades at rostral sites in area 46 and in anterior area 8aD. At these sites, saccades were evoked at high currents and long latencies, and did not exhibit any clear organization of direction or amplitude. As with our observations in other areas of marmoset frontal cortex, this finding is consonant with previous work in macaque (Robinson & Fuchs, 1969). Further investigation in the frontal pole of the marmoset brain is required to characterize this region.

In a previous resting-state fMRI study, the FEF of marmoset was localised provisionally at the border of areas 8aD and 6DR based on the strength of functional connectivity between this region and the SC (Ghahremani et al., 2017). This finding appears at odds with previous task-based fMRI studies which observed robust visual and saccadic responses in areas 8aV (Hung et al., 2015b; Schaeffer, Gilbert, Hori, Hayrynen, et al., 2019). More recent resting-state fMRI in awake marmosets may serve to clarify this discrepancy, with SC showing peaks of connectivity in both lateral 8aV and 8aD/6DR (Schaeffer, Gilbert, Hori, Hayrynen, et al., 2019, Figure 7). Indeed, isoflurane anaesthesia has been shown to obfuscate the full extent of resting state connectivity profiles (Hutchison et al., 2014). Here, we found that the characteristics of ICMS-evoked saccades in area 8aV were consistent with the classically defined FEF in macaque, while those in area 8aD were not. A potential explanation for this discrepancy may lie in the differences in the density and termination patterns of corticotectal projections between the FEF and more medial frontal areas. In macaques, it has been shown that the projections from area 6DR terminate in a more widespread area within the SC than those from FEF (Shook et al., 1990). If such a difference exists also in marmosets, it may account for the greater SC functional connectivity observed at the 6DR/8aD border. From this account, both sets of findings can be reconciled, since the resting-state data would be consistent with the strength of anatomical connections, while evidence from functional studies using fMRI and ICMS point to a common locus of FEF. A definitive appraisal of such an explanation awaits more detailed anatomical investigations of the connectivity of the physiologically defined FEF and medial frontal cortex in the marmoset.

In a recently published study, we carried out an electrophysiological investigation of preparatory activity for pro- and anti-saccades, in which we recorded in area 8aD (Johnston et al., 2019) which we referred to as the putative FEF of the marmoset based on the strength of resting-state functional connectivity as discussed above (Ghahremani et al., 2017). In that work, we carried out recordings with laminar electrodes which were inserted into the cortex daily at sites corresponding to approximately the border of areas 8aD and 6DR. As noted above, a more recent resting-state fMRI study has shown a peak of SC connectivity in this region, in addition to the more lateral area 8aV. We found here that microstimulation evoked larger amplitude saccades from the region corresponding to area 8aD/6DR. Given the broad tuning of FEF neurons (Bruce et al., 1985), and the positioning of our stimuli on the horizontal meridian at an eccentricity of roughly 7 degrees, we believe that although not optimized, our stimuli were

within the response fields of saccade-related neurons in this area. We thus do not believe that our current results affect the interpretation of our findings there. Future work characterizing the tuning characteristics of these areas for visual stimuli and saccades should prove illuminating.

Altogether, our data demonstrate a similar functional organization of the FEF in marmosets and macaques and provide a combined physiological characterization and anatomical localization that opens avenues for future exploration of FEF microcircuitry in marmosets. Electrophysiological studies in marmosets have the potential to complement ongoing work in the macaque model and human participants by advancing our understanding of laminar processes and their contributions to the oculomotor and cognitive functions of this area.

2.5   References

Avants, B. B., Tustison, N. J., Song, G., Cook, P. A., Klein, A., & Gee, J. C. (2011). A Reproducible Evaluation of ANTs Similarity Metric Performance in Brain Image Registration. *NeuroImage*, *54*(3), 2033–2044. https://doi.org/10.1016/j.neuroimage.2010.09.025

Awh, E., Armstrong, K. M., & Moore, T. (2006). Visual and oculomotor selection: Links, causes and implications for spatial attention. *Trends in Cognitive Sciences*, *10*(3), 124–130. https://doi.org/10.1016/j.tics.2006.01.001

Blum, B., Kulikowski, J., Carden, D., & Harwood, D. (1982). Eye Movements Induced by Electrical Stimulation of the Frontal Eye Fields of Marmosets and Squirrel Monkeys. *Brain, Behavior and Evolution*, *21*(1), 34–41. https://doi.org/10.1159/000121613

Bruce, C. J., Goldberg, M. E., Bushnell, M. C., & Stanton, G. B. (1985). Primate frontal eye fields. II. Physiological and anatomical correlates of electrically evoked eye movements. *Journal of Neurophysiology*, *54*(3), 714–734. https://doi.org/10.1152/jn.1985.54.3.714

Burish, M. J., Stepniewska, I., & Kaas, J. H. (2008). Microstimulation and architectonics of frontoparietal cortex in common marmosets (Callithrix jacchus). *Journal of Comparative Neurology*, *507*(2), 1151–1168. https://doi.org/10.1002/cne.21596

Collins, C. E., Lyon, D. C., & Kaas, J. H. (2005). Distribution across cortical areas of neurons projecting to the superior colliculus in new world monkeys. *The Anatomical Record Part A: Discoveries in Molecular, Cellular, and Evolutionary Biology*, *285A*(1), 619–627. https://doi.org/10.1002/ar.a.20207

Corneil, B. D., Elsley, J. K., Nagy, B., & Cushing, S. L. (2010). Motor output evoked by subsaccadic stimulation of primate frontal eye fields. *Proceedings of the National Academy of Sciences of the United States of America*, *107*(13), 6070–6075. https://doi.org/10.1073/pnas.0911902107

Elsley, J. K., Nagy, B., Cushing, S. L., & Corneil, B. D. (2007). Widespread Presaccadic Recruitment of Neck Muscles by Stimulation of the Primate Frontal Eye Fields. *Journal of Neurophysiology*, *98*(3), 1333–1354. https://doi.org/10.1152/jn.00386.2007

Ferrier, D. (1875). The Croonian Lecture: Experiments on the Brain of Monkeys (second series). *Philosopical Transactions of the Royal Society of London*, *165*, 433–488. https://royalsocietypublishing.org/doi/pdf/10.1098/rstl.1875.0016

Foerster, O. (1926). Zur operativen Behandlung der Epilepsie. *Deutsche Zeitschrift für Nervenheilkunde*, *89*(1), 137–147. https://doi.org/10.1007/BF01653863

Ghahremani, M., Hutchison, R. M., Menon, R. S., & Everling, S. (2017). Frontoparietal Functional Connectivity in the Common Marmoset. *Cerebral Cortex*, *27*, 3890–3905. https://doi.org/10.1093/cercor/bhw198

Gilbert, K. M., Schaeffer, D. J., Gati, J. S., Klassen, M. L., Everling, S., & Menon, R. S. (2019). Open-source hardware designs for MRI of mice, rats, and marmosets: Integrated animal holders and radiofrequency coils. *Journal of Neuroscience Methods*, *312*, 65–72. https://doi.org/10.1016/j.jneumeth.2018.11.015

Gottlieb, J. P., Bruce, C. J., & MacAvoy, M. G. (1993). Smooth eye movements elicited by microstimulation in the primate frontal eye field. *Journal of Neurophysiology*, *69*(3), 786–799. https://doi.org/10.1152/jn.1993.69.3.786

Heiney, S. A., & Blazquez, P. M. (2011). Behavioral responses of trained squirrel and rhesus monkeys during oculomotor tasks. *Experimental Brain Research*, *212*(3), 409–416. https://doi.org/10.1007/s00221-011-2746-4

Hung, C.-C., Yen, C. C.-C., Ciuchta, J. L., Papoti, D., Bock, N. A., Leopold, D. A., & Silva, A. C. (2015a). Functional Mapping of Face-Selective Regions in the Extrastriate Visual Cortex of the Marmoset. *The Journal of Neuroscience*, *35*(3), 1160. https://doi.org/10.1523/JNEUROSCI.2659-14.2015

Hung, C.-C., Yen, C. C.-C., Ciuchta, J. L., Papoti, D., Bock, N. A., Leopold, D. A., & Silva, A. C. (2015b). Functional MRI of visual responses in the awake, behaving marmoset. *NeuroImage*, *120*, 1–11. https://doi.org/10.1016/j.neuroimage.2015.06.090

Hutchison, R. M., Culham, J. C., Everling, S., Flanagan, J. R., & Gallivan, J. P. (2014). Distinct and distributed functional connectivity patterns across cortex reflect the domain-specific constraints of object, face, scene, body, and tool category-selective modules in the ventral visual pathway. *NeuroImage*, *96*, 216–236. https://doi.org/10.1016/j.neuroimage.2014.03.068

Johnston, K. D., Barker, K., Schaeffer, L., Schaeffer, D. J., & Everling, S. (2018). Methods for chair restraint and training of the common marmoset on oculomotor tasks. *Journal of Neurophysiology*, *119*, 1636–1646.

Johnston, K. D., Ma, L., Schaeffer, L., & Everling, S. (2019). Alpha Oscillations Modulate Preparatory Activity in Marmoset Area 8Ad. *Journal of Neuroscience*, *39*(10), 1855–1866. https://doi.org/10.1523/JNEUROSCI.2703-18.2019

Knight, T. A., & Fuchs, A. F. (2007). Contribution of the Frontal Eye Field to Gaze Shifts in the Head-Unrestrained Monkey: Effects of Microstimulation. *Journal of Neurophysiology*, *97*(1), 618–634. https://doi.org/10.1152/jn.00256.2006

Li, X., Morgan, P. S., Ashburner, J., Smith, J., & Rorden, C. (2016). *The first step for neuroimaging data analysis: DICOM to NIfTI conversion*.

Liu, C., Ye, F. Q., Yen, C. C.-C., Newman, J. D., Glen, D., Leopold, D. A., & Silva, A. C. (2018). A digital 3D atlas of the marmoset brain based on multi-modal MRI. *NeuroImage*, *169*, 106–116. https://doi.org/10.1016/j.neuroimage.2017.12.004

Mitchell, J. F., & Leopold, D. A. (2015). The marmoset monkey as a model for visual neuroscience. *Neuroscience Research*, *93*, 20–46. https://doi.org/10.1016/j.neures.2015.01.008

Mitchell, J. F., Reynolds, J. H., & Miller, C. T. (2014). Active Vision in Marmosets: A Model System for Visual Neuroscience. *Journal of Neuroscience*, *34*(4), 1183–1194. https://doi.org/10.1523/JNEUROSCI.3899-13.2014

Mott, F. W., Schuster, E., & Halliburton, W. D. (1910). Cortical Lamination and Localisation in the Brain of the Marmoset. *Proceedings of the Royal Society of London. Series B, Containing Papers of a Biological Character*, *82*(553), 124–134. http://www.jstor.org/stable/80317

Peterson, J., Chaddock, R., Dalrymple, B., Van Sas, F., Gilbert, K. M., Klassen, M. L., Gati, J. S., Handler, W. B., & Chronik, B. A. (2018). Development of a Gradient and Shim Insert System for Marmoset Imaging at 9.4 T. Retrieved July 22, 2019, from http://archive.ismrm.org/2018/4421.html

Reser, D. H., Burman, K. J., Yu, H.-H., Chaplin, T. A., Richardson, K. E., Worthy, K. H., & Rosa, M. G. P. (2013). Contrasting Patterns of Cortical Input to Architectural Subdivisions of the Area 8 Complex: A Retrograde Tracing Study in Marmoset Monkeys. *Cerebral Cortex*, *23*(8), 1901–1922. https://doi.org/10.1093/cercor/bhs177

Robinson, D. A., & Fuchs, A. F. (1969). Eye movements evoked by stimulation of frontal eye fields. *Journal of Neurophysiology*, *32*(5), 637–648. https://doi.org/10.1152/jn.1969.32.5.637

Russo, G. S., & Bruce, C. J. (1993). Effect of eye position within the orbit on electrically elicited saccadic eye movements: A comparison of the macaque monkey's frontal and supplementary eye fields. *Journal of Neurophysiology*, *69*(3), 800–818. https://doi.org/10.1152/jn.1993.69.3.800

Schaeffer, D. J., Gilbert, K. M., Hori, Y., Gati, J. S., Menon, R. S., & Everling, S. (2019). Integrated radiofrequency array and animal holder design for minimizing head motion during awake marmoset functional magnetic resonance imaging. *NeuroImage*, *193*, 126–138. https://doi.org/10.1016/j.neuroimage.2019.03.023

Schaeffer, D. J., Gilbert, K. M., Hori, Y., Hayrynen, L. K., Johnston, K. D., Gati, J. S., Menon, R. S., & Everling, S. (2019). Task-based fMRI of a free-viewing visuo-saccadic network in the marmoset monkey. *NeuroImage*, *202*, 116147. https://doi.org/10.1016/j.neuroimage.2019.116147

Schall, J. D. (1997). Visuomotor areas of the frontal lobe. In *Extrastriate cortex in primates* (pp. 527–638). Springer. http://www.psy.vanderbilt.edu/faculty/schall/pdfs/VisuomotorAreasOfTheFro Ch13.pdf

Schlag, J., & Schlag-Rey, M. (1987). Evidence for a supplementary eye field. *Journal of Neurophysiology*, *57*(1), 179–200. https://doi.org/10.1152/jn.1987.57.1.179

Schlag-Rey, M., Amador, N., Sanchez, H., & Schlag, J. (1997). Antisaccade performance predicted by neuronal activity in the supplementary eye field. *Nature*, *390*(6658), 398–401. https://doi.org/10.1038/37114

Shook, B. L., Schlag-Rey, M., & Schlag, J. (1990). Primate supplementary eye field: I. Comparative aspects of mesencephalic and pontine connections. *The Journal of Comparative Neurology*, *301*(4), 618–642. https://doi.org/10.1002/cne.903010410

Smith, S. M., Jenkinson, M., Woolrich, M. W., Beckmann, C. F., Behrens, T. E. J., Johansen-Berg, H., Bannister, P. R., De Luca, M., Drobnjak, I., Flitney, D. E., Niazy, R. K., Saunders, J., Vickers, J., Zhang, Y., De Stefano, N., Brady, J. M., & Matthews, P. M. (2004). Advances in functional and structural MR image analysis and implementation

as FSL. *NeuroImage*, *23*, S208–S219. https://doi.org/10.1016/j.neuroimage.2004.07.051

Stanton, G. B., Deng, S.-Y., Goldberg, M. E., & McMullen, N. T. (1989). Cytoarchitectural characteristic of the frontal eye fields in macaque monkeys. *Journal of Comparative Neurology*, *282*(3), 415–427. https://doi.org/10.1002/cne.902820308

Tomlinson, R. D., & Bahra, P. S. (1986). Combined eye-head gaze shifts in the primate. I. Metrics. *Journal of Neurophysiology*, *56*(6), 1542–1557. https://doi.org/10.1152/jn.1986.56.6.1542

Wakabayashi, M., Koketsu, D., Kondo, H., Sato, S., Ohara, K., Polyakova, Z., Chiken, S., Hatanaka, N., & Nambu, A. (2018). Development of stereotaxic recording system for awake marmosets (Callithrix jacchus). *Neuroscience Research*, *135*, 37–45. https://doi.org/10.1016/j.neures.2018.01.001

Chapter 3

Laminar dynamics of target selection in the lateral intraparietal area

3.1   Introduction

At any given moment, we are faced with many more stimuli than can be processed simultaneously. To cope with this limitation, the process of attention acts to filter irrelevant stimuli and preferentially select those relevant for the guidance of behaviour. In foveate animals such as primates, visual attention and eye movements are closely linked, and the neural mechanisms underlying these processes and their relation to one another has been a topic of intensive investigation. Convergent evidence from anatomical, lesion, fMRI, TMS, and neurophysiological studies has demonstrated that attention and eye movements are supported by an extensively interconnected and largely overlapping network that includes the frontal eye fields (FEF) within prefrontal cortex, the lateral intraparietal area (LIP) within the posterior parietal cortex (PPC), and the midbrain superior colliculus (SC), an area critical for the generation of eye movements (see for review (Johnston & Everling, 2008; McDowell et al., 2008)).

The role of LIP in attentional and oculomotor control has been a topic of considerable interest, owing in part to its anatomical interposition between sensory and motor areas. LIP receives extensive inputs from multiple visual cortical areas, and as noted above is reciprocally interconnected with FEF and SC (Andersen et al., 1990; Baizer et al., 1991; Lewis & Van Essen, 2000; Lynch et al., 1985; Schall, 1995). As such, it has been conceptualized as a transitional link between visual processing and saccade generation. Consistent with this, single neurons in LIP have been shown to exhibit both visual and saccade related responses (Andersen et al., 1987). More direct evidence has been provided by studies in macaque monkeys trained to perform variants of the visual search task, in which a target stimulus is selected from an array of distractors. Pharmacological inactivation of LIP has been shown to induce deficits in visual search performance (Wardak et al., 2002). Neurophysiological studies have revealed that the activity of LIP neurons evolves to discriminate targets from distractors presented within their response fields prior to saccades to the target location (Ipata et al., 2006; Mirpour et al., 2009; Thomas & Paré, 2007), and that the time of this discrimination is predictive of the reaction times of targeting saccades (Thomas & Paré, 2007). Thus, the activity of LIP neurons may be said to instantiate a process of saccade target selection, in which an initial stage of visual

selection is followed by activity related to the forthcoming saccade.

Broadly speaking, for tasks requiring target selection, the activity of LIP neurons resembles closely that of areas to which it projects. Neurons both in FEF (Thompson et al., 1996) and SC (McPeek & Keller, 2002; Shen et al., 2011) discriminate targets from distractor stimuli and discharge prior to saccades. Although activity in both of these areas (Dorris et al., 1997; Hanes & Schall, 1996; Paré & Hanes, 2003) has been more directly linked to saccade initiation than that in LIP (Gottlieb & Goldberg, 1999), the considerable overlap in discharge properties across areas invites detailed investigations of the intrinsic mechanisms shaping the selection process within each area which in turn regulate the signals sent between them to fully understand their respective contributions to target selection. Anatomical and physiological evidence has demonstrated that area LIP possesses separate output channels to the FEF and SC. Cortico-cortical projections exhibit a visual bias and originate predominately in layers II/III, while corticofugal projections originate exclusively in layer V and exhibit a bias toward saccade-related activity (Ferraina et al., 2002; Lynch et al., 1985; Schall, 1995). To date, the laminar dynamics shaping these activity differences remain poorly understood, and although canonical circuit models have provided theoretical accounts with respect to visual cortex (Douglas & Martin, 1991) and the FEF (Heinzle et al., 2007) few studies have investigated directly the laminar flow of information by conducting simultaneous recordings across cortical layers (but see Bastos et al., 2018; Godlove et al., 2014; Nandy et al., 2017; Ninomiya et al., 2015; Pettine et al., 2019). The flow of neural activity in the primate posterior parietal cortex is unknown.

The lack of laminar recordings in fronto-parietal networks is due in large part to the practical difficulty in accessing areas such as FEF and LIP in macaques due to their locations deep within sulci. In contrast, the common marmoset monkey (Callithrix jacchus) has a relatively lissencephalic cortex, making it well-suited for such investigations. Recent work has identified homologous regions to macaque and human FEF and LIP in marmosets using a variety of methods, including cyto- and myeloarchitectural features, anatomical connections, resting state functional connectivity, task-based fMRI activations, intracortical microstimulation, and single-unit electrophysiology (Collins et al., 2005; Feizpour et al., 2021; Ghahremani et al., 2017; Ghahremani et al., 2019; Ma et al., 2020; Reser et al., 2013; Rosa et al., 2009; Schaeffer et al., 2019; Selvanayagam et al., 2019). Here, we addressed the knowledge gap in the understanding of laminar dynamics and their role in instantiating the process of saccadic target selection by carrying out laminar electrophysiological recordings in the posterior parietal cortex of marmosets using ultra-high density Neuropixels probes (Jun et al., 2017) while they performed a simple visual target selection task in which they generated saccades to a target stimulus presented in either the presence or absence of a distractor. We observed neural correlates of visual target selection similar to those observed in macaques and humans, the timing of which varied across neuron type and cortical layer.

3.2   Methods

3.2.1   Subjects

Two adult common marmosets (Marmoset M, female, age 22-24 months, weight 328-337 g; Marmoset N, male, age 23-35 months, weight 421-443g) served as subjects in the present study.

Prior to these experiments, both animals were acclimated to restraint in two separate custom-designed primate chairs for MRI and electrophysiological experiments which placed them in sphinx and upright positions, respectively. The animals additionally underwent an aseptic surgical procedure in which a combination recording chamber/head restraint was implanted, the purpose of which was to stabilize the head for MRI imaging, eye movement recording, and electrode insertions, and to allow access to cortex for electrophysiological recordings. These procedures have been described in detail previously (Johnston et al., 2018; Schaeffer et al., 2019). All experimental procedures were conducted in accordance with the Canadian Council on Animal Care policy on the care and use of laboratory animals and a protocol approved by the Animal Care Committee of the University of Western Ontario Council on Animal Care. The animals were additionally under the close supervision of university veterinarians throughout all experiments.

3.2.2   Behavioural training

For training on eye movement tasks, marmosets were seated in a custom primate chair (Johnston et al., 2018) inside a sound attenuating chamber (Crist Instrument Co. Hagerstown MD), with the head restrained. A spout was placed at animals' mouth to allow delivery of a viscous liquid reward (acacia gum) via an infusion pump (Model NE-510, New Era Pump Systems, Inc., Farmingdale, New York, USA). All visual stimuli were presented on a CRT monitor (ViewSonic Optiquest Q115, 76 Hz non-interlaced, 1600 x 1280 resolution) using either the CORTEX real-time operating system (NIMH, Bethesda, MD, USA) or Monkeylogic (Hwang et al., 2019). Eye positions were digitally recorded at 1 kHz via infrared video tracking of the left pupil (EyeLink 1000, SR Research, Ottawa, ON, Canada).

Marmosets were first trained to fixate on visual stimuli by rewarding 300-600 ms fixations within a circular electronic window with a diameter of 5°centred on circular stimuli consisting of dots with a diameter of 2°presented centrally on the display monitor. Once they were able to perform this subtask reliably, the number of potential fixation locations was increased with the addition of four stimuli presented at +/- 5°abscissa and +/- 5°ordinate. This served both as an initial training stage and allowed us to verify and adjust eye position calibration at the beginning of each experimental session.

Marmosets were then trained on the visual target selection task (see Figure 1a). This task consisted of two trial types. On "single-target" trials, the animals were required to generate a saccade to the location of a single peripheral visual stimulus in order to obtain a liquid reward. On each trial, they were required to maintain fixation within an electronic window with a diameter of 5°centred on a 0.5°dot presented at the centre of the display monitor for a variable duration of 300-500 ms. Following this, a single target stimulus, a marmoset face (2°diameter), was presented at +/- 6°abscissa. Animals were rewarded for single saccades to the target stimulus which landed within a circular electronic window of 5°, centred on the stimulus. Saccades landing elsewhere were marked as "incorrect". If no saccade was made within 1 s of target onset, the trial was marked as "no response". Once marmosets were consistently able to perform 100 or more correct trials of this task within a session, we added an additional "distractor" condition in which a distractor stimulus, a 1°radius black circle, was presented in the opposite hemifield at equal eccentricity to the target stimulus. All fixation and saccade requirements and the timing of trial events was identical to that of single target trials. On distractor trials,

single saccades to the target stimulus were rewarded while those made to the distractor location were classified as errors. In the final version of the task the "single target" and "distractor" conditions were run in alternating 20 trial blocks. Marmosets were trained on this task until they could complete 200 trials with at least 70% accuracy in the distractor blocks excluding "no response" trials. At this point we commenced collection of electrophysiological data. The final blocked version of the task including single target and distractor conditions was used for all electrophysiological recording sessions.

3.2.3   fMRI-Based Localization of Recording Locations

To target LIP for electrophysiological recordings, we conducted an fMRI localizer prior to commencing electrophysiological recordings. To provide landmarks for the location of this area relative to the recording chamber and guide the placement of trephinations allowing access to cortex, a custom-designed in-house printed grid matched to the inside dimensions of the chamber, consisting of 1mm holes at a spacing of 1.5mm, was placed into the chamber and the grid holes filled with iodine solution prior to scanning. This allowed visualization of the chamber and grid coordinates in the MRI images. We then acquired awake anatomical T2 images from each animal and aligned these to a high-resolution ex-vivo MRI template aligned with a group RS-fMRI functional connectivity map (see https://www.marmosetbrainconnectome.org) of the SC (Schaeffer et al., 2022). This group RS-fMRI map is based on over 70 hours of RS-fMRI collected at ultra-high fields from 31 awake adult marmosets.

Marmosets then underwent a second aseptic surgical procedure in which a microdrill (Foredom SR series, Blackstone Industries LLC, Bethel CT) was used to open burr holes of roughly 3mm diameter over the region of PPC identified as described above. This corresponded to approximately to the stereotaxic location of 1.4mm anterior, 6mm lateral indicated for area LIP in the marmoset stereotaxic atlas of Paxinos and colleagues (2012), and explored in a previous microstimulation study in our lab (Ghahremani et al., 2019). As in that study, we were additionally able to visually identify a small blood vessel and shallow sulcus thought to be homologous to the intraparietal sulcus of macaque. The sites were then sealed with a silicone adhesive (Kwik Sil, World Precision Instruments, Sarasota, FLA, USA) which served to prevent infection and reduce growth of granulation tissue on the dural surface. This seal was removed prior to and replaced following recording sessions after thorough flushing and cleaning of the trephinations.

3.2.4   Electrophysiological recordings

Recordings were conducted using Neuropixels 1.0 NHP short probes (Jun et al., 2017). The external reference and ground were bridged in all recordings. All recordings were referenced to the reference contact at the tip of the electrode. Data were recorded in two streams, a spike stream sampled at 30 kHz and high-pass filtered at 300 Hz, and an LFP stream sampled at 2.5kHz and low-pass filtered at 300 Hz. Custom Neuropixels electrode holders designed to interface with the dovetail structures on metal cap of the probe base were used with Narishige Stereotaxic Manipulators (SM-25A and SMM-200) to manipulate electrodes for all recordings. IMEC headstages were used with a PXIe-8381 acquisition module, the PXIe-1082 chassis and the MXIe interface were used for data acquisition. 8-bit digital event signals emitted by

CORTEX or Monkeylogic and calibrated analog signals for the horizontal and vertical eye positions were recorded using the PXI-6133. Neural and auxiliary signals were synchronized by a TTL pulse emitted by CORTEX or Monkeylogic at target onset. All data was acquired using the SpikeGLX application (v20190413-phase3B2 Karsh, 2019).

For each recording session, we removed the chamber cap and cleaned the recording chamber and dural surface to mitigate the risk of infection. First, we cleaned the outside of the chamber with sterile gauze soaked with 70% isopropyl alcohol solution. The silicone adhesive sealing the trephination was then removed and the dural surface was first flushed with sterile saline delivered via a syringe with a sterile catheter tip. Saline filling the chamber was absorbed with sterile gauze between flushing bouts. A 10% iodine solution was then applied, and the area was scrubbed extensively with sterile swabs. We then repeated saline flushing of the area until the solution appeared clear. Any blood or moisture on the dural surface was removed using absorbent surgical eye spears prior to electrode insertion, to avoid fouling of the electrode contacts. Probes were then advanced through the dura using stereotaxic micromanipulators until neural activity no longer appeared on the tip of the electrode where possible. Electrodes were allowed to settle for 30-45 minutes to minimize drift during the recording session. During this time, the animal's eye position was calibrated as described above. Then, animals performed the visual target selection task as described above until approximately 50 correct trials were obtained in each of the conditions or 45 minutes had passed. Finally, a visual field mapping paradigm was conducted, in which 0.2°dots were briefly flashed (100-200ms SOA, 0-100ms ISI) in a pseudorandomized manner in an evenly spaced 5 x 5 grid spanning +/- 8°abscissa and ordinate. Animals were not required to fixate during this period, and trials where the eyes were closed or moved within +/- 200ms of stimulus onset were removed from analysis offline.

In total, 26 penetrations were conducted across 22 sessions (8 in Marmoset M, 14 in Marmoset N), where 8 penetrations in Marmoset N were conducted with two Neuropixels probes simultaneously. For these penetrations, two probes were adhered back-to-back using dental adhesive (Bisco All-Bond, Bisco Dental Products, Richmond, BC, Canada) and advanced together using a single electrode holder.

3.2.5   Semi-automated spike sorting

Data collected in the spike stream were additionally high-pass filtered offline at 300 Hz. Putative single unit clusters were then extracted using Kilosort 2 (Pachitariu et al., 2023). Briefly, a common median filter is applied across channels and a "whitening" filter is applied to reduce correlations between channels and maximize local differences among nearby channels. Following these preprocessing steps, templates are constructed based on some initial segment of the data and adapted throughout session with some accommodation for drift over time. Then clusters are separated and merged as necessary.

Following this process, putative single unit clusters were manually curated using the Phy application (Rossant, 2019). Here, clusters were merged or split on the basis of waveforms, cross-correlations and distributions of spike amplitudes. Following merging and splitting clusters as needed, clusters with consistent waveforms, normally distributed amplitudes, a dip in the autocorrelogram at time 0, and consistently observed throughout the recording session were marked as single units, and all others were marked as multi-unit clusters or noise clusters as appropriate. Single unit clusters where the firing rate across the session was at least 0.5 Hz

and at most 1% of interspike intervals (ISIs) were within 1 ms (i.e., short ISIs that fall within the refractory period) were retained for all subsequent analyses. For these neurons, short ISI spikes were discarded.

3.2.6   Layer assignment based on spectrolaminar LFP analysis

Layer assignment was done as in previous work, using an established spectrolaminar pattern (Mendoza-Halliday et al., 2023). Powerline artifacts were removed at 60 Hz using a butterworth bandstop filter. As these recordings were referenced to the tip of the electrode, as compared to the surface reference used in the recordings of Mendoza-Halliday and colleagues (2023), to recover the pattern they observed, we subtracted the mean activity in channels visually identified as being above the surface from all other channels. Then, the LFP activity aligned to stimulus onset was extracted and the power spectral density (PSD) was computed for each trial using the multi-taper method (Mitra & Pesaran, 1999). This was then averaged across tapers and trials to obtain the mean PSD for a given penetration. The PSD of adjacent channels was then averaged to obtain the mean PSD at each depth (Figure 2d-e). Following visual inspection, power in the 15-22 Hz range was used for the low frequency range and 80-150 Hz was used for the high frequency range. The crossing point in the power of these ranges across depth was marked as the center of layer IV. Upon visual inspection of the density of neurons anchored to this point and the known thickness of layer IV in marmoset PPC, we assigned neurons found from 200 μm below this point to 300 μm above as being in layer IV. Neurons superficial to this range were assigned to layers II/III and those found deeper to layers V/VI.

3.2.7   Putative cell type classification using peak-trough widths

We clustered neurons as broad and narrow spiking cells on the basis of peak-trough width, which has been suggested to correspond to putative pyramidal cells and interneurons respectively (Ardid et al., 2015; Hussar & Pasternak, 2012; McCormick et al., 1985; Mitchell et al., 2007). For each neuron, the channel at which the spike amplitude had the largest magnitude was selected. The mean waveform at this channel was upsampled to 1 MHz and interpolated using a cubic spline. For cells where the largest amplitude was a peak, i.e. positive-first waveforms, we identified a nearby channel with a negative-first waveform as the estimated depth of the soma and discarded neurons for which such a waveform could not be identified. For the retained neurons, the large and well isolated positive-first waveform was inverted to ensure that all waveforms exhibited a negative-going pattern and the peak-trough duration could be estimated reliably. Then, the duration between this trough and the subsequent peak were computed as the peak-trough widths (see Figure 2f). Neurons with a peak-trough width greater than 300 ms were classified as broad spiking (BS) and those with a peak-trough width smaller than 300 ms were classified as narrow spiking (NS).

3.2.8   Identification of task modulated and target discriminating neurons

Neurons were classified as task modulated if activity 40ms from stimulus onset to 25ms after saccade offset significantly differed from baseline activity (200 ms prior to stimulus onset) on contralateral "single-target" trials or "distractor trials". Significance was assessed using paired

samples t-tests for each neuron at an alpha level of .05. For these neurons, activity in the 50ms interval preceding saccade onset was correlated with saccade reaction times for contralateral and ipsilateral "single-target" trials via pearson r correlations at an alpha level of .05. Neurons were classified as target discriminating if activity 50-100 ms following stimulus onset significantly differed ipsilateral and contralateral "distractor" trials. Significance was assessed using independent samples t-tests for each neuron at an alpha level of .05. Neurons were classified as post-saccadic if the activity 50-150 ms following saccade offset differed from the pre-stimulus baseline separately for each condition and across all conditions using paired samples t-tests for each neuron at an alpha level of .05. For all above neurons, we conducted Receiver Operating Characteristics (ROC) analyses (Green & Swets, 1966) comparing the distributions of discharge activity in 15 ms sliding windows to determine the onset times of the observed effects. Significance was determined by comparing to a null distribution constructed via permutation testing using 1000 iterations. We evaluated differences in the proportions of neurons with significant stimulus-related, discrimination or post-saccadic activity (i.e. epoch) across layers and cell types using a logistic regression analysis: $P \propto epoch * layer * celltype$(lme4::glmer v1.1-31 in R v4.2.2). Model significance was estimated by comparison using likelihood ratio chi squared test with reduced models excluding each of these terms. Pairwise differences were computed using Bonferroni corrections (emmeans v1.8.4 in R).

3.2.9 Assessing differences in the timing of stimulus-related and discrimination activity across layers and putative cell classes

To assess the contribution of neurons from different cortical layers and putative cell classes to the stimulus-related and discrimination activity across the population, we employed a generalized additive model (GAM). Here, the odds of a spike at a given point in time are estimated using the time from stimulus onset and depth relative to the crossing point described above (as a tensor product smooth predictor), and putative cell class (NS or BS), with trial and neuron as random effects: $P \propto te(time * depth, by = celltype * condition) + (time|trial) + (time|neuron)$; (mgcv:bam v1.8-41 in R). That is, a two-dimensional spline function is evaluated over time and depth, where the parameters of these functions vary for the cell classes and conditions. Spiking odds over time are allowed to vary randomly across neurons and trials. For the stimulus-related activity condition (ipsilateral and contralateral) was added as a predictor. For the discrimination activity, condition (preferred and nonpreferred) was added as a predictor, where, for each neuron, the stimulus (target or distractor) which elicited the greatest discharge activity was labelled as preferred. Goodness of fit of models as compared to reduced and null models was assessed using the likelihood-ratio chi-squared test. Pairwise differences were examined by estimating difference smooths; i.e. smooth functions corresponding to the difference between levels of a categorical predictor interacting with the time by depth tensor product smooths. The time where significant stimulus-related activity first emerged was computed by determining where the 99.9% CI of the difference smooth between ipsilateral and contralateral trials for the "single-target" condition deviated from 0. Similarly, to determine the time at which neurons first significantly discriminated between target and distractor stimuli, we determined where the 99.9% CI of the difference smooth between preferred and non-preferred trials for the "distractor" condition deviated from 0.

3.3   Results

3.3.1   Behavioural Performance

Marmosets performed visually guided saccades in a simple target selection task wherein blocks of "single-target" and "distractor" trials were presented to the animal (see Figure 3.1a). Animals were required to fixate on a central fixation stimulus (0.5° radius black circle on a grey background) for 300-500 ms at the beginning of each trial. On "single-target" trials, a single target (1° diameter image of a marmoset face) was presented 6° to the left or right of the fixation stimulus and subjects were required to make a saccade to the target to obtain a viscous liquid reward of acacia gum. On "distractor" trials, a distractor stimulus (0.5° radius black circle) was simultaneously presented in the opposite hemifield. Trials in which no saccade at least 4° in amplitude was made were marked as "no response" and were not included in further analysis. Trials in which saccades were made to the target were marked as correct and trials in which saccades landed anywhere else were marked as incorrect. We conducted 22 recording sessions, 8 in Marmoset M and 14 in Marmoset N, in which animals performed 162-438 trials (M=248.7 trials). Accuracy was significantly lower on "distractor" trials (Mean ± SEM; Marmoset M: 89.9 ± 2.2%; Marmoset N: 74.0 ± 4.0%, see Figure 3.1b) than on "single-target" trials (Marmoset M: 100.0 ± 0.0% , Marmoset N: 96.4 ± 0.5%, see Figure 3.1c), Marmoset M: $t(7) = 4.57, p = .003$, Marmoset N: $t(13) = 5.82, p < .001$, and median SRTs were significantly longer, Marmoset M: $t(7) = 3.29, p = 0.013$, Marmoset N: $t(13) = 3.79, p = .002$, (Marmoset M: "distractor"=110.0±4.0ms vs "single-target"=99.4±1.6ms; Marmoset N: "distractor"=146.8±6.5ms vs "single-target"=139.0±5.2ms). Saccade amplitude and durations did not differ significantly between conditions nor on correct vs incorrect trials (all $p's \geq .05$; see Figure 3.1d-e). Taken together, these results reveal a distractor- induced reduction in performance suggesting an additional stage of processing on these trials.

3.3.2   Determining recording locations, cortical layers, and putative neuron classes

To determine recording locations we acquired high resolution, anatomical T2 images from each animal. Prior to scanning, a custom-designed grid with 1.5mm diameter holes spaced at 1mm was inserted in the animals' recording chambers and filled with iodine solution. The filled grid holes provided landmarks for determining the locations of identified areas within the recording chamber. We then aligned these images to a high-resolution ex-vivo MRI template aligned with a group RS-fMRI functional connectivity map of the SC (Schaeffer et al., 2022). We identified a region of strong functional connectivity in the PPC corresponding to the location of area LIP (see Figure 3.2a-b; Ghahremani et al., 2019; Schaeffer et al., 2019). Marmosets subsequently underwent aseptic surgeries in which we opened trephinations of approximately 3 mm in diameter over this region.

We conducted 26 electrode penetrations in two animals (Marmoset M: 8 penetrations in 8 sessions; Marmoset N: 18 penetrations in 14 sessions) in which we advanced either one or two Neuropixels electrodes (Jun et al., 2017) in this region and recorded the activity of 1366 well-isolated single neurons. For each penetration, we determined cortical layers by identifying the crossover point between the power spectral density (PSD) of low (15-22 Hz)

Figure A. Experimental paradigm with contralateral and ipsilateral single-target and distractor conditions.

Panels B–E: Histograms for Marmoset 1 and Marmoset 2 showing Proportion versus Saccade Reaction Time (ms), Saccade Amplitude (deg), and Saccade Duration (ms).
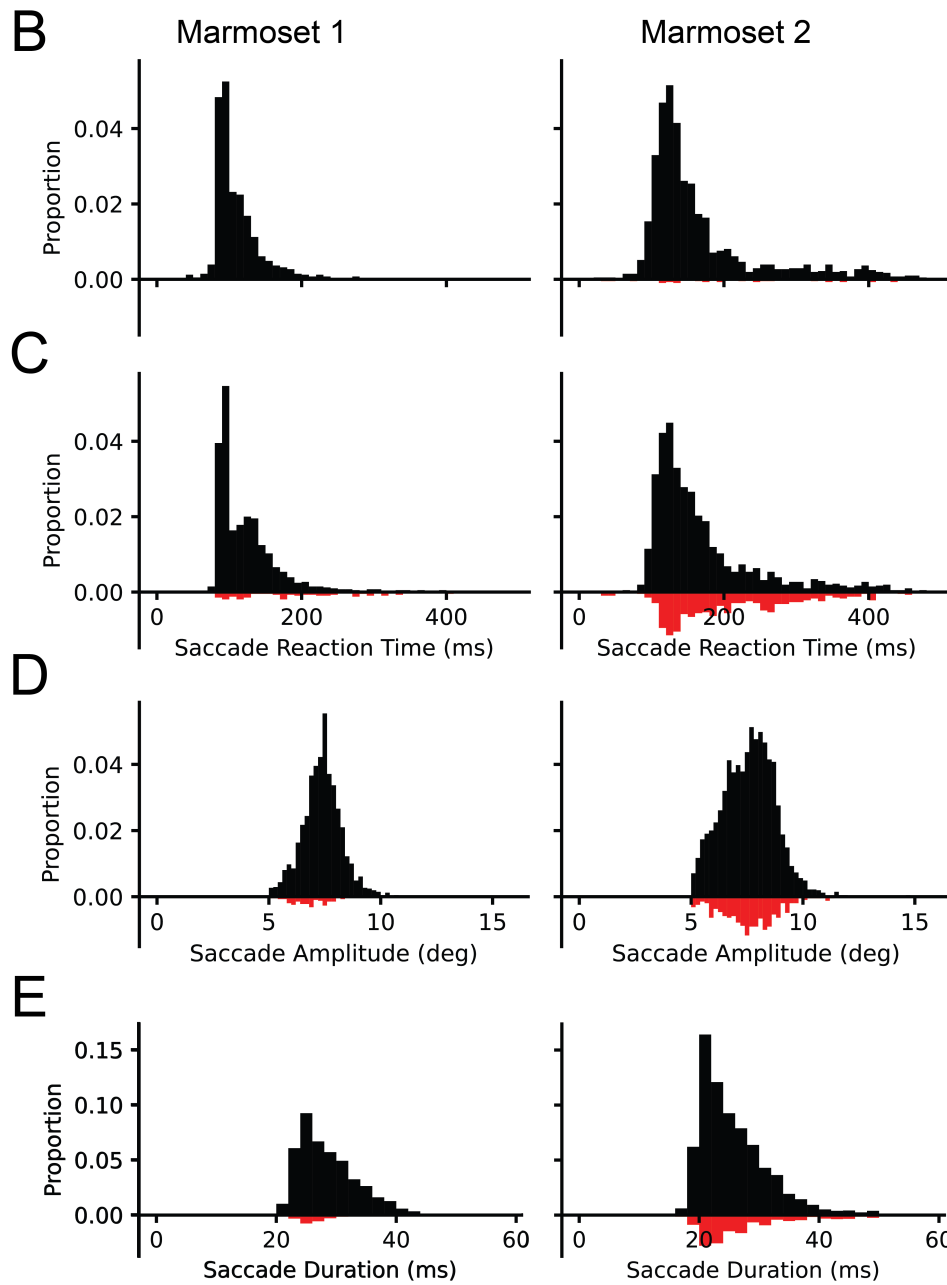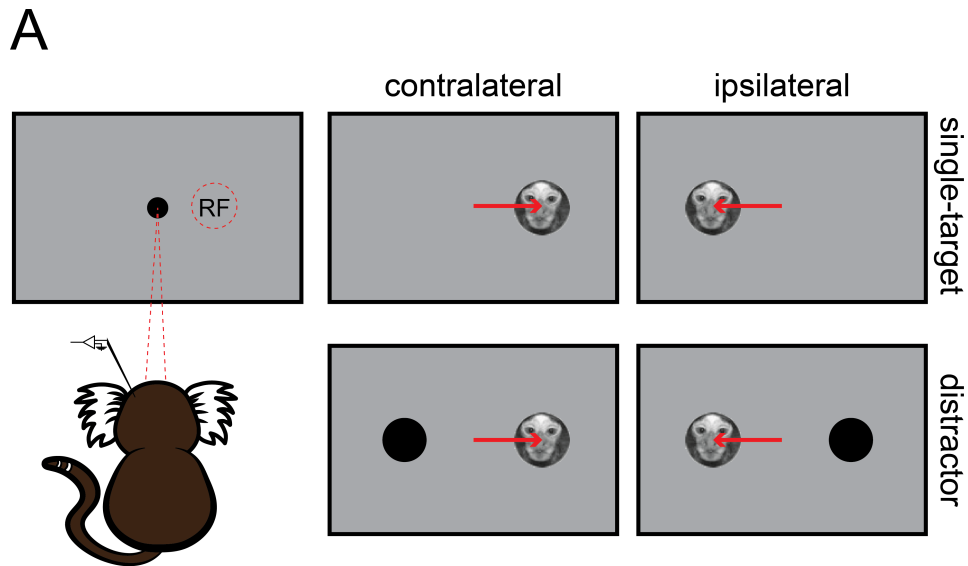
Figure 3.1: *Task design and behavioural performance (continued).* (A) Schematic representing task design for "single-target" and "distractor" trials, where the target falls in (contralateral) or out of (ipsilateral) the receptive field (RF). Saccade metrics for Marmoset 1 (left) and Marmoset 2 (right) for correct (black) and error (red) trials. Saccade reaction time histograms for "single-target" (B) and "distractor" (C) trials for each animal separately. Saccade amplitude (D) and duration (E) histograms for each animal separately across all conditions.

and high (80-150 Hz) frequency ranges in the local field potentials (LFP) across depths as done in previous work (Mendoza-Halliday et al., 2023) (see Figure 3.2c). Based on visual inspection of the distribution of isolated neurons distributed along the length of the electrode shank, and the known density of neuronal distributions within the cortical layers in this region of marmoset cortex, we classified all neurons that fell within 200 μm below to 300 μm above as being in granular Layer IV, and all others as supragranular or infragranular. To classify putative interneurons and pyramidal cells, the established approach of using the peak-trough duration was employed (Ardid et al., 2015; Hussar & Pasternak, 2012; McCormick et al., 1985; Mitchell et al., 2007) (see Figure 3.2d). Interestingly, a large proportion of neurons with positive-first waveforms were observed (198, 14.5 %), which were largely restricted to the broad waveforms observed in deeper layers. For 90 of these neurons, we were able to identify a nearby or deeper channel, where we observed a negative-first waveform and for these neurons we reassigned the relative depths accordingly (see white circles in Figure 3.2f). For the remaining 108 neurons, we were unable to identify a negative-first waveform, in part due to very small amplitudes or the neuron being clipped by the spatial extent of the probe. As these waveforms may also correspond to axons corresponding to a soma in a superficial layer, we excluded these neurons from the analysis. For the neurons we retained, we inverted the positive-first waveform before evaluating the peak-trough duration, as often the negative-first waveform was of a small amplitude and may lead to poor estimates of peak-trough duration.

3.3.3   Evaluating stimulus and saccade-related responses in LIP neurons

To identify task-modulated neurons, we computed the mean discharge rates from 50 ms after stimulus onset to 25 ms after saccade onset for conditions and compared it to the mean baseline activity 200 ms before stimulus onset. Examining the conditions separately, 319 (23.35%) neurons were significantly modulated in the "single target" contralateral condition as compared to 112 (8.2%) in the "single-target" ipsilateral condition; for the "distractor" trials, 329 (24.08%) were significantly modulated when the target was presented in the contralateral hemifield as compared to 262 (19.18%) when the distractor was presented in the contralateral hemifield. Overall, pooling across conditions, a total of 390 (28.55%) neurons exhibited significant modulations in discharge rates during task performance (see Figure 3.3). The proportion of modulated neurons per layer and putative cell class were as follows (see Table 3.1): supragranular (BS: 28.18%, NS: 37.04%), granular (BS: 26.82%, NS: 27.61%), and infragranular (BS: 17.12%, NS: 21.59%).

For these neurons, we conducted Pearson R correlations to determine whether activity preceding saccade onset correlated with the SRTs for contralateral and ipsilateral trials separately; the discharge activity of 32 (8.2%) and 33 (8.5%) neurons were significantly correlated with
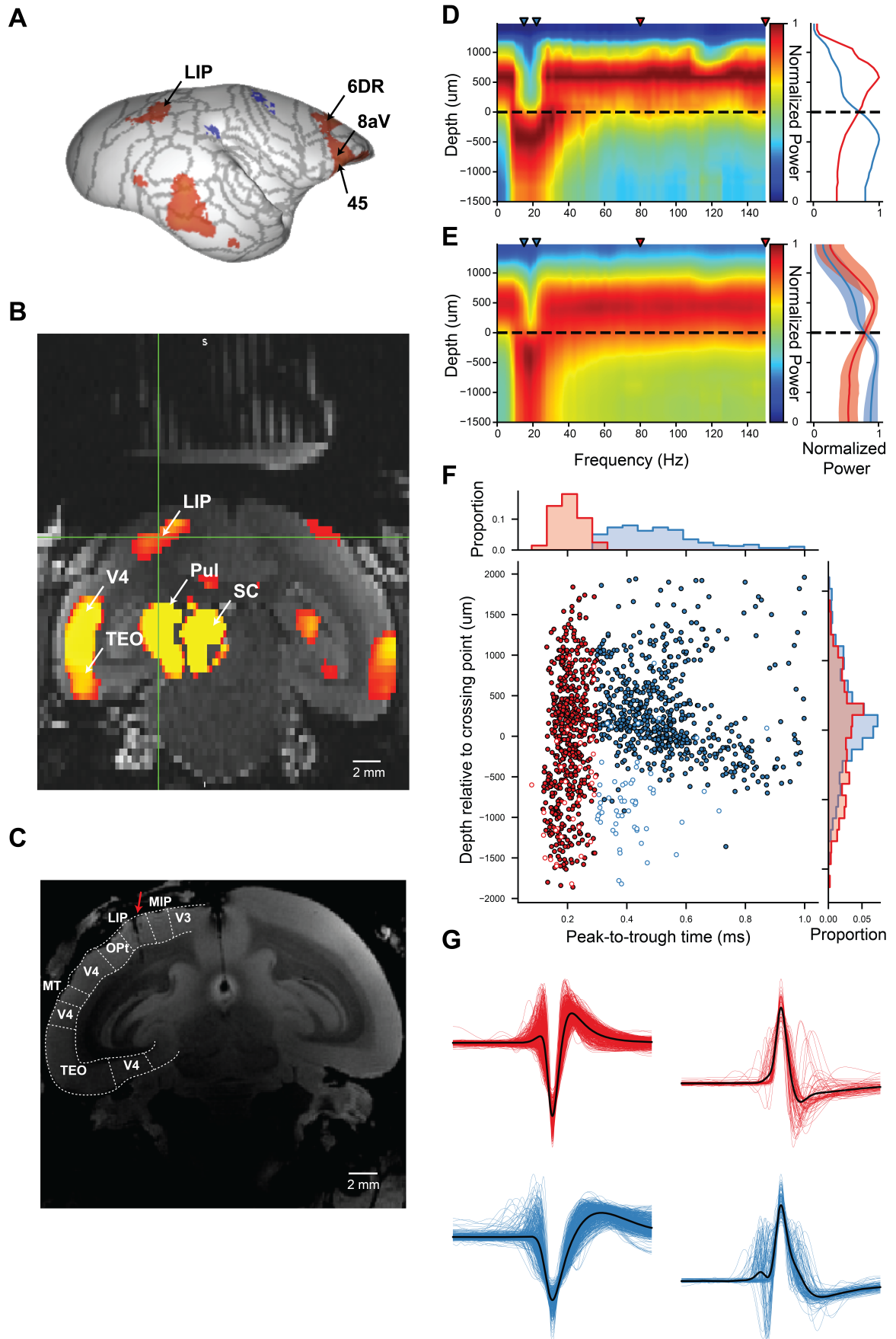
Figure 3.2: Localization of recording locations, layer assignment and cell type classification.

Figure 3.2: *Localization of recording locations, layer assignment and cell type classification (continued).* (A) Surface map of resting state functional magnetic resonance imaging (RS-fMRI) functional connectivity (FC) with superior colliculus to identify lateral intraparietal area (LIP). (B) Coronal slice of anatomical MRI of Marmoset M with an overlay of FC maps from A interpolated to native space of Marmoset M to identify location of LIP relative to the grid. (C) Ex-vivo anatomical MRI of Marmoset N with Paxinos et al., (2012) boundaries overlaid confirming electrode tract locations (as indicated by red arrow) in LIP. LFP power aligned to stimulus onset across depths and frequencies (left) and normalized power in selected ranges (right; blue: 15-22 Hz, red: 80-150 Hz) are shown for an example session (D) and the average of all sessions (E). The crossing point between lower and higher frequencies is marked by a dotted line. Peak-to-trough times for all recorded neurons across depth relative to the crossing point described above (F) and example waveforms of "broad" and "narrow" waveforms (G). Note that neurons for which we observed a positive-first waveform (N=198) are identified by white circles in (F) and plotted separately in (G). LIP = Lateral intraparietal area, MIP = Medial intraparietal area, TEO = temporal area TE occipital part, MT = middle temporal area, OPt = occipito-parietal transitional area

Table 3.1: Proportions of units with significant task modulated activity

Layer	Cell-type	Stimulus-related	Discrimination	Post-saccadic
infragranular	NS	49 (21.58%)	23 (10.13%)	137 (60.35%)
	BS	19 (17.11%)	8 (7.20%)	71 (63.96%)
granular	NS	37 (27.61%)	22 (16.41%)	83 (61.94%)
	BS	70 (26.81%)	42 (16.09%)	147 (56.32%)
supragranular	NS	90 (37.03%)	35 (14.40%)	151 (62.13%)
	BS	82 (28.17%)	27 (9.27%)	181 (62.19%)

SRTs ($p's < .05$) respectively, suggesting there may be little correspondence between the activity of these neurons and the motor planning of the upcoming saccades.

For these neurons, to examine the evolution of stimulus-related activity over time, we conducted receiver operating characteristics (ROC) analyses (Green & Swets, 1966) comparing the distributions of discharge activity following stimulus onset as compared to a prestimulus baseline interval. We computed area under the receiver operating characteristics curve (auROC) values on discharge rates within successive 15ms intervals from stimulus onset to 200 ms after stimulus onset as compared to 200 ms before stimulus onset. To evaluate the significance of auROC values, we compared these values to a null distribution created by shuffling the labels of baseline vs stimulus-related 1000 times at each interval. For each neuron we determined the first time point where a significant auROC value was observed and determined cumulative distributions for each layer (see Figure 3.4). No significant differences were observed between layers for the onset of stimulus-related activity.

We then compared the activity of these neurons in the same interval on distractor trials in which the target was in the contralateral or ipsilateral hemifield. One-hundred and sixty-eight (12.3%) neurons significantly discriminated between targets and distractor presented in the contralateral hemifield, of which 135 (80% of discriminating neurons) showed greater activity
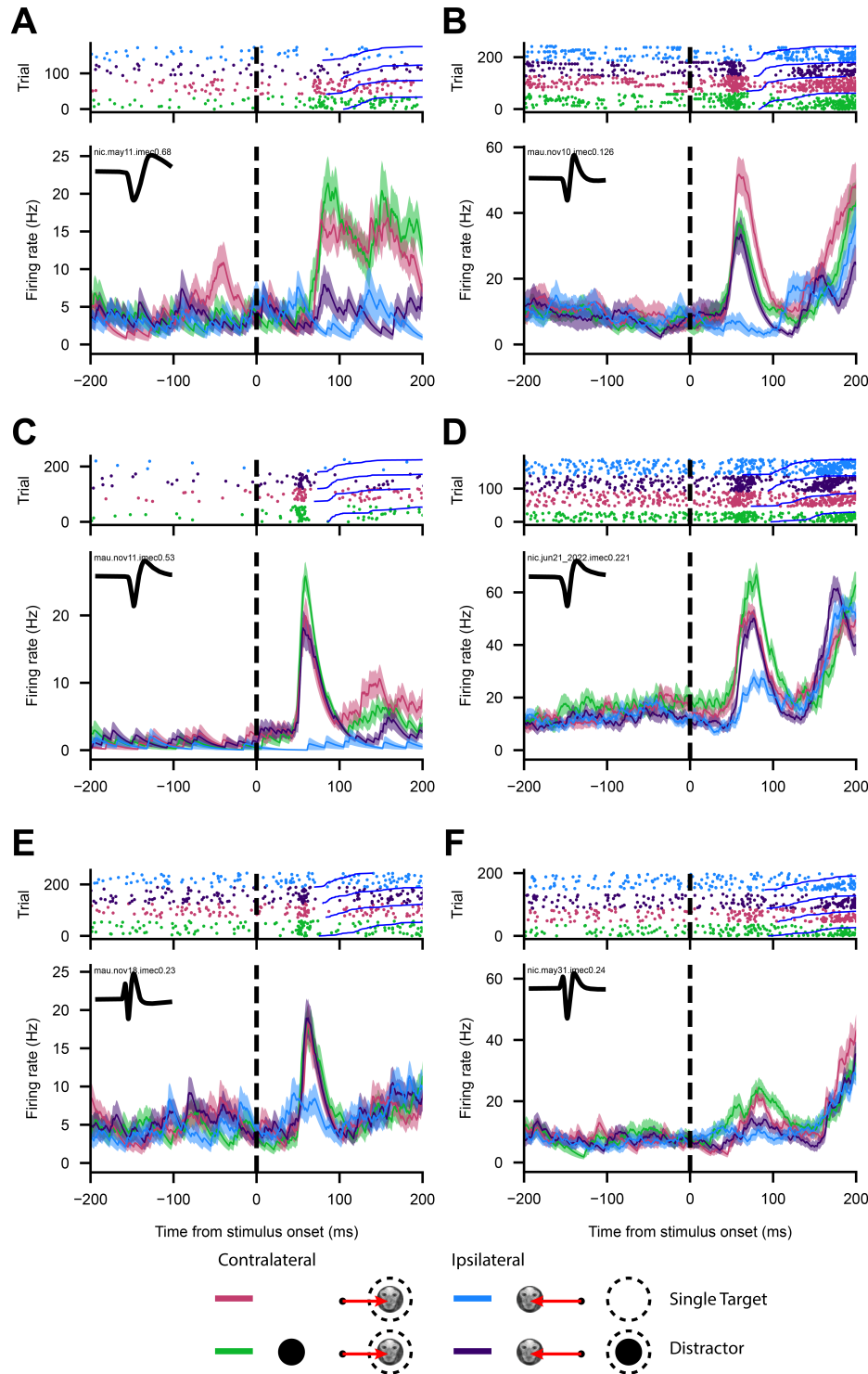
Figure 3.3: Example neurons with stimulus-related activity. Raster plots and spike density functions (SDF) aligned to stimulus onset for example broad (A, C, E) and narrow (B, D, F) - spiking neurons from supragranular (A, B), granular (C, D) and infragranular (E, F) layers with visual activity. Red = target contralateral, Green = target contralateral & distractor ipsilateral, Blue = target ipsilateral, Purple = target ipsilateral & distractor contralateral. Blue lines in raster plot represent saccade onset. Trials are sorted into conditions and in order of increasing saccade reaction times in raster plots. Mean waveform in inset SDF figure. Shaded regions in SDF figures represent +/- 1 SEM for each condition.

Figure 3.4: ROC analyses for stimulus and saccade related activity. Cumulative distributions of neurons over time with significant auROC as compared to a null distribution generated from 1000 randomized shuffles. (A) significant stimulus-related activity as compared to a pre-stimulus baseline in single-target contralateral over time from stimulus onset separately for each cortical layer. (B) significant target discriminating activity comparing ipsilateral and contralateral distractor trials over time from stimulus onset separately for each cortical layer. (C) significant post-saccadic activity comparing each condition separately to a pre-saccadic baseline over time from saccade onset. Shaded region indicates 95% CI.

for the target stimulus (see Figure 3.5, Table 3.1); supragranular (BS: 9.28%, NS: 14.40%), granular (BS: 16.09%, NS: 16.42%), infragranular (BS: 7.21%, NS: 10.13%).

For these neurons, to assess the magnitude and timing of the discrimination activity, we conducted auROC analyses comparing the distributions of activity on the trials in which the preferred (i.e., the stimulus with the greater mean discharge activity in the task epoch) or non-preferred stimulus was presented in the contralateral hemifield. We computed auROC values on discharge rates within successive 15 ms intervals from stimulus onset to 200 ms after stimulus onset. As with the stimulus-related activity, we compared the auROC values to null distributions for each neuron at each time point and determined the discrimination times for each neuron, and evaluated cumulative distributions for each layer (see Figure 3.4). We also determined the magnitude and time from stimulus onset of the maximal auROC value for each neuron. Medians across layers and putative cell class were as follows: supragranular (BS: .602, 76 ms; NS: .598, 78 ms), granular (BS: .583, 94 ms; NS: .645, 83 ms), infragranular (BS: .613, 100 ms; NS: .599, 77ms). Notably, the maximal auROC values were generally observed before the median SRTs, however, the timing and magnitude of the discrimination did not differ appreciably between layers and cell types.

We additionally observed a large proportion of neurons that displayed strong post-saccadic modulations in activity across conditions. Generally, this activity started at saccade offset, peaked approximately 50-100 ms later and often persisted for 300-500 ms. To identify neurons with significant post-saccadic activity, we computed the mean discharge rates from 50-150ms after saccade offset where we observed the peak of the activity and compared it to the 200 ms prestimulus baseline used above, separately for each condition. For correct trials, 969 neurons (70.94%) had significant post-saccadic activity in at least one condition, 688 neurons in at least two conditions, 391 in at least three conditions, 203 in all four conditions; 551-581 neurons

Figure 3.5: Example target discriminating neurons. Raster plots and spike density functions (SDF) aligned to stimulus onset for example broad (A, C, E) and narrow (B, D, F) -spiking neurons from supragranular (A, B), granular (C, D) and infragranular (E, F) layers with activity discriminating between target and distractor stimuli. Red = target contralateral, Green = target contralateral & distractor ipsilateral, Blue = target ipsilateral, Purple = target ipsilateral & distractor contralateral. Blue lines in raster plot represent saccade onset. Trials are sorted into conditions and in order of increasing saccade reaction times in raster plots. Mean waveform in inset SDF figure. Shaded regions in SDF figures represent +/- 1 SEM for each condition.
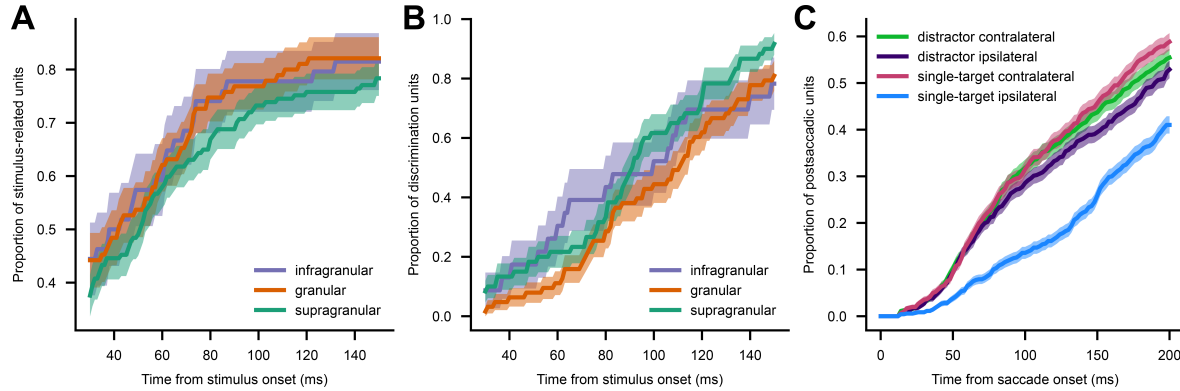
for each condition; see Figure 3.6. Post-saccadic activity did not appear to correspond with stimulus-related activity; of the 329 neurons with significant stimulus-related activity in the contralateral "single-target" condition 58 neurons had significant post-saccadic activity in the ipsilateral "single-target" condition, 71 in the contralateral and 101 in both. For the "distractor" conditions, we examined post-saccadic activity on error trials and observed that only half the number of neurons had significant post-saccadic activity (ipsilateral: 231 neurons as compared to 551, 119 neurons in both; contralateral: 288 neurons as compared to 566, 165 in both). In sum, a large proportion of neurons exhibited post-saccadic activity and this activity varied depending on stimulus identity and task performance.

To examine how this activity evolves over time, we conducted auROC analyses for each neuron, comparing the distributions of discharge activity in 15ms steps from saccade onset for 200 ms to a 50ms pre-saccadic baseline. As we did not have specific predictions about laminar or cell-type differences regarding this activity, we computed the cumulative distribution of significant auROC values across all neurons, separately for each neuron. We observed that many of the neurons exhibited significant increases in discharge activity 25-75ms following saccade onset (50 ms from saccade offset), which would be too early for stimulus related activity in response to stimuli at the saccade landing position. However, many neurons did respond after 75 ms from saccade onset, and some of these neurons may possess perifoveal receptive fields. Notably, post-saccadic increases discharge activity were observed significantly later, $F(1, 177) = 9.81$, $p = .002$, in the ipsilateral single-target condition (M=121.3 ms) compared to all three other conditions (M=101-103 ms), further suggesting this activity may not be strictly related to stimulus related properties following saccade offset but rather reflect the target selection and saccade processes pertaining to those saccades.

For comparison with the above, we determined the proportion of neurons with significant post-saccadic activity across conditions. We then conducted a logistic regression to investigate the effects of layer, cell-type, and epoch (task, discrimination, post-saccadic) on the likelihood that a neuron has significantly different discharge activity. This model explained significantly more variance than the reduced two-way models (p ¡ .05), and revealed that NS infragranular neurons were less likely to be significantly modulated in the task interval, and BS infragranular neurons were less likely to significantly discriminate between target and distractor but were more likely to have significant post-saccadic activity as compared to respective granular and supragranular layer neurons ($p's < .05$, see 3.1).

In sum, we observed in marmosets LIP neurons which were significantly modulated in a visual target selection task and, in particular, those that discriminated between target and distractor stimuli before making a saccade. Further, this activity was observed across cortical laminae and cell types, albeit in slightly different proportions; supragranular and granular neurons were more likely to demonstrate stimulus and target selection related activity whereas infragranular neurons were more likely to have significant post-saccadic activity.

3.3.4 Stimulus related activity first emerges in narrow spiking granular layer neurons

To examine if and how the emergence of stimulus-related activity differs across cortical layers and cell types, we investigated the population activity using generalized additive models
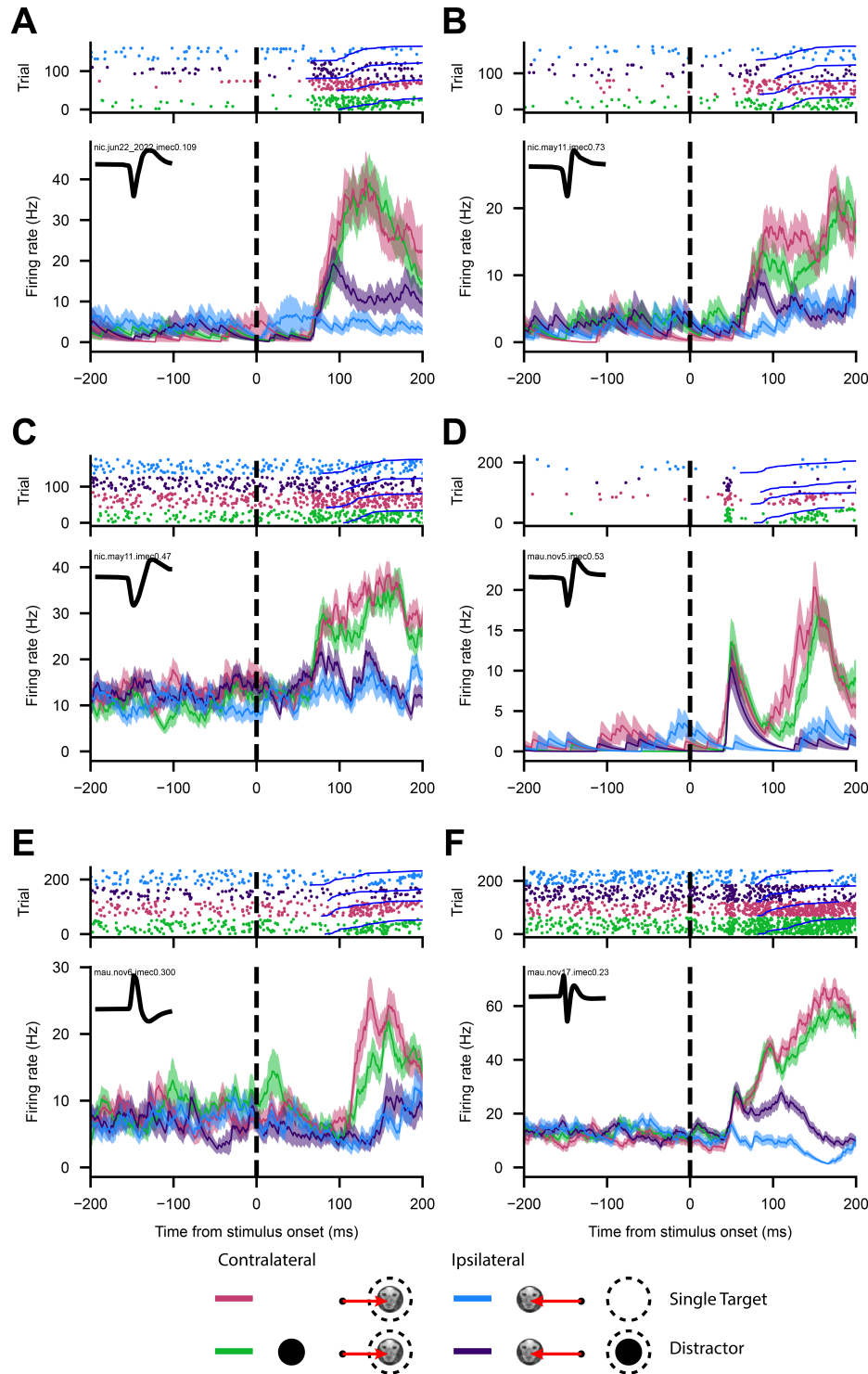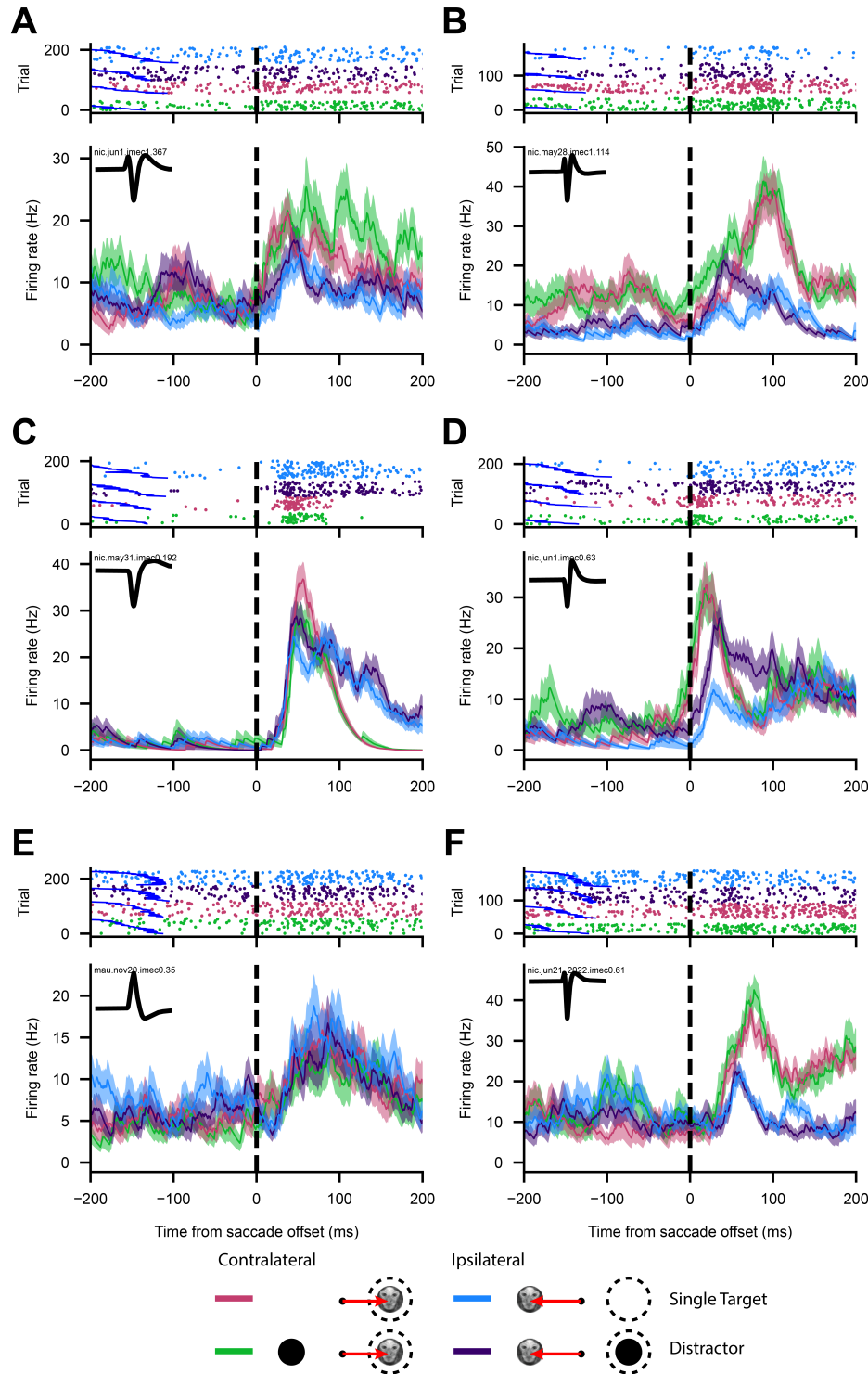
Figure 3.6: Example post-saccadic neurons. Raster plots and spike density functions (SDF) aligned to saccade offset for example broad (A, C, E) and narrow (B, D, F) -spiking neurons from supragranular (A, B), granular (C, D) and infragranular (E, F) layers with significant post-saccadic activity. Red = target contralateral, Green = target contralateral & distractor ipsilateral, Blue = target ipsilateral, Purple = target ipsilateral & distractor contralateral. Blue lines in raster plot represent saccade onset. Trials are sorted into conditions and in order of increasing saccade reaction times in raster plots. Mean waveform in inset SDF figure. Shaded regions in SDF figures represent +/- 1 SEM for each condition.

(GAMs). GAMs are a type of statistical model which fits data to a "smooth" curve comprised of many line segments by estimating the value at each "knot", the boundaries of these segments (Hastie & Tibshirani, 1986). In this manner, GAMs can capture complex, non-linear relationships such as how neural activity varies over time (Cadarso-Suarez et al., 2006). Here, for the entire population of recorded neurons, we modelled the odds of a spike at each point in time and depth as a function of time from stimulus onset (ms), relative depth from the crossing point of low and high frequency power (μm), and cell type (BS, NS) for the contralateral and ipsilateral "single-target" condition. We employed a traditional stepwise regression approach for model selection wherein we constructed reduced models which successively excluded the factors of cell-type, depth, condition and time as well as the random effects of neuron and trial. We then compared these models using the chi-squared likelihood ratio test. This model significantly improved fit as compared to the reduced models (p ¡ .001). As the vast majority of neurons only exhibited significant increases in discharge activity for contralateral as compared to ipsilateral "single-target" trials, we could evaluate the onset of stimulus-related activity by comparing the activity between these conditions. To examine differences between these conditions across time and depth, we may compute estimates of the pairwise differences between conditions for the time by depth tensor smooths separately for BS and NS neuron populations. Points in time and depth where these difference smooths deviate significantly from zero (evaluated here at a 99.9% CI) are where the conditions significantly differ. As such, we can determine the earliest time point and depths where stimulus-related activity was first observed for each cell type (see Figure 3.7). The earliest stimulus related activity first emerges in narrow-spiking neurons 0-500 μm below the crossing point 35 ms following stimulus onset, followed by more superficial narrow-spiking and broad-spiking neurons 38-40 ms following stimulus onset, likely corresponding to granular and supragranular neurons respectively. For ease of exposition, the model was discretized across depth into supragranular, granular and infragranular layers as was done for the single neuron analyses above (see Figure 3.8). Here, stimulus-related activity first emerged in NS granular and BS supragranular neurons (35ms), followed by NS supragranular neurons (37 ms) and finally in BS granular layer neurons (42 ms). In sum, this suggests that stimulus-related activity first emerges in the granular layer, then in supragranular layers and occurs first in NS, i.e., putative interneurons. The population stimulus-related activity in infragranular layers did not reach significance at any time point.

3.3.5   Target discrimination related activity first emerges in broad spiking supragranular neurons

Next, we examined how target discrimination activity first emerges in the population activity using a GAM where we modelled odds of spiking using time, depth, cell type and condition (ipsilateral vs contralateral "distractor" trials; p ¡ .05). We then computed difference smooths between the conditions with a 99.9% CI, identified time points where this difference smooth deviated from 0 (see Figure 3.7), and determined the earliest time point and depths where target discrimination activity was observed for each cell type. The earliest discrimination activity was observed in broad-spiking neurons 1000 μm above the crossing point 56 ms after stimulus onset, followed by broad-spiking and narrow-spiking neurons around the crossing point 58-65ms after stimulus onset. As above, when using discrete layer categories across depth (see
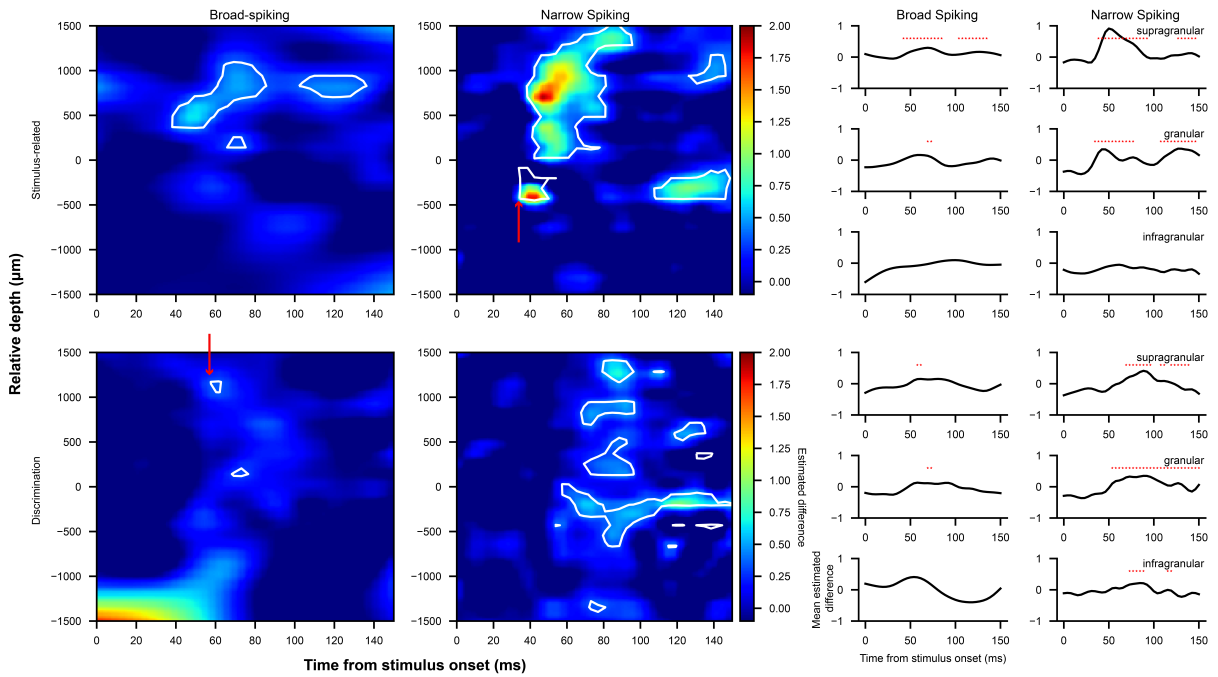
Figure 3.7: Generalized additive model fit of population activity continuously across depth. Odds of a spike at a given point in time are estimated using the time from stimulus onset, the relative depth from the crossing point, putative cell class (NS or BS), and the condition of the given trial (stimulus-related: ispilateral vs contralateral single target trials; discrimination: preferred vs non-preferred distractor trials) with trial and neuron as random effects. Estimated differences across depth and time are plotted separately for stimulus-related (top) and discrimination (bottom), broad-spiking (left) and narrow-spiking (right) as heatmaps, with significant differences between conditions as determined by a 99.9% CI highlighted in white contours. Mean difference traces across depth ranges roughly corresponding to cortical layers are plotted on the right, separately for comparison and cell-type. Significant differences are indicated by red *.

Figure 3.8: Generalized additive model fit for population activity discretely across depth. Odds of a spike at a given point in time are estimated using the time from stimulus onset, the putative layer the neuron is found in (supragranular, granular, or infragranular), putative cell class (NS or BS), and the condition of the given trial (stimulus-related: ispilateral vs contralateral single target trials; discrimination: preferred vs non-preferred distractor trials) with trial and neuron as random effects. Spike probability in the preferred/contralateral (red) and non-preferred/ipsilateral (black) conditions are plotted here for broad (left) and narrow (right) spiking neurons for supragranular, granular and infragranular layers. * = significant difference between conditions at 99.9% CI. First significant time point noted in bottom right corner in ms. Shaded region indicates +/- 1 SEM.

Figure 3.8): we observed target discrimination activity first in BS supragranular neurons (35 ms), followed by infragranular neurons (NS: 36 ms, BS: 37 ms), then in BS granular layer neurons (39 ms), then in NS supragranular neurons (41 ms) and finally in NS granular layer neurons (44ms). Altogether, we see target discrimination emerges rapidly in superficial layers and predominantly in BS neurons.

In sum, although neurons with stimulus-related and target discrimination activity were observed across cortical laminae, subtle differences in the timing of this activity were observed at the population level, suggesting the granular layer as the primary input and supragranular layers as the first to discriminate between targets and distractors.

3.4 Discussion

The laminar microcircuitry underlying visual target selection and saccade control in PPC remains poorly understood due to limitations of previously used animal models and experimental approaches. Here, we employed ultra-high density laminar electrophysiology in the PPC of common marmosets as they completed a saccadic target selection task to address this gap. As expected, we observed neurons with stimulus-related activity and, for the first time in the marmoset, neurons that discriminated between target and distractor stimuli. The stimulus-related activity observed here first emerged in the granular layer, followed by supragranular layers, with population activity in infragranular layers never reaching significance. This activity emerged first in putative interneurons followed by putative pyramidal neurons. Conversely, activity discriminating between target and distractor stimuli first emerged in supragranular neurons, followed by infragranular and finally granular layers, usually first appearing in putative pyramidal neurons. Altogether, the observed patterns support the existence of a canonical circuit consistent with previous models (Douglas & Martin, 2004; Heinzle et al., 2007).

Since its first description in (Andersen et al., 1987; Barash et al., 1991a, 1991b), LIP has been the focus of intensive investigation for its role in the control of visual attention and eye movements. Single neuron recordings in macaque LIP have demonstrated that neurons in this area respond selectively to relevant visual stimuli and are critical in guiding visual attention and saccadic eye movements (Andersen et al., 1987; Barash et al., 1991a, 1991b; Colby et al., 1996; Gnadt & Andersen, 1988; Kusunoki et al., 2000). Subsequent work, typically employing variants of the visual search task, has demonstrated activity in LIP which evolves to discriminate the presence of targets or distractors within their response fields (Ipata et al., 2006; Mirpour et al., 2009; Thomas & Paré, 2007). Investigations using pharmacological interventions and cortical cooling have further demonstrated a causal role for LIP in regulating visual salience (Chen et al., 2020; Wardak et al., 2002). Consistent with these observations, for the first time in the common marmoset, we observed a number of neurons that in a simple target selection task, responded to visual stimuli, a large proportion of which discriminated targets from distractors. Further, this discrimination activity generally peaked prior to the upcoming saccade to the target location, consistent with a visual selection process preceding saccade generation. However, for these neurons, the magnitude of the discharge activity preceding the saccade did not correlate with the SRTs, though this is not surprising as the activity of LIP neurons does not strictly predict the motor plan underlying upcoming saccadic eye movements, but rather represents the current locus of attention across the visual field (Bisley & Goldberg, 2003; Bisley

et al., 2011; Goldberg et al., 2002; Kusunoki et al., 2000).

Surprisingly, a large proportion of neurons displayed significant post-saccadic activity across conditions which began immediately after saccade offset and often persisted up to 500 ms. As this activity is observed for both ipsilateral and contralateral trials in the "single-target" condition, it is unlikely to reflect remapping signals for a stimulus passing through the future receptive field of a neuron, as is observed in LIP neurons for "double-step" saccade paradigms (Duhamel et al., 1992). While it is possible that for some neurons this activity could be explained by stimulus-related activity for the target stimulus in a perifoveal receptive field at saccade offset, this is unlikely to be the sole source of this activity as for many neurons this activity is observed immediately following saccade offset. Additionally, the onset of this activity is delayed in the single-target ipsilateral trials, and is observed in fewer neurons, despite the same perifoveal visual input. This activity could reflect the efference copy of the saccade i.e. corollary discharge (Sommer & Wurtz, 2008). In FEF, corollary discharge activity can be observed which is relayed from SC by the medial dorsal nucleus of the thalamus (Sommer & Wurtz, 2004, 2006). The observed activity here could be corollary discharge activity from SC in a similar pathway through pulvinar or from FEF. It has been previously observed that this activity in PPC can reflect saccadic error or saccade duration (Munuera & Duhamel, 2020; Zhou et al., 2016; Zhou et al., 2018). It is worth noting that for many of these neurons, this activity varied across conditions and as a function of task performance while saccade amplitude and duration did not, suggesting this activity is not merely an efference copy but may encode other task-relevant variables.

While the activity of LIP neurons has not been shown to be tightly linked to saccade initiation, such activity can be observed in other frontoparietal structures such as FEF and SC with which LIP is strongly interconnected. Notably, LIP projections to these areas are largely segregated within distinct cortical laminae; cortico-cortical projections originate primarily in supragranular layers II/III and tend to convey visual information whereas corticotectal projections originate exclusively from infragranular layer V and primarily carry saccade-related information (Ferraina et al., 2002; Lynch et al., 1985; Schall, 1995). Indeed, computational models based on studies of macaque FEF and observed laminar circuits in cat primary visual cortex (Douglas & Martin, 2004; Heinzle et al., 2007) propose layer IV as the input, layers II/III as being responsible for the rule-based allocation of attention, and layer V as the primary output. These observations motivate investigations of laminar dynamics of areas such as FEF and LIP underlying these differences. Although these are challenging to pursue in the macaque due to the location of these areas in sulci prohibiting laminar electrophysiology, the lissencephalic cortex of the marmoset lends itself well to such investigations.

To this end, we used established methods of identifying cortical layers based on the PSD (Mendoza-Halliday et al., 2023) and classifying putative cell classes on the basis of peak-trough widths (Ardid et al., 2015; Hussar & Pasternak, 2012; McCormick et al., 1985; Mitchell et al., 2007). We reliably observed a crossing point in the power of low and high frequencies across depths, indicative of granular layer IV, from which we were able to separate cortex into supragranular, granular, and infragranular layers. Regarding cell type classification, we observed a larger than expected proportion of positive-negative waveforms, which were largely restricted to BS infragranular neurons. These waveforms likely correspond to spikes recorded at the apical dendritic trunk of pyramidal neurons with large apical dendritic arbors which may be more commonly encountered in deeper layers (Boulton et al., 1990, p. 9). For many of

these neurons, we observed lower amplitude, negative-positive waveforms on deeper electrode contacts consistent with spikes recorded at the soma. To classify these neurons, we simply inverted the waveform before computing the peak-trough width.

We then assessed how the observed activity varied across cortical laminae and putative cell classes. First, we examined the proportion of neurons with significant stimulus-related, discrimination and post-saccadic activity. NS supragranular/granular layer neurons were more likely to have stimulus-related activity as compared to infragranular neurons. Similarly, superficial BS neurons were more likely to discriminate between targets and distractors. Conversely, BS infragranular neurons were more likely than their superficial counterparts to display significant post-saccadic activity. These observations are consistent with the proposed role of superficial layers in visual input and attentional deployment and deeper layers for output.

Interestingly, we observed no difference in the maximal magnitude of the discrimination between target and distractor stimuli across layers or putative cell classes. However, the timing of how this activity evolves did differ. We first observed stimulus-related activity in putative interneurons in the granular layer followed by supragranular layer neurons. This is consistent with what is observed in other cortical areas and proposed by theoretical models. Moreover, this is consistent with the anatomy as corticocortical feedforward projections and thalamic input primarily terminate in granular layer IV and to a lesser extent, supragranular layers (Baizer et al., 1991; Matsuzaki et al., 2004). That it is observed first in putative interneurons as compared to pyramidal neurons is perhaps surprising as the primary target of long-range cortical projections are spiny neurons, which are generally pyramidal neurons (Anderson et al., 2011). However, this is characteristic of thalamocortical feedforward inhibition as observed in mouse barrel cortex (Swadlow, 2002). Here it is observed that monosynaptic thalamocortical input to somata of broadly tuned and highly sensitive layer IV interneurons act to rapidly drive inhibition which in turn sharpens the tuning properties of nearby pyramidal cells. Next, also consistent with our hypothesis, we observed discrimination between target and distractor stimuli first in putative pyramidal neurons in supragranular layers. Neurons in this layer are known to share reciprocal projections other key cortical structures involved in visual target selection such as FEF (Ferraina et al., 2002).

In sum, we identified single neurons exhibiting stimulus-related activity and those that discriminate between target and distractor stimuli across all layers and cell types albeit at different proportions and times. These observations are consistent with observations in single neuron investigations of LIP. Ferraina and colleagues (2002) antidromically identified populations of LIP neurons that were either a more superficial cortico-cortical, FEF projecting population, or a deeper corticotectal, SC projecting population. While these populations did possess similar stimulus-related, delay and saccade-related activity, a greater proportion of the more superficial cortico-cortical population exhibited stimulus-related activity whereas a greater proportion of the deeper corticotectal population exhibited delay and saccade-related activity. These observations are consistent with our own, highlighting a role of more superficial neurons in earlier visual processing and deeper neurons in later saccadic stages. This can also be observed in FEF, where layer V corticotectal neurons represent activity at nearly all stages of visuomotor processing but tended to be more related to movement than more superficial cortico-cortical neurons (Everling & Munoz, 2000; Wurtz et al., 2001). Similarly in V4, a greater proportion of neurons with visual activity and feature selectivity can be observed in superficial layers as compared to a greater representation of eye movement related signals in deeper layers (Pettine

et al., 2019; Westerberg et al., 2021).

Altogether, our findings demonstrate single neuron target selection related activity in the posterior parietal cortex of marmoset monkeys. Critically, we found interlaminar dynamics underlying this activity in primate association cortex consistent with a "canonical circuit" resembling that observed in primary visual cortex and proposed for the frontal eye fields. These dynamics are characterized by a flow of neural activity from granular, to supragranular, to infragranular layers, with stimulus-related activity emerging first in granular layer putative interneurons and target discrimination first emerging in supragranular putative pyramidal neurons.

3.5 References

Andersen, R. A., Bracewell, R. M., Barash, S., Gnadt, J. W., & Fogassi, L. (1990). Eye position effects on visual, memory, and saccade-related activity in areas LIP and 7a of macaque. *The Journal of Neuroscience*, *10*(4), 1176–1196. https://doi.org/10.1523/JNEUROSCI. 10-04-01176.1990

Andersen, R. A., Essick, G. K., & Siegel, R. M. (1987). Neurons of area 7 activated by both visual stimuli and oculomotor behavior. *Experimental Brain Research*, *67*(2), 316–322. https://doi.org/10.1007/BF00248552

Anderson, J. C., Kennedy, H., & Martin, K. A. C. (2011). Pathways of Attention: Synaptic Relationships of Frontal Eye Field to V4, Lateral Intraparietal Cortex, and Area 46 in Macaque Monkey. *The Journal of Neuroscience*, *31*(30), 10872–10881. https://doi.org/ 10.1523/JNEUROSCI.0622-11.2011

Ardid, S., Vinck, M., Kaping, D., Marquez, S., Everling, S., & Womelsdorf, T. (2015). Mapping of Functionally Characterized Cell Classes onto Canonical Circuit Operations in Primate Prefrontal Cortex. *The Journal of Neuroscience*, *35*(7), 2975–2991. https://doi. org/10.1523/JNEUROSCI.2700-14.2015

Baizer, J. S., Ungerleider, L. G., & Desimone, R. (1991). Organization of visual inputs to the inferior temporal and posterior parietal cortex in macaques. *The Journal of Neuroscience*, *11*(1), 168–190. https://doi.org/10.1523/JNEUROSCI.11-01-00168.1991

Barash, S., Bracewell, R. M., Fogassi, L., Gnadt, J. W., & Andersen, R. A. (1991a). Saccade-related activity in the lateral intraparietal area. II. Spatial properties. *Journal of Neurophysiology*, *66*(3), 1109–1124. https://doi.org/10.1152/jn.1991.66.3.1109

Barash, S., Bracewell, R. M., Fogassi, L., Gnadt, J. W., & Andersen, R. A. (1991b). Saccade-related activity in the lateral intraparietal area. I. Temporal properties; comparison with area 7a. *Journal of Neurophysiology*, *66*(3), 1095–1108. https://doi.org/10.1152/jn. 1991.66.3.1095

Bastos, A. M., Loonis, R., Kornblith, S., Lundqvist, M., & Miller, E. K. (2018). Laminar recordings in frontal cortex suggest distinct layers for maintenance and control of working memory. *Proceedings of the National Academy of Sciences of the United States of America*, *115*(5), 1117–1122. https://doi.org/10.1073/pnas.1710323115

Bisley, J. W., & Goldberg, M. E. (2003). Neuronal Activity in the Lateral Intraparietal Area and Spatial Attention. *Science*, *299*(5603), 81–86. https://doi.org/10.1126/science.1077395

Bisley, J. W., Mirpour, K., Arcizet, F., & Ong, W. S. (2011). The Role of the Lateral Intra-parietal Area in Orienting Attention and its Implications for Visual Search. *The European journal of neuroscience*, *33*(11), 1982–1990. https://doi.org/10.1111/j.1460-9568.2011.07700.x

Boulton, A. A., Baker, G. B., & Vanderwolf, C. H. (1990, September 12). *Neurophysiological Techniques, II* (Vol. 15). Humana Press. https://doi.org/10.1385/0896031853

Cadarso-Suarez, C., Roca-Pardinas, J., Molenberghs, G., Faes, C., Nacher, V., Ojeda, S., & Acuna, C. (2006). Flexible modelling of neuron firing rates across different experimental conditions: An application to neural activity in the prefrontal cortex during a discrimination task. *Journal of the Royal Statistical Society: Series C (Applied Statistics)*, *55*(4), 431–447. https://doi.org/10.1111/j.1467-9876.2006.00545.x

Chen, X., Zirnsak, M., Vega, G. M., Govil, E., Lomber, S. G., & Moore, T. (2020). Parietal cortex regulates visual salience and salience-driven behavior. *Neuron*, *106*(1), 177–187.e4. https://doi.org/10.1016/j.neuron.2020.01.016

Colby, C. L., Duhamel, J.-R., & Goldberg, M. E. (1996). Visual, presaccadic, and cognitive activation of single neurons in monkey lateral intraparietal area. *Journal of Neurophysiology*, *76*(5), 2841–2852. https://doi.org/10.1152/jn.1996.76.5.2841

Collins, C. E., Lyon, D. C., & Kaas, J. H. (2005). Distribution across cortical areas of neurons projecting to the superior colliculus in new world monkeys. *The Anatomical Record Part A: Discoveries in Molecular, Cellular, and Evolutionary Biology*, *285A*(1), 619–627. https://doi.org/10.1002/ar.a.20207

Dorris, M. C., Paré, M., & Munoz, D. P. (1997). Neuronal Activity in Monkey Superior Colliculus Related to the Initiation of Saccadic Eye Movements. *The Journal of Neuroscience*, *17*(21), 8566–8579. https://doi.org/10.1523/JNEUROSCI.17-21-08566.1997

Douglas, R. J., & Martin, K. A. (1991). A functional microcircuit for cat visual cortex. *The Journal of Physiology*, *440*, 735–769. Retrieved July 23, 2021, from https://www.ncbi.nlm.nih.gov/pmc/articles/PMC1180177/

Douglas, R. J., & Martin, K. A. (2004). Neuronal Circuits of the Neocortex. *Annual Review of Neuroscience*, *27*(1), 419–451. https://doi.org/10.1146/annurev.neuro.27.070203.144152

Duhamel, J.-R., Colby, C. L., & Goldberg, M. E. (1992). The Updating of the Representation of Visual Space in Parietal Cortex by Intended Eye Movements. *Science*, *255*(5040), 90–92. Retrieved February 14, 2023, from https://www.jstor.org/stable/2876068

Everling, S., & Munoz, D. P. (2000). Neuronal Correlates for Preparatory Set Associated with Pro-Saccades and Anti-Saccades in the Primate Frontal Eye Field. *Journal of Neuroscience*, *20*(1), 387–400. https://doi.org/10.1523/JNEUROSCI.20-01-00387.2000

Feizpour, A., Majka, P., Chaplin, T. A., Rowley, D., Yu, H.-H., Zavitz, E., Price, N. S. C., Rosa, M. G. P., & Hagan, M. A. (2021). Visual responses in the dorsolateral frontal cortex of marmoset monkeys. *Journal of Neurophysiology*, *125*(1), 296–304. https://doi.org/10.1152/jn.00581.2020

Ferraina, S., Paré, M., & Wurtz, R. H. (2002). Comparison of Cortico-Cortical and Cortico-Collicular Signals for the Generation of Saccadic Eye Movements. *Journal of Neurophysiology*, *87*(2), 845–858. https://doi.org/10.1152/jn.00317.2001

Ghahremani, M., Hutchison, R. M., Menon, R. S., & Everling, S. (2017). Frontoparietal Functional Connectivity in the Common Marmoset. *Cerebral Cortex*, *27*, 3890–3905. https://doi.org/10.1093/cercor/bhw198

Ghahremani, M., Johnston, K. D., Ma, L., Hayrynen, L. K., & Everling, S. (2019). Electrical microstimulation evokes saccades in posterior parietal cortex of common marmosets. *Journal of Neurophysiology*, *122*(4), 1765–1776. https://doi.org/10.1152/jn.00417.2019

Gnadt, J. W., & Andersen, R. A. (1988). Memory related motor planning activity in posterior parietal cortex of macaque. *Experimental Brain Research*, *70*(1), 216–220. https://doi.org/10.1007/BF00271862

Godlove, D. C., Maier, A., Woodman, G. F., & Schall, J. D. (2014). Microcircuitry of Agranular Frontal Cortex: Testing the Generality of the Canonical Cortical Microcircuit. *The Journal of Neuroscience*, *34*(15), 5355–5369. https://doi.org/10.1523/JNEUROSCI.5127-13.2014

Goldberg, M. E., Bisley, J., Powell, K. D., Gottlieb, J. P., & Kusunoki, M. (2002). The Role of the Lateral Intraparietal Area of the Monkey in the Generation of Saccades and Visuospatial Attention. *Annals of the New York Academy of Sciences*, *956*(1), 205–215. https://doi.org/10.1111/j.1749-6632.2002.tb02820.x

Gottlieb, J. P., & Goldberg, M. E. (1999). Activity of neurons in the lateral intraparietal area of the monkey during an antisaccade task. *Nature Neuroscience*, *2*(10), 906–912. https://doi.org/10.1038/13209

Green, D. M., & Swets, J. A. (1966). *Signal detection theory and psychophysics*. John Wiley.

Hanes, D. P., & Schall, J. D. (1996). Neural Control of Voluntary Movement Initiation. *Science*, *274*(5286), 427–430. https://doi.org/10.1126/science.274.5286.427

Hastie, T., & Tibshirani, R. (1986). Generalized Additive Models. *Statistical Science*, *1*(3), 297–318.

Heinzle, J., Hepp, K., & Martin, K. A. C. (2007). A Microcircuit Model of the Frontal Eye Fields. *Journal of Neuroscience*, *27*(35), 9341–9353. https://doi.org/10.1523/JNEUROSCI.0974-07.2007

Hussar, C. R., & Pasternak, T. (2012). Memory-Guided Sensory Comparisons in the Prefrontal Cortex: Contribution of Putative Pyramidal Cells and Interneurons. *The Journal of Neuroscience*, *32*(8), 2747–2761. https://doi.org/10.1523/JNEUROSCI.5135-11.2012

Hwang, J., Mitz, A. R., & Murray, E. A. (2019). NIMH MonkeyLogic: Behavioral control and data acquisition in MATLAB. *Journal of neuroscience methods*, *323*, 13–21. https://doi.org/10.1016/j.jneumeth.2019.05.002

Ipata, A. E., Gee, A. L., Gottlieb, J. P., Bisley, J. W., & Goldberg, M. E. (2006). LIP responses to a popout stimulus are reduced if it is overtly ignored. *Nature neuroscience*, *9*(8), 1071–1076. https://doi.org/10.1038/nn1734

Johnston, K. D., Barker, K., Schaeffer, L., Schaeffer, D. J., & Everling, S. (2018). Methods for chair restraint and training of the common marmoset on oculomotor tasks. *Journal of Neurophysiology*, *119*, 1636–1646.

Johnston, K. D., & Everling, S. (2008). Neurophysiology and neuroanatomy of reflexive and voluntary saccades in non-human primates. *Brain and Cognition*, *68*(3), 271–283. https://doi.org/10.1016/j.bandc.2008.08.017

Jun, J. J., Steinmetz, N. A., Siegle, J. H., Denman, D. J., Bauza, M., Barbarits, B., Lee, A. K., Anastassiou, C. A., Andrei, A., Aydın, Ç., Barbic, M., Blanche, T. J., Bonin, V., Couto, J., Dutta, B., Gratiy, S. L., Gutnisky, D. A., Häusser, M., Karsh, B., . . . Harris, T. D. (2017). Fully integrated silicon probes for high-density recording of neural activity. *Nature*, *551*(7679), 232–236. https://doi.org/10.1038/nature24636

Karsh, B. (2019). *SpikeGLX: Synchronized acquisition from imec neural probes and NI-DAQ devices.* (Version v20190413-phase3B2). https://github.com/billkarsh/SpikeGLX

Kusunoki, M., Gottlieb, J. P., & Goldberg, M. E. (2000). The lateral intraparietal area as a salience map: The representation of abrupt onset, stimulus motion, and task relevance. *Vision Research*, *40*(10), 1459–1468. https://doi.org/10.1016/S0042-6989(99)00212-6

Lewis, J. W., & Van Essen, D. C. (2000). Corticocortical connections of visual, sensorimotor, and multimodal processing areas in the parietal lobe of the macaque monkey. *Journal of Comparative Neurology*, *428*(1), 112–137. https://doi.org/10.1002/1096-9861(20001204)428:1⟨112::AID-CNE8⟩3.0.CO;2-9

Lynch, J. C., Graybiel, A. M., & Lobeck, L. J. (1985). The differential projection of two cytoarchitectonic subregions of the inferior parietal lobule of macaque upon the deep layers of the superior colliculus. *Journal of Comparative Neurology*, *235*(2), 241–254. https://doi.org/10.1002/cne.902350207

Ma, L., Selvanayagam, J., Ghahremani, M., Hayrynen, L. K., Johnston, K. D., & Everling, S. (2020). Single-unit activity in marmoset posterior parietal cortex in a gap saccade task. *Journal of Neurophysiology*, *123*(3), 896–911. https://doi.org/10.1152/jn.00614.2019

Matsuzaki, R., Kyuhou, S.-i., Matsuura-Nakao, K., & Gemba, H. (2004). Thalamo-cortical projections to the posterior parietal cortex in the monkey. *Neuroscience Letters*, *355*(1), 113–116. https://doi.org/10.1016/j.neulet.2003.10.066

McCormick, D. A., Connors, B. W., Lighthall, J. W., & Prince, D. A. (1985). Comparative electrophysiology of pyramidal and sparsely spiny stellate neurons of the neocortex. *Journal of Neurophysiology*, *54*(4), 782–806. https://doi.org/10.1152/jn.1985.54.4.782

McDowell, J. E., Dyckman, K. A., Austin, B., & Clementz, B. A. (2008). Neurophysiology and Neuroanatomy of Reflexive and Volitional Saccades: Evidence from Studies of Humans. *Brain and cognition*, *68*(3), 255–270. https://doi.org/10.1016/j.bandc.2008.08.016

McPeek, R. M., & Keller, E. L. (2002). Saccade Target Selection in the Superior Colliculus During a Visual Search Task. *Journal of Neurophysiology*, *88*(4), 2019–2034. https://doi.org/10.1152/jn.2002.88.4.2019

Mendoza-Halliday, D., Major, A. J., Lee, N., Lichtenfeld, M., Carlson, B., Mitchell, B., Meng, P. D., Xiong, Y. (, Westerberg, J. A., Maier, A., Desimone, R., Miller, E. K., & Bastos, A. M. (2023, May 12). *A ubiquitous spectrolaminar motif of local field potential power across the primate cortex.* https://doi.org/10.1101/2022.09.30.510398

Mirpour, K., Arcizet, F., Ong, W. S., & Bisley, J. W. (2009). Been There, Seen That: A Neural Mechanism for Performing Efficient Visual Search. *Journal of Neurophysiology*, *102*(6), 3481–3491. https://doi.org/10.1152/jn.00688.2009

Mitchell, J. F., Sundberg, K. A., & Reynolds, J. H. (2007). Differential Attention-Dependent Response Modulation across Cell Classes in Macaque Visual Area V4. *Neuron*, *55*(1), 131–141. https://doi.org/10.1016/j.neuron.2007.06.018

Mitra, P. P., & Pesaran, B. (1999). Analysis of Dynamic Brain Imaging Data. *Biophysical Journal*, *76*(2), 691–708. https://doi.org/10.1016/S0006-3495(99)77236-X

Munuera, J., & Duhamel, J.-R. (2020). The role of the posterior parietal cortex in saccadic error processing. *Brain Structure and Function*, *225*(2), 763–784. https://doi.org/10.1007/s00429-020-02034-5

Nandy, A. S., Nassi, J. J., & Reynolds, J. H. (2017). Laminar organization of attentional modulation in macaque visual area V4. *Neuron*, *93*(1), 235–246. https://doi.org/10.1016/j.neuron.2016.11.029

Ninomiya, T., Dougherty, K., Godlove, D. C., Schall, J. D., & Maier, A. (2015). Microcircuitry of agranular frontal cortex: Contrasting laminar connectivity between occipital and frontal areas. *Journal of Neurophysiology*, *113*(9), 3242–3255. https://doi.org/10.1152/jn.00624.2014

Pachitariu, M., Sridhar, S., & Stringer, C. (2023, January 7). *Solving the spike sorting problem with Kilosort*. https://doi.org/10.1101/2023.01.07.523036

Paré, M., & Hanes, D. P. (2003). Controlled Movement Processing: Superior Colliculus Activity Associated with Countermanded Saccades. *The Journal of Neuroscience*, *23*(16), 6480–6489. https://doi.org/10.1523/JNEUROSCI.23-16-06480.2003

Paxinos, G., Charles, W., Michael, P., Rosa, M. G. P., & Hironobu, T. (2012). *The marmoset brain in stereotaxic coordinates*. Academic
OCLC: 794295103.

Pettine, W. W., Steinmetz, N. A., & Moore, T. (2019). Laminar segregation of sensory coding and behavioral readout in macaque V4. *Proceedings of the National Academy of Sciences of the United States of America*, *116*(29), 14749–14754. https://doi.org/10.1073/pnas.1819398116

Reser, D. H., Burman, K. J., Yu, H.-H., Chaplin, T. A., Richardson, K. E., Worthy, K. H., & Rosa, M. G. P. (2013). Contrasting Patterns of Cortical Input to Architectural Subdivisions of the Area 8 Complex: A Retrograde Tracing Study in Marmoset Monkeys. *Cerebral Cortex*, *23*(8), 1901–1922. https://doi.org/10.1093/cercor/bhs177

Rosa, M. G. P., Palmer, S. M., Gamberini, M., Burman, K. J., Yu, H.-H., Reser, D. H., Bourne, J. A., Tweedale, R., & Galletti, C. (2009). Connections of the Dorsomedial Visual Area: Pathways for Early Integration of Dorsal and Ventral Streams in Extrastriate Cortex. *Journal of Neuroscience*, *29*(14), 4548–4563. https://doi.org/10.1523/JNEUROSCI.0529-09.2009

Rossant, C. (2019). *Phy: Interactive visualization and manual spike sorting of large-scale ephys data* (Version 2.0b1).

Schaeffer, D. J., Gilbert, K. M., Hori, Y., Hayrynen, L. K., Johnston, K. D., Gati, J. S., Menon, R. S., & Everling, S. (2019). Task-based fMRI of a free-viewing visuo-saccadic network in the marmoset monkey. *NeuroImage*, *202*, 116147. https://doi.org/10.1016/j.neuroimage.2019.116147

Schaeffer, D. J., Klassen, L. M., Hori, Y., Tian, X., Szczupak, D., Yen, C. C.-C., Cléry, J. C., Gilbert, K. M., Gati, J. S., Menon, R. S., Liu, C., Everling, S., & Silva, A. C. (2022). An open access resource for functional brain connectivity from fully awake marmosets. *NeuroImage*, *252*, 119030. https://doi.org/10.1016/j.neuroimage.2022.119030

Schall, J. D. (1995). Neural Basis of Saccade Target Selection. *Reviews in the Neurosciences*, *6*(1), 63–85. https://doi.org/10.1515/REVNEURO.1995.6.1.63

Selvanayagam, J., Johnston, K. D., Schaeffer, D. J., Hayrynen, L. K., & Everling, S. (2019). Functional Localization of the Frontal Eye Fields in the Common Marmoset Using Microstimulation. *Journal of Neuroscience*, *39*(46), 9197–9206. https://doi.org/10.1523/JNEUROSCI.1786-19.2019

Shen, K., Valero, J., Day, G. S., & Paré, M. (2011). Investigating the role of the superior colliculus in active vision with the visual search paradigm. *The European Journal of Neuroscience*, *33*(11), 2003–2016. https://doi.org/10.1111/j.1460-9568.2011.07722.x

Sommer, M. A., & Wurtz, R. H. (2004). What the Brain Stem Tells the Frontal Cortex. I. Oculomotor Signals Sent From Superior Colliculus to Frontal Eye Field Via Mediodorsal Thalamus. *Journal of Neurophysiology*, *91*(3), 1381–1402. https://doi.org/10.1152/jn.00738.2003

Sommer, M. A., & Wurtz, R. H. (2006). Influence of the thalamus on spatial visual processing in frontal cortex. *Nature*, *444*(7117), 374–377. https://doi.org/10.1038/nature05279

Sommer, M. A., & Wurtz, R. H. (2008). Visual Perception and Corollary Discharge. *Perception*, *37*(3), 408–418. Retrieved August 3, 2023, from https://www.ncbi.nlm.nih.gov/pmc/articles/PMC2807735/

Swadlow, H. A. (2002). Thalamocortical control of feed-forward inhibition in awake somatosensory 'barrel' cortex. *Philosophical Transactions of the Royal Society B: Biological Sciences*, *357*(1428), 1717–1727. https://doi.org/10.1098/rstb.2002.1156

Thomas, N. W. D., & Paré, M. (2007). Temporal Processing of Saccade Targets in Parietal Cortex Area LIP During Visual Search. *Journal of Neurophysiology*, *97*(1), 942–947. https://doi.org/10.1152/jn.00413.2006

Thompson, K. G., Hanes, D. P., Bichot, N. P., & Schall, J. D. (1996). Perceptual and motor processing stages identified in the activity of macaque frontal eye field neurons during visual search. *Journal of Neurophysiology*, *76*(6), 4040–4055. https://doi.org/10.1152/jn.1996.76.6.4040

Wardak, C., Olivier, E., & Duhamel, J.-R. (2002). Saccadic Target Selection Deficits after Lateral Intraparietal Area Inactivation in Monkeys. *The Journal of Neuroscience*, *22*(22), 9877–9884. https://doi.org/10.1523/JNEUROSCI.22-22-09877.2002

Westerberg, J. A., Sigworth, E. A., Schall, J. D., & Maier, A. (2021). Pop-out search instigates beta-gated feature selectivity enhancement across V4 layers. *Proceedings of the National Academy of Sciences of the United States of America*, *118*(50), e2103702118. https://doi.org/10.1073/pnas.2103702118

Wurtz, R. H., Sommer, M. A., Paré, M., & Ferraina, S. (2001). Signal transformations from cerebral cortex to superior colliculus for the generation of saccades. *Vision Research*, *41*(25), 3399–3412. https://doi.org/10.1016/S0042-6989(01)00066-9

Zhou, Y., Liu, Y., Lu, H., Wu, S., & Zhang, M. (2016). Neuronal representation of saccadic error in macaque posterior parietal cortex (PPC) (W. Schultz, Ed.). *eLife*, *5*, e10912. https://doi.org/10.7554/eLife.10912

Zhou, Y., Liu, Y., Wu, S., & Zhang, M. (2018). Neuronal Representation of the Saccadic Timing Signals in Macaque Lateral Intraparietal Area. *Cerebral Cortex*, *28*(8), 2887–2900. https://doi.org/10.1093/cercor/bhx166

Chapter 4

Laminar dynamics of target selection in the frontal eye fields

4.1 Introduction

The remarkable ability to select and prioritize visual targets within complex scenes is critical for the guidance of behaviour. For primates in particular, visual attention and eye movements function together to select and bring into focus relevant target stimuli. FEF, in conjunction with LIP and the SC form a tightly interconnected network critical for the generation and control of eye movements as well as the deployment of visual attention (see for review, Johnston & Everling, 2008; McDowell et al., 2008).

FEF is defined as a region of frontal cortex wherein low current threshold stimulation elicits fixed vector saccadic eye movements (Bruce et al., 1985; Robinson & Fuchs, 1969). Indeed, joint lesion with the SC, but neither in isolation, permanently abolishes saccade generation (Schiller et al., 1980) demonstrating its role in oculomotor control. However, since its earliest description by Ferrier (1875), there has been significant interest in the role of FEF in visual perception and attention in addition to its role in gaze control (Bruce & Goldberg, 1985; Mohler et al., 1973; Schall, 1991). Indeed FEF neurons may respond following the onset of a visual stimulus (visual), preceding the onset of a saccade (motor) or both (visuomotor) (Bruce et al., 1985) and are directly interconnected with visual and oculomotor regions including LIP, the SC and extrastriate visual cortex (Barone et al., 2000; Huerta et al., 1986, 1987; Stanton et al., 1988). Thus, FEF engagement in visual processing and oculomotor production make it an ideal structure for the investigation of visual attention.

A common approach to investigate visual attention is in the context of the visual search paradigm, in which a target stimulus is presented simultaneously with an array of distractor stimuli, and the subject is tasked with making a saccade to the target stimulus (see for review, Wolfe & Horowitz, 2004). In this task, single neurons in FEF have been shown to have an initially indiscriminate visual response which evolves to discriminate between targets and distractors; this results in an increased response to targets in their RFs and a supressed response for distractors before the saccade is made (Schall & Hanes, 1993; Schall, Hanes, et al., 1995; Thompson et al., 1996). Lesions to FEF result in impairments in visual search paradigms (Schiller & Chou, 2000; van der Steen et al., 1986; Wardak et al., 2006) and ICMS of FEF

below thresholds required for eliciting saccadic eye movements can facilitate covert attention directed to the region of visual space represented by the stimulated location (Moore & Armstrong, 2003; Moore & Fallah, 2004). This process of target selection is dissociable from saccade generation as this activity has been demonstrated to be modulated by visual similarity to target and target history (Bichot & Schall, 1999) and can still be observed in the absence of a saccade or when the response is made manually (Monosov & Thompson, 2009; Schall, 2004; Thompson, Bichot, & Sato, 2005; Thompson et al., 1997). Additionally, increases in discharge activity can be observed for when a cue indicates a target may appear within that neuron's RF (Monosov & Thompson, 2009) even in the absence of any stimuli within the RF (Zhou & Thompson, 2009), highlighting the role of FEF as a source of a top-down spatial attention signal.

Determining how this saccade target selection related activity correlates with anatomical properties such as cortical layer or morphological cell type is of particular interest for disentangling the underlying circuit. Evidence from anatomical and physiological investigations provides some insight into the organization of cortical layers by demonstrating separable projection patterns with LIP and the SC. While reciprocal connections with LIP are found predominantly in supragranular layers, FEF neurons projecting to the SC are found exclusively in layer V and SC projections to FEF via MD likely terminate in layer IV (Fries, 1984; Lynch et al., 1994; Pouget et al., 2009; Sommer & Wurtz, 1998, 2001, 2004). Although target selection related activity can be observed in both LIP (Ipata et al., 2006; Thomas & Paré, 2007; Wardak et al., 2002) and the SC (McPeek & Keller, 2002; Shen et al., 2011), LIP projecting neurons tend to exhibit a visual bias whereas the SC projecting neurons exhibit a motor bias (Ferraina et al., 2002; Segraves & Goldberg, 1987; Sommer & Wurtz, 2001). However, the dynamics of the local laminar circuit underlying target selection activity in FEF remains unknown. Theoretical models have been proposed for an FEF laminar circuit (Heinzle et al., 2007) based on the canonical circuit model proposed by Douglas and Martin (1991) following investigations in cat primary visual cortex. This model would suggest that granular layer neurons receive thalamocortical inputs carrying sensory information, following which supragranular neurons select a target and infragranular neurons convey a motor output. Yet, due to the challenge of conducting laminar recordings in regions like FEF which are located deep within sulci in the macaque, this remains to be investigated.

Here we address this gap by leveraging the relatively lissencephalic cortex of the common marmoset monkey (*Callithrix jacchus*). Homologues of the macaque and human FEF and LIP have recently been identified in the marmoset on the basis of anatomical, resting-state and task-based fMRI, intracortical microstimulation, and single-unit electrophysiological investigations (Collins et al., 2005; Feizpour et al., 2021; Ghahremani et al., 2017; Ghahremani et al., 2019; Ma et al., 2020; Reser et al., 2013; Rosa et al., 2009; Schaeffer et al., 2019; Selvanayagam et al., 2019). We carried out laminar electrophysiological recordings in marmoset FEF using ultra-high density Neuropixels probes (Jun et al., 2017) as they performed a simple visual target selection task. We observed neurons with stimulus-related activity, many of which discriminated between target and distractor stimuli. We also observed strong pre-saccadic activity consistent with the role of FEF neurons in saccade control. Examining the population activity across depth revealed an organization of stimulus-related activity partially consistent with the CCM but target discriminating activity was surprisingly observed in putative infragranular interneurons first. These findings suggest the CCM may not be universally applicable to all

cortical areas, and provides novel insights into the laminar organization of primate FEF.

4.2   Methods

4.2.1   Subjects

Two adult common marmosets (Marmoset J, female, age 22-24 months, weight 328-337 g; Marmoset N, male, age 23-35 months, weight 421-443g) served as subjects in the present study. Marmoset N was the same animal as in Chapter 3. As in Chapter 3, animals were acclimated to restraint for MRI and electrophysiological experiments before surgery in which a combination recording chamber/head restraint was implanted. All experimental procedures were conducted in accordance with the Canadian Council on Animal Care policy on the care and use of laboratory animals and a protocol approved by the Animal Care Committee of the University of Western Ontario Council on Animal Care. The animals were additionally under the close supervision of university veterinarians throughout all experiments.

4.2.2   Data collection

Procedures for behavioural training of animals in the target selection task, electrophysiological recordings and reconstruction of recording locations using fMRI are all the same as in Chapter 3.2. In brief, animals were first trained to fixate on central and eccentric circular stimuli which was used subsequently for calibration. Animals were then trained on the visual target selection task (see Figure 4.1a). Recordings were conducted using Neuropixels 1.0 NHP short probes, synchronized with gaze position and task events. The size and location of the trephination and recording locations were selected on the basis of resting state functional connectivity from a database, registered to the anatomical scan of each monkey, aligned with grids. Recording locations were confirmed *ex vivo*. In total, we conducted 24 electrode penetrations across 17 sessions (Marmoset J: 5 penetrations in 5 session, Marmoset N: 12 penetrations in 19 sessions).

4.2.3   Data Analysis

As described in Chapter 3.2, single unit clusters were manually curated in Phy. Relative depth of units was estimated using the spectrolaminar motif (Mendoza-Halliday et al., 2023). Putative cell-type classifications were made using the peak-to-trough time. Positive-first waveforms were retained only if another negative-first waveform could be observed at an adjacent site (91 of 157 neurons were retained).

 Single neurons were classified as visual, target discriminating, pre-saccadic or post-saccadic using paired-samples or independent-samples t-tests where appropriate (see Chapter 3.2.8 for more info). Significant differences in proportions of single neurons across putative layers and cell types were evaluated using a logistic regression analysis. ROC analyses (Green & Swets, 1966) were conducted to determine the timing of these activity patterns for neurons where significant activity could be detected. Significant differences in latencies across layers or conditions were evaluated using one-way analyses of variance (ANOVAs).

The timing of stimulus-related and target discriminating activity at the population level across time and depth was estimated using generalized additive models (GAMs). Significant differences were determined by estimating difference smooths comparing condition across time, depth and cell-type, and evaluating where the 99.9% confidence intervals (CIs) for these differences did not overlap with 0 (see Chapter 3.2.9 for more info).

4.3 Results

4.3.1 Behavioural performance

Marmosets performed visually guided saccades in a simple target selection task wherein blocks of "single-target" and "distractor" trials were presented to the animal (see Figure 4.1a). Animals were required to fixate on a central fixation stimulus (0.5°radius black circle on a grey background) for 300-500 ms at the beginning of each trial. On "single-target" trials, a single target (1°diameter image of a marmoset face) was presented 6°to the left or right of the fixation stimulus and subjects were required to make a saccade to the target to obtain a viscous liquid reward of acacia gum. On "distractor" trials, a distractor stimulus (0.5°radius black circle) was simultaneously presented in the opposite hemifield. Trials in which no saccade at least 4°in amplitude was made were marked as "no response" and were not included in further analysis. Trials in which saccades were made to the target were marked as correct and trials in which saccades landed anywhere else were marked as incorrect. We conducted 17 recording sessions, 5 in Marmoset J and 12 in Marmoset N, in which animals performed 126-229 trials (M=166.5 trials). Accuracy was significantly lower on "distractor" trials (Mean ± SEM; Marmoset J: 73.2 ± 4.6%; Marmoset N: 62.6 ± 4.6%, see Figure 4.1b) than on "single-target" trials (Marmoset J: 85.3 ± 1.6% , Marmoset N: 93.4 ± 1.3%, see Figure 4.1c), Marmoset J: $t(4) = 3.17, p = .034$, Marmoset N: $t(11) = 7.84, p < .001$, though we observed no significant differences in median SRTs, (Marmoset J: "distractor"=155.2±11.2 ms vs "single-target"=161.7±11.1 ms; Marmoset N: "distractor"=167.2±9.4 ms vs "single-target"=166.0±11.1 ms). The observed distractor-induced reduction in saccades towards the target suggests some target selection process may be underway.

4.3.2 Assigning cortical layers and putative neuron classes

For each penetration, we determined cortical layers by identifying the crossover point between the power spectral density (PSD) of low (15-22 Hz) and high (80-150 Hz) frequency ranges in the local field potentials (LFP) across depths as done in previous work (Mendoza-Halliday et al., 2023) (see Figure 4.2a). Based on visual inspection of the distribution of isolated neurons distributed along the length of the electrode shank, and the known density of neuronal distributions within the cortical layers in this region of marmoset cortex, we classified all neurons that fell within 200 μm below to 300 μm above as being in granular Layer IV, and all others as supragranular or infragranular. To classify putative interneurons and pyramidal cells, the established approach of using the peak-trough duration was employed (Ardid et al., 2015; Hussar & Pasternak, 2012; McCormick et al., 1985; Mitchell et al., 2007) (see Figure 4.2b). Interestingly, a large proportion of neurons with positive-first waveforms were observed (157,
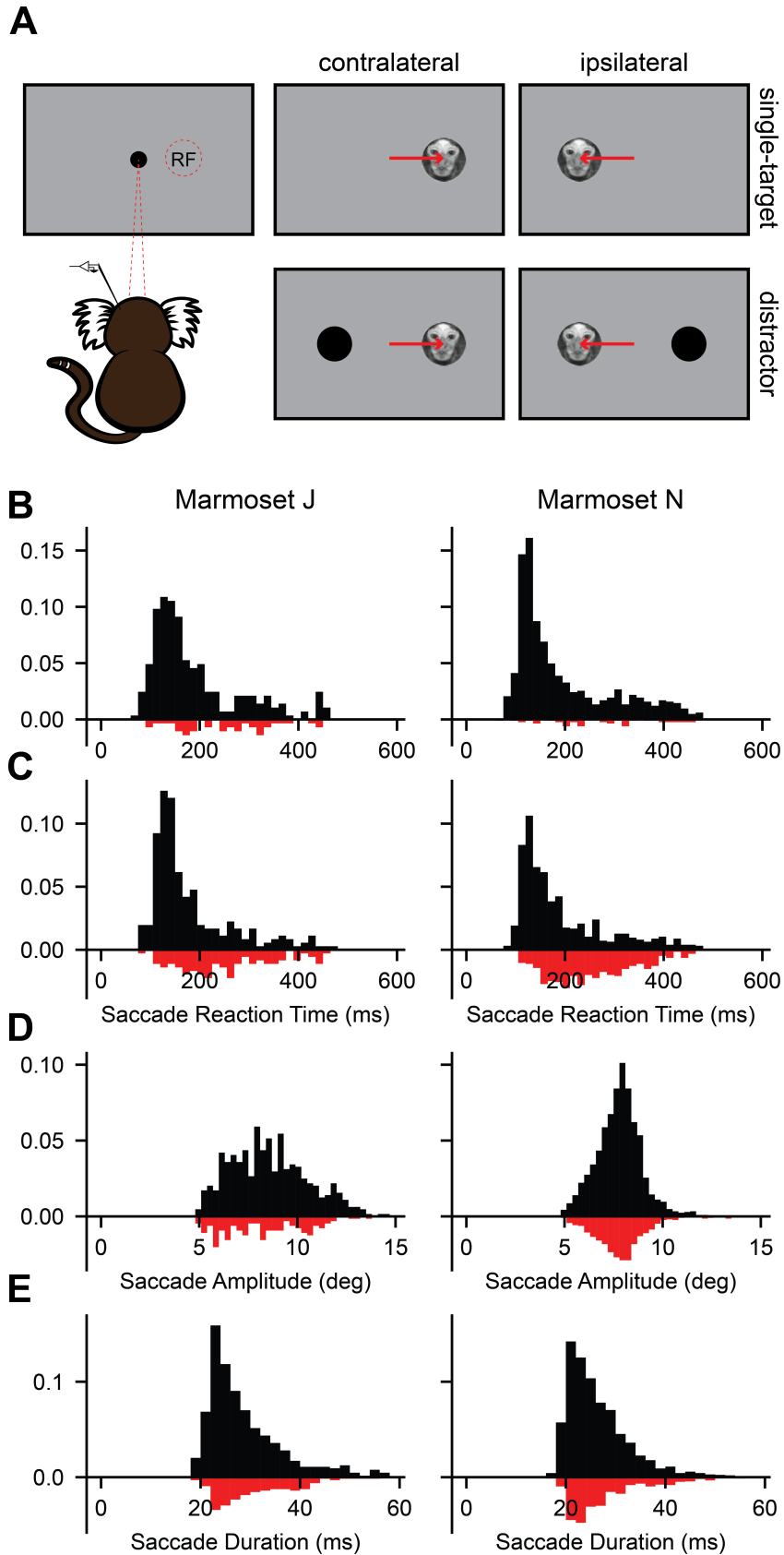
Figure 4.1: Task design and behavioural performance.

Figure 4.1: *Task design and behavioural performance (continued).* (A) Schematic representing task design for "single-target" and "distractor" trials, where the target falls in (contralateral) or out of (ipsilateral) the receptive field (RF). Saccade metrics for Marmoset J (left) and Marmoset N (right) for correct (black) and error (red) trials. Saccade reaction time histograms for "single-target" (B) and "distractor" (C) trials for each animal separately. Saccade amplitude (D) and duration (E) histograms for each animal separately across all conditions.

Table 4.1: Proportions of units with significant task modulated activity

Layer	Cell-type	Stimulus-related	Discrimination	Post-saccadic	Pre-saccadic
infragranular	NS	27 (22.31%)	9 (7.44%)	56 (46.28%)	18 (14.88%)
	BS	27 (25.23%)	8 (7.48%)	55 (51.40%)	14 (13.10%)
granular	NS	58 (25.78%)	39 (17.33%)	95 (42.22%)	41 (18.22%)
	BS	84 (14.84%)	58 (10.25%)	227 (40.11%)	72 (12.73%)
supragranular	NS	20 (21.05%)	10 (10.53%)	46 (48.42%)	14 (14.74%)
	BS	32 (11.76%)	12 (4.41%)	133 (48.90%)	42 (15.44%)

10.8 %), which were largely restricted to the broad waveforms observed in deeper layers. For 91 of these neurons, we were able to identify a nearby or deeper channel, where we observed a negative-first waveform and for these neurons we reassigned the relative depths accordingly (see white circles in Figure 4.2c). For the remaining 66 neurons, we were unable to identify a negative-first waveform, in part due to very small amplitudes or the neuron being clipped by the spatial extent of the probe. As these waveforms may also correspond to axons corresponding to a soma in a superficial layer, we excluded these neurons from the analysis. For the neurons we retained, we inverted the positive-first waveform before evaluating the peak-trough duration, as often the negative-first waveform was of a small amplitude and may lead to poor estimates of peak-trough duration.

4.3.3   Evaluating stimulus and saccade-related responses in FEF neurons

We conducted 24 electrode penetrations in two animals (Marmoset J: 5 penetrations in 5 sessions; Marmoset N: 19 penetrations in 12 sessions) in which we advanced either one or two Neuropixels electrodes in this region and recorded the activity of 1452 well-isolated single neurons.

To identify task-modulated neurons, we computed the mean discharge rates from 50 ms after stimulus onset to 25 ms after saccade onset for all conditions and compared it to the mean baseline activity 200 ms before stimulus onset. Examining the conditions separately, 211 (14.53%) neurons were significantly modulated in contralateral and 111 (7.64%) in the ipsilateral "single-target" conditions; 231 (15.91%) and 146 (10.06%) were modulated in the contralateral and ipsilateral "distractor" conditions respectively. Overall, pooling across conditions, 268 (18.46%) neurons were significantly modulated during task performance. The proportions of these neurons across putative layers and cell types are stated in Table 4.1 and Figure 4.3 for example neurons.

For these neurons, to examine the evolution of stimulus-related activity over time, we con-
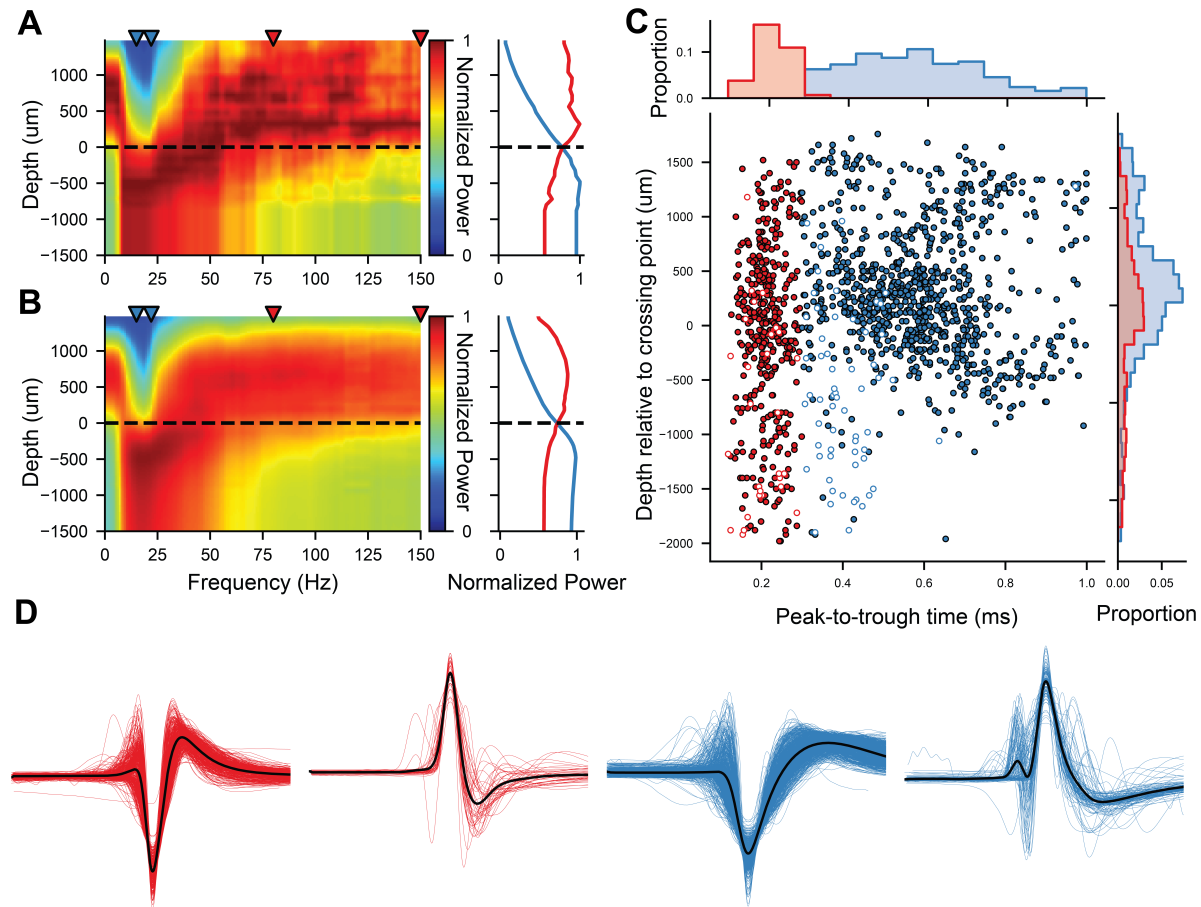
Figure 4.2: Layer assignment and cell type classification. LFP power aligned to stimulus onset across depths and frequencies (left) and normalized power in selected ranges (right; blue: 15-22 Hz, red: 80-150 Hz) are shown for an example session (A) and the average of all sessions (B). The crossing point between lower and higher frequencies is marked by a dotted line. Peak-to-trough times for all recorded neurons across depth relative to the crossing point described above (C) and example waveforms of "broad" and "narrow" waveforms (D). Note that neurons for which we observed a positive-first waveform (N=198) are identified by white circles in (C) and plotted separately in (D).
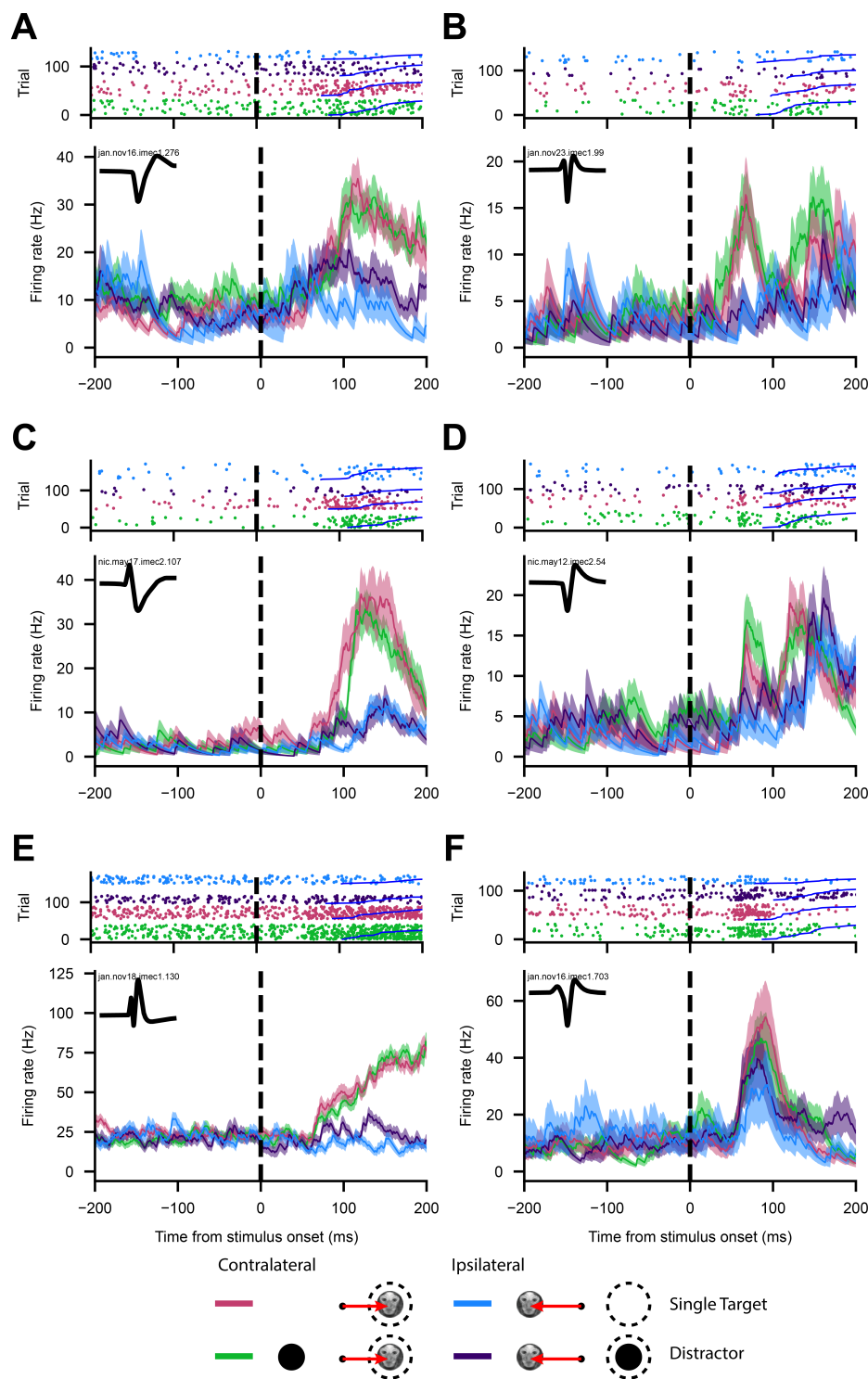
Figure 4.3: Example neurons with stimulus-related activity. Raster plots and spike density functions (SDF) aligned to stimulus onset for example broad (A, C, E) and narrow (B, D, F) - spiking neurons from supragranular (A, B), granular (C, D) and infragranular (E, F) layers with visual activity. Red = target contralateral, Green = target contralateral & distractor ipsilateral, Blue = target ipsilateral, Purple = target ipsilateral & distractor contralateral. Blue lines in raster plot represent saccade onset. Trials are sorted into conditions and in order of increasing saccade reaction times in raster plots. Mean waveform in inset SDF figure. Shaded regions in SDF figures represent +/- 1 SEM for each condition.

Figure 4.4: ROC analyses for stimulus and saccade related activity. Cumulative distributions of neurons over time with significant auROC as compared to a null distribution generated from 1000 randomized shuffles. (A) significant stimulus-related activity as compared to a pre-stimulus baseline in single-target contralateral over time from stimulus onset separately for each cortical layer. (B) significant target discriminating activity comparing ipsilateral and contralateral distractor trials over time from stimulus onset separately for each cortical layer. (C) significant post-saccadic activity comparing each condition separately to a pre-saccadic baseline over time from saccade onset. Shaded region indicates 95% CI.

ducted ROC analyses (Green & Swets, 1966) comparing the distributions of discharge activity following stimulus onset as compared to a prestimulus baseline interval. We computed auROC values on discharge rates within successive 15ms intervals from stimulus onset to 200 ms after stimulus onset as compared to 200 ms before stimulus onset. To evaluate the significance of auROC values, we compared these values to a null distribution created by shuffling the labels of baseline vs stimulus-related 1000 times at each interval. For each neuron we determined the first time point where a significant auROC value was observed and determined cumulative distributions for each layer (see Figure 4.4a). No significant differences were observed between layers for the onset of stimulus-related activity.

As the discharge activity of FEF neurons in the macaque are strongly associated with saccade generation, we additionally evaluated the discharge activity in a perisaccadic interval (50 ms before saccade onset to 25 ms after saccade offset) and determined the proportions of neurons with significant difference in activity from baseline, as well the proportion of neurons with activity correlated to SRTs. We observed 214 (14.74%; see Table 4.1 and Figure 4.5) neurons with significant perisaccadic activity and 27.9% of these neurons were significantly negatively correlated with SRTs. These findings demonstrate a relatively strong association between the activity of recorded neurons and saccade generation, especially when compared to similar recordings in LIP (see Chapter 3.3.3).

We then compared the activity of task modulated neurons on distractor trials where the target was in the contralateral and ipsilateral hemifields. We observed 154 (10.61%) of neurons significantly discriminated between target and distractor stimuli in the contralateral hemifield, 74% of which preferred the target (see Table 4.1 and Figure 4.6). For these neurons, to assess the timing and magnitude of discrimination, we conducted auROC analyses as above, except comparing the activity between ipsilateral and contralateral trials. Again, we observed no significant differences in discrimination times across layers (see Figure 4.4b). We also evaluated
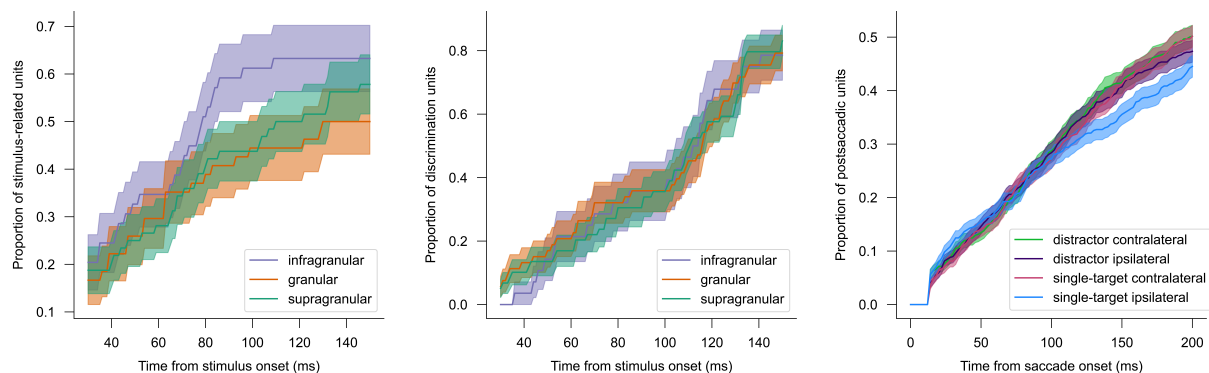
Figure 4.5: Example pre-saccadic neurons. Raster plots and spike density functions (SDF) aligned to saccade onset for example broad (A, C, E) and narrow (B, D, F) -spiking neurons from supragranular (A, B), granular (C, D) and infragranular (E, F) layers with significant increases in activity preceding saccades in the single-target contralateral trials. Red = target contralateral, Green = target contralateral & distractor ipsilateral, Blue = target ipsilateral, Purple = target ipsilateral & distractor contralateral. Blue lines in raster plot represent stimulus onset. Trials are sorted into conditions and in order of increasing saccade reaction times in raster plots. Mean waveform in inset SDF figure. Shaded regions in SDF figures represent +/-1 SEM for each condition.

the magnitude and time of the maximal auROC response: supragranular (BS: .600, 105.1 ms; NS: .513, 71.0 ms), granular (BS: .565, 97.2 ms; NS: .582, 84.9 ms) and infragranular (BS: 0.557, 69.0ms; NS: .619, 94.0ms). While maximal auROC values were generally observed earlier than median SRTs, the did not differ significantly between layers and cell types.

In addition to task modulated neurons, we observed many neurons with significant post-saccadic activity. To characterize this activity, we first evaluated the proportion of neurons with significant increases in activity 50-150 ms following saccade offset as compared to a 200 ms pre-stimulus baseline. For correct trials, 725 neurons (49.93%) had significant post-saccadic activity in at least one condition, 400 neurons in at least two conditions, 195 in at least three conditions, 80 in all four conditions; 319-392 neurons for each condition; see Figure 4.7. This activity did not appear to correspond with stimulus-related activity; of the 159 neurons with significant stimulus-related activity in the contralateral single-target condition, 41 neurons had significant post-saccadic activity in the ipsilateral single-target condition, 49 in the contralateral single-target condition and 24 in both. Additionally, for the distractor conditions, we compared the post-saccadic activity separately for correct and error trials; much fewer neurons had significant post-saccadic activity on error trials (contralateral: 234 vs 420, ipsilateral: 202 vs 359). Also, to evaluate any differences in timing across conditions, we conducted auROC analyses as above, comparing activity from saccade onset compared to a 50 ms pre-saccadic baseline. We observed that many neurons exhibited significant increases in discharge activity 25-75 ms following saccade onset, which would be too early for stimulus-related activity in response to visual refresh at saccade offset. However, this cannot be discounted for neurons that responded later, and some of these neurons may have perifoveal RFs. No significant differences were observed in the timing of post-saccadic activity across conditions (see Figure 4.4c). In sum, a large proportion of neurons exhibited post-saccadic activity rapidly following saccade offset and this activity varied depending on stimulus identity and task performance.

For comparison with above, we determined the proportion of neurons with significant post-saccadic activity across conditions. We then conducted a logistic regression to investigate the effects of putative layer and cell-type, and epoch (task, discrimination, pre-saccadic, post-saccadic) on the likelihood that a neuron has significantly different discharge activity. We observed no significant differences in the proportions of neurons responsive in epochs across layers and cell-types.

In sum, we observed stimulus and saccade related activity for the contralateral hemifield across cortical layers and putative cell-types. Many neurons with stimulus related activity additionally discriminated between target and distractor stimuli. Single neuron analyses did not reveal any differences in the prevalence or timing of these activity patterns across cortical layers.

4.3.4   Stimulus related activity first emerges in narrow spiking granular and supragranular neurons

We employed GAMs to examine differences in the timing of stimulus related activity across depth and putative cell-types. GAMs are a type of statistical model which fits data that cannot easily be fit to some defined function by constructing a "smooth" curve comprised of many segments connecting estimated "knots" (Hastie & Tibshirani, 1986). Complex, non-linear re-
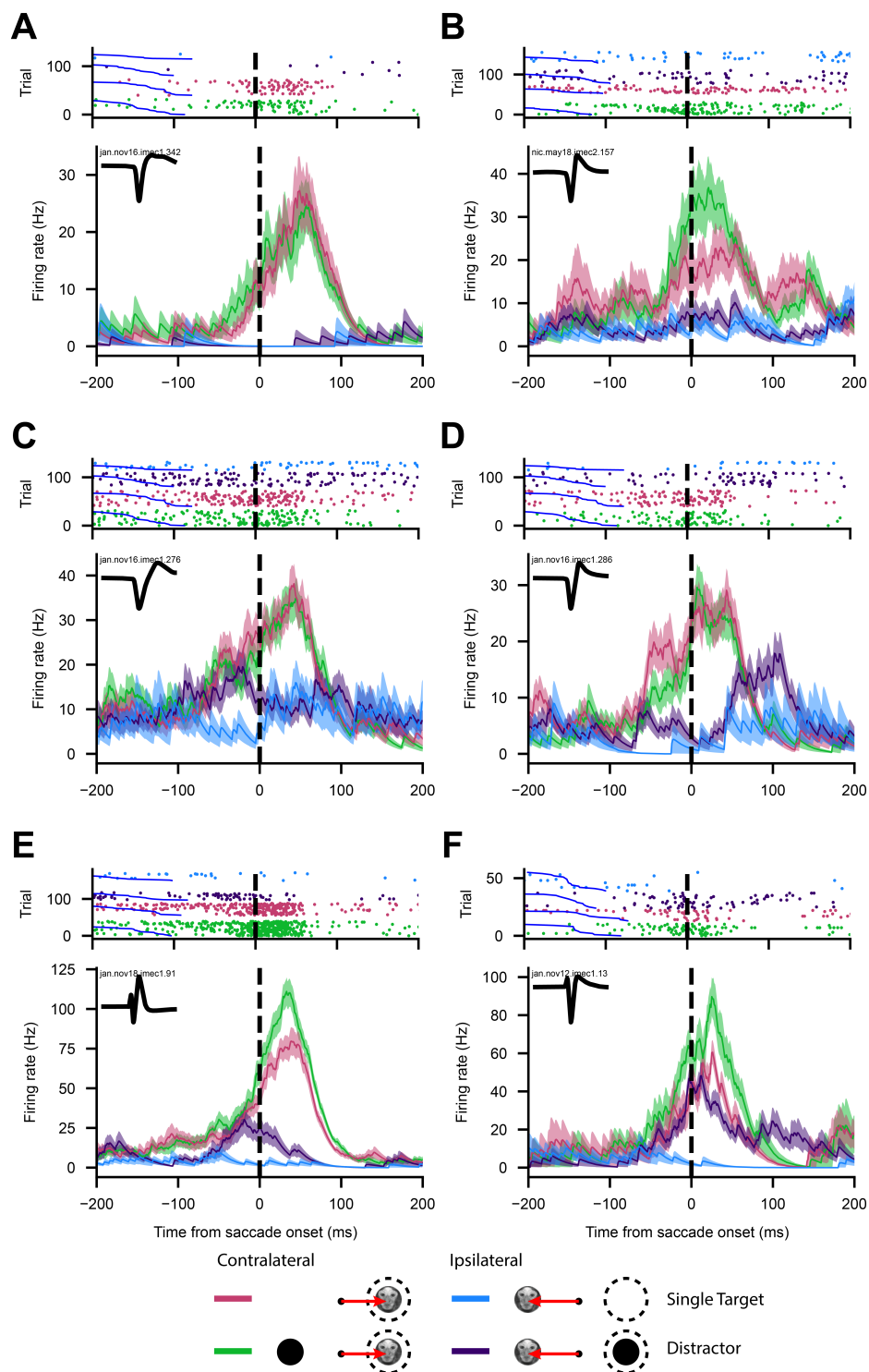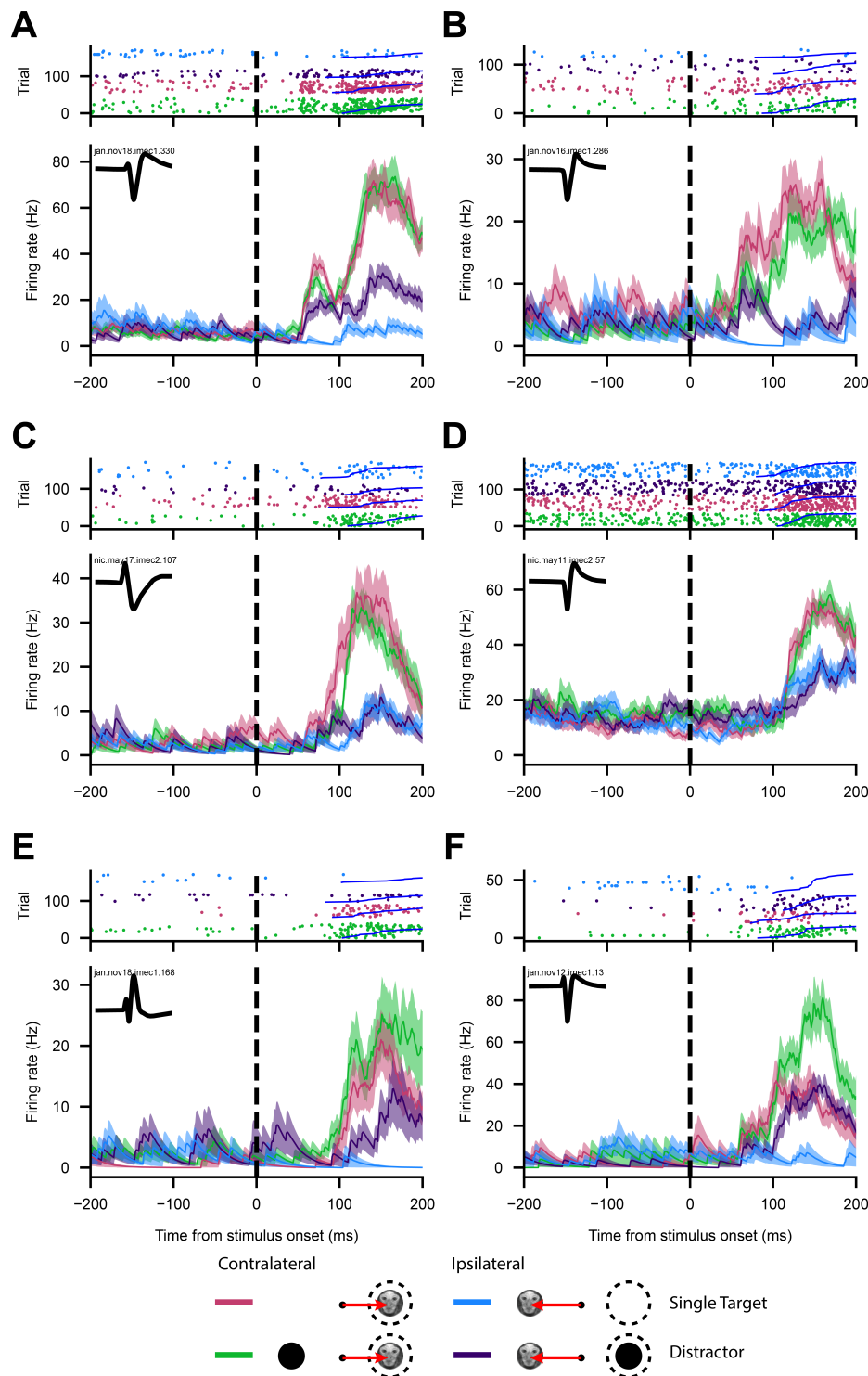
Figure 4.6: Example target discriminating neurons. Raster plots and spike density functions (SDF) aligned to stimulus onset for example broad (A, C, E) and narrow (B, D, F) -spiking neurons from supragranular (A, B), granular (C, D) and infragranular (E, F) layers with activity discriminating between target and distractor stimuli. Red = target contralateral, Green = target contralateral & distractor ipsilateral, Blue = target ipsilateral, Purple = target ipsilateral & distractor contralateral. Blue lines in raster plot represent saccade onset. Trials are sorted into conditions and in order of increasing saccade reaction times in raster plots. Mean waveform in inset SDF figure. Shaded regions in SDF figures represent +/- 1 SEM for each condition.

Figure 4.7: Example post-saccadic neurons. Raster plots and spike density functions (SDF) aligned to saccade offset for example broad (A, C, E) and narrow (B, D, F) -spiking neurons from supragranular (A, B), granular (C, D) and infragranular (E, F) layers with significant post-saccadic activity. Red = target contralateral, Green = target contralateral & distractor ipsilateral, Blue = target ipsilateral, Purple = target ipsilateral & distractor contralateral. Blue lines in raster plot represent saccade onset. Trials are sorted into conditions and in order of increasing saccade reaction times in raster plots. Mean waveform in inset SDF figure. Shaded regions in SDF figures represent +/- 1 SEM for each condition.

lationships such as the evolution of neural activity over time (or depth) can be captured by such models (Cadarso-Suarez et al., 2006). Here, for the entire population of recorded neurons, we modelled the odds of a spike at each point in time and depth as a function of time from stimulus onset (ms), relative depth from the crossing point of low and high frequency power (μm), and cell type (BS, NS) for the contralateral and ipsilateral "single-target" condition. We employed a traditional stepwise regression approach for model selection wherein we constructed reduced models which successively excluded the factors of cell-type, depth, condition and time as well as the random effects of neuron and trial.

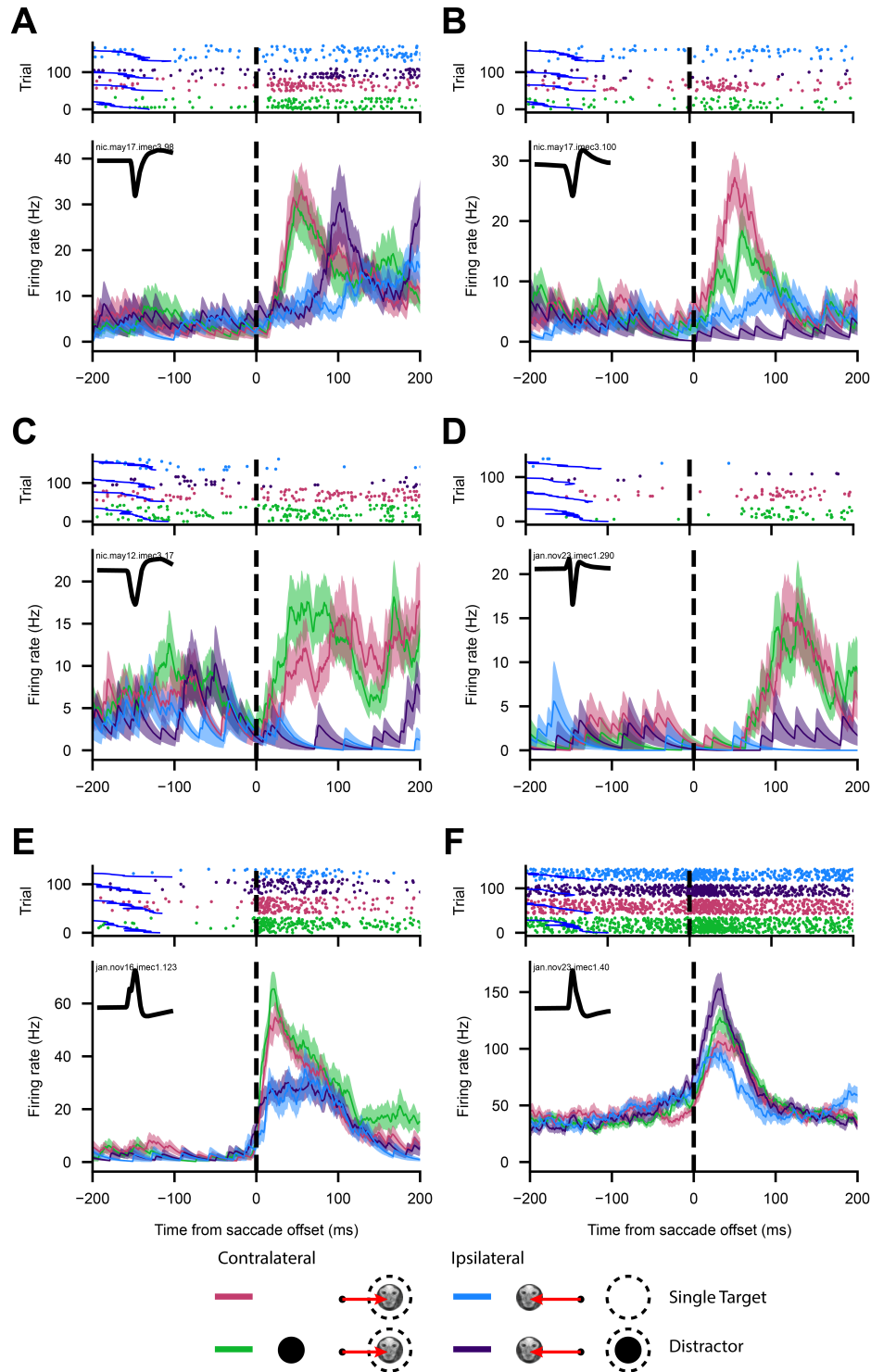We then compared these models using the chi-squared likelihood ratio test. This model significantly improved fit as compared to the reduced models ($p < .001$). As the vast majority of neurons only exhibited significant increases in discharge activity for contralateral as compared to ipsilateral "single-target" trials, we could evaluate the onset of stimulus-related activity by comparing the activity between these conditions. To examine differences between these conditions across time and depth, we may compute estimates of the pairwise differences between conditions for the time by depth tensor smooths separately for BS and NS neuron populations. Points in time and depth where these difference smooths deviate significantly from zero (evaluated here at a 99.9% CI) are where the conditions significantly differ. As such, we can determine the earliest time point and depths where stimulus-related activity was first observed for each cell type (see Figure 4.8).

The earliest stimulus related activity first emerges in narrow-spiking neurons simultaneously at or above the crossing point of low and high frequency power (55 ms), suggesting putative granular and supragranular interneurons simultaneously receive stimulus related information. This activity appears to be transient, followed by a second wave of activity in both narrow and broad-spiking neurons 90-100 ms after stimulus onset, likely corresponding to saccade related activity. In sum, this suggests stimulus-related activity emerges simultaneously in supragranular and infragranular putative interneurons first and never reaches significance in infragranular layers.

4.3.5 Target discrimination activity first emerges in narrow-spiking infragranular neurons

Next, we examined the spatiotemporal pattern of target discrimination activity in the population activity. Here we fit a GAM where we modelled odds of spiking using time, depth, cell type and condition (preferred vs nonpreferred stimulus in contralateral hemifield). This model significantly improved fit over reduced models ($p < .001$). We then computed difference smooths between the conditions with a 99.9% CI, identified time points where the difference smooth significantly deviated from 0, and determined the earliest time points and depths where target discrimination activity was observed separately for each cell type.

Surprisingly, the earliest discrimination activity was observed at 56 ms in infragranular narrow-spiking neurons, followed by supragranular (67 ms) and granular (75 ms) broad-spiking neurons (see Figure 4.8). These findings suggest that target discrimination first occurs in putative infragranular interneurons followed by more superficial putative pyramidal neurons.

In sum, we observe stimulus-related and target discrimination activity across cortical laminae and cell types, with little difference in timing or prevalence of this activity. However, when
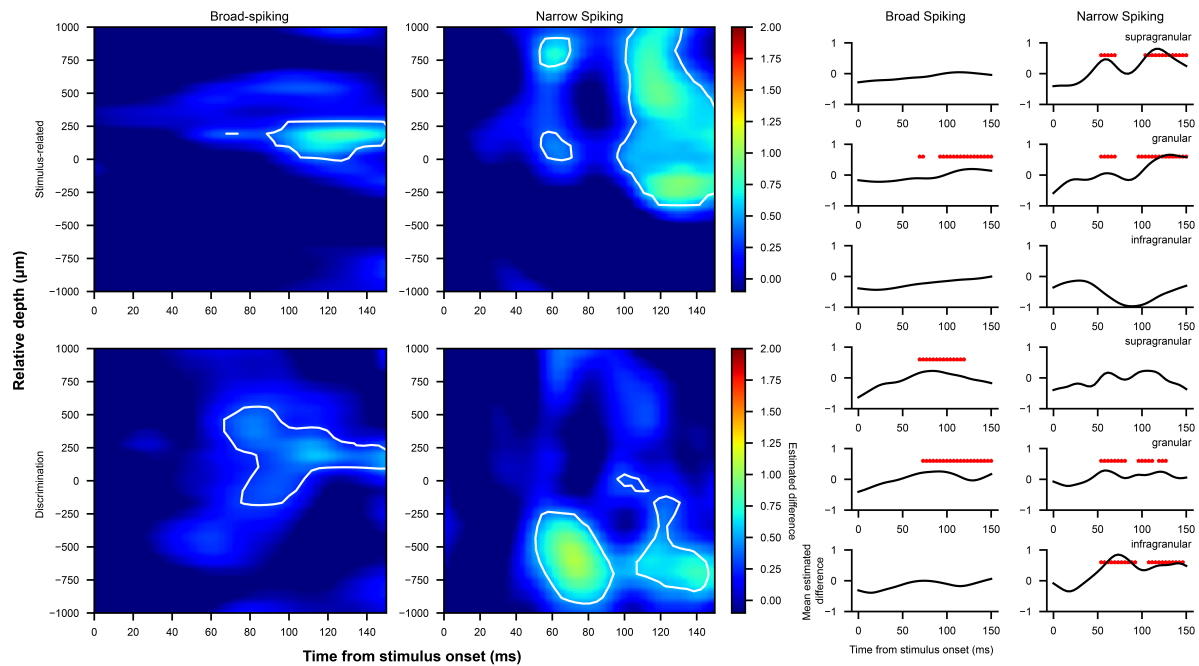
Figure 4.8: Generalized additive model fit of population activity continuously across depth. Odds of a spike at a given point in time are estimated using the time from stimulus onset, the relative depth from the crossing point, putative cell class (NS or BS), and the condition of the given trial (stimulus-related: ispilateral vs contralateral single target trials; discrimination: preferred vs non-preferred distractor trials) with trial and neuron as random effects. Estimated differences across depth and time are plotted separately for stimulus-related (top) and discrimination (bottom), broad-spiking (left) and narrow-spiking (right) as heatmaps, with significant differences between conditions as determined by a 99.9% CI highlighted in white contours. Mean difference traces across depth ranges roughly corresponding to cortical layers are plotted on the right, separately for comparison and cell-type. Significant differences are indicated by red *.

examining the population, clear differences in timing can be observed suggesting simultane-
ous stimulus-related input in granular and supragranular layer interneurons followed by target
discrimination in infragranular interneurons with pyramidal neurons lagging behind.

4.4   Discussion

The neural correlates of visual attention and oculomotor control in primate FEF have been
investigated in detail in the macaque (Schall, 1995). However, the laminar microcircuitry un-
derlying these activity patterns remain to be understood due to the challenges in accessing
this region, found deep in the arcuate sulcus. Here, we conducted ultra-high density laminar
recordings in marmoset FEF as they completed a saccadic target selection task. We observed
strong stimulus and saccade related activity, consistent with the role of FEF as a visuomotor
structure involved in oculomotor control and visual attention. Indeed, many of these neurons
discriminated between target and distractor stimuli. However, neither the proportions of neu-
rons with such activity nor the timing of this activity differed across cortical layers or putative
cell-types at the level of single neurons. When examining spiking-odds across the population
however, we observed striking differences in the timing of stimulus-related and target discrim-
inating activity. Stimulus-related activity first emerged in putative granular and supragranular
interneurons simultaneously, whereas target discriminating activity first emerged in putative in-
fragranular interneurons. Altogether, these results reveal distinct laminar dynamics from those
observed in primary sensory cortical areas (Douglas & Martin, 2004), recently observed in pri-
mate LIP , or previously proposed for FEF (Heinzle et al., 2007), but bears some resemblance
to recent observations in other frontal cortical areas such as SEF (Godlove et al., 2014; Sajad
et al., 2022; Sajad et al., 2019). These observations argue against the existence of a CCM
which is iterated upon throughout all of neocortex.

   First described as an area of frontal cortex from which ICMS can elicit eye and head move-
ments in the primate (Ferrier, 1875), FEF neurons have also been shown to possess visual
activity (Bruce & Goldberg, 1985), which can select from target stimuli from amongst distrac-
tors (Schall, 1995; Schall & Hanes, 1993; Thompson et al., 1996), even covertly (Monosov
& Thompson, 2009; Schall et al., 2004; Thompson et al., 1997; Thompson, Biscoe, et al.,
2005). FEF is interconnected with a variety of visual and oculomotor regions (Barone et al.,
2000; Huerta et al., 1986, 1987; Schall, Morel, et al., 1995; Stanton et al., 1988) and has
been causally implicated in its role in directing attention, overtly with oculomotor (Bruce et
al., 1985; Robinson & Fuchs, 1969) and head-orienting (Elsley et al., 2007; Knight & Fuchs,
2007) movements as well as covertly (Moore & Armstrong, 2003; Moore & Fallah, 2004).
Thus, FEF plays a key role in directing selective spatial visual attention to behaviourally rele-
vant stimuli in a scene. FEF accomplishes this by receiving visual input, using bottom-up and
top-down information to select the most salient target within view, constructing a motor plan
for an orienting response, and transmitting this to downstream oculomotor areas such as the SC
and BSGs. For the first time in the marmoset, we have identified single neurons with discharge
properties corresponding to these functions as has been well established in the macaque.

   Corroborating recent work in anaesthetized marmosets (Feizpour et al., 2021), we observed
strong stimulus-related activity in marmoset FEF primarily for stimuli presented in the con-
tralateral hemifield. The latency of these responses for the majority of these neurons ranged

from 40-100ms, which is slightly earlier than was observed by Feizpour and colleagues (2021), though this could potentially be accounted for by the effects of anaesthesia. Many of these neurons additionally differentiated between target and distractor stimuli in the contralateral hemifield, consistent with decades of single neuron recordings and pharmacological investigations in macaque FEF (Schall, 1995; Schall & Hanes, 1993; Thompson et al., 1996; Wardak et al., 2006). Additionally, this discrimination activity generally peaked prior to the upcoming saccade to the target stimulus, consistent with a process of visual selection preceding saccade generation. These observations of stimulus-related and target discriminating activity are also consistent with our recent investigation in marmoset LIP (see Chapter 3). In contrast with LIP however, FEF has a more direct role in saccade generation, as demonstrated by lesion studies, ICMS, pharmacological inactivation and single neuron recordings (Bisley & Goldberg, 2003; Bisley et al., 2011; Bruce et al., 1985; May & Andersen, 1986; Schiller et al., 1980; Stanton et al., 1988; Thier & Andersen, 1998; Wardak et al., 2006; Wardak et al., 2002, 2004). Recent work from our group in the marmoset similarly reveals lower ICMS thresholds and evoked saccade latencies in FEF ($<= 12\mu A$, $25ms$ Selvanayagam et al., 2019) than in LIP ($<= 40\mu A$, $64ms$ Ghahremani et al., 2019). Accordingly, we observed many neurons in FEF with significant increases in pre-saccadic discharge activity, and this activity is more closely correlated with SRT than observed in LIP. Together, these observations contribute to a growing body of literature establishing the homology of macaque and marmoset FEFs (Collins et al., 2005; Ghahremani et al., 2017; Reser et al., 2013; Rosa et al., 2009; Schaeffer et al., 2019; Selvanayagam et al., 2019).

A large proportion of neurons also demonstrated significant post-saccadic activity, similar to our previous observations in LIP. As in LIP, the activity of FEF post-saccadic for many neurons emerged too rapidly after saccade offset to be visual or remapping signals. We cannot discount this for neurons with post-saccadic activity emerging layer which may also have perifoveal RFs. However, it is worth nothing that post-saccadic activity was often delayed for the ipsilateral single-target trials, for which the perifoveal visual input is the same. This activity could reflect corollary discharge signals i.e., the efference copy of the saccade (Sommer & Wurtz, 2008). It is well established that corollary discharge activity can be observed in FEF, and is relayed here from the SC via MD (Sommer & Wurtz, 2004, 2006). However, the observation that this activity varied across conditions, where saccade metrics were comparable, as well as between correct and error trials, suggests that this activity isn't merely an efference copy but also encodes some task-relevant variables. Future investigations precisely manipulating stimulus presentation, feedback and reward in the post-saccadic interval should prove fruitful in disentangling the nature of this activity.

Inferring the laminar organization of FEF has remained challenging as in the macaque, it is located within the arcuate sulcus, rendering laminar electrophysiology nearly impossible. Indirect evidence for this organization comes from antidromic investigations (Ferraina et al., 2002; Paré & Wurtz, 1997, 2001; Sommer & Wurtz, 2001). The investigators observed a visual bias in neurons projecting between LIP and FEF and a motor bias for neurons projecting from FEF and LIP to the SC. Considering the known bias in cortical projecting neurons, corticocortical neurons tend to be supragranular and corticofugal neurons infragranular, one could infer a possible laminar circuit. However, the strength of such projections are not always proportional to their number, and the relevance is not easily inferred from anatomy alone (Binzegger et al., 2004).

To address this, we carried out ultra-high density laminar recordings (Jun et al., 2017) in the relatively smooth cortices of marmosets. We used the well established spectrolaminar motif (Mendoza-Halliday et al., 2023) to align recording sessions at the center of layer IV. We also used the peak-to-trough width to separate narrow and broad spiking neurons (Ardid et al., 2015; Hussar & Pasternak, 2012; McCormick et al., 1985; Mitchell et al., 2007). For many neurons we observed a positive-first waveform. As these waveforms may correspond to recording at the apical dendritic trunk of pyramidal neurons with large apical dendritic arbors or large axons, both of which may be encountered more commonly in deeper layers (Boulton et al., 1990, p. 9), we identified neurons for which a negative-first waveforms could be observed at nearby channels and retained these for further analysis; all other neurons were discarded as they may correspond to axons from more superficial layers and would pollute the laminar analyses.

We then assessed how the observed activity varied across putative cortical laminae and cell classes. Critically, we observed no differences in timing or prevalence of stimulus-related or target discriminating activity when examining single neurons. Observations regarding timing but not prevalence are similar to those in marmoset LIP. That we did not observe a superficial vs deep bias in the prevalence of visual activity as in marmoset LIP or as suggested by antidromic studies in FEF (Ferraina et al., 2002; Sommer & Wurtz, 2001) might highlight a difference between these areas.

To take a closer look at the spatiotemporal pattern of stimulus-related and target discriminating activity, we examined the population activity fit to GAMs. Here, we observed the stimulus-related activity emerged first in putative supragranular and granular interneurons simultaneously. The granular interneurons receiving stimulus related activity first is consistent with predictions based on the CCM (Douglas & Martin, 2004; Heinzle et al., 2007) and a feedforward inhibition model, as is readily observed in the rodent barrel cortex (Swadlow, 2002). In brief, the anatomy suggests that thalamocortical and corticocortical feedforwardprojections primarily terminate in granular layer IV (Baizer et al., 1991; Matsuzaki et al., 2004). While the primary target of these projections are pyramidal neurons, it is observed in the barrel cortex that monosynaptic thalamocortical input to broadly tuned and rapidly responding granular layer interneurons drives a prepotent inhibitory response which serves to sharpen the tuning properties if interconnected pyramidal neurons. Such an observation is consistent with the excitatory-inhibitory balance necessary for the CCM. However, the CCM would suggest there should only be one input layer, and we have observed an additional, simultaneous, stimulus-related response in supragranular neurons. This is not inconsistent with the anatomy, which also shows feedforward input terminating in superficial layers. It is also possible these may be interneurons which act on the apical dendrites of layer IV neurons and are recruited for stronger feedforward inhibition. It is worth noting that while the CCM does not propose a bilaminar input, such a pattern has been observed in macaque SEF (Godlove et al., 2014), providing a precedent for this observation. It is possible that these frontal cortical structures, being relatively higher in the visual hierarchy than LIP, may have a qualitatively different laminar organization.

Examining the target discriminating activity reveals an even greater discrepancy from proposed models (Heinzle et al., 2007). Target discriminating activity emerges first in putative infragranular interneurons, as opposed to supragranular pyramidal neurons as would be expected, and is the case in LIP. This activity being observed in infragranular layers would perhaps be consistent with an overlap in the population responsible for target selection and motor out-

put, whereas in LIP, these functions are separately observed in supragranular and infragranular layers respectively. Antidromic stimulation experiments in tandem with high-density laminar recordings may prove fruitful in identifying the overlap between these populations. The observation that target discrimination is observed in narrow-spiking but not broad-spiking neurons at the population level is also surprising. It is worth noting that the proportion of broad-spiking neurons in deeper layers was quite low in these recordings, which might point to either a sampling bias in these recordings or a misclassification of cell classes. Such a misclassification is not unlikely, it is known that corticofugal neurons in deeper layers of M1 can often have narrow waveforms (Vigneswaran et al., 2011), and it is possible that this is also the case here. While corticotectal neurons in dlPFC have been shown to have broad waveforms (Johnston et al., 2009), this has not been confirmed for FEF neurons. Cell-type specific optogenetic techniques and antidromic identification experiments may provide great insight into this possible discrepancy. Ultimately, these observations are consistent with previous observations that layer V corticotectal neurons in FEF represent activity at nearly all stages of visuomotor processing (Everling & Munoz, 2000; Wurtz et al., 2001) but are in contrast with the superficial vs deep bias for visual and motor activity respectively observed in other areas such as LIP (Chapter 3) or V4 (Pettine et al., 2019; Westerberg et al., 2021).

Taken together, our findings demonstrate single neuron target selection related activity in marmoset FEF. While there were no differences in the distribution and timing of this activity at the level of single neurons, examining the population revealed striking laminar dynamics. However, these were not consistent with predictions based on a CCM. We observed bilaminar visual input in supragranular and granular layers followed by target selection in infragranular layers. These observations suggest the CCM may not extend to all regions of cortex, and provides novel insight into the organization of FEF.

4.5   References

Ardid, S., Vinck, M., Kaping, D., Marquez, S., Everling, S., & Womelsdorf, T. (2015). Mapping of Functionally Characterized Cell Classes onto Canonical Circuit Operations in Primate Prefrontal Cortex. *The Journal of Neuroscience*, *35*(7), 2975–2991. https://doi.org/10.1523/JNEUROSCI.2700-14.2015

Baizer, J. S., Ungerleider, L. G., & Desimone, R. (1991). Organization of visual inputs to the inferior temporal and posterior parietal cortex in macaques. *The Journal of Neuroscience*, *11*(1), 168–190. https://doi.org/10.1523/JNEUROSCI.11-01-00168.1991

Barone, P., Batardiere, A., Knoblauch, K., & Kennedy, H. (2000). Laminar Distribution of Neurons in Extrastriate Areas Projecting to Visual Areas V1 and V4 Correlates with the Hierarchical Rank and Indicates the Operation of a Distance Rule. *The Journal of Neuroscience*, *20*(9), 3263–3281. https://doi.org/10.1523/JNEUROSCI.20-09-03263.2000

Bichot, N. P., & Schall, J. D. (1999). Saccade target selection in macaque during feature and conjunction visual search. *Visual Neuroscience*, *16*(1), 81–89. https://doi.org/10.1017/S0952523899161042

Binzegger, T., Douglas, R. J., & Martin, K. A. C. (2004). A Quantitative Map of the Circuit of Cat Primary Visual Cortex. *Journal of Neuroscience*, *24*(39), 8441–8453. https://doi.org/10.1523/JNEUROSCI.1400-04.2004

Bisley, J. W., & Goldberg, M. E. (2003). Neuronal Activity in the Lateral Intraparietal Area and Spatial Attention. *Science*, *299*(5603), 81–86. https://doi.org/10.1126/science.1077395

Bisley, J. W., Mirpour, K., Arcizet, F., & Ong, W. S. (2011). The Role of the Lateral Intraparietal Area in Orienting Attention and its Implications for Visual Search. *The European journal of neuroscience*, *33*(11), 1982–1990. https://doi.org/10.1111/j.1460-9568.2011.07700.x

Boulton, A. A., Baker, G. B., & Vanderwolf, C. H. (1990, September 12). *Neurophysiological Techniques, II* (Vol. 15). Humana Press. https://doi.org/10.1385/0896031853

Bruce, C. J., & Goldberg, M. E. (1985). Primate frontal eye fields. I. Single neurons discharging before saccades. *Journal of Neurophysiology*, *53*(3), 603–635. https://doi.org/10.1152/jn.1985.53.3.603

Bruce, C. J., Goldberg, M. E., Bushnell, M. C., & Stanton, G. B. (1985). Primate frontal eye fields. II. Physiological and anatomical correlates of electrically evoked eye movements. *Journal of Neurophysiology*, *54*(3), 714–734. https://doi.org/10.1152/jn.1985.54.3.714

Cadarso-Suarez, C., Roca-Pardinas, J., Molenberghs, G., Faes, C., Nacher, V., Ojeda, S., & Acuna, C. (2006). Flexible modelling of neuron firing rates across different experimental conditions: An application to neural activity in the prefrontal cortex during a discrimination task. *Journal of the Royal Statistical Society: Series C (Applied Statistics)*, *55*(4), 431–447. https://doi.org/10.1111/j.1467-9876.2006.00545.x

Collins, C. E., Lyon, D. C., & Kaas, J. H. (2005). Distribution across cortical areas of neurons projecting to the superior colliculus in new world monkeys. *The Anatomical Record Part A: Discoveries in Molecular, Cellular, and Evolutionary Biology*, *285A*(1), 619–627. https://doi.org/10.1002/ar.a.20207

Douglas, R. J., & Martin, K. A. (1991). A functional microcircuit for cat visual cortex. *The Journal of Physiology*, *440*, 735–769. Retrieved July 23, 2021, from https://www.ncbi.nlm.nih.gov/pmc/articles/PMC1180177/

Douglas, R. J., & Martin, K. A. (2004). Neuronal Circuits of the Neocortex. *Annual Review of Neuroscience*, *27*(1), 419–451. https://doi.org/10.1146/annurev.neuro.27.070203.144152

Elsley, J. K., Nagy, B., Cushing, S. L., & Corneil, B. D. (2007). Widespread Presaccadic Recruitment of Neck Muscles by Stimulation of the Primate Frontal Eye Fields. *Journal of Neurophysiology*, *98*(3), 1333–1354. https://doi.org/10.1152/jn.00386.2007

Everling, S., & Munoz, D. P. (2000). Neuronal Correlates for Preparatory Set Associated with Pro-Saccades and Anti-Saccades in the Primate Frontal Eye Field. *Journal of Neuroscience*, *20*(1), 387–400. https://doi.org/10.1523/JNEUROSCI.20-01-00387.2000

Feizpour, A., Majka, P., Chaplin, T. A., Rowley, D., Yu, H.-H., Zavitz, E., Price, N. S. C., Rosa, M. G. P., & Hagan, M. A. (2021). Visual responses in the dorsolateral frontal cortex of marmoset monkeys. *Journal of Neurophysiology*, *125*(1), 296–304. https://doi.org/10.1152/jn.00581.2020

Ferraina, S., Paré, M., & Wurtz, R. H. (2002). Comparison of Cortico-Cortical and Cortico-Collicular Signals for the Generation of Saccadic Eye Movements. *Journal of Neurophysiology*, *87*(2), 845–858. https://doi.org/10.1152/jn.00317.2001

Ferrier, D. (1875). The Croonian Lecture: Experiments on the Brain of Monkeys (second series). *Philosopical Transactions of the Royal Society of London*, *165*, 433–488. https://royalsocietypublishing.org/doi/pdf/10.1098/rstl.1875.0016

Fries, W. (1984). Cortical projections to the superior colliculus in the macaque monkey: A retrograde study using horseradish peroxidase. *Journal of Comparative Neurology*, *230*(1), 55–76. https://doi.org/10.1002/cne.902300106

Ghahremani, M., Hutchison, R. M., Menon, R. S., & Everling, S. (2017). Frontoparietal Functional Connectivity in the Common Marmoset. *Cerebral Cortex*, *27*, 3890–3905. https://doi.org/10.1093/cercor/bhw198

Ghahremani, M., Johnston, K. D., Ma, L., Hayrynen, L. K., & Everling, S. (2019). Electrical microstimulation evokes saccades in posterior parietal cortex of common marmosets. *Journal of Neurophysiology*, *122*(4), 1765–1776. https://doi.org/10.1152/jn.00417.2019

Godlove, D. C., Maier, A., Woodman, G. F., & Schall, J. D. (2014). Microcircuitry of Agranular Frontal Cortex: Testing the Generality of the Canonical Cortical Microcircuit. *The Journal of Neuroscience*, *34*(15), 5355–5369. https://doi.org/10.1523/JNEUROSCI.5127-13.2014

Green, D. M., & Swets, J. A. (1966). *Signal detection theory and psychophysics*. John Wiley.

Hastie, T., & Tibshirani, R. (1986). Generalized Additive Models. *Statistical Science*, *1*(3), 297–318.

Heinzle, J., Hepp, K., & Martin, K. A. C. (2007). A Microcircuit Model of the Frontal Eye Fields. *Journal of Neuroscience*, *27*(35), 9341–9353. https://doi.org/10.1523/JNEUROSCI.0974-07.2007

Huerta, M. F., Krubitzer, L. A., & Kaas, J. H. (1986). Frontal eye field as defined by intracortical microstimulation in squirrel monkeys, owl monkeys, and macaque monkeys: I. Subcortical connections. *Journal of Comparative Neurology*, *253*(4), 415–439. https://doi.org/10.1002/cne.902530402

Huerta, M. F., Krubitzer, L. A., & Kaas, J. H. (1987). Frontal eye field as defined by intracortical microstimulation in squirrel monkeys, owl monkeys, and macaque monkeys II. cortical connections. *Journal of Comparative Neurology*, *265*(3), 332–361. https://doi.org/10.1002/cne.902650304

Hussar, C. R., & Pasternak, T. (2012). Memory-Guided Sensory Comparisons in the Prefrontal Cortex: Contribution of Putative Pyramidal Cells and Interneurons. *The Journal of Neuroscience*, *32*(8), 2747–2761. https://doi.org/10.1523/JNEUROSCI.5135-11.2012

Ipata, A. E., Gee, A. L., Goldberg, M. E., & Bisley, J. W. (2006). Activity in the Lateral Intraparietal Area Predicts the Goal and Latency of Saccades in a Free-Viewing Visual Search Task. *The Journal of Neuroscience*, *26*(14), 3656–3661. https://doi.org/10.1523/JNEUROSCI.5074-05.2006

Johnston, K. D., DeSouza, J. F. X., & Everling, S. (2009). Monkey Prefrontal Cortical Pyramidal and Putative Interneurons Exhibit Differential Patterns of Activity Between Prosaccade and Antisaccade Tasks. *The Journal of Neuroscience*, *29*(17), 5516–5524. https://doi.org/10.1523/JNEUROSCI.5953-08.2009

Johnston, K. D., & Everling, S. (2008). Neurophysiology and neuroanatomy of reflexive and voluntary saccades in non-human primates. *Brain and Cognition*, *68*(3), 271–283. https://doi.org/10.1016/j.bandc.2008.08.017

Jun, J. J., Steinmetz, N. A., Siegle, J. H., Denman, D. J., Bauza, M., Barbarits, B., Lee, A. K., Anastassiou, C. A., Andrei, A., Aydın, Ç., Barbic, M., Blanche, T. J., Bonin, V., Couto, J., Dutta, B., Gratiy, S. L., Gutnisky, D. A., Häusser, M., Karsh, B., . . . Harris, T. D. (2017). Fully integrated silicon probes for high-density recording of neural activity. *Nature*, *551*(7679), 232–236. https://doi.org/10.1038/nature24636

Knight, T. A., & Fuchs, A. F. (2007). Contribution of the Frontal Eye Field to Gaze Shifts in the Head-Unrestrained Monkey: Effects of Microstimulation. *Journal of Neurophysiology*, *97*(1), 618–634. https://doi.org/10.1152/jn.00256.2006

Lynch, J. C., Hoover, J. E., & Strick, P. L. (1994). Input to the primate frontal eye field from the substantia nigra, superior colliculus, and dentate nucleus demonstrated by transneuronal transport. *Experimental Brain Research*, *100*(1), 181–186. https://doi.org/10.1007/BF00227293

Ma, L., Selvanayagam, J., Ghahremani, M., Hayrynen, L. K., Johnston, K. D., & Everling, S. (2020). Single-unit activity in marmoset posterior parietal cortex in a gap saccade task. *Journal of Neurophysiology*, *123*(3), 896–911. https://doi.org/10.1152/jn.00614.2019

Matsuzaki, R., Kyuhou, S.-i., Matsuura-Nakao, K., & Gemba, H. (2004). Thalamo-cortical projections to the posterior parietal cortex in the monkey. *Neuroscience Letters*, *355*(1), 113–116. https://doi.org/10.1016/j.neulet.2003.10.066

May, J., & Andersen, R. A. (1986). Different patterns of corticopontine projections from separate cortical fields within the inferior parietal lobule and dorsal prelunate gyrus of the macaque. *Experimental Brain Research*, *63*(2). https://doi.org/10.1007/BF00236844

McCormick, D. A., Connors, B. W., Lighthall, J. W., & Prince, D. A. (1985). Comparative electrophysiology of pyramidal and sparsely spiny stellate neurons of the neocortex. *Journal of Neurophysiology*, *54*(4), 782–806. https://doi.org/10.1152/jn.1985.54.4.782

McDowell, J. E., Dyckman, K. A., Austin, B., & Clementz, B. A. (2008). Neurophysiology and Neuroanatomy of Reflexive and Volitional Saccades: Evidence from Studies of Humans. *Brain and cognition*, *68*(3), 255–270. https://doi.org/10.1016/j.bandc.2008.08.016

McPeek, R. M., & Keller, E. L. (2002). Saccade Target Selection in the Superior Colliculus During a Visual Search Task. *Journal of Neurophysiology*, *88*(4), 2019–2034. https://doi.org/10.1152/jn.2002.88.4.2019

Mendoza-Halliday, D., Major, A. J., Lee, N., Lichtenfeld, M., Carlson, B., Mitchell, B., Meng, P. D., Xiong, Y. (, Westerberg, J. A., Maier, A., Desimone, R., Miller, E. K., & Bastos, A. M. (2023, May 12). *A ubiquitous spectrolaminar motif of local field potential power across the primate cortex*. https://doi.org/10.1101/2022.09.30.510398

Mitchell, J. F., Sundberg, K. A., & Reynolds, J. H. (2007). Differential Attention-Dependent Response Modulation across Cell Classes in Macaque Visual Area V4. *Neuron*, *55*(1), 131–141. https://doi.org/10.1016/j.neuron.2007.06.018

Mohler, C. W., Goldberg, M. E., & Wurtz, R. H. (1973). Visual receptive fields of frontal eye field neurons. *Brain Research*, *61*, 385–389. https://doi.org/10.1016/0006-8993(73)90543-X

Monosov, I. E., & Thompson, K. G. (2009). Frontal Eye Field Activity Enhances Object Identification During Covert Visual Search. *Journal of Neurophysiology*, *102*(6), 3656–3672. https://doi.org/10.1152/jn.00750.2009

Moore, T., & Armstrong, K. M. (2003). Selective gating of visual signals by microstimulation of frontal cortex. *Nature*, *421*(6921), 370–373. https://doi.org/10.1038/nature01341

Moore, T., & Fallah, M. (2004). Microstimulation of the Frontal Eye Field and Its Effects on Covert Spatial Attention. *Journal of Neurophysiology*, *91*(1), 152–162. https://doi.org/10.1152/jn.00741.2002

Paré, M., & Wurtz, R. H. (1997). Monkey Posterior Parietal Cortex Neurons Antidromically Activated From Superior Colliculus. *Journal of Neurophysiology*, *78*(6), 3493–3497. https://doi.org/10.1152/jn.1997.78.6.3493

Paré, M., & Wurtz, R. H. (2001). Progression in Neuronal Processing for Saccadic Eye Movements From Parietal Cortex Area LIP to Superior Colliculus. *Journal of Neurophysiology*, *85*(6), 2545–2562. https://doi.org/10.1152/jn.2001.85.6.2545

Pettine, W. W., Steinmetz, N. A., & Moore, T. (2019). Laminar segregation of sensory coding and behavioral readout in macaque V4. *Proceedings of the National Academy of Sciences of the United States of America*, *116*(29), 14749–14754. https://doi.org/10.1073/pnas.1819398116

Pouget, P., Stepniewska, I., Crowder, E. A., Leslie, M. W., Emeric, E. E., Nelson, M. J., & Schall, J. D. (2009). Visual and Motor Connectivity and the Distribution of Calcium-Binding Proteins in Macaque Frontal Eye Field: Implications for Saccade Target Selection. *Frontiers in Neuroanatomy*, *3*, 2. https://doi.org/10.3389/neuro.05.002.2009

Reser, D. H., Burman, K. J., Yu, H.-H., Chaplin, T. A., Richardson, K. E., Worthy, K. H., & Rosa, M. G. P. (2013). Contrasting Patterns of Cortical Input to Architectural Subdivisions of the Area 8 Complex: A Retrograde Tracing Study in Marmoset Monkeys. *Cerebral Cortex*, *23*(8), 1901–1922. https://doi.org/10.1093/cercor/bhs177

Robinson, D. A., & Fuchs, A. F. (1969). Eye movements evoked by stimulation of frontal eye fields. *Journal of Neurophysiology*, *32*(5), 637–648. https://doi.org/10.1152/jn.1969.32.5.637

Rosa, M. G. P., Palmer, S. M., Gamberini, M., Burman, K. J., Yu, H.-H., Reser, D. H., Bourne, J. A., Tweedale, R., & Galletti, C. (2009). Connections of the Dorsomedial Visual Area: Pathways for Early Integration of Dorsal and Ventral Streams in Extrastriate Cortex. *Journal of Neuroscience*, *29*(14), 4548–4563. https://doi.org/10.1523/JNEUROSCI.0529-09.2009

Sajad, A., Errington, S. P., & Schall, J. D. (2022). Functional architecture of executive control and associated event-related potentials in macaques. *Nature Communications*, *13*(1), 6270. https://doi.org/10.1038/s41467-022-33942-1

Sajad, A., Godlove, D. C., & Schall, J. D. (2019). Cortical microcircuitry of performance monitoring. *Nature Neuroscience*, *22*(2), 265–274. https://doi.org/10.1038/s41593-018-0309-8

Bandiera_abtest: a Cg_type: Nature Research Journals Primary_atype: Research Subject_term: Cognitive control;Cortex;Psychology;Schizophrenia Subject_term_id: cognitive-control;cortex;psychology;schizophrenia

Schaeffer, D. J., Gilbert, K. M., Hori, Y., Hayrynen, L. K., Johnston, K. D., Gati, J. S., Menon, R. S., & Everling, S. (2019). Task-based fMRI of a free-viewing visuo-saccadic net-

work in the marmoset monkey. *NeuroImage*, *202*, 116147. https://doi.org/10.1016/j.neuroimage.2019.116147

Schall, J. D. (1991). Neuronal activity related to visually guided saccades in the frontal eye fields of rhesus monkeys: Comparison with supplementary eye fields. *Journal of Neurophysiology*, *66*(2), 559–579. https://doi.org/10.1152/jn.1991.66.2.559

Schall, J. D. (1995). Neural Basis of Saccade Target Selection. *Reviews in the Neurosciences*, *6*(1), 63–85. https://doi.org/10.1515/REVNEURO.1995.6.1.63

Schall, J. D. (2004). On the role of frontal eye field in guiding attention and saccades. *Vision Research*, *44*(12), 1453–1467. https://doi.org/10.1016/j.visres.2003.10.025

Schall, J. D., & Hanes, D. P. (1993). Neural basis of saccade target selection in frontal eye field during visual search. *Nature*, *366*(6454), 467–469. https://doi.org/10.1038/366467a0

Schall, J. D., Hanes, D. P., Thompson, K. G., & King, D. J. (1995). Saccade target selection in frontal eye field of macaque. I. Visual and premovement activation. *The Journal of Neuroscience*, *15*(10), 6905–6918. https://doi.org/10.1523/JNEUROSCI.15-10-06905.1995

Schall, J. D., Morel, A., King, D. J., & Bullier, J. (1995). Topography of visual cortex connections with frontal eye field in macaque: Convergence and segregation of processing streams. *The Journal of Neuroscience*, *15*(6), 4464–4487. https://doi.org/10.1523/JNEUROSCI.15-06-04464.1995

Schall, J. D., Sato, T. R., Thompson, K. G., Vaughn, A. A., & Juan, C.-H. (2004). Effects of Search Efficiency on Surround Suppression During Visual Selection in Frontal Eye Field. *Journal of Neurophysiology*, *91*(6), 2765–2769. https://doi.org/10.1152/jn.00780.2003

Schiller, P. H., True, S. D., & Conway, J. L. (1980). Deficits in eye movements following frontal eye-field and superior colliculus ablations. *Journal of Neurophysiology*, *44*(6), 1175–1189. https://doi.org/10.1152/jn.1980.44.6.1175

Schiller, P. H., & Chou, I.-H. (2000). The effects of anterior arcuate and dorsomedial frontal cortex lesions on visually guided eye movements: 2. Paired and multiple targets. *Vision Research*, *40*(10), 1627–1638. https://doi.org/10.1016/S0042-6989(00)00058-4

Segraves, M. A., & Goldberg, M. E. (1987). Functional properties of corticotectal neurons in the monkey's frontal eye field. *Journal of Neurophysiology*, *58*(6), 1387–1419. https://doi.org/10.1152/jn.1987.58.6.1387

Selvanayagam, J., Johnston, K. D., Schaeffer, D. J., Hayrynen, L. K., & Everling, S. (2019). Functional Localization of the Frontal Eye Fields in the Common Marmoset Using Microstimulation. *Journal of Neuroscience*, *39*(46), 9197–9206. https://doi.org/10.1523/JNEUROSCI.1786-19.2019

Shen, K., Valero, J., Day, G. S., & Paré, M. (2011). Investigating the role of the superior colliculus in active vision with the visual search paradigm. *The European Journal of Neuroscience*, *33*(11), 2003–2016. https://doi.org/10.1111/j.1460-9568.2011.07722.x

Sommer, M. A., & Wurtz, R. H. (1998). Frontal Eye Field Neurons Orthodromically Activated From the Superior Colliculus. *Journal of Neurophysiology*, *80*(6), 3331–3335. https://doi.org/10.1152/jn.1998.80.6.3331

Sommer, M. A., & Wurtz, R. H. (2001). Frontal Eye Field Sends Delay Activity Related to Movement, Memory, and Vision to the Superior Colliculus. *Journal of Neurophysiology*, *85*(4), 1673–1685. https://doi.org/10.1152/jn.2001.85.4.1673

Sommer, M. A., & Wurtz, R. H. (2004). What the Brain Stem Tells the Frontal Cortex. I. Oculomotor Signals Sent From Superior Colliculus to Frontal Eye Field Via Mediodorsal Thalamus. *Journal of Neurophysiology*, *91*(3), 1381–1402. https://doi.org/10.1152/jn.00738.2003

Sommer, M. A., & Wurtz, R. H. (2006). Influence of the thalamus on spatial visual processing in frontal cortex. *Nature*, *444*(7117), 374–377. https://doi.org/10.1038/nature05279

Sommer, M. A., & Wurtz, R. H. (2008). Visual Perception and Corollary Discharge. *Perception*, *37*(3), 408–418. Retrieved August 3, 2023, from https://www.ncbi.nlm.nih.gov/pmc/articles/PMC2807735/

Stanton, G. B., Goldberg, M. E., & Bruce, C. J. (1988). Frontal eye field efferents in the macaque monkey: II. Topography of terminal fields in midbrain and pons. *Journal of Comparative Neurology*, *271*(4), 493–506. https://doi.org/10.1002/cne.902710403

Swadlow, H. A. (2002). Thalamocortical control of feed-forward inhibition in awake somatosensory 'barrel' cortex. *Philosophical Transactions of the Royal Society B: Biological Sciences*, *357*(1428), 1717–1727. https://doi.org/10.1098/rstb.2002.1156

Thier, P., & Andersen, R. A. (1998). Electrical Microstimulation Distinguishes Distinct Saccade-Related Areas in the Posterior Parietal Cortex. *Journal of Neurophysiology*, *80*(4), 1713–1735. https://doi.org/10.1152/jn.1998.80.4.1713

Thomas, N. W. D., & Paré, M. (2007). Temporal Processing of Saccade Targets in Parietal Cortex Area LIP During Visual Search. *Journal of Neurophysiology*, *97*(1), 942–947. https://doi.org/10.1152/jn.00413.2006

Thompson, K. G., Bichot, N. P., & Sato, T. R. (2005). Frontal Eye Field Activity Before Visual Search Errors Reveals the Integration of Bottom-Up and Top-Down Salience. *Journal of neurophysiology*, *93*(1), 337–351. https://doi.org/10.1152/jn.00330.2004

Thompson, K. G., Bichot, N. P., & Schall, J. D. (1997). Dissociation of Visual Discrimination From Saccade Programming in Macaque Frontal Eye Field. *Journal of Neurophysiology*, *77*(2), 1046–1050. https://doi.org/10.1152/jn.1997.77.2.1046

Thompson, K. G., Biscoe, K. L., & Sato, T. R. (2005). Neuronal Basis of Covert Spatial Attention in the Frontal Eye Field. *The Journal of Neuroscience*, *25*(41), 9479–9487. https://doi.org/10.1523/JNEUROSCI.0741-05.2005

Thompson, K. G., Hanes, D. P., Bichot, N. P., & Schall, J. D. (1996). Perceptual and motor processing stages identified in the activity of macaque frontal eye field neurons during visual search. *Journal of Neurophysiology*, *76*(6), 4040–4055. https://doi.org/10.1152/jn.1996.76.6.4040

van der Steen, J., Russell, I. S., & James, G. O. (1986). Effects of unilateral frontal eye-field lesions on eye-head coordination in monkey. *Journal of Neurophysiology*, *55*(4), 696–714. https://doi.org/10.1152/jn.1986.55.4.696

Vigneswaran, G., Kraskov, A., & Lemon, R. N. (2011). Large Identified Pyramidal Cells in Macaque Motor and Premotor Cortex Exhibit "Thin Spikes": Implications for Cell Type Classification. *The Journal of Neuroscience*, *31*(40), 14235–14242. https://doi.org/10.1523/JNEUROSCI.3142-11.2011

Wardak, C., Ibos, G., Duhamel, J.-R., & Olivier, E. (2006). Contribution of the Monkey Frontal Eye Field to Covert Visual Attention. *The Journal of Neuroscience*, *26*(16), 4228–4235. https://doi.org/10.1523/JNEUROSCI.3336-05.2006

Wardak, C., Olivier, E., & Duhamel, J.-R. (2002). Saccadic Target Selection Deficits after Lateral Intraparietal Area Inactivation in Monkeys. *The Journal of Neuroscience*, *22*(22), 9877–9884. https://doi.org/10.1523/JNEUROSCI.22-22-09877.2002

Wardak, C., Olivier, E., & Duhamel, J.-R. (2004). A Deficit in Covert Attention after Parietal Cortex Inactivation in the Monkey. *Neuron*, *42*(3), 501–508. https://doi.org/10.1016/S0896-6273(04)00185-0

Westerberg, J. A., Sigworth, E. A., Schall, J. D., & Maier, A. (2021). Pop-out search instigates beta-gated feature selectivity enhancement across V4 layers. *Proceedings of the National Academy of Sciences of the United States of America*, *118*(50), e2103702118. https://doi.org/10.1073/pnas.2103702118

Wolfe, J. M., & Horowitz, T. S. (2004). What attributes guide the deployment of visual attention and how do they do it? *Nature Reviews Neuroscience*, *5*(6), 495–501. https://doi.org/10.1038/nrn1411

Wurtz, R. H., Sommer, M. A., Paré, M., & Ferraina, S. (2001). Signal transformations from cerebral cortex to superior colliculus for the generation of saccades. *Vision Research*, *41*(25), 3399–3412. https://doi.org/10.1016/S0042-6989(01)00066-9

Zhou, H.-H., & Thompson, K. G. (2009). Cognitively-directed spatial selection in the frontal eye field in anticipation of visual stimuli to be discriminated. *Vision research*, *49*(10), 1205–1215. https://doi.org/10.1016/j.visres.2008.03.024

Chapter 5

General Discussion

5.1 Summary of Main Findings

Selective visual spatial attention and the control of eye movements are critical for our ability to efficiently perceive our visual world. How these processes interact are of particular interest, and the neural correlates of these have been extensively investigated in macaques and humans. However, due to practical challenges, we have yet to uncover the laminar organization of key structures such as LIP and FEF which underlie this behaviour, though some theoretical frameworks exist. The aim of this dissertation work was to establish the marmoset model for neurophysiological investigation of the frontoparietal network for its role in oculomotor control and visual attention as well as to begin to uncover the laminar microcircuitry of its main cortical nodes. In general, we demonstrated via ICMS and ultra-high density laminar recordings, that the marmoset LIP and FEF are highly homologous with those of the macaque. In addition, we observed in LIP a laminar organization of discharge activity consistent with the CCM. However, similar investigation of FEF revealed a more nuanced organization, which challenges the ubiquity of such a model. Future investigations, particularly those with cell-type specificity, are required for the continued examination of laminar circuits underlying attention.

5.1.1 Functional localization of frontal eye fields in the common marmoset

The location of macaque FEF is classically defined as the area of frontal cortex where low current ICMS elicits fixed-vector saccades (Bruce et al., 1985). A confluence of cytoarchitectural, anatomical, resting-state and task-based fMRI, and preliminary ICMS and single-neuron recording studies point to a marmoset homolog of the macaque FEF in marmoset areas 8, 6 and 45 (see Chapter 1.4.2). Here we sought to systematically stimulate marmoset frontal cortex to physiologically identify and characterize the marmoset FEF.

At electrode sites in 8aV and 45, but also the edges of 8aD, 6DR and 8C, we were able to elicit saccades towards the contralateral hemifield with a consistent amplitude and direction. Prolonged stimulation elicited characteristic staircases of saccades driving the orbit to its edge. We also observed a retinotopic organization of saccade vectors, with the dorsal-ventral axis corresponding to large to small amplitude saccades and with saccade direction mapped along

a anterior-dorsal to posterior-ventral axis, corresponding to lower to upper visual field. While saccade vectors at more dorsal sites appeared to be convergent in craniocentric space (i.e. goal directed saccades), this could be better explained by large amplitude saccades being restricted by the more limited oculomotor range of these animals. Indeed, measures of convergence at these sites are correlated with saccade amplitude (Russo & Bruce, 1993). Sites corresponding to larger amplitudes often also recruited neck, ear and shoulder muscles, suggesting these sites may also correspond to head-orienting movements in a head-unrestrained animal (Corneil et al., 2010; Knight & Fuchs, 2007). ICMS applied to a subset of FEF sites produced slow, drifting eye movements for which the velocity but not the direction varied with current intensity. A "smooth pursuit" region of FEF has been described in the macaque, where stimulation produces pursuit-like movements and single neurons are tuned to pursuit (Gottlieb et al., 1993). And marmosets have been demonstrated to be capable of smooth pursuit similar to macaques and humans (Mitchell et al., 2015). Single neuron recordings in this region are required to establish the existence of such a region in the marmoset.

In addition to FEF sites, we observed a rostral eye field where saccades did not have a consistent fixed vector or convergent pattern but rather appeared random (see for similar result Robinson & Fuchs, 1969). At more medial sites, we also observed sites where we could reliably elicit convergent saccades, including ipsiversive saccades, which were not correlated with saccade amplitude. Such observations are reminiscent of SEF, though current thresholds and saccade latencies were higher at these sites than expected (Schlag & Schlag-Rey, 1987). It is likely the case that electrodes here were too lateral to stimulate SEF and observed saccades were elicited via current spread to more medial regions at higher currents.

More posterior to sites where we observed eye movements, or join eye, neck and shoulder movements, we observed sites where no eye movements could be elicited. Here we observed eye blinks, as well as coordinated multi-limb movements consistent with dorsal premotor cortex (Burish et al., 2008; Wakabayashi et al., 2018). Further posterior, we observed skeletomotor of individual limbs and groups of digits as well as orofacial movements which could be evoked at very low current thresholds, consistent with primary motor cortex. Altogether, we observed an organization of marmoset frontal cortex consistent with that of the macaque including primary motor cortex, premotor cortex, and dorsal and ventral aspects of FEF as well as hints of a rostral eye field and SEF.

The observation of retinotopy in marmoset FEF is a novel finding, as while the macaque FEF shows a coarse amplitude mapping along the dorsal-ventral axis, there are often discontinuities and no true direction mapping has been described (Bruce et al., 1985). The complex morphology of the macaque FEF within the sulcus presents challenges in describing the direction mapping, though Savaki and colleagues (2015) have employed ^{14}C-deoxyglucose quantitative autoradiography to explore this. Their findings are in contrast with ours in the marmoset, which may be attributable to a true species difference or a counterintuitive "unfolding" of the arcuate sulcus in the marmoset. In either case, more detailed anatomical and physiological investigations are required. On the other hand, the amplitude mapping, in addition to being consistent with observations in the macaque, was also described by Foerster (1926) in humans. In the macaque, it is also reflected in the segregation of anatomical projections from other retinotopically organized regions, or regions in the ventral visual stream concerned with foveal representations (Schall et al., 1995). A similar organization is present in the marmoset, though these dorsal and ventral aspects were referred to as FEF and FV respectively. A recent

neurophysiological investigation in anaesthetized marmosets (Feizpour et al., 2021) examined the discharge activity of single neurons to visual stimuli and computed RFs for these neurons. These researchers recapitulated the amplitude mapping observed here, but did not observe the direction mapping. More recent work by Chen and colleagues (2023) using careful reconstruction of electrode tracts, viral labelling of corticotectal neuron targets, and one-photon calcium imaging, has replicated the amplitude mapping observed here. Additionally, they observed a very similar direction mapping albeit slightly warped. It appears that direction mapping is primarily along the rostrocaudal axis but is represented radially along the cortical surface and also varies smoothly along the dorsal-ventral axis. Our findings here are consistent with those of Chen and colleagues with a slight rotation of the array of M3. However, the fact this was not observed in the single neuron recordings by Feizpour and colleagues points to a need for further replication of this observation to ensure it is not an idiosyncracy of individual monkeys.

With respect to current thresholds and saccade latencies, results in the marmoset closely resemble those of the macaque (Bruce et al., 1985; Robinson & Fuchs, 1969). However, latencies were slightly longer in marmosets than in macaques. It has been proposed that these longer latency saccades are evoked indirectly via the SC whereas shorter latency saccades are evoked directly via the BSGs (Bruce et al., 1985; Robinson & Fuchs, 1969; Segraves, 1992; Segraves & Goldberg, 1987). It is then possible that the ratio of projections from marmoset FEF to the brainstem as compared to the SC is lower than that of the macaque, which may contribute to longer saccade latencies.

Altogether, this work identifies a region of marmoset frontal cortex wherein low current stimulation elicits saccades with properties consistent with primate FEF. The cytoarchitectural areas corresponding to the newly defined marmoset FEF are consistent with the anatomical and fMRI data from marmosets and those of the macaque. The retinotopic organization of marmoset FEF is largely consistent with that of the macaque, and has been replicated recently (Chen et al., 2023; Feizpour et al., 2021). These findings provide a basis for subsequent investigations in marmoset FEF and generally support the use of the marmoset model for neurophysiological investigations of oculomotor control and visual attention.

5.1.2   Laminar dynamics in the lateral intraparietal area

As previous work in our lab has similarly established the homology of marmoset LIP with that of the macaque (see Chapter 1.4.2), there is now a basis for neurophysiological investigations of marmoset LIP and FEF for examining the laminar circuitry underlying eye movements and attention. Indeed, LIP is a key node of the frontoparietal network, and is strongly interconnected with other visual and oculomotor regions. Activity in LIP is known to correspond to a saliency map, which represents the most behaviourally relevant stimuli in a scene from which targets may be selected for focus. Single neurons in LIP select for target stimuli over distractors and inactivation of this regions impairs target selection but not saccade generation generally. Theoretical models and antidromic stimulation studies suggest there may be an organization cortical layers in LIP such that input arrives in granular layer IV, followed by target selection in supragranular layers and output in infragranular layers (Douglas & Martin, 2004; Heinzle et al., 2007).

To evaluate this, we conducted ultra-high density laminar recordings in marmoset PPC as animals completed a visual target selection task. Marmosets were able to readily complete this

task, showing behavioural patterns such as increased errors and reaction times, consistent with a visual selection process. We observed many single neurons with stimulus-related activity, many of which discriminated target and distractor stimuli in the contralateral hemifield. We also observed post-saccadic activity which may correspond to corollary discharge, feedback signals and.or visual refresh. Additionally, in contrast with observations in FEF, pre-saccadic activity in LIP neurons did not correlate well with SRTs (Bisley & Goldberg, 2003; Bisley et al., 2011; Goldberg et al., 2002; Kusunoki et al., 2000). These observations are consistent with those in macaques showing that while LIP neurons can signal motor plans, these are likely fed back from other more oculomotor areas, and LIP neurons are largely concerned with the current locus of attention.

The observed stimulus-related and target discriminating activity was more dominant in superficial layers whereas post-saccadic activity was more commonly observed in deeper layers, consistent with the CCM and previous antidromic investigations (Douglas & Martin, 2004; Ferraina et al., 2002; Heinzle et al., 2007; Paré & Wurtz, 1997). However, the magnitude and timing of maximal target discrimination did not vary across cortical layers, suggesting all cortical layers ultimately equally represent target selection related activity. These observations are not inconsistent with previous reports in the macaque showing that while slight biases exist in different neuronal populations, ultimately nearly all visuomotor signals tend to be reflected in all populations.

By investigating the stimulus-related and target discrimination activity at the population level, subtle differences in timing could be observed. We observed that stimulus related activity was observed first in putative granular layer interneurons whereas target discrimination activity was observed first in putative supragranular pyramidal neurons. These observations are consistent with the feedforward loop proposed in the CCM and feedforward inhibition observed in rodent barrel cortex (Douglas & Martin, 2004; Heinzle et al., 2007; Swadlow, 2002). Altogether, these findings support a model of LIP laminar function, where incoming visual activity is received by granular layer neurons, with a blanket of inhibition from interneurons briefly preceding the activity of pyramidal neurons to sharpen contrast. Subsequently, supragranular pyramidal neurons, which also receive input from other cortical areas, integrate bottom-up and top-down signals to select the most relevant stimuli for the focus of attention. Finally, these plans are fed back to early visual areas via corticocortical feedback projections and infragranular neurons convey these signals to downstream oculomotor areas.

In sum, we report, for the first time in the marmoset, neural correlates of target selection in single neurons in marmoset LIP. We also identify laminar dynamics consistent with the CCM, extending observations previously restricted to primary cortical areas to association cortex. These findings demonstrate the value of the marmoset model in neurophysiological investigations of oculomotor control and attention, as well as deepening our understanding of primate functional cortical architecture.

5.1.3   Laminar dynamics in the frontal eye fields

Building on the observations of laminar dynamics consistent with the CCM in LIP of marmosets, and the evidence establishing homology between marmoset and macaque FEF (see Chapter 1.4.2 and chapter 4), the final project of this dissertation aimed to investigate the laminar organization of marmoset FEF with regards to visual target selection. As with LIP, FEF

is strongly interconnected with other visual and oculomotor regions and reflects covert and overt attentional processes. In contrast to LIP, which contains a saliency map representing the relative importance of visible stimuli, FEF more closely indexes the actual orienting towards a particular location in space. This is indexed by the stronger association of the discharge properties of FEF neurons with saccade occurence as well as the more pronounced effects of FEF inactivation or lesion on saccade generation. FEF involvement in visual search has been investigated even more extensively than with LIP. FEF neurons show an initially indiscriminate visual response which evolves to signal target stimuli in RF over distractor stimuli before a saccade is made, and do so even in the absence of a saccade (Hanes et al., 1995; Monosov & Thompson, 2009; Schall, 2004; Schall & Hanes, 1993; Thompson et al., 1997; Thompson et al., 2005; Thompson et al., 1996). Lesion to FEF results in significant impairment in visual search performance (Schiller & Chou, 2000; van der Steen et al., 1986; Wardak et al., 2006). FEF neurons also show increases in activity corresponding to covert shifts of attention to eccentric locations based on exogenous and endogenous cues, and this effect can be elicited by ICMS (Monosov & Thompson, 2009; Moore & Armstrong, 2003; Moore & Fallah, 2004; Zhou & Thompson, 2009). Altogether, the role of FEF in the control of eye movements and covert visual attention is well established, however the laminar contributions remain unclear. Here we sought to examine this laminar organization, on the basis of theoretical models constructed based on the activity of FEF neurons (Douglas & Martin, 2004; Heinzle et al., 2007), by conducting ultra-high density laminar recordings in marmoset FEF.

First, we observed stimulus-related and target discriminating activity as in marmoset LIP and as expected of FEF. Additionally, we observed a stronger correspondence between presaccadic activity and saccade occurence in marmoset FEF as compared to marmoset LIP, consistent with its greater role in saccade control. As in LIP, we also observed a preponderance of post-saccadic activity in FEF. Altogether, these observations are consistent with the role of FEF in target selection and saccade control.

Unlike in LIP, we observed no significant differences in the proportion of stimulus-related or target discriminating activity across cortical layers, pointing to a difference between these regions in laminar organization. Further, when examining the population level activity, we observed bilaminar input of stimulus-related activity, with the earliest activity simultaneously appearing in putative granular and supragranular interneurons. As with LIP, the earliest stimulus-related activity being in granular layer interneurons is consistent with feedforward inhibition models (Douglas & Martin, 2004; Swadlow, 2002), but the bilaminar input is in conflict with the CCM. However, similar observations have been made in macaque SEF (Godlove et al., 2014; Sajad et al., 2022; Sajad et al., 2019), which may suggest a unique cortical organization for these frontal cortical areas that are relatively higher in the visual hierarchy.

The target discriminating activity presents an even more distinct pattern. Here, the earliest activity is observed in putative infragranular interneurons. First, this suggests the target selection processes are co-localized with the output of this region, which is markedly distinct from the organization of LIP. Further, the fact this is observed in narrow-spiking and not broad-spiking neurons suggests that either the classification of putative pyramidal and interneurons is not as reliable for this population or these interneurons play a different role for target selection than previous suspected. Future investigations using cell-type specific approaches such as optogenetic identification are required to disentangle these observations.

In sum, we report single neurons in marmoset FEF with stimulus and saccade related activ-

ity consistent with its role in target selection and saccade control as observed in the macaque. However, the laminar organization is markedly different from what is observed in LIP. While the general structure of a feedforward loop from granular to supragranular to infragranular may still be present, an unexpected bilaminar input and shift of target selection to the output layer are observed. These observations are more consistent with recent observations in SEF, challenging the ubiquity of the CCM and providing a greater understanding of functional cortical architecture.

5.2   Limitations and Future directions

A major practical challenge in conducting neurophysiological investigations in the marmoset follows from a key advantage of this model, namely the relative absence of sulci. The cortical regions of interest here are easily identified in the macaque on the basis of sulcal landmarks, which are absent in the marmoset. While this permits techniques required to address the questions presented here, it also offers a practical challenge in targeting these regions for recordings. Here we employed an approach of registering anatomical scans with a awake resting-state functional connectivity database (Schaeffer et al., 2022). We then reconstructed electrode tracts using ultra-high field fMRI to confirm recording locations. In the macaque, detailed atlases have been constructed using a wide variety of anatomical, cyto- and myeloarchitectural and magnetic resonance imaging (MRI) studies collected from a large number of animals (Frey et al., 2011; vs Paxinos et al., 2012). A benefit conferred to this model from decades of dedicated use as a neuroscientific model. Additionally, the relatively larger macaque brain provides a greater margin of error for targeting specific locations. As atlases for the marmoset are improved with greater sample sizes and increased resolution, as well as continued refinement of targeting approaches used here, marmoset neurophysiology will provide even greater insights into cortical circuits underlying attention and cognition in general.

A challenge with all non-human primate models is the inability to instruct subjects in task demands. These investigations require careful training over months, which reduces the external validity of these observations and limits the sophistication of tasks employed. In particular for the marmoset, where food/water restrictions protocols have yet to be developed, and motivation remains a challenge, task complexity and trial counts suffer. While we were able to train reliably train animals to complete a target selection task here, the animals were quickly sated (< 500 trials). These limited trial counts prevented the use of a radial search array, which would permit investigation of RF specific target facilitation/distractor suppression effects (e.g., Schall, 1995). Additionally, we had difficulty in training marmosets to perform delayed or memory guided saccades, which would be necessary to dissociate visual and motor components of the observed activity (e.g., Bruce & Goldberg, 1985). This limited our ability to investigate the motor components of the observed data. However, recent success in training head-unrestrained marmosets to complete delayed-matched to location tasks on a touchscreen, with delays up to 8s (Wong et al., 2022) demonstrates that this is not an issue of the capabilities of marmosets. Indeed, recent work has shown that marmosets can be trained to perform upwards of 3000 trials in visually guided saccade tasks head-fixed (Fakharian et al., 2023) with an appropriate food restriction protocol. Future investigations using employing such protocols, and perhaps pretraining animals using a touchscreen setup, may prove fruitful in conducting more sophisticated

experiments with the marmoset model.

Finally, a limitation of extracellular electrophysiology is the poor spatial resolution. While high-density laminar probes such as the ones used here provide a major advantage in isolating and recording from neurons that may traditionally have been lost to noise, this approach is largely still blind to the cell-types of recorded neurons and does introduce some sampling biases. This limitation may in part explain the observation in FEF wherein putative interneurons as opposed to pyramidal neurons (as was the case in LIP) possessed the earliest target discriminating activity. Future investigations may aim to identify the ground truth in these recordings by employing cell-type specific approaches such as optogenetics targeting various interneuron populations or using "designer receptors exclusively activated by designer drugs" (see for review, Inoue et al., 2021; Roth, 2016). Also, antidromic investigation approaches, previously used in macaques, can also provide some insight as projection neurons in the cortex are obligatorily pyramidal. While the Neuropixels probes, with the data being digitized at the headstage, does not permit for a closed-loop system at present, in a preliminary experiment, we were able to elicit spikes from an LIP neuron with ICMS in FEF. While it is not immediately possible to discount orthodromic activation, it may be possible to identify antidromic activation on the basis of the mean and variability of the spike latency as well as potential spontaneous collisions. Such approaches will provide even greater insights into the present findings and the laminar microcircuits underlying these areas.

In addition to single neuron recordings, it would be of interest to employ causal manipulations to perturb the cortical microcircuit. It may be possible to employ cortical cooling with a thermal probe to selectively cool superficial cortical layers while sparing deeper layers by manipulating the cooling strength (Cooke et al., 2012; Girardin & Martin, 2009; Jeschke et al., 2022). Simultaneously recording from laminar probes may provide insight into the layer specific contributions to behaviour as well as the importance of feedforward and feedback projections for the activity of the local circuit. Alternatively, local drug injection either targeting receptors with known laminar distributions in these regions (e.g., GABA or dopamine) (Douglas & Martin, 1991; Lidow et al., 1998) or approaches with high spatial resolution such as iontophoresis may provide great incite into the laminar microcircuit (e.g., Major et al., 2015, 2018).

The work presented here investigated patterns at the level of single neurons either by investigating onset times of individual neurons, or fitting the data together in a model, for comparison with the existing literature in the macaque monkey. However, examining neuronal population dynamics via state space analyses may reveal additional insights into the laminar organization of these regions (see for review, Vyas et al., 2020). Here, a population state is defined as a vector of the instantaneous firing rate of each neuron in the population. The trajectory of the population activity through this space can be investigated to uncover features of this space; the flow of activity therein can explain neural activity patterns and the cognitive phenomena they underlie. These features, described in detail for many motor functions, such as reaching behaviours (Churchland et al., 2012), have been recapitulated by recurrent neural networks designed to simulate neural activity in a variety of commonly used cognitive tasks (Sohn et al., 2019; see also for review, Vyas et al., 2020). Assessing how these population dynamics evolve across cortical layers can provide unique insights into functions otherwise not detectable from single neurons. However, such analyses may require more trials than available here to capture subtle features (e.g., 800 trials in Churchland et al., 2012), and should be a

focus of future investigations building on this work.

5.3 Concluding Remarks

Visual spatial attention, directed by overt shifts of gaze and covert shifts of attention, are necessary for visual perception. This is comprised of a rich but stereotyped and well characterized behavioural repertoire, which provides a strong foundation for neurophysiological inquiry. While much is known about the neural circuitry underlying attention and eye movements, the cortical microcircuitry of key regions such as LIP and FEF remain largely unknown. To address this, we leveraged the homologous oculomotor behaviour and frontoparietal networks of marmosets as well as their largely lissencephalic cortex.

Throughout the course of this dissertation work, we established the homology of marmoset LIP and FEF with that of macaques and humans, and examined the laminar dynamics of these regions as animals completed a target selection task. First, we observed neural correlates of target selection and saccade control consistent with results obtained in macaques. Next, we observed that LIP is organized in a way that is qualitatively similar to previous observations in primary cortical areas supporting the generalizability of the CCM. Finally, we observed FEF organization is not entirely consistent with what is proposed by the CCM, and more closely resembles unique motifs observed in other frontal cortical areas. Overall, our observations provide additional support for the use of the emerging neuroscientific model, the common marmoset, for neurophysiological investigations of oculomotor control and attention, highlight the diversity of cortical circuits underlying target selection, and provides a deeper understanding of how the frontoparietal supports attention.

5.4 References

Bisley, J. W., & Goldberg, M. E. (2003). Neuronal Activity in the Lateral Intraparietal Area and Spatial Attention. *Science*, *299*(5603), 81–86. https://doi.org/10.1126/science.1077395

Bisley, J. W., Mirpour, K., Arcizet, F., & Ong, W. S. (2011). The Role of the Lateral Intraparietal Area in Orienting Attention and its Implications for Visual Search. *The European journal of neuroscience*, *33*(11), 1982–1990. https://doi.org/10.1111/j.1460-9568.2011.07700.x

Bruce, C. J., & Goldberg, M. E. (1985). Primate frontal eye fields. I. Single neurons discharging before saccades. *Journal of Neurophysiology*, *53*(3), 603–635. https://doi.org/10.1152/jn.1985.53.3.603

Bruce, C. J., Goldberg, M. E., Bushnell, M. C., & Stanton, G. B. (1985). Primate frontal eye fields. II. Physiological and anatomical correlates of electrically evoked eye movements. *Journal of Neurophysiology*, *54*(3), 714–734. https://doi.org/10.1152/jn.1985.54.3.714

Burish, M. J., Stepniewska, I., & Kaas, J. H. (2008). Microstimulation and architectonics of frontoparietal cortex in common marmosets (Callithrix jacchus). *Journal of Comparative Neurology*, *507*(2), 1151–1168. https://doi.org/10.1002/cne.21596

Chen, C.-Y., Watakabe, A., Matrov, D., Ho, K.-T., Amly, W., Onoe, H., Yamamori, T., & Isa, T. (2023). Topographic organization of the saccade related areas in dorsal frontal cortex of common marmoset.

Churchland, M. M., Cunningham, J. P., Kaufman, M. T., Foster, J. D., Nuyujukian, P., Ryu, S. I., & Shenoy, K. V. (2012). Neural population dynamics during reaching. *Nature*, *487*(7405), 51–56. https://doi.org/10.1038/nature11129

Cooke, D. F., Goldring, A. B., Yamayoshi, I., Tsourkas, P., Recanzone, G. H., Tiriac, A., Pan, T., Simon, S. I., & Krubitzer, L. (2012). Fabrication of an inexpensive, implantable cooling device for reversible brain deactivation in animals ranging from rodents to primates. *Journal of Neurophysiology*, *107*(12), 3543–3558. https://doi.org/10.1152/jn.01101.2011

Corneil, B. D., Elsley, J. K., Nagy, B., & Cushing, S. L. (2010). Motor output evoked by sub-saccadic stimulation of primate frontal eye fields. *Proceedings of the National Academy of Sciences of the United States of America*, *107*(13), 6070–6075. https://doi.org/10.1073/pnas.0911902107

Douglas, R. J., & Martin, K. A. (1991). A functional microcircuit for cat visual cortex. *The Journal of Physiology*, *440*, 735–769. Retrieved July 23, 2021, from https://www.ncbi.nlm.nih.gov/pmc/articles/PMC1180177/

Douglas, R. J., & Martin, K. A. (2004). Neuronal Circuits of the Neocortex. *Annual Review of Neuroscience*, *27*(1), 419–451. https://doi.org/10.1146/annurev.neuro.27.070203.144152

Fakharian, M., Shoup, A., Zang, J., Hage, P., Pi, J., & Shadmehr, R. (2023). Temporal coordination of spikes in the cerebellum reveals connectivity patterns of Molecular layer interneurons and Purkinje Cells during saccades.

Feizpour, A., Majka, P., Chaplin, T. A., Rowley, D., Yu, H.-H., Zavitz, E., Price, N. S. C., Rosa, M. G. P., & Hagan, M. A. (2021). Visual responses in the dorsolateral frontal cortex of marmoset monkeys. *Journal of Neurophysiology*, *125*(1), 296–304. https://doi.org/10.1152/jn.00581.2020

Ferraina, S., Paré, M., & Wurtz, R. H. (2002). Comparison of Cortico-Cortical and Cortico-Collicular Signals for the Generation of Saccadic Eye Movements. *Journal of Neurophysiology*, *87*(2), 845–858. https://doi.org/10.1152/jn.00317.2001

Foerster, O. (1926). Zur operativen Behandlung der Epilepsie. *Deutsche Zeitschrift für Nervenheilkunde*, *89*(1), 137–147. https://doi.org/10.1007/BF01653863

Frey, S., Pandya, D. N., Chakravarty, M. M., Bailey, L., Petrides, M., & Collins, D. L. (2011). An MRI based average macaque monkey stereotaxic atlas and space (MNI monkey space). *NeuroImage*, *55*(4), 1435–1442. https://doi.org/10.1016/j.neuroimage.2011.01.040

Girardin, C. C., & Martin, K. A. C. (2009). Cooling in cat visual cortex: Stability of orientation selectivity despite changes in responsiveness and spike width. *Neuroscience*, *164*(2), 777–787. https://doi.org/10.1016/j.neuroscience.2009.07.064

Godlove, D. C., Maier, A., Woodman, G. F., & Schall, J. D. (2014). Microcircuitry of Agranular Frontal Cortex: Testing the Generality of the Canonical Cortical Microcircuit. *The Journal of Neuroscience*, *34*(15), 5355–5369. https://doi.org/10.1523/JNEUROSCI.5127-13.2014

Goldberg, M. E., Bisley, J., Powell, K. D., Gottlieb, J. P., & Kusunoki, M. (2002). The Role of the Lateral Intraparietal Area of the Monkey in the Generation of Saccades and Visuospatial Attention. *Annals of the New York Academy of Sciences*, *956*(1), 205–215. https://doi.org/10.1111/j.1749-6632.2002.tb02820.x

Gottlieb, J. P., Bruce, C. J., & MacAvoy, M. G. (1993). Smooth eye movements elicited by microstimulation in the primate frontal eye field. *Journal of Neurophysiology*, *69*(3), 786–799. https://doi.org/10.1152/jn.1993.69.3.786

Hanes, D. P., Thompson, K. G., & Schall, J. D. (1995). Relationship of presaccadic activity in frontal eye field and supplementary eye field to saccade initiation in macaque: Poisson spike train analysis. *Experimental Brain Research*, *103*(1), 85–96. https://doi.org/10.1007/BF00241967

Heinzle, J., Hepp, K., & Martin, K. A. C. (2007). A Microcircuit Model of the Frontal Eye Fields. *Journal of Neuroscience*, *27*(35), 9341–9353. https://doi.org/10.1523/JNEUROSCI.0974-07.2007

Inoue, K.-i., Matsumoto, M., & Takada, M. (2021). Nonhuman Primate Optogenetics: Current Status and Future Prospects. In H. Yawo, H. Kandori, A. Koizumi, & R. Kageyama (Eds.), *Optogenetics: Light-Sensing Proteins and Their Applications in Neuroscience and Beyond* (pp. 345–358). Springer. https://doi.org/10.1007/978-981-15-8763-4_22

Jeschke, M., Ohl, F. W., & Wang, X. (2022). Effects of Cortical Cooling on Sound Processing in Auditory Cortex and Thalamus of Awake Marmosets. *Frontiers in Neural Circuits*, *15*, 786740. https://doi.org/10.3389/fncir.2021.786740

Knight, T. A., & Fuchs, A. F. (2007). Contribution of the Frontal Eye Field to Gaze Shifts in the Head-Unrestrained Monkey: Effects of Microstimulation. *Journal of Neurophysiology*, *97*(1), 618–634. https://doi.org/10.1152/jn.00256.2006

Kusunoki, M., Gottlieb, J. P., & Goldberg, M. E. (2000). The lateral intraparietal area as a salience map: The representation of abrupt onset, stimulus motion, and task relevance. *Vision Research*, *40*(10), 1459–1468. https://doi.org/10.1016/S0042-6989(99)00212-6

Lidow, M. S., Wang, F., Cao, Y., & Goldman-Rakic, P. S. (1998). Layer V neurons bear the majority of mRNAs encoding the five distinct dopamine receptor subtypes in the primate prefrontal cortex. *Synapse (New York, N.Y.)*, *28*(1), 10–20. https://doi.org/10.1002/(SICI)1098-2396(199801)28:1⟨10::AID-SYN2⟩3.0.CO;2-F

Major, A. J., Vijayraghavan, S., & Everling, S. (2015). Muscarinic Attenuation of Mnemonic Rule Representation in Macaque Dorsolateral Prefrontal Cortex during a Pro- and Anti-Saccade Task. *The Journal of Neuroscience*, *35*(49), 16064–16076. https://doi.org/10.1523/JNEUROSCI.2454-15.2015

Major, A. J., Vijayraghavan, S., & Everling, S. (2018). Cholinergic Overstimulation Attenuates Rule Selectivity in Macaque Prefrontal Cortex. *Journal of Neuroscience*, *38*(5), 1137–1150. https://doi.org/10.1523/JNEUROSCI.3198-17.2017

Mitchell, J. F., Priebe, N. J., & Miller, C. T. (2015). Motion dependence of smooth pursuit eye movements in the marmoset. *Journal of Neurophysiology*, *113*(10), 3954–3960. https://doi.org/10.1152/jn.00197.2015

Monosov, I. E., & Thompson, K. G. (2009). Frontal Eye Field Activity Enhances Object Identification During Covert Visual Search. *Journal of Neurophysiology*, *102*(6), 3656–3672. https://doi.org/10.1152/jn.00750.2009

Moore, T., & Armstrong, K. M. (2003). Selective gating of visual signals by microstimulation of frontal cortex. *Nature*, *421*(6921), 370–373. https://doi.org/10.1038/nature01341

Moore, T., & Fallah, M. (2004). Microstimulation of the Frontal Eye Field and Its Effects on Covert Spatial Attention. *Journal of Neurophysiology*, *91*(1), 152–162. https://doi.org/10.1152/jn.00741.2002

Paré, M., & Wurtz, R. H. (1997). Monkey Posterior Parietal Cortex Neurons Antidromically Activated From Superior Colliculus. *Journal of Neurophysiology*, *78*(6), 3493–3497. https://doi.org/10.1152/jn.1997.78.6.3493

Paxinos, G., Charles, W., Michael, P., Rosa, M. G. P., & Hironobu, T. (2012). *The marmoset brain in stereotaxic coordinates*. Academic OCLC: 794295103.

Robinson, D. A., & Fuchs, A. F. (1969). Eye movements evoked by stimulation of frontal eye fields. *Journal of Neurophysiology*, *32*(5), 637–648. https://doi.org/10.1152/jn.1969.32.5.637

Roth, B. L. (2016). DREADDs for Neuroscientists. *Neuron*, *89*(4), 683–694. https://doi.org/10.1016/j.neuron.2016.01.040

Russo, G. S., & Bruce, C. J. (1993). Effect of eye position within the orbit on electrically elicited saccadic eye movements: A comparison of the macaque monkey's frontal and supplementary eye fields. *Journal of Neurophysiology*, *69*(3), 800–818. https://doi.org/10.1152/jn.1993.69.3.800

Sajad, A., Errington, S. P., & Schall, J. D. (2022). Functional architecture of executive control and associated event-related potentials in macaques. *Nature Communications*, *13*(1), 6270. https://doi.org/10.1038/s41467-022-33942-1

Sajad, A., Godlove, D. C., & Schall, J. D. (2019). Cortical microcircuitry of performance monitoring. *Nature Neuroscience*, *22*(2), 265–274. https://doi.org/10.1038/s41593-018-0309-8
Bandiera_abtest: a Cg_type: Nature Research Journals Primary_atype: Research Subject_term: Cognitive control;Cortex;Psychology;Schizophrenia Subject_term_id: cognitive-control;cortex;psychology;schizophrenia

Savaki, H. E., Gregoriou, G. G., Bakola, S., & Moschovakis, A. K. (2015). Topography of Visuomotor Parameters in the Frontal and Premotor Eye Fields. *Cerebral Cortex*, *25*(9), 3095–3106. https://doi.org/10.1093/cercor/bhu106

Schaeffer, D. J., Klassen, L. M., Hori, Y., Tian, X., Szczupak, D., Yen, C. C.-C., Cléry, J. C., Gilbert, K. M., Gati, J. S., Menon, R. S., Liu, C., Everling, S., & Silva, A. C. (2022). An open access resource for functional brain connectivity from fully awake marmosets. *NeuroImage*, *252*, 119030. https://doi.org/10.1016/j.neuroimage.2022.119030

Schall, J. D. (1995). Neural Basis of Saccade Target Selection. *Reviews in the Neurosciences*, *6*(1), 63–85. https://doi.org/10.1515/REVNEURO.1995.6.1.63

Schall, J. D. (2004). On the role of frontal eye field in guiding attention and saccades. *Vision Research*, *44*(12), 1453–1467. https://doi.org/10.1016/j.visres.2003.10.025

Schall, J. D., & Hanes, D. P. (1993). Neural basis of saccade target selection in frontal eye field during visual search. *Nature*, *366*(6454), 467–469. https://doi.org/10.1038/366467a0

Schall, J. D., Morel, A., King, D. J., & Bullier, J. (1995). Topography of visual cortex connections with frontal eye field in macaque: Convergence and segregation of processing

streams. *The Journal of Neuroscience*, *15*(6), 4464–4487. https://doi.org/10.1523/JNEUROSCI.15-06-04464.1995

Schiller, P. H., & Chou, I.-H. (2000). The effects of anterior arcuate and dorsomedial frontal cortex lesions on visually guided eye movements: 2. Paired and multiple targets. *Vision Research*, *40*(10), 1627–1638. https://doi.org/10.1016/S0042-6989(00)00058-4

Schlag, J., & Schlag-Rey, M. (1987). Evidence for a supplementary eye field. *Journal of Neurophysiology*, *57*(1), 179–200. https://doi.org/10.1152/jn.1987.57.1.179

Segraves, M. A. (1992). Activity of monkey frontal eye field neurons projecting to oculomotor regions of the pons. *Journal of Neurophysiology*, *68*(6), 1967–1985. https://doi.org/10.1152/jn.1992.68.6.1967

Segraves, M. A., & Goldberg, M. E. (1987). Functional properties of corticotectal neurons in the monkey's frontal eye field. *Journal of Neurophysiology*, *58*(6), 1387–1419. https://doi.org/10.1152/jn.1987.58.6.1387

Sohn, H., Narain, D., Meirhaeghe, N., & Jazayeri, M. (2019). Bayesian Computation through Cortical Latent Dynamics. *Neuron*, *103*(5), 934–947.e5. https://doi.org/10.1016/j.neuron.2019.06.012

Swadlow, H. A. (2002). Thalamocortical control of feed-forward inhibition in awake somatosensory 'barrel' cortex. *Philosophical Transactions of the Royal Society B: Biological Sciences*, *357*(1428), 1717–1727. https://doi.org/10.1098/rstb.2002.1156

Thompson, K. G., Bichot, N. P., & Schall, J. D. (1997). Dissociation of Visual Discrimination From Saccade Programming in Macaque Frontal Eye Field. *Journal of Neurophysiology*, *77*(2), 1046–1050. https://doi.org/10.1152/jn.1997.77.2.1046

Thompson, K. G., Biscoe, K. L., & Sato, T. R. (2005). Neuronal Basis of Covert Spatial Attention in the Frontal Eye Field. *The Journal of Neuroscience*, *25*(41), 9479–9487. https://doi.org/10.1523/JNEUROSCI.0741-05.2005

Thompson, K. G., Hanes, D. P., Bichot, N. P., & Schall, J. D. (1996). Perceptual and motor processing stages identified in the activity of macaque frontal eye field neurons during visual search. *Journal of Neurophysiology*, *76*(6), 4040–4055. https://doi.org/10.1152/jn.1996.76.6.4040

van der Steen, J., Russell, I. S., & James, G. O. (1986). Effects of unilateral frontal eye-field lesions on eye-head coordination in monkey. *Journal of Neurophysiology*, *55*(4), 696–714. https://doi.org/10.1152/jn.1986.55.4.696

Vyas, S., Golub, M. D., Sussillo, D., & Shenoy, K. V. (2020). Computation Through Neural Population Dynamics. *Annual Review of Neuroscience*, *43*(1), 249–275. https://doi.org/10.1146/annurev-neuro-092619-094115

Wakabayashi, M., Koketsu, D., Kondo, H., Sato, S., Ohara, K., Polyakova, Z., Chiken, S., Hatanaka, N., & Nambu, A. (2018). Development of stereotaxic recording system for awake marmosets (Callithrix jacchus). *Neuroscience Research*, *135*, 37–45. https://doi.org/10.1016/j.neures.2018.01.001

Wardak, C., Ibos, G., Duhamel, J.-R., & Olivier, E. (2006). Contribution of the Monkey Frontal Eye Field to Covert Visual Attention. *The Journal of Neuroscience*, *26*(16), 4228–4235. https://doi.org/10.1523/JNEUROSCI.3336-05.2006

Wong, R. K., Selvanayagam, J., Johnston, K. D., & Everling, S. (2022). Delay-related activity in marmoset prefrontal cortex. *Cerebral Cortex*, bhac289. https://doi.org/10.1093/cercor/bhac289

Zhou, H.-H., & Thompson, K. G. (2009). Cognitively-directed spatial selection in the frontal eye field in anticipation of visual stimuli to be discriminated. *Vision research*, *49*(10), 1205–1215. https://doi.org/10.1016/j.visres.2008.03.024

Appendix A

Ethics Approval

Western🛡

AUP Number: 2021-111
PI Name: Everling, Stefan
**AUP Title:** Functional imaging and neurophysiology in the common marmoset Callithrix jacchus

Official Notification of ACC Approval: A modification to Animal Use Protocol **2021-111** has been approved.

Please at this time review your AUP with your research team to ensure full understanding by everyone listed within this AUP.

As per your declaration within this approved AUP, you are obligated to ensure that:

1. This Animal Use Protocol is in compliance with:
   - Western's Senate MAPP 7.12 [PDF]; and
   - Applicable Animal Care Committee policies and procedures.
2. Prior to initiating any study-related activities—as per institutional OH&S policies—all individuals listed within this AUP who will be using or potentially exposed to hazardous materials will have:
   - Completed the appropriate institutional OH&S training;
   - Completed the appropriate facility-level training; and
   - Reviewed related (M)SDS Sheets.

Submitted by: McInnis, Jennifer on behalf of the Animal Care Committee
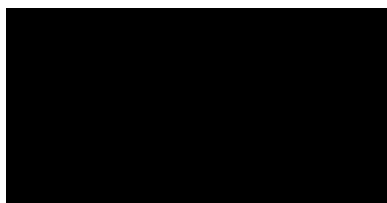
Dr. Lisa Hoffman,
Acting Animal Care Committee Chair

Animal Care Commitee
The University of Western Ontario
London, Ontario Canada N6A 5C1
▓▓▓▓▓▓▓▓▓ | ACC Website

Curriculum Vitae

Janahan Selvanayagam

Education

2018-
PhD in Neuroscience, University of Western Ontario
Supervisor: Stefan Everling

2014-2018
BSc in Neuroscience, Brock University
Supervisor: Veena D. Dwivedi

Grants, honours & awards

2020-2023
Canadian Graduate Scholarship (Doctoral) **$ 105,000**
Natural Sciences and Engineering Research Council (NSERC) - Federal Grant

2020
Ontario Graduate Scholarship **declined**
OGS - Provincial Grant

2019-2020
Canadian Graduate Scholarship (Masters) **$ 17,500**
Natural Sciences and Engineering Research Council (NSERC) - Federal Grant

2019
Ontario Graduate Scholarship **declined**
OGS - Provincial Grant

2019
Neuroscience Travel Award **$ 500**
University of Western Ontario - Internal Grant

2018
Distinguished graduating student - Neuroscience
Brock University - Top student in graduating class

2018
Match of Minds **$ 5,000**
Brock University - Internal Grant

2014-2018
Brock Scholar's Award **$ 14,000**
Brock University - Internal Grant

Publications & talks

Journal articles

submitted
Selvanayagam, J., Johnston, K.D., & Everling, S. Laminar Dynamics of Target Selection in the Posterior Parietal Cortex of the Common Marmoset. *Journal of Neuroscience*.

2023
Zanini, A., Dureux, A., **Selvanayagam, J.**, & Everling, S. Ultra-high field fMRI identifies an action-observation network in the common marmoset. *Communications Biology, 6*, 553.

2023
Dureux, A., Zanini, A., **Selvanayagam, J.**, Menon, R.S., & Everling, S. Gaze patterns and brain activations in humans and marmosets in the Frith-Happé theory-of-mind animation task. *eLife, 12*, e86327.

2023
Wong, R. K., **Selvanayagam, J.**, Johnston, K. D., & Everling, S. Delay-related activity in marmoset prefrontal cortex. *Cerebral Cortex, 33*(7), 3523-3537.

2021
Gilbert, K.M., Clery, J.C. **Selvanayagam, J.**, ... & Everling, S. Simultaneous functional MRI of two awake marmosets. *Nature Communications, 12*, 6608.

2021
Hori. Y., Clery, J.C., **Selvanayagam, J.**, ... & Everling, S. Interspecies activation correlations reveal functional correspondences between marmoset and human brain areas. *Proceedings of the National Academy of Sciences, 118*(37), e2110980118.

2021
Selvanayagam, J., Johnston, K. D., Wong, R. K., Schaeffer, D., & Everling, S. Ketamine disrupts gaze patterns during face viewing in the common marmoset. *Journal of Neurophysiology, 126*(1), 330-339.

2021
Dwivedi, V. D., & **Selvanayagam, J.**(2021). Effects of Dispositional Affect on the N400: Language Processing and Socially Situated Context. *Frontiers in Psychology, 12*, 566894.

2020
Schaeffer, D. J., **Selvanayagam, J.**, Johnston, K. D., Menon, R. S., Freiwald, W. A., & Everling, S. Face

selective patches in marmoset frontal cortex. *Nature Communications, 11*(1), 4856.

2020   Ma, L., **Selvanayagam, J.**, Ghahremani, M., Hayrynen, L. K., Johnston, K. D., & Everling, S. Single-unit activity in marmoset posterior parietal cortex in a gap saccade task. *Journal of Neurophysiology, 123*(3), 896-911.

2019   **Selvanayagam, J.**, Johnston, K. D., Schaeffer, D.J., Hayrynen, L.K., & Everling, S. Functional Localization of the Frontal Eye Fields in the Common Marmoset Using Microstimulation. *Journal of Neuroscience, 39*(46), 9197–9206.

2019   **Selvanayagam, J.**, Witte, V., Schmidt, L.A., & Dwivedi, V.D. A preliminary investigation of dispositional affect, the P300, and sentence processing. *Brain Research, 1721*, 146309.

2018   Dwivedi, V.D., Goertz, K.E., & **Selvanayagam, J.**. Heuristics in Language Comprehension. *Journal of Behavioral and Brain Science, 8*(7), 430-446.

Talks

2022, Nov   **Selvanayagam, J.**, Johnston, K. D., Everling, S. Cortical microcircuitry underlying target discrimination in marmoset LIP. *Marmoset Bioscience Symposium*, San Diego, USA.

2022, Oct   **Selvanayagam, J.**, Johnston, K. D., Everling, S. Cortical microcircuitry underlying target discrimination in marmoset posterior parietal cortex. *Mental Health Research Day*, [virtual].

Selected Posters

* = Presenting author

2023, May   ***Selvanayagam, J.**, Johnston, K. D., Everling, S. Laminar microcircuitry underlying target selection in marmoset posterior parietal cortex. *Canadian Association for Neuroscience*, Montreal, Canada.

2023, Nov   ***Selvanayagam, J.**, Johnston, K. D., Everling, S. Cortical microcircuitry underlying target discrimination in marmoset LIP. *Society for Neuroscience*, San Diego, USA.

2021, Nov   ***Selvanayagam, J.**, Johnston, K. D., Everling, S. Cortical microcircuitry underlying target discrimination in the posterior parietal cortex of the common marmoset. *Society for Neuroscience* [virtual].

2021, Nov   *Johnston, K. D., **Selvanayagam, J.**, Everling, S. Visual receptive fields in the posterior parietal cortex of the common marmoset. *Society for Neuroscience* [virtual].

2021, Oct   ***Selvanayagam, J.**, Johnston, K. D., Wong, R. K., Everling, S. Ketamine disrupts holistic face processing in the common marmoset. *Marmoset Bioscience Symposium*, [virtual].

2019, Oct   ***Selvanayagam, J.**, Johnston, K. D., Schaeffer, D., Hayrynen, L. K., Everling, S. Functional localization of the frontal eye fields in the common marmoset using microstimulation. *Society for Neuroscience*, Chicago, USA.

2019, Apr   ***Selvanayagam, J.**, Johnston, K. D., Hayrynen, L. K., Everling, S. Identification of the frontal eye fields in the common marmoset using microstimulation. *Society for the Neural Control of Movement*, Toyama, Japan.

2018, May   Dwivedi, V.D., ***Selvanayagam, J.**. N400 and dispositional affect. *Southern Ontario Neuroscience Association*, Guelph, Canada.

2018, Mar   ***Selvanayagam, J.**, Witte, V., Schmidt, L., Dwivedi, V.D. P300, dispositional affect and sentence processing. *Cognitive Neuroscience Society*, Boston, USA.

2017, May   Dwivedi, V. D., Tarkowski, V., ***Selvanayagam, J.**. Dispositional affect and sentence processing. *Southern Ontario Neuroscience Association*, St. Catharines, Canada.

2017, Feb   Dwivedi, V. D., Curtiss, K., ***Selvanayagam, J.**. Numerical cognition and the activation of event knowledge. *Lake Ontario Visionary Establishment*, Niagara Falls, Canada.